The repair of DSBs catalyzed by VMA1 derived endonuclease by homologous recombination during meiosis

A thesis submitted in part fulfillment of the requirements

for the degree of Doctor of Philosophy

by Darpan K. Medhi

B.Sc. (Dual Hons) University of Sheffield

Department of Molecular Biology and Biotechnology

University of Sheffield

(July 2013)

Summary

The repair of DSBs catalyzed by VMA1 derived endonuclease by homologous recombination during meiosis

Darpan Medhi

PhD Thesis

Homologous recombination (HR) during meiosis is initiated by programmed DNA double strand breaks (DSBs). Some of these DSBs are repaired to give crossovers (COs), which connect maternal and paternal homologous chromosomes and thus ensure proper segregation during meiosis I. In contrast, HR in mitotic cells forms mostly noncrossovers (NCOs); this prevents deleterious genome rearrangement and loss of heterozygosity. Therefore, meiotic HR is regulated to enrich for COs, but much remains to be understood regarding the basis of this regulation. Meiotic cells express unique HR proteins, and these global factors might facilitate the distinct regulation of meiotic HR. In addition, meiosis-specific proteins localize to the chromosome axis, and these proteins interact with the meiotic Spo11 complex during DSB formation. Thus, the substrate for meiotic HR forms in a unique local chromatin context, and is then acted upon by unique global recombination factors. In order to better understand the balance between local and global influences, we studied the meiotic repair of DSBs formed by the VMA1-derived endonuclease (VDE). Repair of these breaks, which form independent of the meiotic chromosome axis, should still be influenced by global cell wide meiotic recombination proteins, but may or may not be influenced by the localized meiotic chromosome axis.

We studied repair of two VDE DSBs: one located in a region that is "hot" for Spo11 DSBs and is enriched for axis proteins; and one in a Spo11 DSB "cold" region that is not enriched for axis proteins. VDE DSBs are repaired at both loci to produce NCOs in excess over COs, but more COs are formed at the hot-spot locus. The hot-spot also accumulated more joint molecules (JMs), which are the intermediates of CO formation. In addition, CO formation shows different resolvase dependence at the two loci. Hot-spot COs are Mlh3-dependent but largely independent of the "mitotic" Mus81-Mms4 structure-selective nuclease; whereas cold-spot COs are Mlh3-independent but show dependence on Mus81-Mms4. Finally, in *spo11-Y135F* cells lacking genome wide meiotic DSBs, VDE-initiated COs are reduced at both loci, which now display an identical NCO-CO ratio. This effect is partially attributable to the lack of pairing in these cells, as ectopic repair of VDE DSBs in *SPO11* cells also have a similar NCO-CO ratio. Thus, COs in meiosis require a specific global recombination environment. COs are also influenced by factors that act locally, such that VDE initiated COs at a hot-spot and a cold-spot are reminiscent of meiosis and mitosis respectively.

“There is a pony in there somewhere”

- Michael Lichten

For my father Dr. Dilip Medhi, who, despite his best attempts, inspired me to follow his footsteps.

For my mother, Anjali Medhi, who, despite my best attempts, still believes I can accomplish anything I put my mind to.

For my brother, Prabal Medhi, for holding the fort while I wandered off chasing my dreams.

Acknowledgements

I would like to thank my supervisor at NCI, Dr. Michael Lichten, for his advice, supervision and constant support and encouragement during the course of this project. He has also been a wonderful teacher, and learning from him has been a joy and a privilege. I would also like to thank by my supervisor at the University of Sheffield Dr. Alastair Goldman, who gave me this opportunity to work on this challenging and wonderful project and none of this would have been possible if he hadn't put his faith in me and supported my PhD candidacy. His support and advice has been invaluable for this project.

I would like to thank my mother, father and brother, who have been there for me through thick and thin and made it possible for me to take this monumental journey from the Northeast of India to Sheffield and Bethesda. I would also like to thank all my friends, who have shared my joys and sorrows in this relatively solitary existence during my education away from my home.

Abbreviations

DNA	Deoxyribonucleic acid
DSB	Double strand break
HR	Homologous Recombination
CO	Crossover
NCO	Noncrossover
HJ	Holliday junction
DSBR	Double Strand Break Repair
dHJ	double Holliday junction
JMs	Joint Molecules
SDSA	Synthesis Dependent Strand Annealing
ssDNA	single stranded DNA
SSA	Single strand annealing
BIR	Break induced replication
LOH	loss of heterozygosity
nt	nucleotide
S phase	Synthesis phase
bp	base pairs
kb	kilo bases
kDa	kilo Daltons
NDR	nucleosome depleted region
TF	transcription factor
SC	Synaptonemal Complex
EM	electron microscope

AE	Axial Element
LM	light microscopy
ChIP	Chromatin immunoprecipitaion
PAR	Pseudo Autosomal Region
VDE	*VMA1* derived endonuclease
S. cerevisiae	*Saccharomyces cerevisiae*
S. pombe	*Schizosaccharomyces pombe*
C. elegans	*Caenorhabditis elegans*
E. coli	*Escherichia coli*

Table of Contents

List of Figures

List of Tables

1 Introduction

Double strand breaks (DSBs) in DNA are potentially lethal lesions for all organisms and defects in their repair can block replication, transcription, and lead to the build up of mutations in the genome (Jackson and Bartek. 2009). Homologous recombination (HR) is a pathway for repairing DSBs in DNA by using an intact chromosome as template for repair. Such repair leads to minimal loss of genetic information, and thus during the S-G2 phase of the cell cycle when chromosomes have replicated, HR is the preferred mode of DSB repair (Ira et al. 2004, Chen et al. 2011, Huertas and Jackson. 2009, Esashi et al. 2005). Somatic or vegetative cells divide via mitosis to create two daughter cells with identical chromosome complement by equational segregation of their replicated chromosomes. Therefore, HR in these cells is primarily required for genome maintenance.

However, sexual reproduction involving the union of cells cannot arise from the fusion of mitotically dividing cells, as this will lead to the doubling of ploidy with every generation. Thus, germ cells form by a process called meiosis. In meiosis, cell division consists of one round of chromosome replication followed by two successive rounds of reductional and equational chromosome segregation to give gametes with haploid complement of chromosomes (Figure 1-1). The union of these gametes to form a zygote restores the normal diploid chromosome complement. The reductional segregation in the first meiotic division separates homologous paternal and maternal chromosomes, and this requires physical connections called chiasmata between these homologues (Koszul et al. 2012, Janssens. 1909). HR in meiosis forms the chiasmata between homologues due to the repair of programmed DSBs, and these physical linkages between homologous chromosomes ensure their faithful segregation. This is evident from studies of recombination deficient mutants in *Saccharomyces cerevisiae* (Engebrecht et al. 1990, Nakagawa and Ogawa. 1999, Khazanehdari and Borts. 2000) and studies of human chromosome aneuploidies (Lamb et al. 1997). Also, meiotic recombination rates vary in human populations and these correlate with the occurrence of aneuploidies (Hussin et al. 2011, Bleazard et al. 2013).

Thus, HR plays different roles in mitotic cells vs. meiotic cells (Figure 1-2) and these different roles of HR are mediated by differences at multiple levels in the repair process. This introductory chapter will begin with an introduction to HR and some alternate DNA repair processes, and then proceed to elaborate on the contrasting roles of HR in mitosis and meiosis. Finally, it will explore the possible basis of this difference between mitotic and meiotic HR.

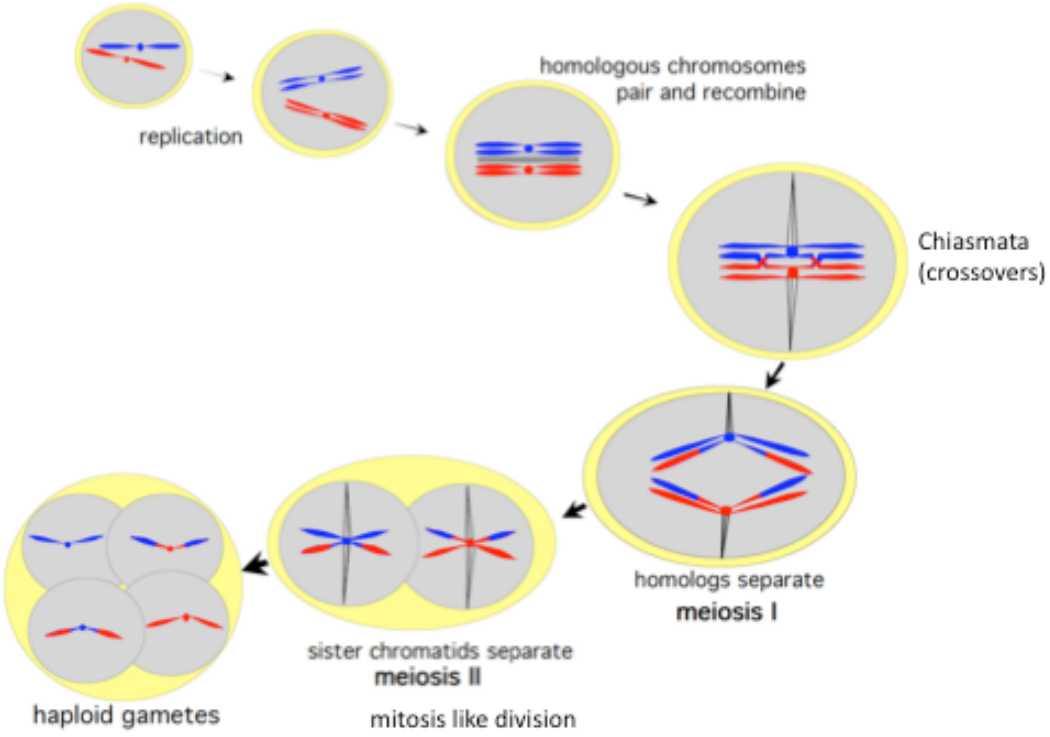

Figure 1-1 Meiotic recombination consists of one round of DNA replication followed by two successive rounds of reductional and equational chromosome segregation. Reductional segregation in meiosis I requires chiasmata to physically connect homologous chromosomes.

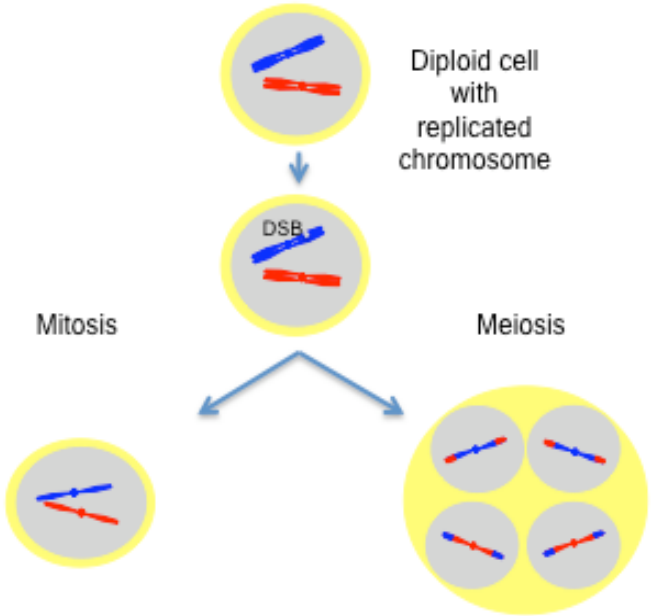

Figure 1-2 Homologous recombination to repair DNA DSBs performs contrasting functions between mitosis and meiosis. In mitosis, homologous recombination repairs DSBs as NCOs that lead to minimum alteration of the genome. In meiosis, DSBs are repaired to give COs to ensure faithful segregation of homologous chromosomes, this also leads to genomic alterations.

1.1 Molecular models for repair of DNA double strand breaks by homologous recombination

As mentioned previously, homologous recombination (HR) is an important pathway for the repair of DNA double strand breaks, but the earliest studies into recombination were done from a perspective of looking at the haploid products of meiosis, mainly by analysis of eight spore asci of fungi such as *Ascobolus, Neurospora* and *Sordoria* and sectored spore clones arising from the first mitotic division after sporulation in *Saccharomyces* and *Schizosaccharamyces* tetrads (Holliday. 1964, Szostak et al. 1983, Roman. 1985). A diploid cell that undergoes meiosis first replicates its DNA, such that it posses 4 DNA duplexes consisting of a two pairs of sister chromatids, for a total of 8 strands of DNA. Therefore, the examination of the 8 spores in fungal ascus or sectored spore colonies in a yeast 4 spore ascus allows one to determine the identity of all 8 strands of DNA that embark upon meiotic divisions. A heterozygous marker in a diploid would normally segregate in a 4:4 ratio, in line with Mendel's laws.

However, occasionally, aberrant asci were seen which deviated from this 4:4 segregation. These events were first described as 3:1 segregation events by Winkler. (1930), from the study of 4 spore asci of *Hymenomycetes* and mosses, and Winkler coined the term "gene conversion". This term was re-introduced by Lindegren. (1953), who described the 6:2 (3:1) segregation pattern as gene conversions in *Saccharomyces* (Figure 1-3). Other types of aberrant segregation are caused by post meiotic segregation, which give a sectored spore colony in a tetrad ascus or two non-identical sister spores in an octad ascus. These events would be classed as aberrant 6:2, 5:3, aberrant 5:3 and aberrant 4:4 segregations (Figure 1-3). The existence of these events implied the existence of heteroduplex DNA, i.e. DNA where the two complementary strands have mismatches, which upon semi conservative replication would give daughter DNA molecules with different alleles. Extensive tetrad analysis also demonstrated that such aberrant segregation events had a high probability of reciprocal exchange between flanking DNA markers (Holliday. 1964, Szostak et al. 1983).

1.1.1 Early models for homologous recombination

The first widely accepted molecular model that accounted for these phenomena was proposed by Holliday (1964) (Figure 1-4). This model postulated the initiation of gene conversion by formation of a single strand nick on two DNA molecules at homologous sites. This is followed by an exchange of nicked strands between the two DNA molecules, thereby forming a four way DNA junction, referred to as a Holliday junction, and flanked by heteroduplex DNA on both DNA duplexes, i.e. a symmetric heteroduplex. Resolution of this Holliday junction by cleavage of the uncrossed strands would cause an exchange of nearby DNA i.e. a

crossover (CO) while cleavage of the crossed strands would give a noncrossover (NCO). Thus, this model was able to explain the existence of aberrant segregation pattern, because if a heterozygous DNA marker falls within the region of the hetroduplex DNA, mismatches are created on both DNA duplexes. If both DNA mismatches are then corrected in favour of one allele, 6:2 segregation is observed. If only one mismatch is corrected while the other segregates post-meiotically, 5:3 segregation or aberrant 5:3 segregation is observed. If neither mismatch is corrected, an aberrant 4:4 tetrad would be seen, where there are two sectored spores.

The Holliday model predicts the formation of symmetrical hetroduplex, where both chromatids have heteroduplex DNA. However, Stadler and Towe. (1971) reported that most NCO tetrads in *Ascobolus* had segregation patterns consistent with 5:3 segregation, but very few showed aberrant 5:3 pattern. This suggested that in most case of recombination, only one chromatid had heteroduplex DNA, i.e. recombination was capable of forming an asymmetric heteroduplex. Also, the aberrant 4:4 segregation pattern predicted by Holliday model was infrequently observed in *Sordaria* (Kitani and Whitehouse. 2008) and was never observed in *S. cerevisiae* (Fogel and Mortimer. 1969, Klar et al. Gene 1979). To account for these discrepancies, Meselson and Radding (1975) proposed a model where a single stranded nick on one DNA molecule, called the donor, initiates recombination (Figure 1-5). Synthesis of new DNA initiates at the 3' end of the nick, while the 5' end displaces one strand of DNA in another recipient DNA homologue. This creates a D-loop on the recipient strand and creates a region of heteroduplex DNA. The D-loop is subsequently degraded while the invading strand ligates to the recipient. The region of heteroduplex DNA on the recipient can be extended by further synthesis of DNA on the donor strand and exonucleolytic degradation of the displaced recipient strand. Branch migration and isomerization of the newly synthesized strand from the donor to the recipient can form a Holliday junction. The Holliday junction can then be resolved to form an asymmetric heteroduplex, while migration of the Holliday junction away from the initiation site followed by resolution can also give rise to symmetric heteroduplex on both donor and recipient chromatids. Thus, this model accounted for the presence of both types of heteroduplex DNA. However, this model also predicted that newly synthesized DNA would be on the donor strand, whereas experimental data suggested that synthesized DNA was usually present on the recipient strand (Stahl. 1979). Additionally, heteroduplex DNA associated with COs is usually found to be positioned near the initiation site, but heteroduplex DNA in COs would always be positioned away from the initiation site (Fogel et al. 1978).

Early studies in *S. cerevisiae* on the repair of DSBs caused by ionizing radiation concluded that such repair in haploid cells was only possible in G2 phase (Brunborg et al. 1980). Chlebowicz and Jachymczyk (1979) also observed the same requirement for the repair of MMS induced DSBs and

thus, it appeared that DSBs in yeast DNA required a homologous DNA molecule for repair. Resnick and Martin (1976) also studied the repair of DSBs formed by ionizing radiation, and these studies led Resnick (1976) to propose a model for recombination that is initiated by a DNA DSB, 7 years before the DSBR model and around the same time as the Meselson and Radding model (Figure 1-6). In this model, the DSB is processed by 5' to 3' exonuclease degradation. A single stranded nick is then created on the intact donor DNA strand, and this anneals to the resected single stranded region on the recipient strand. This intermediate has two different fates. In one pathway, DNA synthesis is then primed from the 3' end of the resected strand, using the annealed donor strand as template. Once sufficient synthesis has been achieved, the newly synthesized strand can unwind from the donor strand and anneal back to the other end of the DSB, and the donor strand anneals back to the nick. Ligation and DNA synthesis to fill the gaps now creates an NCO with asymmetric heteroduplex i..e heteroduplex DNA is only on the recipient strand, not the donor. In the other pathway, the resected DNA strand on the other end of the DSB anneals to the single stranded region on the donor. A subsequent nick on the donor strand and isomerization now leads to a exchange of flanking DNA strands to form COs with symmetric heteroduplex, and the process is completed by ligation and synthesis to fill any gaps in the two strands.

The Resnick model has several features of note, which ought to be highlighted. Firstly, the initiation of recombination in this model is via a DSB in DNA, which is then resected, and this feature is now a canonical part of all current HR models. Secondly, newly synthesized DNA in this model is always on the recipient strand, thus this was the first model which was consistent with experimental evidence in this regard. Thirdly, this model allows for an NCO exclusive pathway with asymmetric heteroduplex, and the current exclusive NCO models bear strong similarities to this model. Finally, the Resnick model proposed separate pathways for the formation of NCOs and COs via homologous recombination, and this is indeed the case for meiotic recombination in cells. Therefore, it is rather unfortunate that the Resnick model was largely ignored in its day, but as noted above, several features of this model are now accepted features of HR.

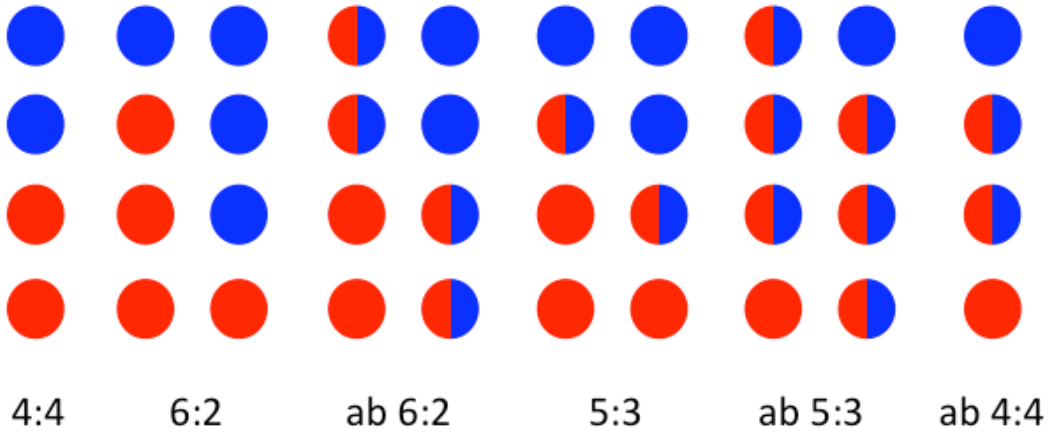

Figure 1-3 Various classes of tetrad asci with different segregation patterns for the red and blue heterozygous markers. ab stands for aberrant.

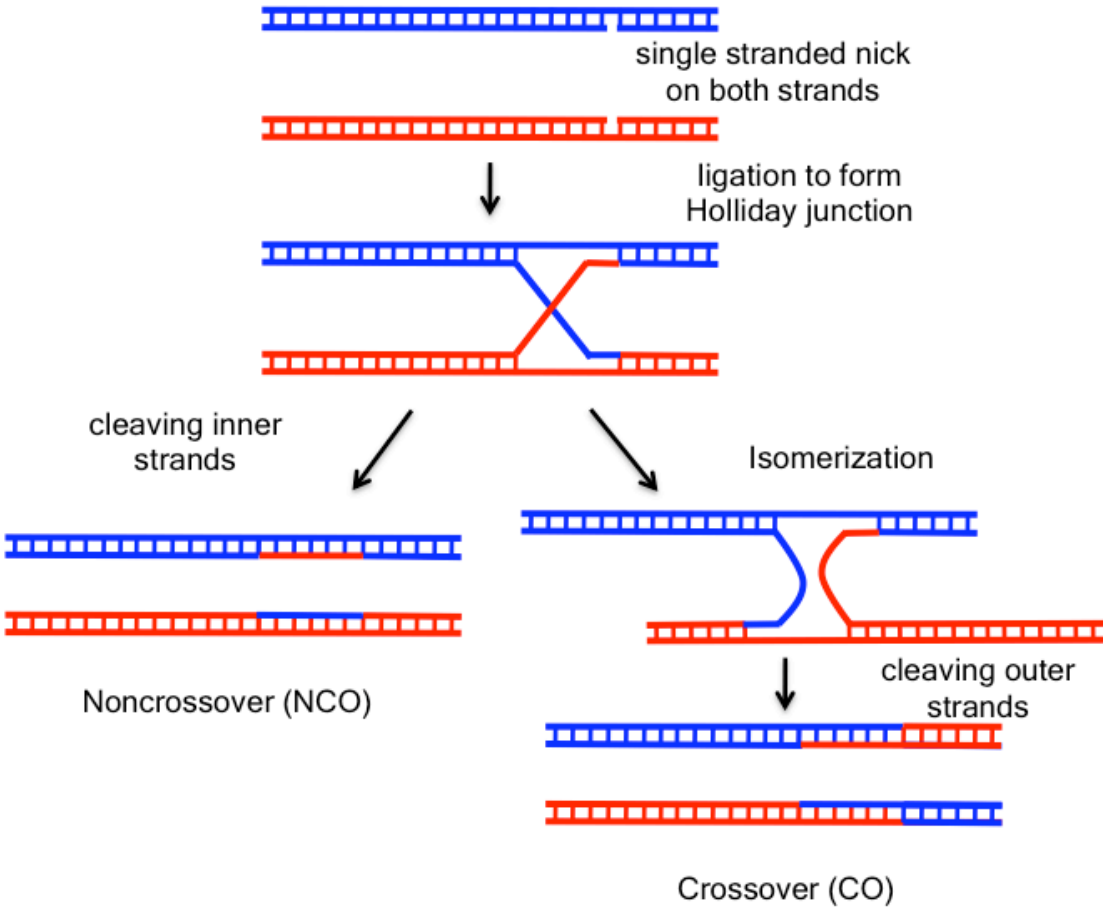

Figure 1-4 Holliday model of recombination. The various steps in these pathways are mentioned in text alongside the figures.

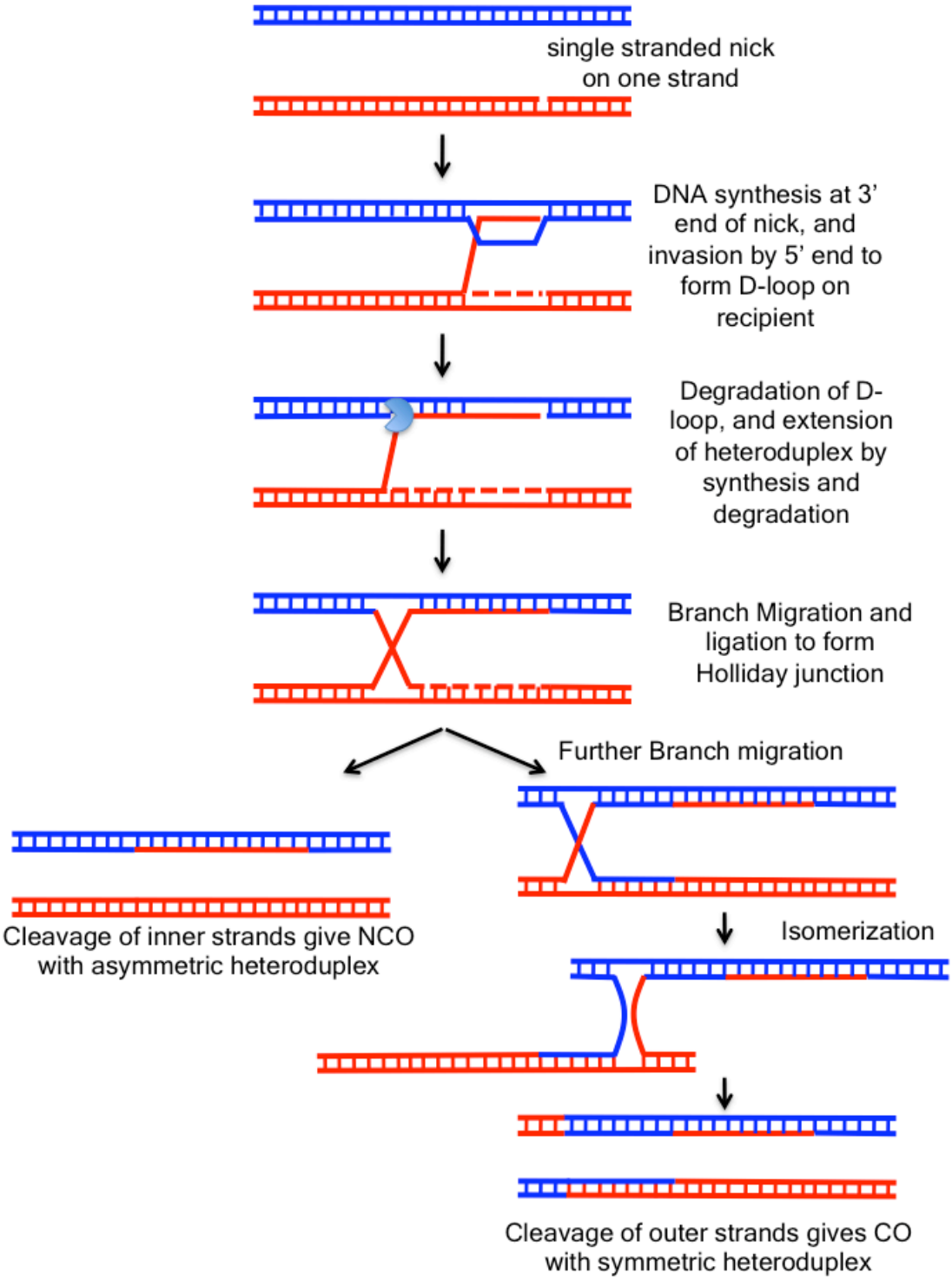

Figure 1-5 Meselson-Radding model of homologous recombination. Also referred to as the Aviemore model. The various steps in these pathways are mentioned in text alongside the figures.

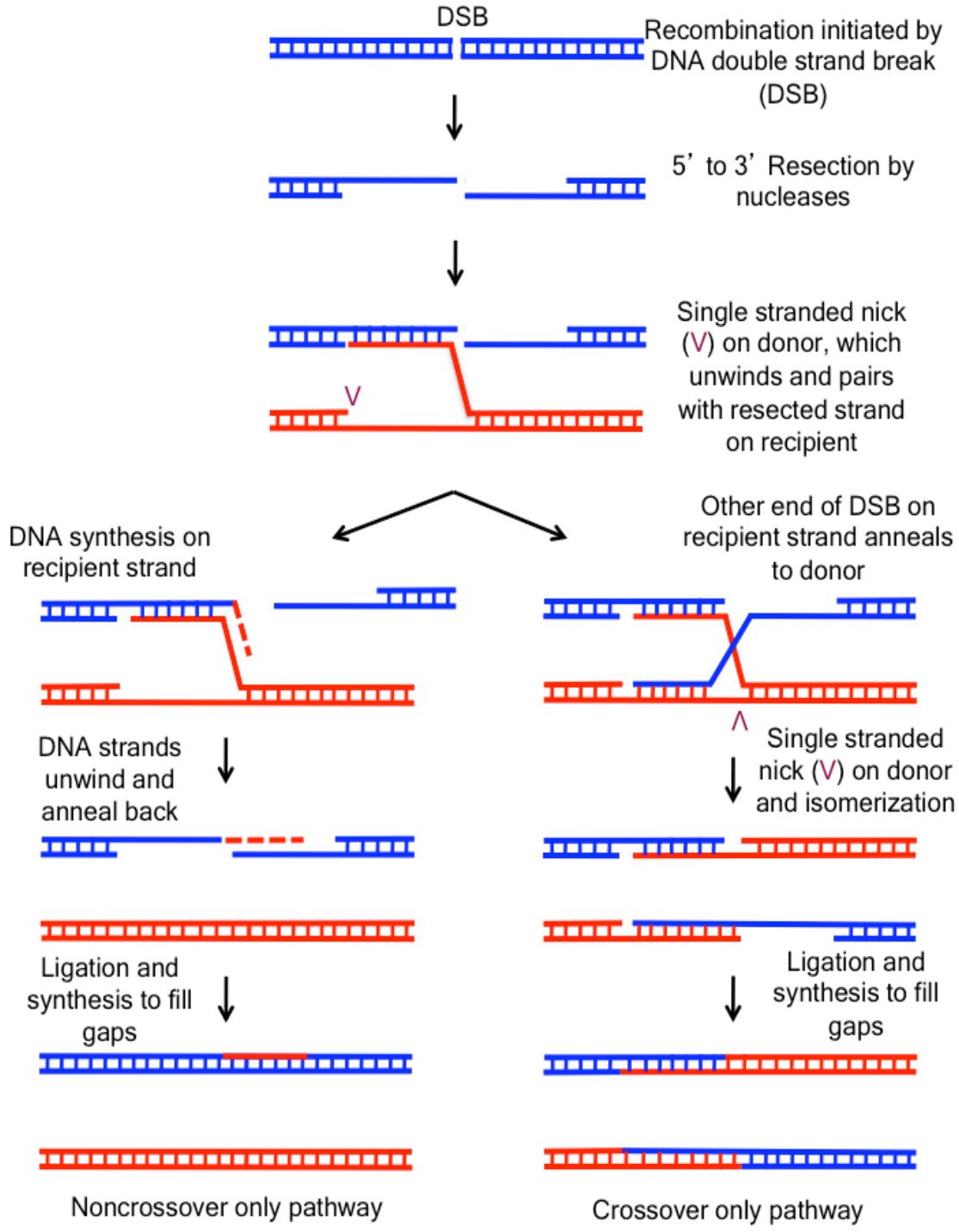

Figure 1-6 Resnick model of recombination. The various steps in these pathways are mentioned in text alongside the figures.

1.1.2 The Double Strand Break Repair model of homologous recombination

The current favoured model of homologous recombination was formally proposed by Szostak et al. in 1983(Figure 1-7). This model was based on some key observations from the study of recombination between plasmid and chromosomal sequences made in plasmid transformation assays by Orr-Weaver et al. (1981) and also observations from genetic studies by Resnick and Martin (1976). Introducing a DSB into a plasmid via restriction digestion in a region of homology with the chromosome improved transformation efficiency by 3000 fold. Cuts made elsewhere on the plasmid had no such effect, and the structure of integrated plasmids was identical for both cut and intact plasmids (Orr-Weaver et al. 1981). Furthermore, a plasmid with two regions of homology to the yeast genome could integrate at either locus when an intact plasmid was used, but cutting the plasmid at one of the loci would specifically target the plasmid to that locus (Orr-Weaver et al. 1981). Taken together, these observations showed that DNA DSB ends are recombinogenic and that these ends directly interact with homologous sequences. Finally Orr-Weaver et al. (1981) also showed that if a gapped plasmid was used for transformation, that gap is fully repaired in the integrated plasmid using sequences from the chromosome. This transfer of genetic information from one DNA duplex to another could result in gene conversion. Subsequent studies of plasmid transformation with an autonomously replicating plasmid showed similar occurrences of integrated plasmids which correspond to COs and unintegrated plasmids which correspond to NCOs (Orr-Weaver and Szostak. 1983). This demonstrated that gene conversions were frequently associated with COs. When a *his3* strain was transformed with a plasmid gapped at *his3*, occasional *HIS3* transformants were obtained. These could arise from transfer of genetic information from the plasmid to the chromosome, thereby demonstrating that gap repair is associated with formation of heteroduplex DNA in adjacent regions (Orr-Weaver and Szostak. 1983). Since this model also fulfilled the observations made in meiotic recombination in yeast, this mechanism was also proposed to act during meiosis (Sun et al. 1989, Cao et al. 1990, Zenvirth et al. 1992, Gilbertson and Stahl. 1994, Schwacha and Kleckner 1995, Allers and Lichten 2001a).

The Double Strand Break Repair (DSBR) model as originally proposed has the following features: 1) initiation of recombination with the formation of a double strand break on the recipient chromatid; 2) the DSB is then enlarged to a gap and acted upon by exonucleases to form 3' single stranded termini; 3) one of these strands then invades an intact homologous duplex, displacing a D-loop; 4) synthesis is primed from the invading strand, which also enlarges the D-loop; 5) eventually, the D-loop enlarges to expose complementary sequences to the other end of the DSB, and these strands also anneal and prime synthesis from the other 3' end of the DSB, thus forming two regions of heteroduplex DNA; 6) once synthesis has sufficiently progressed, branch migration and ligation result

in the formation of two adjacent Holliday junctions with symmetric heteroduplex DNA; 7) resolution of the two Holliday junctions in the same sense (cutting both inner or both outer strands) results in NCOs, while resolution in opposite sense (one inner, one outer strand) results in COs (Figure 1-7).

Subsequent studies of meiotic recombination in yeast have confirmed features of the DSBR model. Sun et al. (1989) demonstrated the presence of DSBs in the promoter region of the *ARG4* gene during meiosis. Cao et al. (1990) created an artificial meiotic reciprocal recombination hotspot by inserting a 2.8Kb fragment of the *LEU2* gene adjacent to *HIS4*, and they were also able to identify discrete DNA bands, obtained by digestion of DNA of synchronously sporulating cultures of SK1 yeast, which correspond to DSBs. These DSBs were also reported to be dependent on the function meiosis-specific genes such as *SPO11*; these will be discussed in detail in a latter section. Zenvirth et al. (1992) used pulsed-field gels of whole chromosomes in DSB repair deficient *rad50S* mutants of *S. cerevisiae* to show the presence of multiple DSBs, some of which coincided with known hot-spots" for meiotic recombination. Also, Gilbertson and Stahl (1994) showed that DSBs arose in meiosis even in the absence of corresponding homologous sequences on the other chromosome. These studies therefore showed that that DSBs were the initiating events of meiotic recombination, which then catalyze interhomologue interactions between DNA strands. Schwacha and Kleckner (1995) used the same chromosomal recombination reporter system, the *HIS4*-*LEU2* interval on chromosome III of yeast, and 2-D gel electrophoresis to identify branched double Holliday junction (dHJ) joint molecules as intermediates of meiotic recombination. Allers and Lichten (2001b) used a recombination reporter consisting of a defined 3.5 kb interval of *URA3* and *ARG4* sequences inserted at *LEU2* and *HIS4* on two homologue. The *HIS4* insert was marked with a 36 bp palindrome, which is poorly corrected by mismatch repair and thus allows the detection of heteroduplex DNA. Joint Molecules (JMs) formed during meiosis in synchronous sporulating cultures were analyzed by 2-D native/denaturing gels, and it was found that a population of these JMs contained heteroduplex DNA at the site of the palindrome, thereby fulfilling another central prediction of the DSBR model. Finally, Hunter and Kleckner (2001) identified yet another intermediate in meiotic recombination, an asymmetric joint molecule that was postulated to represent the strand invasion intermediate (SEI). However, interhomologue alignment and formation of co-axial bridges between homologous chromosomes in meiosis occurs prior to detectable SEIs, and SEIs themselves appear to precursors of dHJs and subsequently COs only, and not NCOs. Therefore, it is unlikely that these SEIs represent the true nascent strand invasion event in recombination. They may represent a more stabilized intermediate after the initial strand invasion.

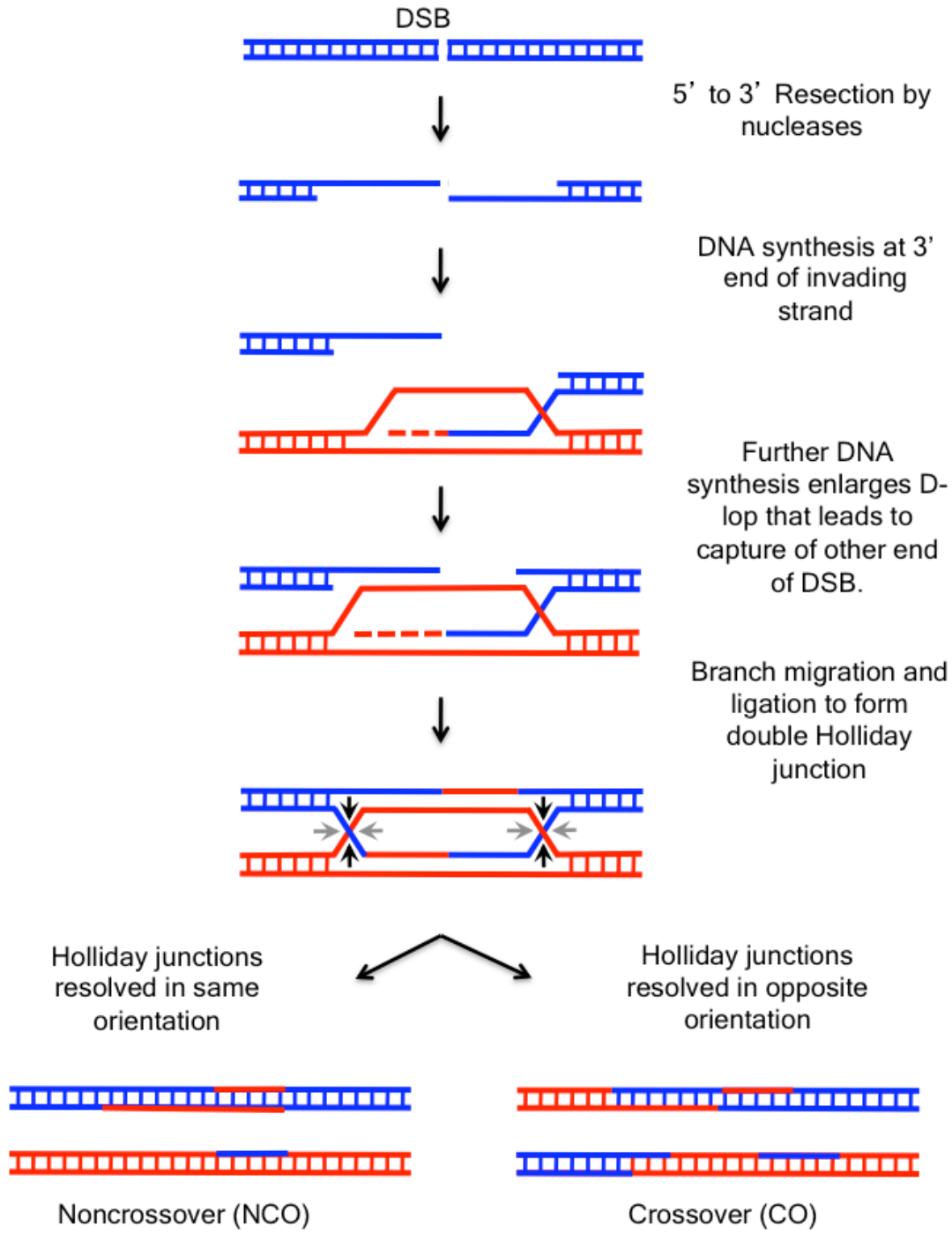

Figure 1-7 The Double Strand Break Repair (DSBR) model of recombination as proposed by Szostak, Orr-Weaver, Rothstein and Stahl. . The various steps in these pathways are mentioned in text alongside the figures.

1.1.3 The Synthesis Dependent Strand Annealing model of homologous recombination

One of the central tenets of the DSBR model is the formation of both COs and NCOs from the alternate resolution of a common dHJ intermediate (Szostak et al. 1983)(Figure 1-7). This would suggest that in all recombination events, COs and NCOs had an equal chance of forming from the common intermediate. In the study of yeast mating type switching, which is initiated by a DSB, Haber et al. (1981) showed that intrachromosomal recombination mostly forms NCOs, and reciprocal CO events form at a much lower rate. Thus, the recombination event in mating type switching greatly favours NCOs over COs. Nassif et al. (1994) also observed a lack of crossing over in P element excision mediated gap repair in *Drosophila*, and they were the first to formally propose the Synthesis Dependent Strand Annealing (SDSA) model (Figure 1-8). The early steps in their model are identical to the DSBR model up to the point of resection. The SDSA model then proposes independent strand invasion by both 3'OH termini to create local D-loops. The newly synthesized DNA is then rapidly displaced from the donor strand, and the D-loop does not enlarge and anneal with ssDNA (single stranded DNA) on the recipient DNA duplex as predicted by the DSBR model. Once synthesis has moved past the break site, the newly synthesized strands anneal back together and any excess DNA that is unpaired is subsequently removed. The important features of this model are that it allows only NCOs to form and DNA synthesis is conservative (newly synthesized DNA is only on one chromatid) and not semi-conservative as in DSBR (where newly synthesized DNA ends up on both chromatids). Finally, only the recipient strand contains heteroduplex DNA in this model. The latter prediction was confirmed by studies of yeast mating type switching, which is initiated by a DSB at *MAT* locus by HO. During mating type switching, the *MAT* locus was almost always the recipient of synthesized DNA and very rarely the donor, and heteroduplex DNA was also seen only at the *MAT* locus which is the recipient chromatid (McGill et al. 1989, Ray et al. 1991). Current versions of the SDSA model usually suggest strand invasion by only one DSB end, which is used to prime synthesis past the site of DSB. The newly synthesized strand then anneals back to the other end of the DSB and the other strand then synthesized from this strand (Figure 1-8) (Pâques and Haber. 1999, Mazón et al. 2010).

Further evidence for existence of repair by SDSA came from heteroduplex patterns in meiotic recombination. Studies into the location of heteroduplex DNA relative to the break site were made at *ARG4* and *HIS4* recombination hotspots and it was found that in most cases the heteroduplex is restricted to only one side of the DSB, referred to as *cis* heteroduplex (Gilbertson and Stahl. 1996, Porter et al. 1993, Merker et al. 2003). This is in line with predictions made by the SDSA model, as the DSBR model predicts heteroduplex to form on both sides of the DSB. However, Gilbertson and Stahl (1996) also found a class of tetrads with

heteroduplex on both sides of the DSB on the same duplex, this suggested the presence of still another NCO pathway; this is discussed in the following section. Allers and Lichten (2001a) showed that there was a difference in the timing of appearance of NCOs and CO in synchronous meiotic cultures of yeast. NCOs appeared around the same time as dHJ intermediates, while COs appear around half an hour later. This result is incompatible with NCOs and COs being formed by alternate resolution of a common dHJ intermediate as predicted by DSBR, in which case both should appear simultaneously. In addition, in mutants lacking a meiotic transcription factor Ndt80, dHJs accumulate and only CO formation is affected (Allers and Lichten. 2001a). Sourirajan and Lichten (2008) further expanded on this by showing that induction of the polo like kinase Cdc5 caused dHJs to be resolved but only to form COs. In wild-type meiosis, Cdc5 expression is activated by Ndt80. Thus, these data suggest that Ndt80 and its downstream target Cdc5 control a CO-exclusive pathway via the formation of dHJs (Sourirajan and Lichten 2008, Matos et al. 2011). Merker et al. (2003) also showed that at the *HIS4* locus, unidirectional heteroduplex (heteroduplex on only one chromatid) was mostly associated with NCOs, while bi-directional heteroduplex pattern (heteroduplex on both chromatids) was mostly associated with COs. This is consistent with DSBR in meiosis mostly forming COs and SDSA forming NCOs. Finally, McMahill et al. (2007) showed, from genetic analysis of random spores, a class of NCOs where two flanking heterozygous markers were gene converted without conversion of an intervening heterology. Such a pattern of heteroduplex DNA cab be explained with a model invoking discontinuous DNA synthesis followed strand annealing, and this is therefore an SDSA mechanism. However, such discontinuous tracts of gene conversion can also arise from defects in the mismatch repair mechanism, and the observations in McMahill et al. (2007) do not rule out this possibility.

1.1.4 The double Holliday junction dissolution model of homologous recombination

A critical feature of SDSA is that the heteroduplex DNA is relegated to only one side of the DSB on a DNA duplex, and donated DNA sequence are present on one strand of the recipient chromosome. This is referred to as a *cis* heteroduplex. However, Gilbertson and Stahl (1996) found a class of tetrads where heteroduplex DNA spanned markers on both sides of an *ARG4* DSB on the same DNA duplex, and donated DNA sequence were also on two sides on opposite strands of the same recipient DNA duplex. This is referred to as a trans heteroduplex. Nasmyth (1982) had proposed an alternate mechanism for mating type switching, which would only give NCOs, that involved topoisomerase unwinding of the dHJ rather than resolution and then subsequent replication. Gilbertson and Stahl (1996) noted that such NCOs would contain a trans heteroduplex pattern. Studies using *in vitro* dHJ substrates by Wu and Hickson (2003) showed that the concerted action of the BLM helicase and human Topoisomerase IIIα

could unwind such substrates into two equally sized molecules, in a process they called dHJ dissolution (Figure 1-8). Plank et al. (2006) additionally demonstrated that this dissolution activity was unique to topoisomerase IIIα. The dHJ dissolution activity is further promoted by BLAP75/RMI1 (Wu et al. 2006, Raynard et al. 2006. Raynard et al. 2008). Raynard et al. (2008) and Cejka et al. (2010) demonstrated *in vitro* that RmiI does not affect the initial HJ migration in dissolution, but stimulates the decatenation of the intercrossed donor and recipient DNA strands. *in vivo* evidence for dHJ dissolution was provided by Bzymek et al. (2010), who showed that in mitotic cells, interhomologue dHJs accumulate to a greater degree in mutants lacking the Sgs1 helicase, which is the yeast orthologue of BLM. Further, Dayani et al. (2011) showed that meiotic dHJs, which accumulate in *ndt80* mutants, were dissolved by Sgs1 to mostly form NCOs upon return to mitotic growth by transfer into rich media. These data strongly suggest that dissolution is the common fate for dHJs in mitotic cells. In meiosis, Martini et al. (2011) determined the pathways of CO and NCO formation by heteroduplex patterns in an *msh2* hybrid yeast strain defective for mismatch repair, which allowed preservation of highly dense heteroduplex patterns. Based on the frequencies of *cis* or *trans* heteroduplex patterns, Martini et al. (2011) concluded that SDSA and dHJ dissolution had roughly equal contributions to NCO formation in meiosis.

1.1.5 The early D-loop cleavage model of homologous recombination

In the fission yeast *Schizosaccharomyces pombe*, the Mus81-EmeI flap endonuclease has been shown to be responsible for formation of the majority of COs (Boddy et al. 2001, Smith et al. 2003, Hyppa and Smith. 2010). However, *in vitro* analysis showed that recombinant fission yeast Mus81-Eme1 poorly cleaved intact HJs (Whitby et al 2003), which was also true for budding yeast orthologue Mus81-Mms4 (Doe et al. 2002). Instead, Mus81-EmeI was better able to cleave D-loop substrates and nicked HJs (Osman et al. 2003). Thus, to reconcile this *in vivo* and *in vitro* data, Osman et al. (2003) proposed a new model for the generation of COs without a fully ligated HJ intermediate (Figure 1-8). Once again, the initial steps of this model are common to DSBR up to the capture of the 2nd end of the DSB by the D-loop. This intermediate however is not allowed to branch migrate and form a fully ligated dHJ. This intermediate is instead cleaved by Mus81-EmeI in precise orientation to only form COs (Figure 1-8).

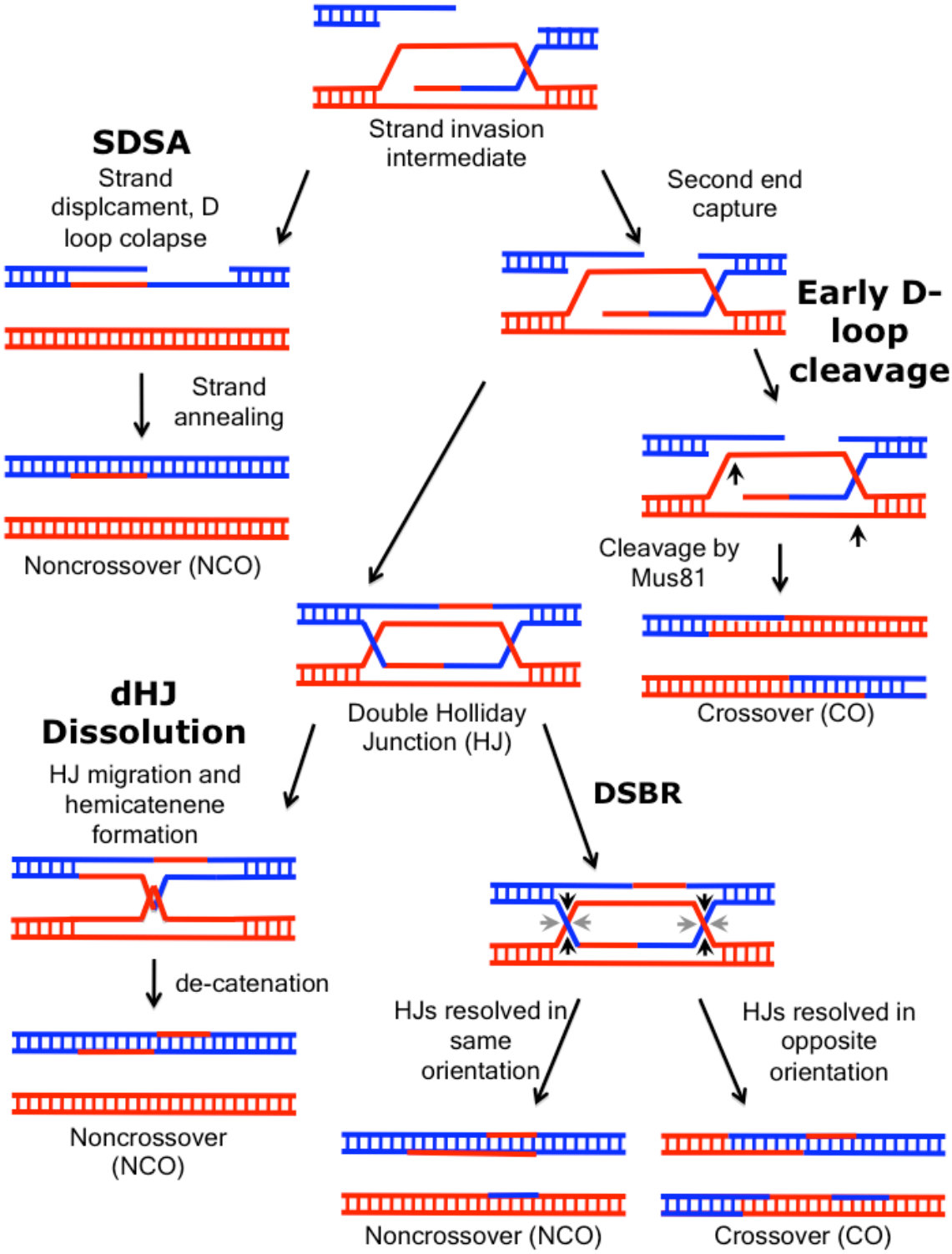

Figure 1-8 Current models of homologous recombination. All of these models begin with a DSD in DNA that is procressed by 5' to 3' exonucleolytic processing to five 3'OH ssDNA. From thereon in, different HR models are indicated in bold, at the point of divergence for their unique features. The various steps in these pathways are mentioned in text alongside the figures.

1.1.6 Relative contributions of different homologous recombination pathways in mitosis and meiosis as revealed by heteroduplex DNA analysis

As discussed above, there are four major models of HR to repair DSBs, DSBR; SDSA; dHJ dissolution and early D-loop cleavage. One of the key experimentally observable differences between these models is the pattern of heteroduplex DNA formed by each of them (Figure 1-8). Analysis of heteroduplex DNA patterns is a very powerful tool that has allowed us to understand the differing contributions of different HR pathways in meiosis and mitosis. Early studies into heteroduplex patterns were performed by genetic analysis of tetrads (Gilbertson and Stahl 1996, Porter et al. 1993, Merker et al. 2003). These gave initial clues the existence of different repair pathways in meiotic recombination. However, these studies were limited to mismatches that show an observable phenotype. Newer studies have utilized DNA sequencing methods, which does not require mismatches in heteroduplex DNA to generate a phenotype. Mitchel et al. (2010) and Mitchel et al. (2013) used a transformation-based gap-repair system in mitotically growing mismatch repair defective *mlh1* yeast to identify the pathways acting in recombination. They concluded that 90% of all repair events produced NCOs, and 90% of these NCOs were consistent with SDSA. A similar study was made in meiotic cells made by Martini et al. (2011), in a *msh2* hybrid yeast strain defective for mismatch repair, thereby allowing for the preservation of highly dense heteroduplex patterns. They showed that in meiosis, about half the recombinants were NCO, and SDSA and dHJ dissolution had roughly equal contributions to NCO formation. Patterns of heteroduplex in COs were quite complex, but could be reconciled with DSBR by invoking of multiple rounds of strand invasion and template switching. No meiotic COs were seen by Martini et al. (2011) that showed heteroduplex consistent with early D-loop cleavage. However, mutants of *mus81* or its partner *mms4* have very mild defects in meiotic CO formation in the budding yeast *Saccharomyces cerevisiae*, (De Muyt et al. 2012, Zakharyevich et al. 2012) and thus Mus81 dependent early D-loop cleavage model may form very few COs in this organism.

The studies Martini et al. (2011), Mitchel et al. (2010) and Mitchel et al. (2013) have been all been performed in mismatch repair deficient mutants. *msh2* mutants in *S. cerevisiae* are still competent for short patch mismatch repair of <12 nucleotides (Coïc et al. 2000). Such short patch mismatch repair may generate heteroduplex patterns, which could be misinterpreted as the consequence of different recombination pathways. However, earlier studies by Porter et al. (1993), Allers and Lichten (2001b) and Merker et al. 2003 used palindromic insertions which are poorly recognized by the mismatch repair complex and they reported similar conclusions regarding COs and NCOs arising from different homologous recombination pathways. Therefore it is unlikely that the conclusions from DNA sequence analysis in mismatch repair deficient

hybrid strains by Martini et al. (2011), Mitchel et al. (2010) and Mitchel et al. 2013 are artifacts of short patch mismatch repair.

In addition to looking at heteroduplex patterns, Terasawa et al. (2007) examined DNA synthesis patterns in meiotic recombination by looking at BrdU incorporation on meiotic recombination products. They showed that newly synthesized DNA spans the gap in NCOs, as predicted by the SDSA model (Figure 1-8), where the invading strand is ejected after DNA synthesis goes past the DSB end, and the resected DNA from the other DSB end is filled in. Conversely, newly synthesized DNA in COs was found to be only on one side of the DSB, and this is also consistent with the predictions of DSBR, where resolution of a dHJ to form COs splits the newly synthesized DNA between the recipient and donor strand, such that each of them have newly synthesized DNA on opposite sides of the DSB. This is further evidence that different pathways of recombination form NCOs and COs in meiosis, as suggested by heteroduplex studies.

1.2 Alternate DSB repair pathways

Before we elaborate on the different roles of HR between mitosis and meiosis, we shall very briefly discuss the other major alternate DSB repair pathways. This section is not meant to give a detailed elucidation on these processes, references are listed at the end of each paragraph.

Non Homologous End Joining (NHEJ) is a DSB repair pathway where both ends of the break are first bound by the Ku70/Ku80 heterodimer, which then recruits the catalytic subunit of the DNA dependent protein kinase DNA-PKcs. The DNA ends can be processed if necessary. Nucleases such as Artemis can chew back ends; or DNA polymerases such as Polμ or Polλ can fill in ends; to create compatible ends. The ends are finally ligated back by the ligation complex, which consists of DNA ligase IV, X-ray cross-complementation group 4 (XRCC4) and Xrcc4 like factor (XLF)/Cernunnos. NHEJ is reviewed in Pâques and Haber (1999) and by Lieber (2010). NHEJ is repressed in MATa/MATα diploids, which are competent for meiosis (Valencia et al. 2001). Therefore this is little flux through this pathway during the repair of VDE DSBs during meiosis.

Single strand annealing (SSA) is another alternate repair pathway that can repair DSBs that occur between two flanking homologous regions. In SSA, the DNA DSB ends are similarly resected as in HR, but such resection continues until the flanking homologous sequences are exposed, these then reanneal. In yeast, SSA is nearly 100% efficient when homologous regions flanking the DSB are at least 415 bps, and even with 60 bps of homology, efficiency of SSA is about 5% (Sugawara et al. 2000). Repair by SSA is also efficient even if the repeats are separated by as much as 15 kb (Ivanov et al. 1996). SSA is reviewed in Pâques and Haber (1999) and by Pastink et al. (2001).

Break induced replication (BIR) is the final major alternate repair pathway. The initial steps of BIR are again identical to HR, up to strand invasion by a single stranded DSB end. However, unlike HR, during BIR, the invading strand is then extended by DNA synthesis to the end of the chromosome, with the displaced intact DNA strand forming a migrating d-loop (Saini et al. 2013). This structure is unstable and can undergo dissociation and reinvasion events during the extended synthesis. DNA synthesis in BIR is conservative; and lagging strand synthesis to restore the DNA duplex follows leading strand synthesis and is templated from the newly synthesized leading strand (Saini et al. 2013). Since the second end of the DSB is not involved in this repair process, BIR is believed to occur when one of the ends of a DSB is lost, leaving only one end to repair from. The end result of BIR resembles a non-reciprocal crossover. BIR is reviewed by Pâques and Haber (1999) and by Llorente et al. (2008).

1.3 Homologous recombination plays distinct roles during mitosis and meiosis

HR is required for the repair of DNA DSBs in mitotic cells. These may arise spontaneously due to environmental insults, or during replication, or as part of programmed DNA recombination events such as mating type switching in yeast. However, mitotic COs can result in loss of heterozygosity (LOH) in the entire region distal to the CO, if the recombinant sister chromatids segregate towards opposite poles. Such events have the potential to aggregate deleterious recessive alleles, which is commonly seen in many cancers (Gallie and Worton. 1986) Also, COs between dispersed repeats in the genome can cause chromosomal rearrangements, which could also be potentially deleterious (Sasaki et al. 2010). In human populations, mutations in the BLM helicase increase the level of COs between sister chromatids, referred to as sister chromatid exchange (Ray and German. 1984, Ray et al. 1987). BLM mutation causes a condition known as Bloom's Syndrome, which is characterized pre-natal and post-natal growth retardation, immunodeficiency and high pre disposition to cancer, which are indicative of genome instability (Watt and Hickson. 1996). Similarly, mutations in the human FancM helicase, along with other FA genes, lead to the condition known as Fanconi Anemia, the main features of which are aplastic anemia in childhood, multiple congenital abnormalities, susceptibility to leukemia and other cancers, and cellular hypersensitivity to interstrand DNA cross-linking agents, such as cisplatin and other bifunctional alkylating agents. All of these phenotypes again point towards genome instability and repair defects in these patients (D'Andrea. 2010).

On the other hand, HR in meiosis is required to generate COs between homologous chromosomes to physically connect them for faithful segregation in meiosis I (Figure 1-1). The presence of these

interhomologue contacts and the dis-concordant separation of sister chromatid arms and centromeres differentiates meiosis from mitosis in terms of chromosome morphogenesis. During S phase, when chromosomes are replicated in both mitotic and meiotic cells, a ring shaped complex called cohesin is established which pairs sister chromatids together (Sherwood et al. 2010). This pairing of sister chromatids allows their alignment on the metaphase plate and subsequent segregation (Bickel and Orr-Weaver. 1996). However, in meiotic cells, association between sister chromatids cannot contribute to alignment of homologous chromosomes during metaphase I, unless there has been an exchange of sister chromatid arms due to crossovers (COs) formed by HR (Figure 1-1). These COs create physical attachments between homologous chromosomes due to sister chromatid cohesion distal to the CO site (Buonomo et al. 2000). Defective homologous recombination causing a lack of COs leads to random segregation of chromosomes in meiosis (Klapholz et al. 1985, Dernburg et al. 1998, Sharif et al. 2002, Xu et al. 2003).

Therefore, during meiosis, every pair of homologous chromosome requires at least one CO event to ensure their correct segregation, and there are meiotic mechanisms that ensure this, such as non-random distribution of COs. From the very genetic analyses of COs, in model organism such as *Drosophilla melanogaster* (Stevens. 1936) and *Neurospora crassa* (Perkins. 1962), it was established that COs show positive interference, such that the probability of double COs in adjacent intervals in much lower than the product of frequencies of single COs in those intervals. Similarly, on a cytological level, the distribution of chiasmata in bivalents deviates from random and the frequency of non-exchange bivalents (i.e homologous chromosomes lacking COs) and multiple exchange bivalents (homologous chromosomes with multiple COs) is much lower than expected. This has been observed in many early microscopic studies in organisms including *Drosophila melanogaster, Primula sinensis*/Chinese Primrose, *Pisum sativum*/Gardem Pea, *Lilium longiflorum*/Easter lily, *Fritillaria imperialis*/Crown Imperial, *Campanula persicifolia*/ Peach-leaved Bellflower, *Matthiola incana* and *Tulipa australis* (reviewed in Haldane. 1931). The lack of bivalents without COs in meiosis is referred to as CO assurance. These mechanisms of CO interference and assurance thus ensure an even distribution of COs among homologous chromosomes. Finally, Martini et al. (2006) demonstrated an interesting phenomenon in yeast, where CO levels are maintained in meiosis at the expense of NCOs, despite the reduction of DSBs. This effect was referred to as CO homeostasis. CO homeostasis is also shown to occur in mouse, where the number of cytologically detected CO foci remain constant despite varying levels of DSBs (Cole et al. 2012). Thus, meiotic HR is regulated to ensure sufficient CO formation and distribution to enable the faithful segregation of homologous chromosomes.

The contrasting requirement of COs in meiotic versus mitotic HR is reflected in the regulation of HR in these respective cells. During HR in mitosis in the budding yeast *Saccharomyces cerevisiae*, which is arguably the best studied organism for this process and also the model system for this thesis, as many as 90% of mitotic DSBs are repaired to form NCOs (Bzymek et al. 2010, Pâques et al. 1998). Limited studies in *S pombe* and mammalian cells also reveal an excess of NCOs to COs during mitotic HR (Virgin et al. 2001, Stark and Jasin. 2003). Also, mitotic HR events such as mating type switching in budding yeast (Haber et al. 1981) and *Drosophila* P element excision mostly give rise to NCOs (Nassif et al. 1994). As previously mentioned, Mitchel et al. (2010) and Mitchel et al. (2013) reported that 91% of recombination events in a transformation based gap repair assay were NCOs.

Conversely, during meiosis, there is a substantial enrichment of COs in order to ensure faithful segregation of every homologue pair. Studies at the artificial meiotic recombination hot-spot *HIS4-LEU2* hotspot have determined the level of cumulative Spo11 DSBs to be at ~20% of chromosomes (Keeney and Kleckner. 1995), and half of these DSBs are repaired to give COs (De Muyt et al. 2012). Studies to map meiotic DSBs in *Saccharomyces cerevisiae* at a genome wide level have determined the total number of DSBs in each meiotic cell to be 140-170 (Buhler et al. 2007, Pan et al. 2011), while genome wide studies in hybrid yeast strains with a high degree of sequence polymorphisms have determined the total number of COs in meiosis to be around 90 (Mancera et al. 2008, Qi et al. 2009, Esberg et al. 2011). Therefore, more that ½ of the DSBs in meiosis in *Saccharomyces* cerevisiae are repaired to give COs. Martini et al. (2011) also reported 51% of meiotic recombination events detected in their hybrid yeast strain to be COs. In other model systems such as *Sordaria, C elegans* and *Drosophila*, the ratio of DSBs to CO is around 2-5:1 (Serrentino and Borde. 2012). In higher metazoans such as *Mus musculus* and plants such as *Arabidopsis*, there are 15-30 times more DSBs than COs in meiotic cells (Serrentino and Borde. 2012), but it is conceivable that this still represents a substantial enrichment of COs when compared to mitotic recombination in these organisms.

Thus, mitotic and meiotic HR differs significantly in the frequency of NCOs and COs (Figure 1-9). The various pathways of HR, expounded upon in the previous section, can lead to different CO or NCO outcomes. SDSA and dHJ dissolution are believed to be NCO only pathways, while early D-loop cleavage is supposed to only form COs. DSBR can theoretically lead to both CO and NCO outcomes, but it is shown to be regulated in meiosis to only form COs (Sourirajan and Lichten. 2008). Therefore, one can postulate that the differential regulation of HR in mitosis vs. meiosis regarding the NCO-CO distribution is mediated by controlling the flux of DSBs into these different pathways, which allow the cell to enrich for COs or NCOs.

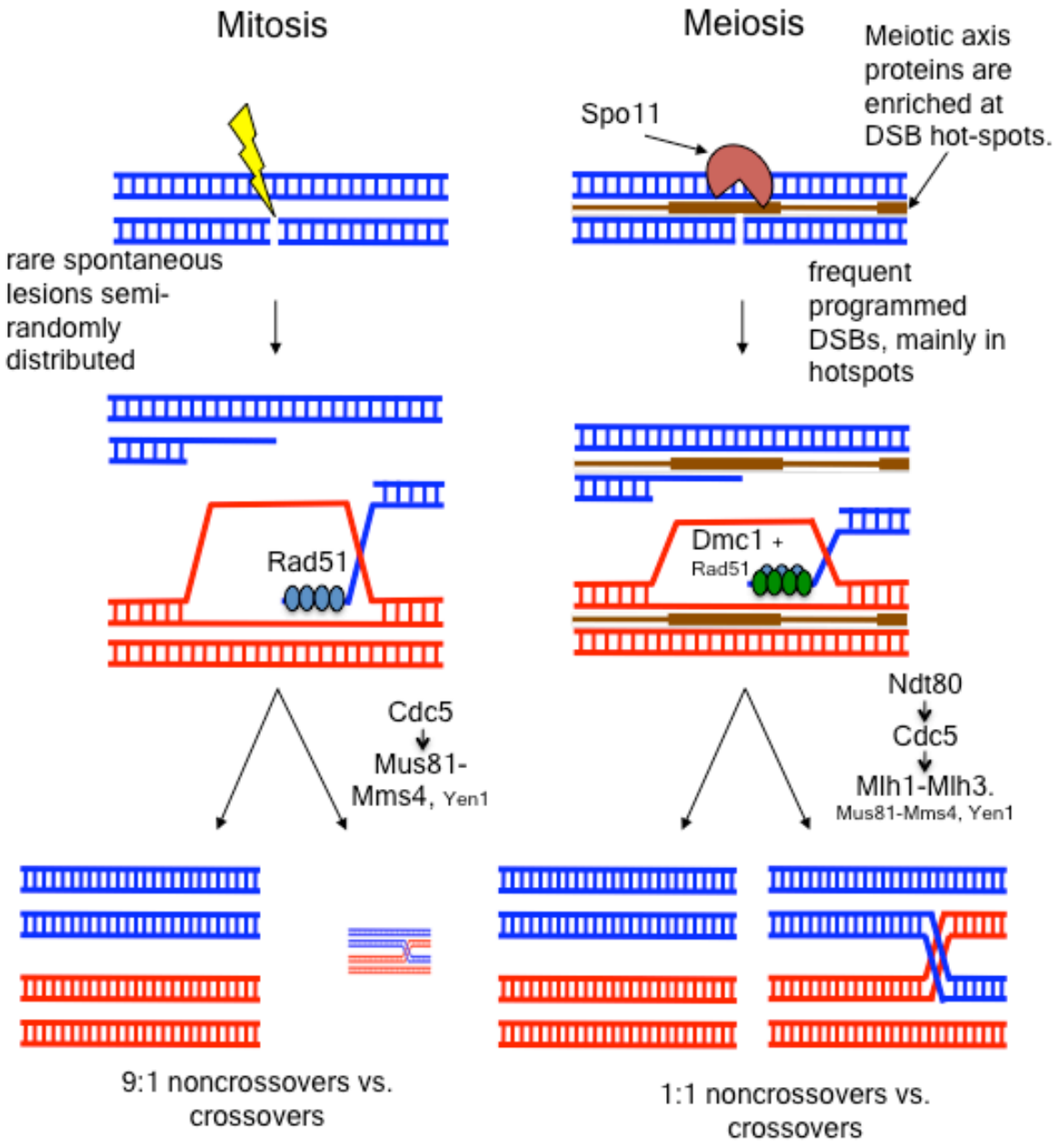

Figure 1-9 Homologous recombination has distinct roles in mitosis and meiosis, and this is also reflected in the molecular level. Firstly, the HR in mitosis repairs spontaneous lesions, while HR in meiosis repairs programmed DSBs made within the context of meiosis-specific axial proteins. Subsequently, different proteins are involved in HR repair during mitosis and meiosis. Finally, the outcome of HR is very different between mitosis and meiosis, with mitotic HR forming mostly NCOs, while meiotic HR enriching for COs.

1.4 DSBs in meiosis are in a unique local chromosome context as opposed to DSBs in mitosis

The primary goal of this thesis is to understand the basis of this differential regulation between HR in mitosis and HR in meiosis. We shall examine this in the context of two fundamental differences between mitotic and meiotic HR. The first major difference between mitotic and meiotic HR concerns the very DSBs that form the substrate for HR. DSBs in mitosis and meiosis are different with respect to their origin and local chromosome context, and it is very probable that the chromosome environment of the DSB can have profound effects on its repair. We shall examine this in the following sections in greater detail.

1.4.1 Mitotic DSBs are semi-random events whose formation is not dependent on chromosome context.

Mitotic DNA damage arising from replication has been long known to form at "common fragile sites", which are present in human genomes (Glover et al. 1984, Freudenreich. 2007, Ozeri-Galai et al. 2012), and these sites have also been identified in yeast (Lemoine et al. 2005). Additionally, another class of fragile sites, referred to as early replicating fragile sites, accumulate due to replication or mis-targeted DNA damage by activation-induced cytidine deaminase (AID), which induces class switching in lymphocytes (Barlow et al. 2013). Studies in yeast have shown such DNA damage can arise due to changes in stoichiometry of replicative polymerases (Lemoine et al. 2008), or due to sequences that are difficult to replicate such as palindromes or spaced inverted repeats (Casper et al. 2009). Thus, although replication induced mitotic DSBs cannot be described as being entirely random, these events can still be considered accidental, as they aren't part of a cellular programme and haven't been shown to fulfill any physiological function. DNA DSBs in mitosis can also arise from environmental insults such as radiation; and it is again conceivable that there might be loci that are more sensitive to damage than others.

Lee et al. (2009) have recently mapped mitotic COs on a 120 Kb region of chromosome V in *Saccharomyces cerevisiae*, and their analysis indicates that the distribution of these COs significantly deviates from a random distribution. Therefore, this may be further evidence that mitotic DSBs, which give rise to these COs, are not randomly distributed. But it can still be argued that these mitotic DSBs are accidental and serve no physiological function.

Finally, there are mitotic DSBs that are part of physiological processes. Homothallic mating type switching in *S. cerevisiae* is initiated with a programmed DSB at *MAT* by HO (Haber. 2012), and V(D)J recombination during immunoglobin gene rearrangement is initiated by DSBs that are formed by RAG1 (Schatz and Ji. 2011). However, both HO and RAG1 are

targeted in a sequence specific manner, and in the case of HO, moving the recognition sequence is sufficient to target the DSB elsewhere in the genome (Nickoloff et al. 1986, Kolodkin et al. 1986). Thus, in general, mitotic DBSs do not form in a manner that is dependent on the chromosomal context, and there are no reported chromatin modifications that precede the formation of such DSBs.

1.4.2 Meiotic DSBs are formed by Spo11 along with its accessory factors

DSBs are formed in meiosis as part of the cellular programme, by the Spo11 protein, which was identified in screen for temperature- sensitive mutations that eliminated ascospore formation (Esposito and Esposito. 1969, Esposito et al. 1972, Esposito and Esposito. 1974). It must be noted that in most currently used laboratory strain of *S. cerevisiae*, *spo11* mutants have limited defects in spore formation, but they show whole scale chromosome non-disjunction and generate aneuploid inviable spores. *SPO11* was shown to be required for both inter-chromosomal recombination (Klapholz et al. 1985) and intra-chromosomal recombination (Wagstaff et al. 1985), and Cao et al. (1990) showed that *spo11* mutants had no DSBs. Keeney and Kleckner (1995), using a mutant of the Rad50 protein that is deficient in the processing of DSBs, noted that the 5' end of DSBs were covalently linked to protein and de Massy et al. (1995) also noted that DNA strands ending with 5' end of the DSB had an altered migration compared to strands ending at the 3' end. Keeney et al. (1997) purified these complexes and identified the protein as Spo11. The Spo11 protein contains homology to the A subunit of a type II topoisomerase from the archaebacteria *Sulfolobus shibatae* and changing the predicted tyrosine residue to phenylalanine abolished Spo11 function. (Bergerat et al. 1997). Thus, these studies were strong indicators that Spo11 is the catalytic activity for DSB formation in meiosis. This is done in a manner that is mechanistically analogous manner to type II topoisomerases, whereby Spo11 forms covalent linkages between the 5' strand phosphate and its catalytic tyrosine residue, to form a 5' phosphotyrosyl protein-DNA intermediate.

In addition to Spo11, DSB formation in meiosis requires a number of accessory factors, mostly identified from studies in budding yeast. These accessory factors include Rec114, Mei4 and Mer2, which together form the RMM sub-complex (Li et al. 2006, Maleki et al. 2007, Sasanuma et al. 2008) and for the timely recruitment of Spo11 to DSB hot-spots (Prieler et al. 2005). Mer2 is phosphorylated by the cyclin dependent kinase Cdc28, which is the primary cell cycle regulator in *S. cerevisiae.* Thus, Mer2 couples DSB formation to the cell cycle (Henderson et al. 2006). Mer2 is also phosphorylated by the DDK kinase Cdc7 (Sasanuma et al. 2008), which controls the initiation of DSB formation after meiotic DNA replication (Blitzblau and Hochwagen. 2013). Additional roles of the RMM sub-complex will be elaborated in a future section. Other proteins required for DSB formation are Ski8, Rec102 and Rec104. Ski8 directly

interacts with Spo11 and is thought to play a role in Spo11 dimerization and recruiting other accessory proteins to the DSB forming pre initiation complex (Arora et al. 2004, Maleki et al. 2007). Rec102 and Rec104 require Ski8 for their recruitment to chromosomes (Kee et al. 2004) and are believed to connect the RMM sub-complex to Spo11 by interacting with Mei4 and Rec114 (Maleki et al. 2007). Finally, Mer1 and Nam8/Mre2 are RNA splicing factors that are required for meiosis-specific splicing of the *MER2* transcript (Engebrecht et al. 1991, Nandabalan and Roeder. 1995, Ogawa et al. 1995, Nakagawa and Ogawa. 1997)

Once Spo11 forms DSBs in meiosis, the DSB ends are then bound by a complex of Mre11-Rad50-Xrs2 (MRX), in association with Sae2/Com1 (Krogh and Symington. 2004). The MRX complex, in association with Sae2, removes the covalently bound Spo11 from the DNA end as a Spo11-oligonucleotide complex, and in mutants like *rad50S*, *sae2Δ* or *mre11-58S*, Spo11 remains covalently attached to the 5′-strand termini of DSBs and thus these DSBs remain unrepaired (Alani et al. 1990, Keeney and Kleckner. 1995, Tsubouchi and Ogawa. 1998). The removal of the Spo11-oligo from the DSB ends then allows the initiation of 5' to 3' resection of DNA from the DSB and subsequent repair by HR (reviewed in Mimitou and Symington. 2009).

1.4.3 Meiotic DSBs are non-randomly distributed in the genome and accumulate in "hot-spots"

Meiotic DSBs are the initiating events of HR in meiosis and have been best studied in the budding yeast *Saccharomyces cerevisiae*, including cartographic studies at a single nucleotide resolution by sequencing Spo11 associated oligonucleotides (Pan et al. 2011). This builds on earlier studies of DSB mapping, which were initially made for chromosome III by Southern blotting (Baudat and Nicolas. 1997) and subsequently at the genomic level by using microarrays (Gerton et al. 2000, Buhler et al. 2007, Blitzblau et al. 2007). These studies reveal that Spo11 DSBs are non-randomly distributed in the genome; they tend to cluster at sites referred to as "hot-spots". Recently, meiotic DSBs have been also mapped at a genome wide scale in mouse (*Mus musculus)* to a 200 nt (nucleotide) resolution. These DSBs also show a non-random distribution in the genome, and similarly concentrate in hot-spots (Smagulova et al. 2011). In the course of this introduction, I shall use the terms recombination or DSB hot-spot, and this can be arbitrarily defined as a specific site on the genome where the probability of DSB formation and thus meiotic recombination is 100 to 1000 times greater than elsewhere in the genome (Baudat and Nicolas. 1997, Gerton et al. 2000, Buhler et al. 2007, Blitzblau et al. 2007, Pan et al. 2011, Smagulova et al. 2011). Similarly, the term "cold-spot" will be used to refer to genomic sites, which show no such enrichment of meiotic DSB formation. On the other hand, I will also refer to "DSB hot regions" and 'DSB cold regions", to signify the larger domains

in the genome which are respectively enriched or suppressed for overall meiotic DSB formation.

1.4.4 Meiotic DSB formation by Spo11 in budding yeast is dependent on chromosome context rather than primary sequence

The mechanism underlying the specification of these DSB hot-spots has been long studied. Early studies into this considered the possibility of sequence specific targeting. One of the earliest known recombination hot-spots in yeast was reported on a plasmid containing the promoter region of *ARG4* (Nicolas et al. 1989). de Massy and Nicolas (1993) replaced the sequences around this DSB site, but this did not affect DSB formation. Goyon and Lichten (1993) moved the *ARG4* promoter sequences to the *MAT* locus, this insert was however not cut during meiosis. Wu and Lichten (1995) and Borde et al. (1999) further showed that identical recombination reporters containing *URA3* and *leu2* or *arg4* sequences would show different recombination frequencies and DSB levels when inserted at different locations in the genome. Thus, these early studies indicated that DSB frequency is not determined by DNA sequence; rather it is the chromosomal context that determines hot-spot activity. Further evidence that hot-spots are determined more in terms of chromosome context than primary DNA sequence came from experiments with sequence specific targeting of Spo11. Robine et al. (2007) used a Gal4-DNA binding domain-Spo11 fusion protein to specifically target Spo11 to Gal4 binding sites on the genome, but only a subset of these sites were cleaved by Spo11. Similar to this, Fukuda et al. (2008) inserted Gal4 binding sequences (UAS sites) at known hot-spots and cold-spots, but despite the fact that the Gal4BD-Spo11 fusion protein bound efficiently at all loci, DSBs were made only in hot-spots. Finally, in DSB hot-spots as mapped by Pan et al. (2011), the specific break site still displays a distribution with a median width of ~189 bps. Thus even within a hot-spot there is no specific sequence that Spo11 targets. However, it ought to be noted that there may be some loose preferences for Spo11 in terms of DNA sequence, as hot-spots tend to be mostly AT rich. Also, within a hot-spot, Spo11 has certain preferences of nucleotide composition at the point of cleavage and also in bases around the cleavage site (Murakami and Nicolas. 2009, Pan et al. 2011).

1.4.5 Meiotic DSBs in many mammals have primary sequence preference specified by the histone methyl transferase Prdm9

In contrast to yeast meiosis, recent studies in mice, chimpanzees and humans have implicated a unique meiosis-specific methyl-transferase Prdm9, which contains multiple DNA binding zinc finger motifs, in specifying meiotic recombination hot-spots in an allele specific manner (Baudat et al. 2010, Parvanov et al. 2010 and Myers et al. 2010). The primary difference between different Prdm9 alleles is the DNA binding specificity of their zinc fingers. Different Prdm9 alleles bind different

sequence motifs, and these DNA sequence motifs were shown to be directly predictive of hot-spot usage in mice (Grey et al. 2011). Grey et al. (2011) also showed that the Prdm9 bound its consensus motif at the center of three hot-spots and that mutation in this sequence decreased Prdm9 binding and hot-spot activity. In a genome wide DSB mapping study in mouse, Smagulova et al. (2011) found that 73% of hot-spots have the predicted binding site of the corresponding Prdm9 allele in their center. In humans as well, individuals with different Prdm9 alleles were shown to have different hot-spot usage (Baudat et al. 2010) and genetic variation in Prdm9 affects sperm hot-spot usage (Berg et al. 2010). Consistent with Prdm9 having DNA sequence preferences, Webb et al. (2008) and Myers et al. (2008) reported that 40% of human recombination hot-spots in their study sample have a 13 base pair consensus motif. Thus, in contrast to yeast, primary DNA sequences have a much greater role in DSB hot-spot specification in higher metazoans, and this sequence specificity is directly dependent on Prdm9, as hot-spots containing Prdm9 consensus sequence are stronger, and the quality of motif alignment directly correlates with hot-spot strength (Smagulova et al. 2011). However, in the absence of Prdm9, meiotic DSBs in mice still accumulate in hot-spots, but 99% of these are different from Prdm9 dependent hot-spots, and about half of them localize to promoters, similar to most DSB hot-spots in yeast (Brick et al. 2012). Thus, Prdm9 represents an additional layer of regulation for meiotic DSB localization, and it appears in the absence of Prdm9, sites for DSB formation in metazoans are chosen more like the ancestral process in yeast.

1.4.6 Meiotic DSB hot-spots in budding yeast are in nucleosome depleted regions

As noted previously, the promoter region of *ARG4* was one of the first reported DSB hot-spots in budding yeast (Sun et al. 1991, Nicolas et al. 1989). Subsequently, other DSB hot-spots were reported to exist in the 5' upstream region of *HIS4* (Detloff et al. 1992, White and Petes. 1994, Fan et al. 1995) and the 5' upstream region of *CYS3* (Cherest and Surdin-Kerjan. 1992, Vedel and Nicolas. 1999). Subsequent studies showed that both the *ARG4* and *CYS3* regions are hypersensitive to micrococcal nuclease (Ohta et al. 1994), and the *HIS4* hot-spot showed DNase-I hypersensitivity (Wu and Lichten. 1995). Wu and Lichten (1994) also examined DSB sites in regions surrounding *THR4*, *ARG4* and the *LEU2-CEN3* interval, all of which showed DNase-I hypersensitivity. Sensitivity of chromatin to nuclease stems from a nucleosome depleted open chromatin structure, and this was first observed in actively transcribed genes (Weintraub and Groudine. 1976). Most *S. cerevisiae* promoter regions have a short nucleosome depleted region (NDR) flanked by well-positioned nucleosomes (Radman-Livaja and Rando 2010), and most Spo11 DSBs in *S cerevisisae* have been mapped to these NDRs (Pan et al. 2011). The association between DSBs and NDRs has been explained by postulating that an open chromatin structure is necessary for the accessibility of Spo11 to its DNA substrate (Lichten 2008). However, though an open

chromatin structure is necessary for DSB formation, it is not sufficient. Wu and Lichten (1995) and Borde et al. (1999) also showed that their recombination reporter cassettes had similar DNase-I hypersensitivity in all genomic loci, but DSB formation was enriched at only in recombinationally hot-regions. Thus, merely inserting a region of open chromatin in a recombinationally cold region is not enough to stimulate DSB formation.

1.4.7 Transcription factor binding affects DSB formation at hot-spots, but not hot-spot specification

Since most DSB hot-spots *S. cerevisiae* coincide with promoter regions (Pan et al. 2011), binding of transcription factors and chromatin modifiers can influence DSB formation. The binding of transcription factors (TFs) Rap1, Bas1 and Bas2 was shown to stimulate recombination at *HIS4*, and mutations in their respective binding sites or deletion of the genes encoding these TFs reduced the rate of recombination (White et al. 1991, White et al. 1993). In *Schizosaccharomyces pombe,* the well-known DSB hotspot at the *ade6-M26* allele is created by single base pair change that allows the binding of the Mts1/Mts2 TF (Kon et al. 1997). However, DSB formation does not require any specific TFs, as replacing Bas1 and Bas2 binding regions for two Rap1 binding regions restored WT levels of recombination at *HIS4* (White et al. 1993). Also, neither is transcription required for DSB formation, as deletion of an upstream TATAA sequence at *HIS4* substantially reduced transcription but not meiotic recombination (White et al. 1992). Similarly, deletion of promoter elements upstream of *ARG4* lowers transcript levels but not recombination (Schultes and Szostak. 1991). Thus, the effect of TF binding on DSB formation appears to be an indirect one, altering the chromatin structure at promoter regions provides an opportunity for Spo11 to create DSBs. It is also conceivable that TF binding may occlude DSB sites from Spo11. Pan et al. (2010) performed a comprehensive comparison between TF binding sites and Spo11 oligos from the same regions, and concluded that some TFs tightly occupy nucleosome free promoters and thereby indirectly prevent Spo11 DSB formation.

1.4.8 Post translational histone modifications are associated with DSB hot-spots in budding yeast and mouse

Borde et al. (2009) reported a correlation between sites of histone H3 lysine 4 trimethylation (H3K4me3) and DSB formation in meiosis in yeast. Set1, which is the only histone methyl transferase acting on lysine 4 on histone H3, had been previously shown to affect the onset of meiotic S phase, DSB formation and the expression of middle meiotic genes (Sollier et al. 2004). Borde et al. (2009) showed that in a *set1Δ dmc1Δ* mutant, 84% of DSB hot-spots show a ≥ 1.5 fold reduction in activity compared to a *dmc1Δ* strain (70% showed a ≥ 2 fold reduction). Therefore, Set1 affects DSB hot-spot activity. However, all DSB hot-spots are not equally affected

in *set1Δ* mutants, and some sites on the genome that are cold-spots, such as the *PES4* locus on chromosome VI and the *SET4* locus on chromosome X, become DSB hot-spots in *set set1Δ* mutants.

Consistent with the effect of Set1 on meiotic DSB formation, abolishing H3K4 trimethylation by an H3K4A mutation also reduces genome wide DSB formation. However, the relation between H3K4 trimethylation levels and DSB formation is not straightforward. Both H3R2A and H3K14A mutations also reduce H3K4 trimethylation levels, but only H3R2A affects DSB formation (Sommermeyer et al. 2013). Similar to this, members of the Set1 complex *swd3Δ* and *spp1Δ* both affect H3K4 trimethylation, but DSB levels are reduced only in *spp1Δ* mutants, resembling DSB levels in *set1Δ* mutants (Sommermeyer et al. 2013). In fact, Spp1 has been shown to be directly involved in connecting H3K4 trimethylation to DSB formation, as the targeting of Spp1 by a Gal4-BD fusion can target DSBs in loci with Gal4 binding sites, similar to the effect of a Gal4-BD-Spo11 fusion protein (Acquaviva et al. 2013). Both Sommermeyer et al. 2013 and Acquaviva et al. 2013 have shown that Spp1 directly interacts with Mer2, which is a part of the Spo11 DSB forming complex. Thus, in budding yeast, there appears to be a functional role of the H3K4 trimethylation complex to DSB formation, however, this is not an essential role. Although hot-spot usage in *set1Δ* is reduced, DSBs are still formed in the absence of H3K4me3.

As with yeast, H3K4Me3, H3K4Me2 and also H3K9Ac have been reported to be specifically enriched near active recombination initiation sites in mice, and this enrichment is also seen in the absence of DSBs in $Spo11^{-/-}$ mice (Buard et al. 2009). In mouse, 94% of DSB hot-spots overlap with H3K4me3 (Smagulova et al. 2011), but these H3K4me3 marks are different from the more widespread H3K4me3 marks in promoter regions. Since Prdm9 has a histone H3K4 trimethyl transferase activity, H3K4me3 marks at DSBs could be unique to meiosis. But, similar to yeast, H3K4me3 is not sufficient to promote DSB formation, as DSBs are not formed in H3K4me3 marks at transcription promoters in wild-type spermatocytes (Smagulova et al. 2011, Brick et al. 2012).

1.4.9 Meiotic DSBs are formed in a meiosis-specific chromosome axis structure and DSB formation is also dependent on axis elements

The chromosomes of meiotic prophase cells are arranged in a meiosis-specific tripartite structure referred to as the Synaptonemal Complex (SC), first observed by electron microscope (EM) studies of thin sections of meiotic chromosomes made by Moses (1956) in spermatocytes of crayfish, and was subsequently confirmed by electron microscopy of cat and human spermatocytes (Fawcett. 1956). The SC is evolutionarily conserved and is composed of a pair of axial/lateral elements connected by a transverse central element (Westergaard and von Wettstein. 1972, Heyting. 1996). Axial elements (AEs) are assembled between the two

sister chromatids in leotptene, as first shown by ammoniacal silver staining of leptotene chromosomes in the fungus *Neotiella rutilans* (Westergaard and von Wettstein 1970). Subsequently, in zygotene, partial SCs appear at sites where the lateral elements are connected by transverse central elements, as was observed in *Neotiella* (Westergaard and von Wettstein 1970), *Lilium longiflorum*/lily (Holm 1977), in the mushroom *Coprinus cinereus* (Rasmussen et al. 1982) and in human spermatocytes (Rasmussen and Holm 1984). The temporal relation between the appearance of AEs and full SCs varies between different organisms. In the fungi *Sordaria macrospora* (Zickler 1977)*, S. humana* (Zickler and Sage 1981) and *Neurospora crassa* (Bojko. 1989, Lu 1993) and plants such as *Lilium longiflorum* /lily (Holm. 1977), *Zea mays*/maize (Anderson et al 1988), *Lycopersicon esculentum* /tomato (Stack and Anderson 1986) and *Allium cepa* /onion (Albini and Jones 1987), full-length AEs are observed well before any significant SC assembly. In other organisms such as budding yeast (Alani et al. 1990, Dresser and Giroux 1988, Padmore et al. 1991), *Locusta migratoria* (Moens 1969), *Coprinus cinereus* (Rasmussen et al 1982), *Bombyx mori*/silkworm (Rasmussen 1976), *Drosophila* (Carpenter 1975), mouse (Dietrich and Boer 1983) and human spermatocytes (Rasmussen and Holm 1978) and oocytes (Bojko 1983), AEs appear in short segments and then elongate as the SC begins to appear. Within the AE and eventually in the SC, chromosomes are arranged as an array of loops on a structural axis. This was proposed in EM studies of pigeon spermatocytes by Nebel and Coulon (1962), and human spermatocytes by Baker and Franchi (1967). These loops were also seen in light microscopy (LM) studies of diplotene chromosomes in the fungus *Coprinus lagopus* (Lu 1967); early microscopy studies of chromatin loops are reviewed in Henderson (1971a,b). Finally, individual chromosome loops could also be distinguished by whole mount surface spread preparations of hypotonically lysed testis of mice, quail, crayfish, and frogs (Comings and Okada 1970) and spread lampbrush chromosomes in primary spermatocytes of the non-biting midge *Chironomus pallidivittatus* (Keyl 1975). Within a species, the size of these loops was observed to be relatively constant, but between species, average loop lengths (in kb) show considerable variation from ~20kb in yeast (Møens and Pearlman 1988) to ~75kb in *Bombyx* (Rattner et al. 1981), to ~330-400kb in mouse (Møens and Pearlman 1988, Heng et al. 1994, Borde and De Massy 2013) to ~2500kb in the DNA rich *Chloealtis conspersa*/grasshopper (Møens and Pearlman 1988).

Meiotic DSBs are formed during leptotene in yeast (Prieler et al. 2005) and mice (Mahadevaiah et al. 2001). Therefore, Spo11 and its associated partners form DSBs in context chromosomes organized into the AE and chromatin loops. The yeast *HOP1* gene was identified in a screen that detected mutants defective in homologous chromosome pairing but unaffected in intrachromosomal recombination (Hollingsworth and Byers 1989). Subsequently, the Hop1 protein was shown to have a zinc finger motif and localize to meiotic chromosomes. Thus Hop1 was the first

structural member of meiotic chromosomes to be identified (Hollingsworth et al. 1990). *HOP1* was also identified in an additional screen for genes defective in meiotic recombination (Ajimura et al. 1993). *RED1* was identified in a screen for mutants that were proficient in spore formation but formed inviable spores (Rockmill and Roeder 1988). Smith and Roeder (1997) also showed that both Hop1 and Red1 localized to cores of unsynapsed and synapsed chromosomes, and staining in synapsed chromsomes was discontinuous, suggesting a restrained tendency to spread. Red1 was also shown to extensively co-localize with Hop1. No Hop1 staining was found in a *red1*Δ mutant, while Red1 was still present on chromosomes in *hop1* mutants (Smith and Roeder 1997). Thus, Red1 appears to be required for Hop1 localization. Also, Red1 overexpression is able to suppress a conditional allele of Hop1 (Hollingsworth and Johnson 1993, Friedman et al. 1994) and Red1 and Hop1 co-immunoprecipitate (Bailis and Roeder 1998). Red1 and Hop1 have also been shown to influence DSB formation in yeast meiosis. Both *red1* and *hop1* mutants showed reduced DSB levels at the *HIS2* meiotic recombination hot-spot (Mao-Draayer et al. 1996). *red1* mutants also reduce DSB formation at the *HIS4-LEU2* hotspot to 25% of WT (Schwacha and Kleckner 1997), and similarly, a *hop1Δ* mutant only makes 10% of WT DSB levels (Schwacha and Kleckner. 1994). Hop1 appears to be more directly involved in DSB formation than Red1, as the *hop1-628* temperature sensitive allele is also suppressed by overexpression of Rec102, which is a part of the Spo11 DSB forming complex. Also, the *hop1 red1* double mutants have the same level of meiotic recombination as *hop1,* therefore *HOP1* is epistatic to *RED1* in terms of meiotic recombination (Rockmill and Roeder. 1990). Finally, in *hop1* mutants, no heteroduplex DNA was detected in a diploid reporter strain heterozygous for *HIS4*, while it was observed at much reduced level in *red1* (Nag et al. 1995). Therefore, Red1 may be partially dispensable for DSB formation but Hop1 appears to be indispensable. Peciña et al. (2002) examined the genetic requirements for targeted meiotic DSBs by the Spo11-GalBD fusion protein, and found significant DSB formation in *red1* mutants but no DSBs were formed in *hop1* mutants. This also suggests partial dispensability for Red1 in DSB formation but not Hop1.

1.4.10 Axial elements define domains of DSB formation during meiosis, by directly interacting with Spo11 accessory proteins

The earliest microscopic reports of the axial elements reported a banding pattern of alternating thick and thin silver staining (Westergaard and von Wettstein. 1970), referred to as the G-band (chromomeric) and R band (interchromomeric). Chandley (1986) proposed a model that postulated meiotic recombination to be effectively established only in R-regions. Blat et al. (2002), using ChIP to determine protein binding at chromosome III, showed that at low resolution, both Red1 (axial element component) and Dmc1 (meiosis-specific recombinase used as proxy for DSB formation) bound along the length of chromosomes but were co-enriched in R-bands,

which they defined as GC rich, as opposed to AT rich G-bands. . Also, elimination of Red1 uniformly lowered DSBs levels all along chromosome III and the enrichment of Dmc1 at R-bands was lost (Blat et al. 2002). These results suggest that the AE component Red1 is directly responsible for establishing the chromosome context for DSB formation. However, at finer resolution, peaks of Dmc1 (i.e DSBs) correspond to valleys of Red1 and vice versa (Blat et al. 2002). Therefore, broader domains of DSB formation are specified by axial elements, but the specific DSB sites are in loop sequences away from the axis. This raised an apparent contradiction that despite the fact that DSB formation requires axial elements, the DSBs themselves form in loops away from the axis. This contradiction was resolved with a genome wide ChIP study by Panizza et al. 2011 of Red1, Hop1, the meiotic cohesin Rec8, the SC central element Zip1. Panizza et al. 2011 compared the ChIP profiles to the genome wide DSB map by Buhler et al. 2007, and reconfirmed the data from Blat et al. 2002 on a genome wide scale by showing the enrichment of Hop1, Red1, Rec8 and Zip1 at axis association sites, and the co-enrichment of Red1 and Hop1 at DSB rich domains. In addition, they demonstrated that the ChIP profiles of Rec114, Mer2 and Mei4, which form the RMM complex that directly associates with Spo11 and is essential for DSB formation, actually coincide with the axial element proteins Hop1 and Red1 rather than DSB sites. This suggests that DSB formation involves bridging between sites on the loops and the axis. This localization to the axis was shown to be dependent on Mer2 phosphorylation by S phase cyclin dependent kinase Cdc28, thereby providing a basis for temporal control of DSB formation post-S phase (Panizza et al. 2011). Thus, Red1 and Hop1, as members of the meiosis-specific chromosome axis structure, provide the loop-axis chromosomal context for meiotic DSB formation.

In addition to Hop1 and Red1, Rec8, which is a member of the cohesin ring complex that hold sister chromatids together, had also been reported to affect Spo11 distribution (Kugou et al. 2009) and *rec8* mutants have reduced DSB formation at *HIS4-LEU2* (Kim et al. 2010). Panizza et al. 2011 looked at Hop1 and Rec114 localization in *REC8* and *rec8* cells, and hypothesized that cohesin is required for Hop1 deposition at some genomic loci, which correspondingly affects Rec114 localization to those loci and subsequent DSB formation.

The loop-axis context also influences DSB formation in higher eukaryotes. HORMA domain containing homologues of Hop1, such as Him3 in *C elegans* and HORMAD-1 in mice, are known to influence meiotic DSB formation (Goodyer et al. 2008, Daniel et al. 2011). Further, in male mice, the specific region of homology between the X and Y chromosome, referred to as the Pseudo Autosomal Region (PAR), has a longer meiotic axis and shorter loops than the genome average, which creates a very high loop density. Correspondingly, the PAR region has the highest DSB formation frequency in the mouse genome (Kauppi et al. 2011). This region was also shown by Smagulova et al. (2011) to have the “hottest”

cluster of DSBs, directly correlating its denser loop-axis organization with DSB formation. Lynn et al. (2002) have demonstrated that in both mice and humans, increased SC length correlates with a higher CO frequency, presumably due to increased loop density in a longer SC.

Thus, meiotic DSBs are formed by Spo11 in a meiosis-specific chromosome context, defined by the axial elements and chromatin loop organization, and further influenced by nucleosome density and their post translational modifications. It is conceivable that in addition to controlling DSB formation, the chromosome context that envelopes a meiotic DSB might also influence its repair, by controlling the access of repair factors to the DSB. Thus, the meiosis-specific chromosome context could differentiate meiotic HR from mitotic HR.

1.5 Meiotic DSBs are acted upon by unique meiosis-specific recombination activities

HR is initiated by a DNA DSB, which is initially processed by 5' to 3' resection. The ssDNA then invades an intact DNA duplex and primes synthesis from the intact template strand. The strand invasion intermediate is then processed to give NCOs or COs. These fundamental steps in HR are unchanged from mitosis to meiosis. In the previous section, we have discussed how the DSB in meiosis form in a unique meiosis-specific chromosome context that differentiates it from mitosis. However, in addition to a unique context of DSB formation, there are unique recombination proteins that are solely expressed in meiosis. Also, the recombination activities of mitotic proteins may also be modulated during meiosis. Thus, another basis for the differentiation of HR from mitosis to meiosis could be the action of the meiosis-specific recombination activities. This section is not meant to be an exhaustive list describing all of the recombination proteins that act in mitosis and meiosis. Rather, I will highlight specific examples as I serially progress through signaling, resection, strand invasion, and CO/NCO formation.

1.5.1 DNA DSB signaling is mediated by Rad53 in mitosis versus Mek1 in meiosis

DNA DSB are potentially lethal lesions, and as such, DSBs lead to a cascade of signaling events that activate repair pathways and lead to cell cycle arrest. The Mre11-Rad50-Xrs2, complex in association with Sae2 can process DSB ends to initiate repair (Lobachev et al. 2002, Lengsfeld et al. 2007). In cells in the S-G2 phase of the cell cycle, this is controlled by the phosphorylation of Sae2 by the yeast cyclin dependent kinase Cdc28, to initiate resection for HR (Terasawa et al. 2008, Huertas et al. 2008, Manfrini et al. 2010). This is also conserved in mammalian cells, where the Mre11-Rad50-Nbs1 (MRN) complex recruits ATM (Tel1 orthologue) and CtIP/Ctp1 (Sae2 orthoulogue) to DSB ends (Langerak et al. 2011). In *S. cerevisiae*, Mre11 protein and the ATM-related signaling kinase Tel1 are

the first proteins detectable at DSB ends by fluorescence microscopy (Lisby et al. 2004). The MRX complex is believed to recruit Tel1 via the C-terminus of Xrs2 (Nakada et al. 2003). Tel1 might be the first signaling kinase to be recruited to a DSB, but it plays a minor role compared to the other signaling kinase Mec1, which is related to the ATR kinase in mammalian cells. In the absence of Mec1, Tel1 activation by a single DSB is unable to activate downstream targets and induce cell cycle arrest, and multiple DSBs are required to activate the DNA damage response via Tel1 in the absence of Mec1 (Mantiero et al. 2007). However, Tel1, together with MRX increases the efficiency of single stranded DNA accumulation, which in turn induces Mec1 (Mantiero et al. 2007). Single stranded DNA generated by resection is coated by the replication protein A (RPA) (Alani et al. 1992), which in turn recruits Mec1 through its partner Ddc2 (Zou and Elledge. 2003). RPA also stimulates the loading of the heterotrimeric checkpoint clamp, which comprises of Rad17, Mec3 and Ddc1 (Zou et al. 2003, Majka et al. 2006a). The Tel1 and Mec1 kinases, in association with the checkpoint clamp, then hyper-phosphorylate the Rad9 checkpoint protein, (Vialard et al. 1998, Usui et al. 2001, Majka et al. 2006b).

In mitotic cells, the Rad9 protein then acts as an adaptor between the upstream signaling kinases and the downstream effector kinase Rad53, which mediates the checkpoint arrest (Sweeney et al. 2005). In contrast, Rad9 in meiotic cells interacts with a different protein, the Rad53 paralogue Mre4/Mek1 (Usui et al. 2001). Mek1 activation also requires Red1 and Hop1 (Wan et al. 2004). In meiotic cells, Mek1, which promotes dimerization of Hop1, is required for promoting interhomologue recombination and suppressing inter sister recombination (Niu et al. 2005, Niu et al. 2007). However, other than partner choice, it is not entirely clear if Rad53 phosphorylation in mitosis versus Mek1 phosphorylation in meiosis has other consequences for repair of DSBs by HR.

1.5.2 5’ to 3’ resection in meiosis is comparable to resection in mitosis

As mentioned previously, the first step in HR after DSB formation is 5’ to 3’ resection, which is initiated by the MRX complex in concert with Sae2 (Stracker et al. 2004, Borde. 2007). Garcia et al. (2011) have proposed a mechanism of initiation beginning with an endonucleolytic cleavage by MRX-Sae2 ~300 nucleotides away from the DSB. DNA resection then proceed bi-directionally on each strand via the 3’-5’ exonuclease activity of Mre11 and a 5’ to 3’ exonuclease activity of Exo1. Hodgson et al. (2011) have further argued that this bidirectional resection is also required beyond the initial resection step, as resection for a Spo11-independent meiotic DSB with free ends is still impaired in a nuclease dead mutant of Mre11. The 3’ to 5’ resection by Mre11 leads to the release of the Spo11-DNA oligo complex in meiosis and may also clean damaged DNA ends in mitosis. Once resection is initiated, it is further extended in a 5’ to 3’ direction, which in budding yeast is primarily mediated by the 5’ to 3’

exonuclease Exo1. Exo1 has been shown to mediate resection in both mitotic cells (Fiorentini et al. 1997) and meiotic cells (Tsubouchi and Ogawa. 2000, Manfrini et al. 2010, Zakharyevich et al. 2010, Hodgson et al. 2011). In meiotic cells, such DNA resection generates ssDNA extending from the DSB site to ~800 nucleotides (Sun et al. 1991, Zakharyevich et al. 2010). Since *exo1* mutants do not affect the kinetics of mating type switching in mitotic cells (Tsubouchi and Ogawa. 2000, Moreau et al. 2001), there must be redundancy in the role of the Exo1 for resection. An *sgs1Δ* mutant shows normal resection close to an HO DSB site in mitotic cells, but resection is reduced for sequences greater than 3 kb away (Zhu et al. 2008). Also, an *exo1Δ sgs1Δ* mutant shows a more severe defect in repair by single strand annealing (SSA) that required extensive resection; and processing of an HO DSB at *MAT* locus than either single mutant (Mimitou and Symington. 2008). These results suggest that Sgs1 plays a redundant role to Exo1 for DNA resection in mitotic cells, and this is done together with the Dna2 nuclease (Zhu et al. 2008, Cejka et al. 2010a, Cannavo et al. 2013).

In contrast, in meiosis, there is almost no resection in *exo1* mutants, though meiotic recombination proceeds with normal kinetics (Zakharyevich et al. 2010). This is because even in *exo1* mutants, there are ~150-250 bps of ssDNA at break ends (Zakharyevich et al. 2010), probably from the action of endonucleolytic cleavage and 3 to 5' resection by Mre11 (Garcia et al. 2011, Hodgson et al. 2011). A meiotic null allele of Sgs1, *pCLB2-SGS1* shows no resection defect on its own at the *HIS4-LEU2* DSB hot-spot, and *pCLB2-SGS1 exo1Δ* is no worse for resection that the *exo1Δ* single mutant (Zakharyevich et al. 2010). Thus, the role of Sgs1-Dna2 may be very limited in meiotic resection.

Overall, the roles of MRX-Sae2 and Exo1 in DNA resection during HR seem quite comparable in meiosis and mitosis, while Sgs1-Dna2 may play a redundant role to Exo1 in mitotic cells.

1.5.3 Dmc1 is a unique meiosis-specific recombinase that may differentiate strand invasion in meiosis from mitosis.

The 3' ssDNA tails formed by resection are the substrates for recombinases that catalyze the strand invasion step of homologous DNA pairing and strand exchange. The *RAD51* gene was identified in genetic screens for mutants with elevated sensitivities to ionizing radiation (Nakai and Matsumoto. 1967, Averbeck et al. 1970, Game and Mortimer 1974) as a member of the *RAD52* epistasis group. *rad51* mutants were subsequently also shown to be sensitive to the DSB-inducing drug bleomycin (Moore. 1978). *RAD51* was also identified in screen for mutator loci, initially referred to as *mut5-1,* and these mutants were shown to be defective for both mitotic and meiotic recombination (Hastings et al. 1976, Morrison and Hastings. 1979). Rad51 is homologous to the *E coli* recombinase RecA, and *rad51* mutants accumulate meiotic

DSBs at *HIS4-LEU2* and reduce the formation of CO recombinants (Shinohara et al. 1992). The strand exchange activity of Rad51 is facilitated by a number of accessory proteins that act as mediators of Rad51 loading onto ssDNA for strand invasion (Krejci et al. 2012).

Most eukaryotes contain second meiosis-specific recombinase, Dmc1, which was identified in *S. cerevisiae* in a screen for genes whose expression was enhanced in meiosis (Bishop et al. 1992). Bishop et al. (1992) showed that the Dmc1 protein was homologous to both RecA and Rad51, and that *dmc1* mutants accumulate meiotic DSBs which continue to resect, form recombinants at only 10% of WT levels, show incomplete SC and arrest at late prophase. In mice, *dmc1* males and females are sterile, with an arrest of gametogenesis in meiotic prophase I. These mice also show asynapsed homologous chromosomes (Pittman et al. 1998, Yoshida et al. 1998, Di Giacomo et al. 2005). In *Arabidopsis*, *dmc1* mutants do not show meiotic arrest, but are still infertile due to random chromosome segregation (Couteau et al. 1999). However, *dmc1* mutants of the fission yeast *S. pombe* still show significant levels of recombination (Young et al. 2004), and Dmc1 has been shown to be required for interhomologue Holliday junction intermediates only at DSB cold-spots (Hyppa and Smith. 2010). Also, *Drosophila melanogaster*, *Caenorhabditis elegans* and *Neurospora crassa* have Rad51 but lack a Dmc1 orthologue, so some organisms accomplish meiosis without a meiosis-specific recombinase.

Rad51 is required for both mitotic and meiotic recombination, while Dmc1 only functions in meiosis (reviewed in Krogh and Symington. 2004), and the exact nature of their respective roles in meiosis has long been studied. In *S. cerevisiae,* both *rad51* and *dmc1* mutants show asynapsed axial elements that are indicative of unrepaired DSBs (Rockmill et al. 1995). Rad51 and Dmc1 foci co-localize during meiosis in budding yeast, and the normal formation of Dmc1 foci is dependent on Rad51 (Bishop. 1994). The Dmc1 accessory factor Tid1/Rdh54 promotes this co-localization (Shinohara et al. 2000). The co-localization of Rad51 and Dmc1 has also been observed in lily (Terasawa et al. 1995, Anderson et al. 1997) and mouse (Tarsounas et al. 1999). Rad51 is also able to catalyze meiotic recombination, as over-expression of the Rad51 accessory protein Rad54 can suppress *dmc1* mutants of *S. cerevisiae* and restore spore viability to close to WT levels (Bishop et al. 1999). A *hed1* mutant is also able to overcome the meiotic arrest in *dmc1* mutants (Tsubouchi and Roeder. 2006). Hed1 inhibits the action of Rad51 during meiosis by preventing its interaction with one of its accessory factors Rad54 (Busygina et al. 2008). Thus the *hed1* mutant releases this inhibition allowing Rad51 to catalyze strand invasion.

The DSB repair defect and meiotic arrest that is seen in *dmc1* mutants can also be alleviated by combining *dmc1* and *red1* mutations. However, inter homologue single end invasion intermediates and interhomologue double

Holliday junction intermediates are not detected at wild type levels in these double mutants (Hunter and Kleckner. 2001, Schwacha and Kleckner. 1997). Lydall et al. (1996) and Grushcow et al. (1999) showed that checkpoint mutants *mec1, rad17* and rad24 also alleviate the meiotic arrest in *dmc1,* but these double mutants have elevated levels of ectopic recombination. These results have been used to argue for an interhomologue-only recombinase function for Dmc1 and consequently, an intersister recombinase function for Rad51. However, *hed1 dmc1* mutants, where strand invasion is catalyzed by Rad51, still have significant levels of interhomologue recombinants. Also, *rad51* mutation causes an increase in intersister Holliday junction intermediates at *HIS4-LEU2* (Schwacha and Kleckner. 1997). Thus, Rad51 and Dmc1 appear to have distinct but interdependent roles in meiosis. A recent study by Cloud et al. (2012) has further elaborated on this interdependence by identifying a separation of function mutant of Rad51 that that retains presynaptic filament-forming activity but loses strand invasion activity. Cloud et al. (2012) showed that the latter activity is fully dispensable for meiotic recombination, but the corresponding mutation in Dmc1 is catastrophic for meiosis. Therefore, Rad51 appears to function as a Dmc1 accessory factor in meiosis, and Dmc1 is responsible for the meiotic strand invasion activity. Thus, the strand invasion step of recombination is modified in meiosis, with the meiosis-specific recombinase Dmc1 and its accessory factors. This is an example of how unique recombination activities can be responsible for differentiating meiotic HR from mitotic.

1.5.4 Mitotic cells drive HR to NCO outcomes by the action of helicases

Once strand invasion has been accomplished and DNA synthesis goes past the site of the DSB, the intermediate can then go down different recombination pathways that will lead to NCO or CO outcomes. As described previously, SDSA and dHJ dissolution lead to NCOs only. These pathways are more prominent in mitosis (Mitchel et al. 2010, Mitchel et al. 2013), and they are primarily executed by the action of helicases, which can unwind DNA strands (Mitchel et al. 2013). Such helicase activity can dissociate the invading strand from the donor strand after DNA synthesis, which will lead to D-loop collapse. Subsequent annealing of the newly synthesized strand with the other end of the DSB results in a NCO outcome by SDSA. Similarly, the combined action of a helicase and topoisomerase on a double Holliday junction intermediate can move the two Holliday junctions inwards and resolve the resultant hemicatanated DNA strands to create exclusively NCOs by a process called dHJ dissolution (Wu and Hickson 2003). Thus, helicase are vital in their role of suppressing CO formation in mitotic cells. The budding yeast helicase Srs2, which belongs to the superfamily I of DNA helicases and is homologous to the *E coli* protein UvrD (Gorbalenya et al. 1988), was identified in a genetic screen for mutants with increased intrachromosomal recombination between duplicated *leu2* genes (Aguilera and Klein. 1988). Srs2 can unwind Rad51 nucleoprotein

filaments *in vitro* (Krejci et al. DNA 2003, Veaute et al. 2003). Sgs1, the budding yeast homologue of *E coli* RecQ helicase, was identified as a suppressor of the slow growth phenotype of *top3* mutants in *S. cerevisiae* (Gangloff et al. 1994), and was also shown to interact with the C terminal region of *S. cerevisiae* topoisomerase II in a two-hybrid screen (Watt et al. 1995). Sgs1 was also identified as a homologue of the eukaryotic Bloom's syndrome helicase (BLM) and Werner's syndrome helicase (WRN) (discussed in a previous section), and *sgs1* mutants have increased level of genome insertions and translocations caused by homeologous recombination (Myung et al. 2001). Topoisomerase III interacts with *SGS1* (Ng et al. 1999) and as mentioned previously, their combined action along with Rmi1 can dissolve double Holliday junctions (Wu and Hickson. 2003, Cejka et al. 2010b). Both Srs2 and Sgs1 are required to maintain genome integrity by regulating homologous recombination (Vaze et al. 2002, Lee et al. 1999, Gangloff et al. 2000). In budding yeast mitotic cells, loss of the helicases Srs2 and Sgs1 increases COs in an ectopic recombination system by 2-3 fold (Ira et al. 2003). Another helicase, Mph1, was identified in a screen for mutators (Entian et al. 1999). Mph1 is the yeast orthologue of the human FancM helicase (Meetei et al. 2005, Mosedale et al. 2005). *mph1* mutants also show 4 fold increased COs in both ectopic and allelic recombination assays (Prakash et al. 2009). The role of helicases in CO suppression in mitotic cells has been further demonstrated with a plasmid gap repair assay and subsequent analysis of heteroduplex DNA by Mitchel et al. (2013), who show that Srs2, Sgs1 and Mph1 affect NCO bias by promoting SDSA, and Srs2 and Sgs1 further promote NCOs formation by dismantling Holliday junction containing intermediates. The role of Sgs1 in dHJ dissolution is well known, but Srs2 was thought to promote NCO formation by SDSA alone by unwinding Rad51 nucleoprotein filaments (Krejci et al. DNA 2003, Veaute et al. 2003). Mitchel et al. (2013) are the first to report a role for Srs2 in reducing NCOs with bidirectional trans heteroduplex DNA, which can arise from dHJ intermediates. Blanck et al. (2009) showed an *in vitro* activity for *Arabidopisis* Srs2 on nicked Holliday junctions, and Mitchel et al. (2013) have proposed this activity as the basis of Srs2's role in dismantling dHJs.

As regards the infrequent COs in mitotic yeast cells, these are formed by the action of the endonucleases Mus81 and Yen1 (Ho et al. 2010). But Matos et al. (2011) and Matos et al. (2013) have shown that the activity of Mus81 and Yen1 and their respective human orthologues MUS81 and GEN1 is temporally restricted in mitotic cells by the polo-like kinase Cdc5 in yeast and PLK1 in humans, so that these nuclease are only active during the period immediately after mitosis in anaphase, mostly likely to prevent JMs from interfering with chromosome segregation. Therefore, mitotic cells specifically tailor their recombination activities to bias HR towards NCOs.

1.5.5 Meiotic cells enrich for COs by attenuating helicases and providing additional resolvase activities

The repair of meiotic DSBs by HR has to ensure sufficient CO formation so that all homologue pairs receive at least one CO. In the DSBR model of homologous recombination, the cleavage of dHJs in opposite orientations forms COs, while cleavage in the same orientation forms NCOs ((Szostak et al. 1983). Allers and Lichten (2001a) showed that there was a timing difference in the appearance of NCOs and COs, and that the meiosis-specific Ndt80 transcription factor only affected the formation of COs. Subsequently, Sourirajan and Lichten (2008) showed that dHJs are resolved in meiosis to only form COs, and this resolution is dependent on the Cdc5 polo like kinase, whose expression in turn is activated by Ndt80. Therefore, dHJs are specifically driven towards resolution by an endonuclease to enrich for COs in meiosis. Thus, it is conceivable that to ensure a CO fate for meiotic DSB repair, intermediates of HR have to be protected from helicases, which antagonize CO formation in mitotic cells. The ZMM proteins Zip1, Zip2, Zip3, Mer3 and Msh5 (also referred to as the synapsis initiation complex) are involved in both establishing synapsis between homologous chromosomes and are also required for CO formation (Lynn et al. 2007, Börner et al. 2004). Börner et al. (2004) examined the effect of ZMM proteins Zip1, Zip2, Zip3, Mer3, and Msh5 on recombination and showed that mutants lacking ZMM proteins are specifically deficient in CO formation and SC formation. COs are reduced in these mutants to 40-50% of wild type cells at 23°C and 15% at 33°C. These ZMM proteins were also shown to antagonize the anti-CO activity of the helicase Sgs1 (Jessop et al. 2006). Zip1, which is the central element of the synaptonemal complex (Sym et al. 1993), and the remaining ZMM proteins are distributed along meiotic chromosomes in foci that show interference, akin to meiotic COs (Fung et al. 2004). Zip3 is a SUMO E3 ligase (Cheng et al. 2006) and is believed to mark CO designated DSBs (Agarwal and Roeder 2000, Henderson and Keeney 2004, Serrentino et al. 2013). Msh4 and Msh5 are meiosis-specific MutS homologues in yeast. The proteins have no roles in mismatch repair but their mutants are deficient in meiotic CO formation (Ross-Macdonald and Roeder. 1994, Hollingsworth et al. 1995, Novak et al. 2001). Snowden et al. (2004) and Snowden et al. (2008) were able to perform biochemical studies on purified human Msh4 and Msh5 (hMSH4 and hMSH5), and showed that hMSH4 and hMSH5 form a heterodimer that binds uniquely to Holliday junctions and that Holliday junction binding stimulates the ATP hydrolysis activity of hMSH4-hMSH5. hMSH4-hMSH5 can also bind proto Holliday junctions (Snowden et al. 2004). In addition, binding of ATP by hMSH4-hMSH5 induces the formation of a sliding clamp that embraces the opposing duplex arms of a Holliday junction in an ATP hydrolysis independent manner; this activity could potentially stabilize dHJs *in vivo* (Snowden et al. 2004 and Snowden et al. 2008). Therefore, Snowden et al. (2004) showed a direct association between the Msh4-Msh5 heterodimer and Holliday junctions *in vitro*, and this could provide a mechanistic basis

for the role of Msh4-Msh5 in CO formation *in vivo.* Thus, these genetic and biochemical studies support the notion that the ZMM proteins stabilize recombination intermediates to ensure CO formation.

In addition to SC and CO formation, ZMM proteins are also involved in CO interference. Mutations in Zip1, Mer3, Msh4 and Msh5 abolish CO interference; residual COs in these mutants do not show interference (Sym and Roeder. 1994, Nakagawa and Ogawa. 1999, Novak et al. 2001, Argueso et al. 2004). Getz et al. (2008) looked at interference properties of COs with different heteroduplex patterns using palindromes that are poorly corrected by mismatch repair. They showed that COs with a 5:3 segregation pattern do not show interference and are unaffected by *msh4* mutation, while COs that show a 6:2 or 4:4 interference pattern show interference and are dependent of Msh4. The ZMM proteins are therefore responsible for the formation of the interfering class of COs in meiosis, and these are believed to then evenly distribute themselves along all homologue pairs such that there are no homologue pairs without COs. This is referred to as CO assurance, and it has been cytologically observed in many organisms, such that meiotic chromosomes seldom show bivalents with no chiasmata between them (reviewed in Haldane. 1931). The ZMM pathway is therefore involved in both SC formation and formation of interfering COs. However, *spo16* and *spo22* mutants in *S. cerevisiae* also have defective SC formation and reduced COs like other ZMM mutants, but the residual COs still show interference (Shinohara et al. 2008). Therefore, the exact relation between SC and CO interference is not entirely clear.

The ZMM pathway represents the primary CO pathway in meiosis, although the identity of the resolvase that forms COs from dHJs upon Cdc5 activation is not clear. The yeast MutL homogues Mlh1 and Mlh3 were also shown to be deficient in CO formation (Wang et al. 1999, Zakharyevich et al. 2010). This function of the Mlh1/3 proteins is mediated by an interaction with Exo1 (Zakharyevich et al. 2010, Zakharyevich et al. 2012). This led Zakharyevich et al. 2012 to propose Mlh1/3-Exo1 as the resolvase activity for the ZMM pathway.

Orthologues of ZMM proteins have been found in *Arabidopsis* including Mer3 (Chen et al. 2005, Mercier et al. 2005), Zip4 (Chelysheva et al. 2007), Zip3 (Chelysheva et al. 2012) and Msh4 (Higgins et al. 2004) and COs in *Arabidopsis* show interference (Copenhaver et al. 2002). Evidence for the ZMM CO pathway also exists in *Drosophila, Oriza sativa*/rice, *C elegans*, mice and humans (Lynn et al. 2007). In *C elegans*, which form exactly one CO per homologue pair, almost all COs appear to form via the ZMM pathway (Zalevsky et al. 1999).

In budding yeast, residual COs still remain in the absence ZMM proteins. These COs do not show interference and are dependent on the 3' to 5' flap endonuclease Mus81 and its partner Mms4 (de los Santos et al. 2003,

Argueso et al. 2004). The fission yeast *Schizosaccharomyces pombe* has no observable synaptonemal complex (Kohli and Bähler. 1994, Roeder. 1997) and most CO formation is dependent on Mus81-Eme (Boddy et al. 2001, Smith et al. 2003, Hyppa and Smith. 2010). Osman et al. (2003) suggested an alternate method of CO formation by cleavage of early D-loop intermediates (discussed in section 1.1.5). Mus81-Mms4 has also been proposed as the resolvase for a backup CO pathway in *Saccharomyces cerevisiae* (Hollingsworth and Brill. 2004). Matos et al. 2011 have showed that the Mus81 and Yen1 endonucleases are sequentially hyperactivated by Cdc5 dependent phosphorylation during meiosis, which may further promote CO formation in meiosis.

dHJ formation is promoted in meiosis as compared to mitosis (Oh et al. 2007, Jessop and Lichten. 2008, Bzymek et al. 2010). However, JMs with HJs can form not only between two homologues; they can also form between sister chromatids or heterologous chromosomes, and can engage more that two DNA duplexes. Such branched molecules involving multiple DNA strands can be deleterious (Larsen and Hickson. 2013). Therefore, there must be a balance in meiosis that allows HJ containing JM formation, but not to the extent that it becomes unregulated and starts engaging multiple chromatids. De Muyt et al. (2012) demonstrated that in the absence of Sgs1, the Mus81 dependent alternate CO pathway becomes dominant in meiosis. This might represent a meiotic cell wide CO control mechanism that prevents the formation of JM intermediates outside the context of ZMM proteins under normal circumstances, and the absence of Sgs1 results in an altered cell wide JM population. Consistent with this, Sgs1 and Mus81 prevent the accumulation of multi-chromatid JMs in meiosis (Oh et al. 2007, Jessop and Lichten. 2008). Thus, meiotic cells have ZMM proteins to protect dHJs from helicases and also hyper-activate other Holliday junction resolution activites, and these unique recombination proteins enrich for COs in meiosis.

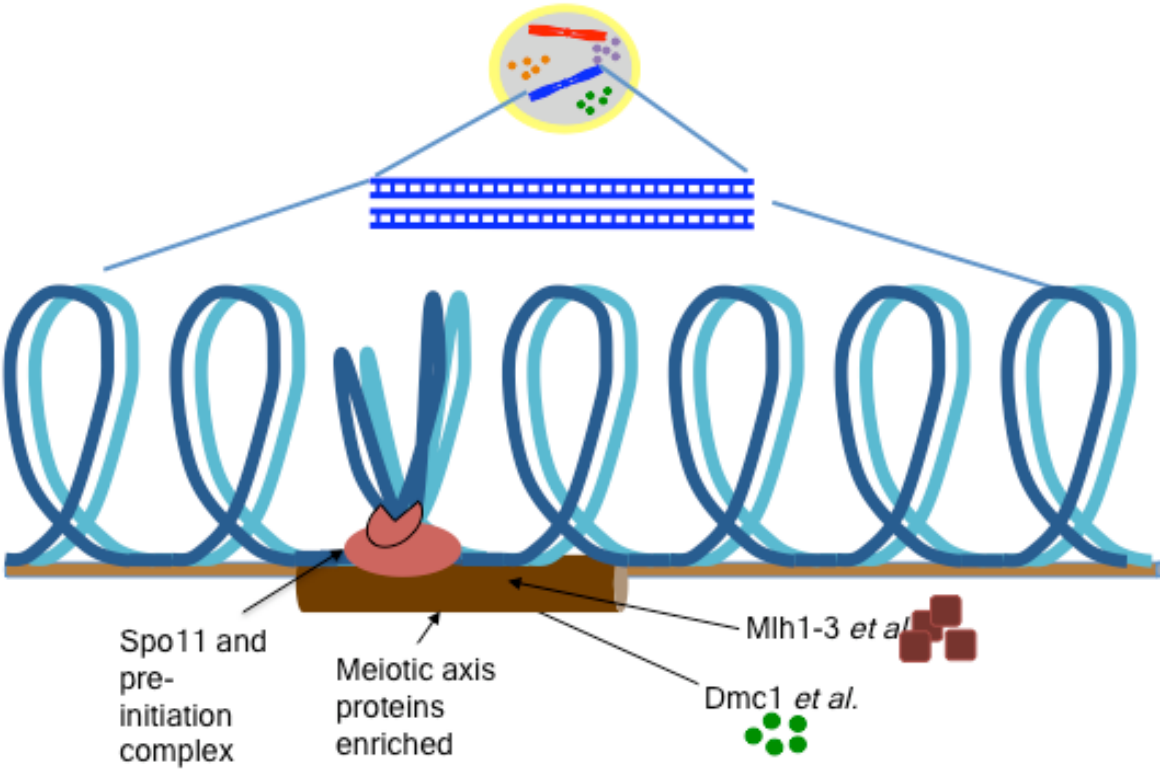

Figure 1-10 DSBs in meiosis are formed in a meiosis-specific chromosome axis context, and they are acted on by meiosis-specific recombination activities

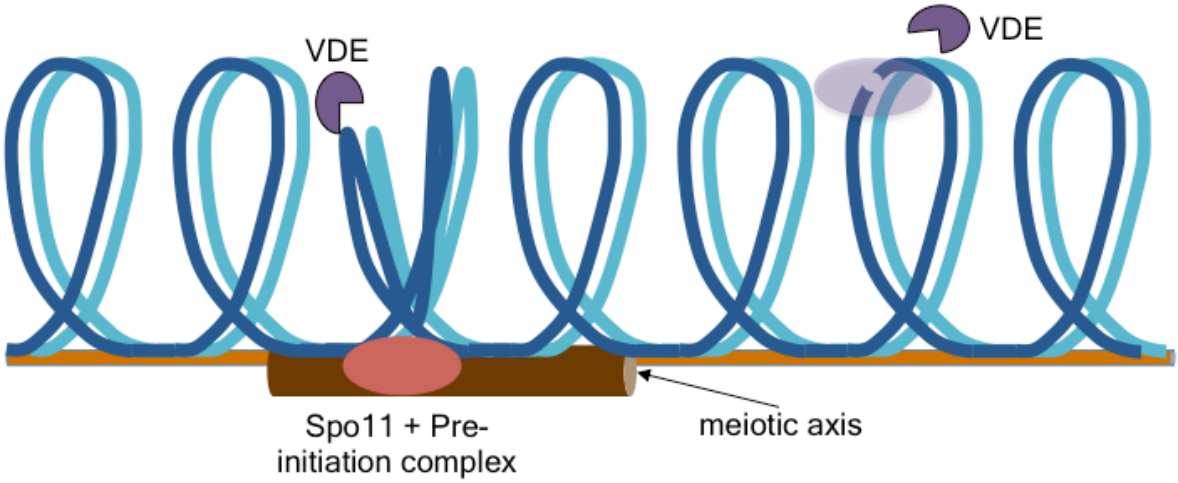

Figure 1-11 The VDE DSB forms in during meiosis, but outside the context of the meiotic axis, thus study of VDE DSB repair can separate the local influence of the axis from the cell wide global influence of meiotic recombination activities.

1.6 Understanding local and global factors of meiosis from the study of Spo11 independent meiotic DSBs formed by VDE

As stated above, homologous recombination (HR) is an important mechanism for repairing double strand breaks (DSBs) in DNA by interacting with an intact copy of DNA as a template for repair. In mitotic cells, HR is almost exclusively regulated to form NCOs; this prevents any alterations to the genome that can be deleterious. Conversely, meiotic cells enrich for COs, which are required to create physical association between maternal and paternal homologous chromosomes for segregation in meiosis I, to produce haploid gametes from diploid cells by halving ploidy. The basis of such contrasting regulation is not completely understood. Meiotic cells have specific HR proteins present in addition to the mitotic HR proteins; these may facilitate the altered regulation of meiotic recombination. On the other hand, meiotic axis proteins are enriched in DSB-hot regions on chromosomes; these then interact with the meiosis-specific endonuclease Spo11 to form DSBs. Thus, the substrate for meiotic recombination is in a unique meiosis-specific chromatin context, unlike the spontaneous lesions that are the major target of mitotic repair, and this could also provide the basis for altered regulation of HR in meiosis.

If meiotic recombination is primarily regulated by the cell wide meiosis-specific recombination activities, then all DSBs in meiosis should be similarly repaired to enrich for COs. Malkova et al. (2000) studied the repair of a *SPO13::HO* DSB, which is specifically expressed in meiosis as its expression is controlled by the *SPO13* promoter, at the *LEU2* locus. They reported that about half the recombinants arising from the *SPO13::HO* DSB were COs, therefore the repair of this break resembled Spo11 DSB repair. This would argue that all DSBs in meiosis are similarly repaired. However, it is worth noting that the *SPO13::HO* DSB was placed at the *LEU2* locus, which is a hot-spot for meiotic recombination (White and Petes. 1994). In addition, the experimental setup for Malkova et al. (2000) had a 113 bp *HO* DSB site inserted on one homologue, with no homology on the other homologue. Heterology right at the DSB site affects the NCO to CO ratio; this will be elaborated upon at the discussion section of this thesis, after relevant experimental evidence has been presented. Cartagena-Lirola et al. (2008) generated exogenous DSBs in meiotic cells, by treating *spo11Δ* cells with phleomycin after completion of pre-meiotic DNA synthesis. They found that these exogenous DSBs are able to trigger both Rad53 and Mek1 phosphorylation, whereas Spo11 DSBs do not trigger Rad53 phosphorylation. Only fusing Rad53 to Ddc2, which is the partner of Mec1, allows Rad53 activation by Spo11 DSBs. This suggests that Rad53 itself cannot access endogenous meiotic DSBs, while Rad53 can access a subset of exogenous DSBs in meiosis. Therefore, contrary to Malkova et al. (2000), the data from Cartagena-Lirola et al. (2008) indicates that all meiotic DSBs are not equal, and the unique local environment of Spo11 DSBs can affect downstream steps of DSB

signaling. Also, genome wide mapping of COs and NCOs by Mancera et al. 2008 revealed regions in the genome where either crossovers or non-crossovers are favoured more than expected by chance, so even all Spo11 DSBs in meiosis may not be equally repaired, with some being pre-disposed to NCO or CO fates. Finally, in another model organism for meiosis, *C. elegans*, Youds et al. (2010) showed that exogenous DSBs generated by ionizing radiation are primarily repaired as NCOs via the action of the RTEL-1 helicase, and this is further evidence that all DSBs in meiosis are not equally repaired to enrich for COs.

The purpose of this thesis is to further study DSB repair in meiosis by HR, to differentiate between global versus local regulation. Spo11 meiotic DSBs are formed in meiosis-specific chromosome axis context (Cao et al. 1990, Rockmill and Roeder. 1990, Mao-Draayer et al. 1996, Schwacha and Kleckner. 1994, Schwacha and Kleckner. 1997, Blat et al. 2002 and Panizza et al. 2011) and are acted upon by meiosis-specific recombination activities (Bishop et al. 1992, Sym et al. 1993, Ross-Macdonald and Roeder. 1994, Hollingsworth et al. 1995, Shinohara et al. 2000, Novak et al. 2001, Usui et al. 2001, Tsubouchi and Roeder. 2006, Lynn et al. 2007, Börner et al. 2004, Fung et al. 2004, Cheng et al. 2006) (Figure 1-10). Therefore, the study of Spo11 DSBs in meiosis cannot differentiate between the local effects of meiotic chromosome axis to the cell wide effects of meiotic recombination proteins. Consequently, a meiotic DSB that can form independently of the meiotic axis is required for this study.

The *VMA1* derived endonuclease (VDE), also known as PISceI, was discovered by Gimble and Thorner (1992) as a site-specific DNA endonuclease that is encoded as an intein in the budding yeast vacuolar H(+)-ATPase subunit gene. VDE shares 34% identity with the homothallic switching endonucleases, and cleaves a specific VDE recognition sequence (VRS) within the *VMA1* allele that lacks the VDE endonuclease segment (Gimble and Thorner 1992). VDE is formed by a protein splicing reaction that joins the N-terminal segment and the C-terminal segment of the 119KDa primary translation product of the *VMA1* gene to yield a 69 kDa vacuolar H(+)-ATPase subunit and an internal 50 kDa endonuclease (Gimble and Thorner. 1993). Interestingly, the cleavage by VDE at the VRS site only occurs during meiosis and it initiates 'homing', a genetic event that converts a *VMA1* allele lacking the endonuclease coding sequence into one that contains it (Nogami et al. 2002). The meiosis-specific cleavage by VDE is due to its selective import into the nucleus in early meiosis, which is induced by the inactivation of TOR kinases due to nutrient depletion, which also triggers sporulation (Nagai et al. 2003). Also, unlike Spo11, VDE cleaves its recognition sequence irrespective of the meiotic chromosome context. VRS sites are effectively cleaved by VDE during meiosis at both DSB-hot regions and DSB-cold regions (Fukuda et al. 2008).

There have been limited studies regarding the repair of VDE DSBs in meiosis at its natural *VMA1* locus. Fukuda et al. (2003) reported that the homing product formed by VDE initiated recombination is unaffected in *spo11Δ*, but is reduced in *mre11Δ, rad50Δ, xrs2Δ, sae2Δ, rad51Δ, rad54Δ, dmc1Δ, tid1Δ and rec8Δ.* However, other than the *spo11Δ*, all other mutants were *SPO11*, so these mutants would also accumulate unrepaired Spo11 DSBs. Johnson et al. (2007) showed that VDE DSB repair by SSA is impaired in *dmc1* mutants, but this can be alleviated in *hop1* and *spo11Y135F* mutants which reduce or completely remove the load of unrepaired DSBs. This is because in repair deficient mutants, which accumulate resected Spo11 DSBs, RPA components become limiting. This affects both DNA damage signaling and recruitment of downstream repair proteins. This presents the possibility that the reduction in VDE DSB repair, especially in the resection competent but repair deficient *rad51Δ, rad54Δ, dmc1Δ, tid1Δ and rec8Δ* mutants, may be an indirect consequence of these mutants accumulating resected Spo11 DSBs that sequester RPA. Fukuda et al. (2003) also inserted *URA3* and *LEU2* sequences upstream and downstream of the *VMA1* gene with the VDE cleavage site to determine CO frequencies, which they calculated to be 36% in WT. They observed a reduction of CO frequencies in *exo1Δ* and *msh4Δ,* but this was less than 2-fold reduction which is seen for Spo11 initiated COs. In addition, Fukuda et al. (2003) determined CO frequencies only using 4-spore viable tetrads that have 4:0 segregation. This raises the possibility of biases introduced in the observations due to the elimination of all other tetrads that do not have 4 viable spores. Also, Malkova et al. (2000) reported that 4:0 tetrads in which both sister chromatids are cut are repaired differently from tetrads with 3:1 segregation. Fukuda et al. (2003) concluded that the VDE DSB at *VMA1* was repaired like endogenous Spo11 DSBs, but this conclusion needs further scrutiny. Another study by Fukuda and Ohya. (2006) reported that both recombinases Rad51 and Dmc1 are recruited to the VDE DSB at *VMA1*. Rad51 recruitment is dependent on Rad52, Rad55 and Rad57, and Dmc1 recruitment is dependent on Sae3 and Tid1. This again suggests that VDE DSBs are repaired in the same manner as Spo11 DSBs. But recruitment alone does not indicate functional equivalence, and even though both Rad51 and Dmc1 are also recruited to Spo11 DSBs, only Dmc1 is required for the strand invasion activity to repair DSBs by HR (Cloud et al. 2012). Therefore, further analysis is required to see if these proteins are also functionally equivalent in the repair of Spo11 and VDE DSBs.

The interesting biology of VDE allows one to study the repair of meiotic DSB irrespective of meiotic chromosome axis enrichment. I therefore created a recombination reporter system that undergoes meiotic DSB formation by VDE, in two loci that are hot and cold for Spo11 DSB formation, to examine effects on VDE repair in the vicinity of the axis and away for the axis. This allows us to examine the NCO and CO repair events in an unbiased physical assay, which is unaffected by issues such as spore viability. I reasoned that the study of such VDE DSBs close to and away

from the axis would be able to separate the influence of meiotic axis from the cell wide influence of the meiotic recombination proteins (Figure 1-11). If the primary level of regulation for meiotic HR is at the level of the meiotic axis, then VDE DSBs might not be repaired identically to Spo11 DSBs, which is enriched for CO formation. On the other hand, if meiotic HR is primarily controlled by the altered cell-wide recombination environment, then any DSB formed in meiosis should show repair that is similar to the Spo11 meiotic DSBs.

2 Materials and methods

2.1 Strain list

Strain	Genotype
3549	*MATa ho::LYS2 lys2 leu2-? nuc1Δ::LEU2 VMA1::VDE1* *---- -------- ---- ------ ---------- ----------* *MATl ho::lys2 lys2 leu2-? nuc1Δ::LEU2 VMA1* *ura3:: ura3::Ty1-[arg4-bgl]-URA3* *---------------------------------* *ura3:: NatMX-[arg4-rv::VDE]-KlTRP1* *arg4Δ(eco47iii-hpa1)* *--------------------* *arg4Δ(eco47iii-hpa1)*
3529	*MATa ho::LYS2 lys2 leu2-? nuc1Δ::LEU2 VMA1::VDE1* *---- -------- ---- ------ ---------- ----------* *MATl ho::lys2 lys2 leu2-? nuc1Δ::LEU2 VMA1* *ura3:: ura3::Ty1-[arg4-bgl]-URA3* *---------------------------------* *ura3:: NatMX-[arg4-rv::VDE]-KlTRP1* *spo11(Y135F)-HA3-his6::KanMX arg4Δ(eco47iii-hpa1)* *------------------------- --------------------* *spo11(Y135F)-HA3-his6::KanMX arg4Δ(eco47iii-hpa1)*
3677	*MATa ho::LYS2 lys2 leu2-? nuc1Δ::LEU2 VMA1::VDE1* *---- -------- ---- ------ ---------- ----------* *MATl ho::lys2 lys2 leu2-? nuc1Δ::LEU2 VMA1* *ura3:: ura3::Ty1-[arg4-bgl]-URA3* *---------------------------------* *ura3:: NatMX-[arg4-rv::VDE]-KlTRP1* *red1::LEU2 arg4Δ(eco47iii-hpa1)* *---------- --------------------* *red1::LEU2 arg4Δ(eco47iii-hpa1)*

Strain	Genotype
3673	*MATa ho::LYS2 lys2 leu2-? nuc1Δ::LEU2 VMA1::VDE1* *---- -------- ---- ------ ---------- ----------* *MATl ho::lys2 lys2 leu2-? nuc1Δ::LEU2 VMA1* *ura3:: ura3::Ty1-[arg4-bgl]-URA3* *---------------------------------* *ura3:: NatMX-[arg4-rv::VDE]-KlTRP1* *dmc1::LEU2 arg4Δ(eco47iii-hpa1)* *---------- --------------------* *dmc1::LEU2 arg4Δ(eco47iii-hpa1)*
3674	*MATa ho::LYS2 lys2 leu2-? nuc1Δ::LEU2 VMA1::VDE1* *---- -------- ---- ------ ---------- ----------* *MATl ho::lys2 lys2 leu2-? nuc1Δ::LEU2 VMA1* *ura3:: ura3::Ty1-[arg4-bgl]-URA3 dmc1::LEU2* *--------------------------------- ----------* *ura3:: NatMX-[arg4-rv::VDE]-KlTRP1 dmc1::LEU2* *spo11(Y135F)-HA3-his6::KanMX arg4Δ(eco47iii-hpa1)* *-------------------------- --------------------* *spo11(Y135F)-HA3-his6::KanMX arg4Δ(eco47iii-hpa1)*
3550	*MATa ho::LYS2 lys2 leu2-? nuc1Δ::LEU2 VMA1::VDE1* *---- -------- ---- ------ ---------- ----------* *MATl ho::lys2 lys2 leu2-? nuc1Δ::LEU2 VMA1* *ura3:: ura3::Ty1-[arg4-bgl]-URA3* *---------------------------------* *ura3:: NatMX-[arg4-rv::VDE]-KlTRP1* *ndt80::LEU2 arg4Δ(eco47iii-hpa1)* *---------- --------------------* *ndt80::LEU2 arg4Δ(eco47iii-hpa1)*
3675	*MATa ho::LYS2 lys2 leu2-? nuc1Δ::LEU2 VMA1::VDE1* *---- -------- ---- ------ ---------- ----------* *MATl ho::lys2 lys2 leu2-? nuc1Δ::LEU2 VMA1* *ura3:: ura3::Ty1-[arg4-bgl]-URA3 ndt80::LEU2* *--------------------------------- ----------* *ura3:: NatMX-[arg4-rv::VDE]-KlTRP1 ndt80::LEU2* *spo11(Y135F)-HA3-his6::KanMX arg4Δ(eco47iii-hpa1)* *-------------------------- --------------------* *spo11(Y135F)-HA3-his6::KanMX arg4Δ(eco47iii-hpa1)*

Strain	Genotype
3560	*MATa ho::LYS2 lys2 leu2-? nuc1Δ::LEU2 VMA1::VDE1* *MATl ho::lys2 lys2 leu2-? nuc1Δ::LEU2 VMA1* *ura3:: ura3::Ty1-[arg4-bgl]-URA3 TRP1* *ura3:: NatMX-[arg4-rv::VDE]-KlTRP1 trp1::hisG* *yen1::HphMX arg4Δ(eco47iii-hpa1)* *yen1::HphMX arg4Δ(eco47iii-hpa1)*
3676	*MATa ho::LYS2 lys2 leu2-? nuc1Δ::LEU2 VMA1::VDE1* *MATl ho::lys2 lys2 leu2-? nuc1Δ::LEU2 VMA1* *ura3::ura3::Ty1-[arg4-bgl]-URA3 TRP1* *ura3::NatMX-[arg4-rv::VDE]-KlTRP1 trp1::hisG* *KanMX::pCLB2-3HA-MMS4 arg4Δ(eco47iii-hpa1)* *KanMX::pCLB2-3HA-MMS4 arg4Δ(eco47iii-hpa1)*
3627	*MATa ho::LYS2 lys2 leu2-? nuc1Δ::LEU2 VMA1:103* *MATI ho::lys2 lys2 leu2-? nuc1Δ::LEU2 VMA1:103* *ura3:: ura3::Ty1-[arg4-VRS103]-URA3* *ura3:: NatMX-[arg4-VRS]-KlTRP1* *arg4Δ(eco47iii-hpaI)* *arg4Δ(eco47iii-hpaI)*
3617	*MATa ho::LYS2 lys2 leu2-? nuc1Δ::LEU2 VMA1:103* *MATl ho::lys2 lys2 leu2-? nuc1Δ::LEU2 VMA1:103* *ura3 his4:: his4'-URA3-[arg4-VRS103]-his4'* *ura3 his4:: NatMX-[arg4-VRS]-KlTRP1* *arg4Δ(eco47iii-hpaI)* *arg4Δ(eco47iii-hpaI)*

Strain	Genotype
3624	*MATa ho::LYS2 lys2 leu2-? nuc1Δ::LEU2 VMA1:103* *---- -------- ---- ------ ---------- --------* *MATa ho::lys2 lys2 leu2-? nuc1Δ::LEU2 VMA1:103* *ura3:: ura3::Ty1-[arg4-VRS103]-URA3* *---------------------------------* *ura3:: NatMX-[arg4-VRS]-KlTRP1* *pCUP1-VDE-KanMX-pCUP1-CUP1 arg4Δ(eco47iii-hpaI)* *------------------------- --------------------* *pCUP1-CUP1 arg4Δ(eco47iii-hpaI)*
3618	*MATa ho::LYS2 lys2 leu2-? nuc1Δ::LEU2 VMA1:103* *---- -------- ---- ------ ---------- --------* *MATl ho::lys2 lys2 leu2-? nuc1Δ::LEU2 VMA1:103* *ura3 his4:: his4'-URA3-[arg4-VRS103]-his4'* *---- --* *ura3 his4:: NatMX-[arg4-VRS]-KlTRP1* *pCUP1-VDE-KanMX-pCUP1-CUP1 arg4Δ(eco47iii-hpaI)* *------------------------- --------------------* *pCUP1-CUP1 arg4Δ(eco47iii-hpaI)*
3605	*MATa ho::LYS2 lys2 leu2-? nuc1Δ::LEU2 VMA1:103* *---- -------- ---- ------ ---------- --------* *MATl ho::lys2 lys2 leu2-? nuc1Δ::LEU2 VMA1:103* *ura3:: ura3::Ty1-[arg4-VRS103]-URA3* *---------------------------------* *ura3:: NatMX-[arg4-VDE]-KlTRP1* *pCUP1-VDE-KanMX-pCUP1-CUP1* *--------------------------* *pCUP1-CUP1* *spo11(Y135F)-HA3-his6::KanMX arg4Δ(eco47iii-hpaI)* *-------------------------- --------------------* *spo11(Y135F)-HA3-his6::KanMX arg4Δ(eco47iii-hpaI)*

Strain	Genotype
3606	*MATa ho::LYS2 lys2 leu2-? nuc1Δ::LEU2 VMA1:103* *MATl ho::lys2 lys2 leu2-? nuc1Δ::LEU2 VMA1:103* *ura3 his4:: his4'-URA3-[arg4-VRS103]-his4'* *ura3 his4:: NatMX-[arg4-VRS]-KlTRP1* *pCUP1-VDE-KanMX-pCUP1-CUP1* *pCUP1-CUP1* *spo11(Y135F)-HA3-his6::KanMX arg4Δ(eco47iii-hpaI)* *spo11(Y135F)-HA3-his6::KanMX arg4Δ(eco47iii-hpaI)*
3643	*MATa ho::LYS2 lys2 leu2-? nuc1Δ::LEU2 VMA1:103* *MATI ho::lys2 lys2 leu2-? nuc1Δ::LEU2 VMA1:103* *ura3:: ura3::Ty1-[arg4-VRS103]-URA3* *ura3:: NatMX-[arg4-VRS]-KlTRP1* *sae2::HphMX arg4Δ(eco47iii-hpaI)* *sae2::HphMX arg4Δ(eco47iii-hpaI)*
3645	*MATa ho::LYS2 lys2 leu2-? nuc1Δ::LEU2 VMA1:103* *MATI ho::lys2 lys2 leu2-? nuc1Δ::LEU2 VMA1:103* *ura3 his4:: his4'-URA3-[arg4-VRS103]-his4'* *ura3 his4:: NatMX-[arg4-VRS]-KlTRP1* *sae2::HphMX arg4Δ(eco47iii-hpaI)* *sae2::HphMX arg4Δ(eco47iii-hpaI)*

Strain	Genotype
3659	*MATa ho::LYS2 lys2 leu2-? nuc1Δ::LEU2 VMA1:103* *---- -------- ---- ------ ---------- --------* *MATI ho::lys2 lys2 leu2-? nuc1Δ::LEU2 VMA1:103* *ura3* *----------* *ura3:: NatMX-[arg4-VRS]-KlTRP1* *his4:: his4'-URA3-[arg4-VRS103]-his4'* *----------* *HIS4* *pCUP1-VDE-KanMX-pCUP1-CUP1 arg4Δ(eco47iii-hpaI)* *---------- ----------* *pCUP1-CUP1 arg4Δ(eco47iii-hpaI)*
3660	*MATa ho::LYS2 lys2 leu2-? nuc1Δ::LEU2 VMA1:103* *---- -------- ---- ------ ---------- --------* *MATI ho::lys2 lys2 leu2-? nuc1Δ::LEU2 VMA1:103* *ura3:: ura3::Ty-[arg4-VRS103]-URA3* *----------* *ura3* *HIS4* *----------* *his4:: NatMX-[arg4-VRS]-KlTRP1* *pCUP1-VDE-KanMX-pCUP1-CUP1 arg4Δ(eco47iii-hpaI)* *---------- ----------* *pCUP1-CUP1 arg4Δ(eco47iii-hpaI)*
3630	*MATI ho::LYS2 lys2 leu2-? nuc1Δ::LEU2 VMA1:103* *---- -------- ---- ------ ---------- --------* *MATa ho::lys2 lys2 leu2-? nuc1Δ::LEU2 VMA1:103* *ura3:: ura3::Ty1-[arg4-VRS103]-URA3 ndt80::LEU2* *---------- ----------* *ura3:: NatMX-[arg4-VRS]-KlTRP1 ndt80::LEU2* *pCUP1-VDE-KanMX-pCUP1-CUP1 arg4Δ(eco47iii-hpaI)* *---------- ----------* *pCUP1-CUP1 arg4Δ(eco47iii-hpaI)*

Strain	Genotype
3631	*MATa ho::LYS2 lys2 leu2-? nuc1Δ::LEU2 VMA1:103* *MATl ho::lys2 lys2 leu2-? nuc1Δ::LEU2 VMA1:103* *ura3 his4:: his4'-URA3-[arg4-VRS103]-his4'* *ura3 his4:: NatMX-[arg4-VRS]-KlTRP1* *pCUP1-VDE-KanMX-pCUP1-CUP1 ndt80::LEU2* *pCUP1-CUP1 ndt80::LEU2* *arg4Δ(eco47iii-hpaI)* *arg4Δ(eco47iii-hpaI)*
3621	*MATI ho::LYS2 lys2 leu2-? nuc1Δ::LEU2 VMA1:103* *MATa ho::lys2 lys2 leu2-? nuc1Δ::LEU2 VMA1:103* *ura3:: ura3::Ty1-[arg4-VRS103]-URA3* *ura3:: NatMX-[arg4-VRS]-KlTRP1* *pCUP1-VDE-KanMX-pCUP1-CUP1 ndt80::LEU2* *pCUP1-CUP1 ndt80::LEU2* *spo11(Y135F)-HA3-his6::KanMX arg4Δ(eco47iii-hpa1)* *spo11(Y135F)-HA3-his6::KanMX arg4Δ(eco47iii-hpa1)*
3640	*MATI ho::LYS2 lys2 leu2-? nuc1Δ::LEU2 VMA1:103* *MATa ho::lys2 lys2 leu2-? nuc1Δ::LEU2 VMA1:103* *ura3 his4:: his4'-URA3-[arg4-VRS103]-his4'* *ura3 his4:: NatMX-[arg4-VRS]-KlTRP1* *pCUP1-VDE-KanMX-pCUP1-CUP1 ndt80::LEU2* *pCUP1-CUP1 ndt80::LEU2* *spo11(Y135F)-HA3-his6::KanMX arg4Δ(eco47iii-hpa1)* *spo11(Y135F)-HA3-his6::KanMX arg4Δ(eco47iii-hpa1)*

Strain	Genotype
3665	*MATa ho::LYS2 lys2 leu2-? nuc1Δ::LEU2 VMA1:103* *---- -------- ---- ------ ---------- --------* *MATI ho::lys2 lys2 leu2-? nuc1Δ::LEU2 VMA1:103* *ura3:: ura3::Ty1-[arg4-VRS103]-URA3* *---------------------------------* *ura3:: NatMX-[arg4-VRS]-KlTRP1* *KanMX::pCLB2-3HA-MMS4 pCUP1-VDE-hphMX-pCUP1-CUP1* *-------------------- -------------------------* *KanMX::pCLB2-3HA-MMS4 CUP1* *arg4Δ(eco47iii-hpaI)* *-------------------* *arg4Δ(eco47iii-hpaI)*
3666	*MATa ho::LYS2 lys2 leu2-? nuc1Δ::LEU2 VMA1:103* *---- -------- ---- ------ ---------- --------* *MATI ho::lys2 lys2 leu2-? nuc1Δ::LEU2 VMA1:103* *ura3 his4:: his4'-URA3-[arg4-VRS103]-his4'* *----- ---------------------------------* *ura3 his4:: NatMX-[arg4-VRS]-KlTRP1* *KanMX::pCLB2-3HA-MMS4 pCUP1-VDE-hphMX-pCUP1-CUP1* *-------------------- -------------------------* *KanMX::pCLB2-3HA-MMS4 pCUP1-CUP1* *arg4Δ(eco47iii-hpaI)* *-------------------* *arg4Δ(eco47iii-hpaI)*
3681	*MATa ho::LYS2 lys2 leu2-? nuc1Δ::LEU2 VMA1:103* *---- -------- ---- ------ ---------- --------* *MATI ho::lys2 lys2 leu2-? nuc1Δ::LEU2 VMA1:103* *ura3:: ura3::Ty1-[arg4-VRS103]-URA3* *---------------------------------* *ura3:: NatMX-[arg4-VRS]-KlTRP1* *KanMX::pCLB2-3HA-MMS4 pCUP1-VDE-hphMX-pCUP1-CUP1* *-------------------- -------------------------* *KanMX::pCLB2-3HA-MMS4 CUP1* *yen1::HphMX arg4Δ(eco47iii-hpaI)* *---------- -------------------* *yen1::HphMX arg4Δ(eco47iii-hpaI)*

Strain	Genotype
3682	*MATa ho::LYS2 lys2 leu2-? nuc1Δ::LEU2 VMA1:103* *---- -------- ---- ------ ---------- --------* *MATI ho::lys2 lys2 leu2-? nuc1Δ::LEU2 VMA1:103* *ura3 his4:: his4'-URA3-[arg4-VRS103]-his4'* *----- ----------------------------------* *ura3 his4:: NatMX-[arg4-VRS]-KlTRP1* *KanMX::pCLB2-3HA-MMS4 pCUP1-VDE-hphMX-pCUP1-CUP1* *-------------------- -------------------------* *KanMX::pCLB2-3HA-MMS4 CUP1* *yen1::HphMX arg4Δ(eco47iii-hpaI)* *---------- --------------------* *yen1::HphMX arg4Δ(eco47iii-hpaI)*
3669	*MATa ho::LYS2 lys2 leu2-? nuc1Δ::LEU2 VMA1:103* *---- -------- ---- ------ ---------- --------* *MATI ho::lys2 lys2 leu2-? nuc1Δ::LEU2 VMA1:103* *ura3:: ura3::Ty1-[arg4-VRS103]-URA3* *---------------------------------* *ura3:: NatMX-[arg4-VRS]-KlTRP1* *mlh3Δ::KANMX6 pCUP1-VDE-hphMX-pCUP1-CUP1* *------------ --------------------------* *mlh3Δ::KANMX6 CUP1* *arg4Δ(eco47iii-hpaI)* *--------------------* *arg4Δ(eco47iii-hpaI)*
3670	*MATa ho::LYS2 lys2 leu2-? nuc1Δ::LEU2 VMA1:103* *---- -------- ---- ------ ---------- --------* *MATI ho::lys2 lys2 leu2-? nuc1Δ::LEU2 VMA1:103* *ura3 his4:: his4'-URA3-[arg4-VRS103]-his4'* *----- ----------------------------------* *ura3 his4:: NatMX-[arg4-VRS]-KlTRP1* *mlh3Δ::KANMX6 pCUP1-VDE-hphMX-pCUP1-CUP1* *------------ --------------------------* *mlh3Δ::KANMX6 CUP1* *arg4Δ(eco47iii-hpaI)* *--------------------* *arg4Δ(eco47iii-hpaI)*

2.2 Plasmid list

Plamsid	backbone	contents
911	pMLC28	arg4::VRS103 CAT Chloramphenicol resistance
912	pBR322	URA3 Hind3-Hind3 Hind3 arg4-rv::VRS103 Pst1-Pst1 BamH1-Sal1
913	pBR322	'his4' Pvu2-Cla1 EcoR1-Cla1 Pvu2 site converted to EcoR1 site URA3 Hind3-Hind3 Hind3 arg4::VRS Pst1-Pst1 BamH1-Sal1
914	pBR322	'his4' Pvu2-Cla1 EcoR1-Cla1 Pvu2 site converted to EcoR1 site URA3 Hind3-Hind3 Hind3 arg4::VRS103 Pst1-Pst1 BamH1-Sal1
915	pFA6a	kanMX6 pCUP1-3HA-VDE

2.3 Primer list

Table 2-1 List of primers.

Arg4 del 5' F	GCTCCAGGTGGTGTTGAATTG
Arg4 del 3' R	CTTTGACTGCGGACCTGAACT
	test for *arg4* deletion
FDrug 5 Ura chr	AGTTTTGACCATCAAAGAAGGTTAATGTGGCTGTGGTTTCAGGGTCCATA CCTTGACAGTCTTGACGTGC
RDrug 3 Ura pmj	TAGGGAGCCCAAACAGGTTTCTAAATATAATTGGGAACTTTGGGTCAAGT CGCACTTAACTTCGCATCTG
	PCR *NatMX* for insertion in recombination reporter at *URA3*
F klactrp1 5'pmj	AATCTGCTGTATTGAAGCAATTGGATAATTTGAAATCCCAATTAAATTAG AAGCTTCTGCAGGTCGACTCCGGTTCTGCTGC
New R klactrp1 3'chr	TTAGTTTTGCTGGCCGCATCTTCTCAAATATGCTTCCCAGCCTGCTTTTCT GAATTCGAGCTCGCCTCGAGGCCAGAAGAC
	PCR *KlTRP1* for insertion in heterologous recombination reporter at *URA3*
Arg4 5' add hom new F	AGCTACCGACTTGGCAGATT
Arg4 5' add hom new R	ACAGCAGATTTAGCGGTTCC

Chr V3' addhom new F	AAAGCAGGCTGGGAAGCAT
Chr V3' addhom new R	GTTCTTGATTTGTGCCCCG
	Flanking homology for *KlTRP1* insertion at *URA3*
5'FKlTRP1pbr	AATAACTAAAACGGCCGCAATAATACACACTATTGTAACCTCCCAAAGTCG AAGCTTCTGCAGGTCGACTCCGGTTCTGCTGC
New R klactrp1 3'chr	TTAGTTTTGCTGGCCGCATCTTCTCAAATATGCTTCCCAGCCTGCTTTTCT GAATTCGAGCTCGCCTCGAGGCCAGAAGAC
	PCR *KlTRP1* for insertion in homologous recombination reporter at *URA3*
5' F his4 NatMX	CAGCGTTTCTGTGACCGTCTAGACCCTCCTTCTTGGCAACGCACATAACA CCTTGACAGTCTTGACGTGC
3' R ded81 NatMX	TAGGGAGCCCAAACAGGTTTCTAAATATAATTGGGAACTTTGGGTCAAGT CGCACTTAACTTCGCATCTG
	PCR *NatMX* for insertion in homologous recombination reporter at *HIS4*
5' NatMX F hom	GTTCGCCCTAAATGCCTCT
3' NatMX F hom	ACAGTCACATCATGCCCCTG
5' NatMX R hom	CTCGACATCATCTGCCCAGA
3' NatMX R hom	CAGCTTCTGCAATATCGTCACC
	Flanking homology for *NatMX* insertion at *HIS4*
5' F pbr322 KlTRP1	AATAACTAAAACGGCCGCAATAATACACACTATTGTAACCTCCCAAAGTCG CTGCAGGTCGACTCCGGTTCTGCTGC
3' R his4 KlTRP1	GAAATGAAATCTGGATCAAGGGTGAAACTTCTGGCAATGGCCAAAAGCTT GAATTCGAGCTCGCCTCGAGGCCAGAAGAC
	PCR *KlTRP1* for insertion in homologous recombination reporter at *HIS4*
5' KlTRP1 F hom	ATGGCGACGTTATGCGCAA
3' KlTRP1 F hom	TGGGTATCTAGCAGCAGAACC
5' KlTRP1 R hom	CCTCTTAGTCTTCTGGCCTCGA
3' KlTRP1 R hom	CTGTTCATTGCTAGCCAAGATGC
	Flanking homology for *KlTRP1* insertion at *HIS4*

Arg4 probe 5'F	TTTACGTTCCTCCCTCTCTCT
Arg4 probe 3'R	CATCAAAGGATCGGTTTCAC
	arg4 porbe for southern blots
ded81' F probe	CAGAGCTGAAAAGTCCCACAC
ded81 R probe	CGCTGAAACGTGGATACAAGG
	ded81 porbe for southern blots

2.4 Plasmid PCR DNA preparation

Overnight 5ml LB cultures of E coli are centrifuged for 2 mins at 1500 x*g*, and the pellet is resuspended in 350 μl TENS (1X Tris EDTA, 0.1 M NaOH, 0.5% SDS). Then, quickly, 150 μl of 3 M NaOAc pH5.2 is added and tubes are inverted until a white precipitate forms. The tubes are then centrifuged at 16100x*g* for 5 mins, and the supernatant is transferred to a fresh eppendorf tube. 1:1 volume of phenol-chloroform-isoamyl alcohol is added, tubes are spun at 16.1x*g* for 10 mins and the supernatant is transferred to another fresh tube without touching the phenol: DNA interface. DNA is then precipitated by adding 2 volumes of 100% ethanol and 0.3 M NaOAC, spun at 16100x*g* for 15mins. The resultant pellet, which should be translucent, is then resuspended in 70% ethanol and spun down for 1 min and resuspended in 1X Tris EDTA (TE).

2.5 Transformnation of yeast/*E. coli* with electroporation

Overnight yeast cultures of YEPD for yeast are washed 3X in ice cold 1 M sorbitol at 4˚C and resuspended after the final wash by vortexing the pellet. LB cutures of E coli are washed 3X in ice cold deionized H_2O at 4˚C and resuspended after the final wash by vortexing the pellet. Final yield is approximately 30 μl cells/ml original culture. 40 μl cell suspension is then transferred to a cold eppendorf tube. For yeast transformation, 12.5 μg sonicated carrier fish DNA + 3 μg linear DNA or 1 μg plasmid is added to the cell suspension. If DNA has been digested by restriction enzymes, it is purified with phenol chloroform, precipitated with ethanol and finally resuspended in low salt buffer such as TE before adding to the transformation mix. For plasmid transformation as an episomal entity in *E coli*, no carrier DNA is used. The cell/DNA mix is then added to pre-cooled 0.2 cm electroporation cuvettes, which are completely dried before electroporation. Yeast cells are electroporated at 1.5 kV (kilovolts), 200 ohms, 25 microFarads and 0.5 ml ice-cold 1 M sorbitol is then added immediately. *E coli* cells are electroporated at 2.5 kV (kilovolts), 200 ohms, 25 microFarads, Cells are outgrown for 4 hrs in YEPD + 1 M Sorbitol for yeast at 30°C and LB for E coli at 37°C. Cells are then plated on selective media. For yeast, media is supplemented with 1 M sorbitol.

2.6 Dissection of yeast tetrads

Single colonies of strains to be mated are patched together on YEPD plates and grown at 30°C for one overnight. The mating patch is then replicated to 1% KAc plates and allowed to sporulate for 2 days at 30˚C. A small blob of spores is resuspended in 50 µl 1/10 gluculase (DuPont) and incubated for 5 min at room temperature. Then 0.5 ml water is added, the suspension is incubated at room temperature for another 20 mins and then put on ice at 4°C. Tetrads will soften up over ~1 hr and be easier to dissect. Digested tetrads are dissected onto YEPD plates that have been stored at room temperature. Spore colonies are ready to replica-plate after 2 days at 30°C.

2.7 PCR from yeast colonies

A small amount of a fresh yeast colony is suspended in 20 µl spheroplasting solution (1.2 M sorbitol, 100 mM KPO_4, pH7.4) + 1% β-mercaptoethanol and 1 mg/ml 80T Zymolyase (10 mg/ml). The suspension is incubated at 37°C for 40 mins and then at 98°C for 3 mins. 1µl of supernantant is used for PCR.

2.8 Quick DNA prep for mitotic yeast cultures

An overnight yeast culture is grown in 5 ml YEPD. Cells are centrifuged at 2,033*xg* for 2 mins, resuspended in 0.5 ml spheroplasting solution (1.2 M sorbitol, 0.1 M EDTA, 1% ß-mercaptoethanol, 1 mg/ml zymolyase, pH7.5) and incubated for 4 min at 37˚C until cells lyse when put into a drop of 20% SDS. The spheroplasts are then spun at 16100x*g* for 20 sec in the microfuge and the pellet is resuspended in 0.5 ml resuspension buffer (100 mM NaCl, 50 mM TRIS, 50 mM EDTA pH 8.0.). SDS is then added to 1% final concentration (i.e. 50 µl 10% SDS), the cell suspension mixed by inverting gently and then is incubated at 65˚C for 30 min. After the incubation, 0.2 ml 5 M potassium acetate (CH_3CO_2K) is added; suspension mixed by inverting gently and is then incubated on ice for 15 min. The cell suspension is then centrifuged at 16100x*g* for 30 min in a microfuge at 4˚C, and the supernatant is transferred to a fresh tube. 0.7 ml isopropanol is added and the samples are mixed by gentle inversion to precipitate DNA in a large clump. The clump is allowed to settle and the supernatant is decanted. The DNA pellet is then allowed to dry, resuspended in 0.3 ml TE + 0.3 M sodium acetate (CH_3COONa) + 0.1 µg/ml RNase (DNase free) and incubated at 37˚C for 30 min. 0.2 ml isopropanol is added to precipitate DNA and as before, the DNA pellet is dried and resuspended in 1X TE.

2.9 Meiotic time-course with presporulation in PSP2.

Strains for the meiotic time-course are streaked for single colonies on YEPD plates and incubated at 30˚C. A single colony from YEPD plate is then used to inoculate a 10 ml liquid YEPD culture and incubated for one overnight at 30˚C with aeration. The next day, 0.5 ml, 1.5 ml, 2.0 ml and 3.0 ml of the overnight saturated culture is added to 400 ml PSP2 presporulation medium (0.67% yeast nitrogen base, 0.2% yeast extract, 1% potassium acetate and 0.05M potassium biphtalate) at pH5.5, which is then divided into two 2 L flasks with 200 ml each and is incubated overnight at 30˚C with vigorous aeration for another overnight. On the next day, in the morning, the OD_{600} is measured for a ½ dilution of the PSP2 cultures, the culture with OD_{600} of 0.8-0.9 is pelleted at 2053x*g* for 3 mins at room temperature, washed once in 2 X 200 ml 1% potassium acetate and resuspended together in 400 ml sporulation medium (1% KAc + 0.001% polypropylene glycol) (supplemented for the relevant auxotrophies) and cultured at 30˚C with vigorous aeration in 4 L baffled Fernbach flasks. 30 ml of culture is taken every hour from 0 hr onwards for meiotic DNA and added to 8 ml 50% glycerol + 0.4 ml 10% sodium azide, pelleted as before and washed in 5 ml spherolplasting solution (1 M sorbitol, 0.05 M KPO_4 + 0.01 M EDTA + 20% glycerol pH7.5) and stored in -80°C. 0.75 ml samples are also taken at 0 hr and added to 0.75 ml ethanol and stored at -20°C at 0 hr and every hour onward, for DAPI staining.

2.10 Meiotic Timecourse with presporulation in SPS

Overnight cultures in YPED are prepared as above. These are then inoculated into 230 ml SPS presporulation medium (0.17% yeast nitrogen base, 0.5% yeast extract, 1% peptone, 1% potassium acetate, 0.5% ammonium sulphate and 0.05 M potassium biphtalate) at 1/ 500, 1 / 600, 1/700 and 1 /800 dilutions and are incubated at 30˚C with vigorous aeration for another overnight. On the next morning, the OD_{600} is measured for the SPS cultures, and the culture with OD_{600} of 1.3-1.4 is pelleted at 2053x*g* for 3 mins at room temperature and then resuspended in 230 ml 1% potassium acetate. 30 ml culture is taken for 0 hr meiotic DNA sample and added to 8 ml 50% glycerol + 0.4 ml 10% sodium azide, pelleted as before and washed in 5 ml spherolplasting solution (1 M sorbitol, 0.05 M KPO_4 + 0.01 M EDTA+ 20% glycerol pH7.5) and stored at -80°C. Meanwhile, the remaining 200 ml 1% potassium acetate suspension is pelleted and resuspended in 400 ml sporulation medium (1% potassium acetate + 0.001% polypropylene glycol +supplements) and cultured at 30˚C with vigorous aeration in 4 L Ferbach baffled flasks. Additional 30 ml meiotic DNA samples are taken every hour onwards for and are processed and stored as above. 0.75 ml samples are also taken at 0 hr and then every hour from 4 hrs onward for DAPI staining as above.

2.11 Meiotic DNA prep with CTAB-Cohex

This method achieves separation of nucleic acids from polysaccharides and proteins by exploiting the insolubility of cetyltrimethylammonium (CTAB) - nucleic acid complexes at low salt concentrations (Jones 1953, Dutta et al. 1953, Murray and Thompson. 1980, Allers and Lichten. 2000)

Frozen meiotic cell pellets are thawed on ice, resuspended in 500 µl Zymolyase solution (1 M sorbitol, 50 mM KPO_4 buffer pH7.5, 10 mM EDTA pH 7.5, 5mM hexamine cobalt chloride (CoHex), 1% ß-mercaptoethanol and 0.5 mg/ml zymolyase 100T), transferred to 5 ml (12 X 75 mm) polypropylene round-bottom tubes, and incubated at 37°C for 2-5 mins until spehroplasted (determined as above). Spheroplasts are then pelleted at 3000x*g* for 2 mins at 4°C, the supernatant is removed, and the pellet is resuspended in 500 µl CTAB extraction solution (3% CTAB, 100 mM Tris.HCl pH7.5, 25 mM EDTA pH 8, 2 M NaCl, 2% PVP40, 20 mM CoHex) by vortexing gently. Proteinase K (20mg/ml) to 0.5mg/ml final concentration and RNase (≥10 mg/ml) to 20 µg/ml final concentration are added and samples are mixed by vortexing gently. Samples are then incubated at 37°C for 15 mins, vortexing gently every ~5mins. Soluble DNA-CTAB complexes are formed during this incubation.

The CTAB extraction solution is then transferred to a 1.5 ml eppendorf tube containing 300 µl chloroform:isoamylalcohol (24:1) vortexed at full speed for 10 secs, shook thoroughly, and then vortexed again for 5 secs. Failure to vortex thoroughly leads to poor DNA recovery. Samples are then spun at top speed in microfuge (~6000x*g*) for 5 mins and upper (aqueous) layer is promptly transferred to 5 ml (12 X 75 mm) polypropylene round-bottom tube. 1.5 ml (~3 volumes) CTAB dilution solution (1% CTAB, 50 mM Tris.HCl pH7.5, 10 mM EDTA pH8, 4 mM CoHex) is layered on top, mixed by inverting gently ~5X and left undisturbed at room temperature for 10mins. After inverting ~5X, the solution should be faintly cloudy with little discrete localised precipitation. The tubes are then inverted until a discrete white precipitate is observed, which should sink to the bottom of the tube.

The supernatant is then removed gently. 1 ml TECoHex (10 mM Tris.HCl pH7.5, 1 mM EDTA pH8, 1 mM CoHex) + 0.4 M NaCl, is then added and the tube is shaken gently for the pellet to float. The 0.4 M NaCl TE wash removes excess CTAB that is not complexed with nucleic acid, and most of the acidic polysaccharides that are precipitated by CTAB. After the 0.4M NaCl wash, TECohHeX + 1.42 M NaCl is added and the tube is gently shaken to resuspend pellet. The high salt concentration will re-solubilize the CTAB:DNA complexes. The suspension is then transferred to 1.5 ml eppendorf tubes. 1 ml ethanol is added at room temperature and tubes are inverted until the DNA is completely precipitated. Ethanol only precipitates DNA, as CTAB is highly soluble in ethanol. The supernatant is removed and the pellet is washed in 1ml 70% ethanol, 30% 1 mM CoHex

at room temperature. The pellet is then resuspended in 100 μl of ice cold 10 mM Tris.HCl pH7.5, 10 mM $MgCl_2$, 200 mM NaCl. Once the pellet has completely resuspended, 200 μl ethanol is added to precipitate DNA at room temperature, the DNA pellet is washed twice in 200 μl 70% ethanol-$MgCl_2$ (70% ethanol, 30% 10 mM $MgCl_2$) at room temperature, and DNA is finally suspended in ice cold 10 mM Tris.HCl pH7.5, 2 mM $MgCl_2$, 50 uM sperimidine.

2.12 DAPI staining of nuclei to monitor meiotic progression

1 μl of a 0.1 mg/ml DAPI solution (1 mg/ml) is added to cells in 1.5 ml cells in 50% ethanol, left at room temperature (RT) for 5 mins, and then spun down at 1500*xg* for 3 mins in a microfuge. The supernatant is removed and pellet is washed with 0.5 ml water, pelleted again at 1500*xg* for 3 min and then is resuspended in 0.5 ml water. Samples are observed by fluorescence microscopy under a 63X or 100X objective. Cells with 1 nucleus are counted as undivided, cells with 2 nuclei are past meiosis I and cells with 3-4 nuclei have completed meiosis II.

2.13 Digestion and Sothern Blotting to monitor meiotic recombination at the molecular level

Genomic DNA extracted by CTAB-CoHex can be digested by different enzyme to monitor different species of meiotic recombination. For the heterozygous cassette at *URA3* (Figure 4-1), cumulative VDE DSB levels are determined by monitoring the level of uncut *arg4-VRS* parents, this is analyzed by an *Eco*RV-*Bg*lII digest of genomic DNA at 37°C. The DNA is then loaded onto 0.5% agarose gels in 45 mM Tris Borate + 1 mM EDTA (TBE) in TBE running buffer and run at 2 V/cm for 13 hrs. Free DSB and joint molecules are monitored by digesting genomic DNA with *Hind*III in presence of 0.1 mM spermidine at 37°C . The digested DNA is then loaded onto 0.5% agarose gels in TBE + 4 mM $MgCl_2$ gel in TBE + 3mM $MgCl_2$ running buffer and run at 2 V/cm for 25.25 hrs for the *URA3* reporter and 24.25 hrs for the *HIS4* reporter. NCOs and COs are monitored by digesting genomic DNA with PI-*Sce*I-*Hind*III double digest in NEB buffer PI*Sce*I at 37°C. The digested DNA is then heated at 65°C to denature PI*Sce*I, which aggregates on DNA, and then loaded onto 0.5% agarose gels in TBE in TBE running buffer and run at 2 V/cm for 25.25 hrs for the *URA3* reporter and 24.25 hrs for the *HIS4* reporter.

In the case of $MgCl_2$ gels, Mg^{2+} has to be removed before they can be blotted, which is done by washing these gels twice for 15 mins each in 10 mM and 5 mM EDTA. Gels are then rinsed in water for 5 mins.

Gels are then depurinated by washing in 0.25 M HCl for at least 20 mins. Gels are then rinsed in water again 5 mins and then transferred to a

vacuum blot apparatus over a nylon membrane positively charged with quaternary amine groups and covered in transfer buffer (0.5 M NaOH, 1.5 M NaCl) and blotted under vacuum.

After blotting, the membranes are sequentially rinsed in 250 ml 0.5 M Tris-HCl pH7.5, 1 M NaCl and then 0.15 M sodium chloride, 0.010 M sodium phosphate, 0.001 M EDTA buffer (2X SSPE). DNA is then crosslinked onto the membrane by exposure UV irradiation and the blot is transferred to 40 ml pre-incubated prehybridization buffer (2X SSPE, 1% SDS, 0.5% Not-fat Dry Milk, 200 μg/ml Fish DNA) and incubated with gentle shaking at 65°C for 4 hrs.

During pre hybridization, the DNA probe is made by adding 25 ng probe, 0.2 ng λDNA for DNA size markers, 100 μCi [α-^{32}P] dCTP and High Prime (Roche) in a 20 μl reaction volume and incubating at 37°C for 10 mins. The reactions are then purified on illustra MicroSpin G-50 Columns.

After 4 hrs, pre hybridization buffer is removed and blots and put in 30 ml pre-heated hybridization buffer (2X SSPE, 1% SDS, 0.5% Not-fat Dry Milk, 1.5 g dextran sulphate, 200 μg/ml Fish DNA and [α-^{32}P] dCTP labeled DNA probe) and incubated at 65°C for >16 hrs. Sequences in *arg4* or *ded81* are used to probe Southern blots. The primers for these probes are in the primer list (Table 2-1).

After hybridization, the blot is washed twice in 2X SSPE, 0.1% SDS at room temperature, once in 0.2X SSPE, 0.1% SDS at room temperature and once in 0.2X SSPE, 0.1% SDS at 60°C. The blot is finally rinsed in 0.2X SSPE, wrapped in clingfilm (Saran Wrap, Dow) and exposed on a phosphoimager screen.

3 Design and Construction of the VDE recombination reporter system to study homologous recombination in meiosis

3.1 Designing a recombination reporter at *URA3* to monitor VDE DSB repair by homologous recombination (HR)

The object of this study was to better understand the process of homologous recombination (HR) during meiosis using a VDE DSB initiated reporter system. A recombination reporter with a VDE recognition sequence (VRS) inserted in *arg4* and flanked by *URA3* sequences already existed at the *URA3* locus in *S. cerevisiae* (Neale et al. 2002)(Figure 3-1A). However this cassette was not suitable for our studies because of the following:

1. The recombination reporter in Figure 3-1A from Neale et al. (2002) has *arg4* with a VDE recognition sequence (*arg4-VRS*) flanked by *URA3* sequences and these represent significant flanking homology of ~800 bp, which facilitate an alternate pathway for repair of the VDE DSB by single strand annealing (SSA). During meiosis, as much as ~50% of *arg4* chromatids containing the VRS site are repaired by SSA which leads to deletion of the reporter cassette, while only ~40% of *arg4-VRS* chromatids are repaired by HR (Neale et al. 2002, Terentyev et al. 2010). Repair by SSA rises to as much as ~80% of *arg4-VRS* chromatids in *spo11Y135F* cells lacking genome wide Spo11 DSBs, and HR constitutes a very minor fraction of repair events in these cells (Neale et al. 2002, Terentyev et al. 2010).
2. Also, both homologues in the Neale et al. 2002 recombination cassette are identical, with no flanking heterologous markers. CO recombinants therefore cannot be separated from the parental chromosomes in Southern blots (Neale et al. 2002, Terentyev et al. 2010).
3. The cassette bears homology to the endogenous *ARG4* locus, as the strains in Neale et al. (2002) carried the *arg4-nsp,bgl* allele. This allows the possibility of ectopic recombination and limits the availability of Southern probes that can detect all chromatids.

In order to fix issues 1 and 2, the flanking *URA3* homologies were replaced with *NatMX* upstream of *arg4-VRS*, and *Kluveromyces lactis TRP1 (KlTRP1)* downstream of *arg4-VRS* (Figure 3-1B,C). This also creates flanking restriction site polymorphisms, which allow differentiation of recombinant chromosomes from parental chromosomes in Southern blots. Tetrad dissection of a hemizygous diploid with *arg4-VRS* cassette on one homologue and *ura3::Ty1* on the other homologue shows that less than 1% of VRS containing spores are viable, while 94% of *ura3::Ty1* spores are viable (Table 3-1). This shows that repair of the DSB on the

arg4-VRS chromosomes requires homology on the other chromosome. For the third issue about the possibility of ectopic recombination between the recombination reporters and the endogenous *ARG4* locus, *arg4Δ(eco47iii-hpaI)* was crossed into the new strains. Haploid spores carrying *arg4Δ(eco47iii-hpaI)* were detected by PCR with primer upstream and downstream of *ARG4*, these primers give a larger product for *arg4-nsp,bgl* versus a smaller products for *arg4Δ(eco47iii-hpaI)* (Figure 3-13A).

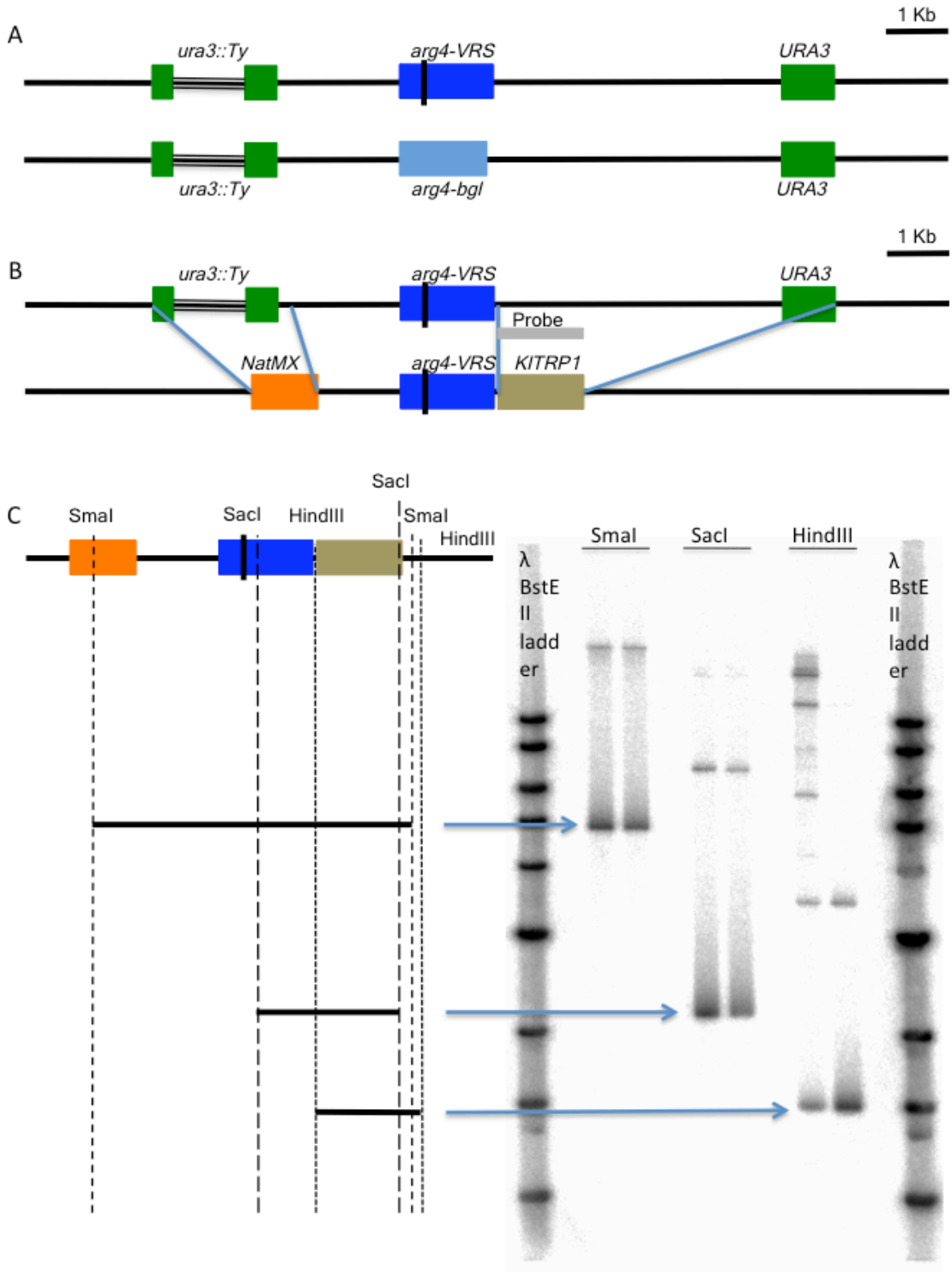

Figure 3-1 Redesigning the recombination cassette to remove flanking *URA3* homologies by transformation with NatMX and KlTrp1 sequences respectively
A) Map of Neale et al. (2002) recombination reporter cassette.
B) Upstream *uar3::Ty1* was replaced with *NatMX*, downstream *URA3* was replaced with *KlTRP1*.
C) Southern blot of transformants after sequential transformation of *NatMX* and *KlTrp1*, digested with *Sma*I, *Sac*I and *Hind*III, and probed with *KlTRP1* sequences. Map of digest bands are illustrated alongside the Southern blot, partial digests of products are seen above main bands.

Total hemizygous tetrads	Viable spores	Spore viability	Viable *arg4-VRS* spores	Viable *ura3::Ty* spores	VRS spore viability	non VRS spore viabilty
40	79	0.49	4	75	0.05	0.94

Table 3-1 Dissection of hemizygous tetrads shows VDE DSB cannot be repaired without homologous partner.

3.2 Inefficient repair of VDE DSBs in recombination reporter and no parity between crossovers suggesting non reciprocal events

Having modified the existing VDE recombination reporter cassette, I assayed for HR recombination products in WT, *spo11Y135F* (henceforth referred to as *spo11*), *ndt80* and *spo11 ndt80* by Southern blotting. However, VDE DSB repair by HR in the new recombination reporter showed the following problems:

1. In all the strains examined for VDE DSB repair, Southern blots of genomic DNA digested *Hind*III and probed for *ARG4* sequences showed that the DSB would persist at ~5% even at 9hrs (Figure 3-2A). This indicated that VDE DSB repair by HR was not efficient in the modified recombination reporter.
2. To confirm if repair of VDE DSBs was indeed impaired in the modified recombination reporter, Southern blots of meiotic DNA were digested with *Hind*III and probed with *DED81* sequences. The *ded81* 3' end is present in the *arg4* PstI to PstI fragment in the recombination cassette and additionally, the probe is also detects the natural *DED81* locus on chromosome 8, which provides a loading control to compare the total chromosome material (Figure 3-2A). When the total material originating from the *arg4-VRS* chromatid (the sum of the parental, free DSB and CO1 bands) was compared to the *DED81* loading control band, it revealed a loss of 50% chromosome material in WT strains while the level of *arg4-bgl* chromosomes remain stable (Figure 3-2C). This loss of *arg4-VRS* chromatids increased further in *spo11, ndt80 and spo11 ndt80* mutants (Figure 3-2D). Thus, half of the *arg4-VRS* chromatids are not repaired during meiosis in the new recombination reporter.
3. Finally, physical analysis of VDE initiated recombination also showed that at 9 hrs, there were about 1½ times as many CO1 products as compared to CO2 (Figure 3-2E). As reciprocal products of HR, levels of CO1 and CO2 should be roughly equal.

The inefficient repair of VDE DSBs was also observed in genetic studies (Table 3-2), where spore viability for WT tetrads was about 55%. The ratio of viable spores that arise from *arg4-VRS* parent (P1 and CO1), to viable spores that arise from *ar4-bgl* parent (P2 and CO2), is 0.46. This also suggests that VDE DSB repair leads to loss of half the VRS containing

chromatids, which is consistent with the ratio of *arg4-VRS* to *arg4-bgl* chromatids obtained from physical analysis.

A possible reason, which could explain the inefficient repair of VDE DSB, was the sequence heterology in the recombination reporter. The VDE recombination reporter has an *arg4-VRS* allele on one homologue, which is cut by VDE and repaired from the *arg4-bgl* allele on the other homologue. Since the other allele has no *VRS* sequences, there is a 74 bp heterology right at the DSB site. This heterology resulted in no residual DSBs or chromosome loss in Neale et al. (2002), however that cassette had ~800 bp flanking homologies upstream and downstream of the VDE DSB, which permits repair by SSA in addition to HR (Neale et al. 2002). SSA is nearly 100% efficient with flanking homologies of ~415 bps (Sugawara et al. 2000), therefore any inefficiency of VDE DSB repair by HR in the Neale et al. (2002) cassette could be compensated for by SSA.

DNA sequence divergence has a significant role in reducing the efficiency of homologous recombination. Studies into recombination rates in diverged sequences in mitotic cells reveal that a sequence divergence of 9% in a 350 bp intronic substrate (~32 nt) reduces the rate of recombination by 50 fold (Datta et al. 1996). The heterology for our recombination reporter is 74 bps right at the DSB site, which suggests there are ~32 bps of non-homologous sequence at the end of the invading strand, which may inhibit strand invasion. Single molecule studies of the prokaryotic recombinase RecA show that during strand invasion, the length of DNA synapsis after strand exchange is ~80 bp (van der Heijden et al. 2008). Thus, a 32 bp stretch of heterologous nucleotides represent ~40% of the DNA involved in the homology search. I therefore sought to reduce this sequence heterology from the VDE recombination reporter.

The second discrepancy observed from physical analysis of VDE initiated meiotic recombination was the significant disparity between the levels of crossovers, with 1½ times greater level of CO1 compared to CO2. (Figure 3-2E). Genetic studies involving tetrad dissection also show a 2 fold excess of CO1 over CO2 spores (Table 3-2). As discussed in introduction section 1.1.2, HR creates reciprocal COs by the resolution of a common dHJ intermediate, and hence the two CO products should be at equal levels. On the other hand, alternate repair processes such as break induced replication (BIR) (discussed in section 1.2) create only non-reciprocal COs, and hence can create disparity between CO products. Genetic studies of a frequent DSB induced by I-SceI in mitotic cells show that ~2% of recombinants are produced by BIR (Ho et al. 2010). As VDE is constitutively expressed of from *VMA1::VDE* promoter in the heterologous system, it is possible that some VDE DSBs may form during meiotic S phase or even mitosis, and these DSBs may be repaired by BIR. In Southern blots, in even the WT strain, faint DSBs and COs were observed in the 0hr time-point (Figure 4-1A,B), suggesting pre-meiotic recombination events which complicate the analysis of meiotic

recombination. Therefore, I sought to remove VDE from the constitutively active *VMA1* promoter, and place it under an inducible promoter system.

In addition to the two goals of reducing the heterology in the VDE recombination reporter and controlling VDE expression, another goal was to clone the recombination reporter in a different locus from *URA3,* which is a cold-spot for Spo11 DSBs and hence is likely to be away from the meiotic axis (Panizza et al. 2011). Moving the VDE recombination reporter to a Spo11 DSB hot-spot locus would provide the opportunity to study VDE DSB repair in the vicinity of the meiotic axis (Blat et al. 2002, Panizza et al. 2011), to see if the local environment of Spo11 DSBs has any effect of DSB repair.

The final issue I sought to address with the VDE recombination reporter system was the possibility that the VDE DSB at the *VMA1* natural locus was also causing some inviability. Examining the genetic data from Table 3-2, we can also determine absolute viability for spores containing the *arg4-VRS* chromatid versus the *arg4-bgl* chromatid, rather than their relative viabilities. Total viable spores containing the *arg4-VRS* chromatid i.e. P1 and CO1 spores number 110 + 80 = 190. *arg4-VRS* spores should be half the total spore population, therefore absolute spore viability for *arg4-VRS* spores is 190/(1092/2) = 0.35. Since the *arg4-VRS* chromatids as determined by physical assay are at 50% the level of starting chromatid material, genetic assays reveal an additional 15% loss, which could be attributed to the VDE DSB at the *VMA1* natural locus. Even *arg4-bgl* spores have an absolute spore viability of (P2+CO2)/(1092/2) = (363 + 40)/546 = 0.74, which could be due to VDE DSB repair at *VMA1* in addition to *URA3*. Therefore, removing the possibility of VDE DSB formation at the *VMA1* loci could remove this additional spore inviability.

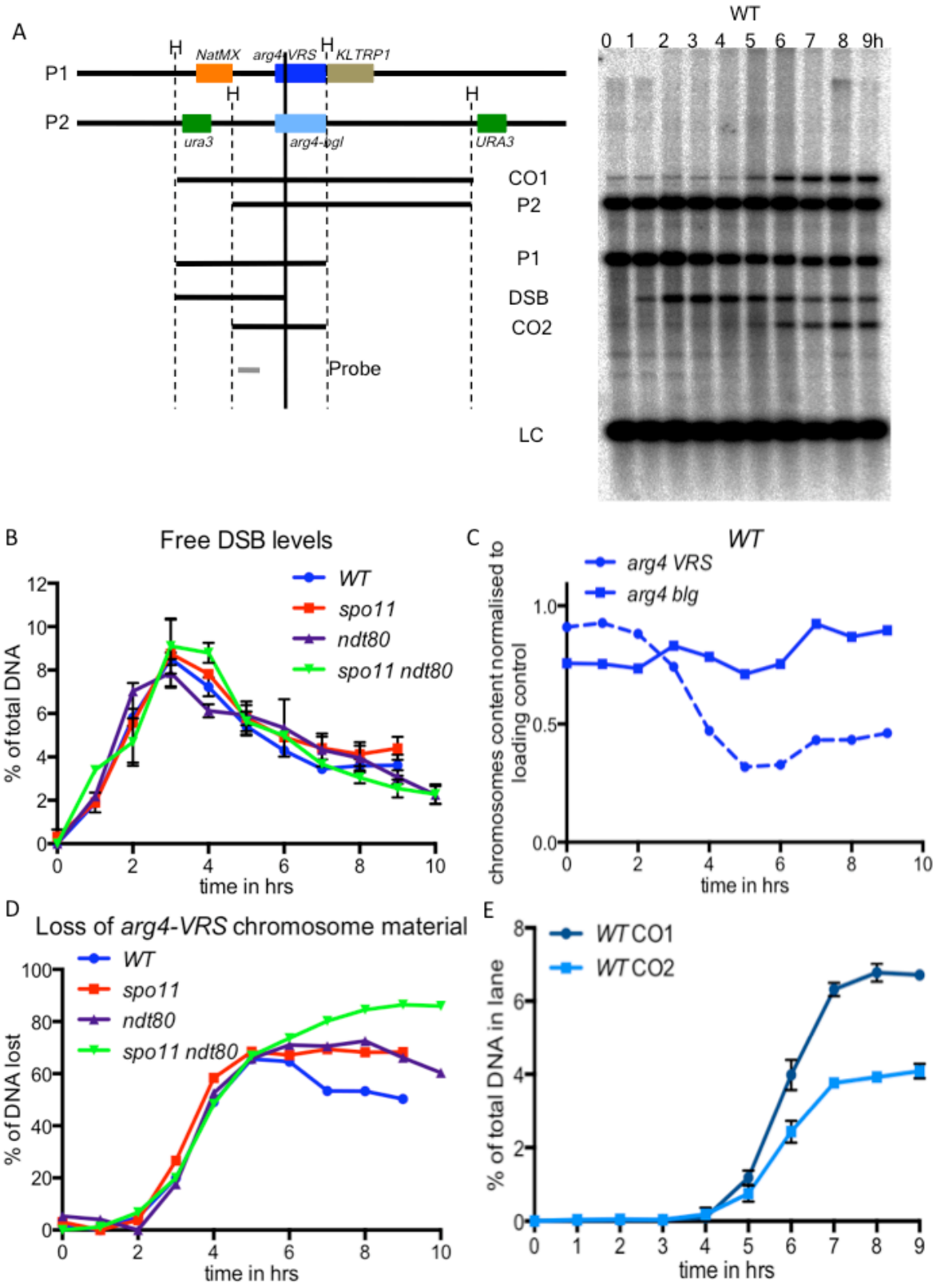

Figure 3-2 Inefficient DSB repair in recombination cassette with heterology at the DSB site
A) *Hind*III digest to separate parental *arg4 –VRS* (P1) and *arg-bgl* (P2) chromosomes, both interhomologue crossovers (CO1 and CO2), the free VDE double strand break (DSB) and also the *arg4* natural locus used as a loading control (LC). The same labeling shall be used for all subsequent Southern blots using the same digest and probe.
B) The VDE DSB is not fully repaired and persists at ~5% even at 9 hrs

C) Comparing the total chromosome material from each parent shows reduction of *arg4-VRS* chromosomes from ~1 to ~0.5, while *arg4-bgl* material remains stable.
D) Loss of *arg4-VRS* chromosome material goes from 50% in WT to 86% in *spo11 ndt80.*
E) Reciprocal homologous crossovers are not equal, CO1 is at 6/76% while CO2 is at 4.09%

Tetrads dissected	Viable spores	Spore viability	P1 spores	P2 spores	CO1 spores	CO2 spores	VRS chromaitds spore viabilty (P1+CO1) (P2+CO2)	CO1 CO2 ratio
273	595	0.55	110	363	80	40	0.46	2

Table 3-2 Genetic analysis of VDE DSB repair by tetrad dissection in heterologous reporter strain MJL 3549.

3.3 Removing heterology at the repair site on the homologue corresponding to DSB by cloning *arg4-VRS103* in place of *arg4-bgl* on the other homologue at *URA3*.

As explained in the previous section, the repair of the VDE DSB in the heterologous cassette with *arg4-VRS* opposite *arg4-bgl* is not efficient. In this cassette, there are 74 bps of *VRS* sequence that are absent on the other homologue. Homologous recombination requires a homology-based search by the single stranded DNA at the break site to find a template partner for repair. Therefore, to improve the rate of homologous recombination in our VDE reporter system, I sought to remove the heterology at the DSB site by cloning a mutated VRS sequence which is resistant to VDE cleavage. This sequence is from a allele of *VMA1,* called *VMA1-103*, which is WT for *VMA1* function, but resistant to cleavage by VDE due to 4 bp mutations adjacent to the VDE cut-site (Gimble and Stephens. 1995). This sequence will be henceforth referred to as *VRS103*, and PCR product of the *VMA1-103* cut-site i.e the *VRS103* sequence is not cleaved by VDE/PI*Sce*I in vitro (Figure 3-13B). The *VRS103* sequence would be then inserted into the *ARG4* gene in the recombination cassette on the other homologue. The scheme of this cloning is described in Figure 3-3. The *VRS103* oligonucleoitde sequence was initially synthesized and then was cloned into the *Eco*RV site of *ARG4* in pMJ77 (Figure 3-3). The *arg4-VRS103* allele so created was then inserted into pMJ391, which contains the recombination reporter cassette, replacing *arg4-VRS* to make pMJ912 (Figure 3-4A). Transformants were genetically tested (data not shown). Genomic DNA was then extracted from the final transformants of *arg4-VRS103* at the *URA3* locus, digested with *Bsa*XI, which cuts within *arg4* and also in flanking regions (Figure 3-4B). Probing these digests with *arg4* gives one band for single insertion, but two bands if more than one copy of the recombination insert is present (Figure 3-4B).

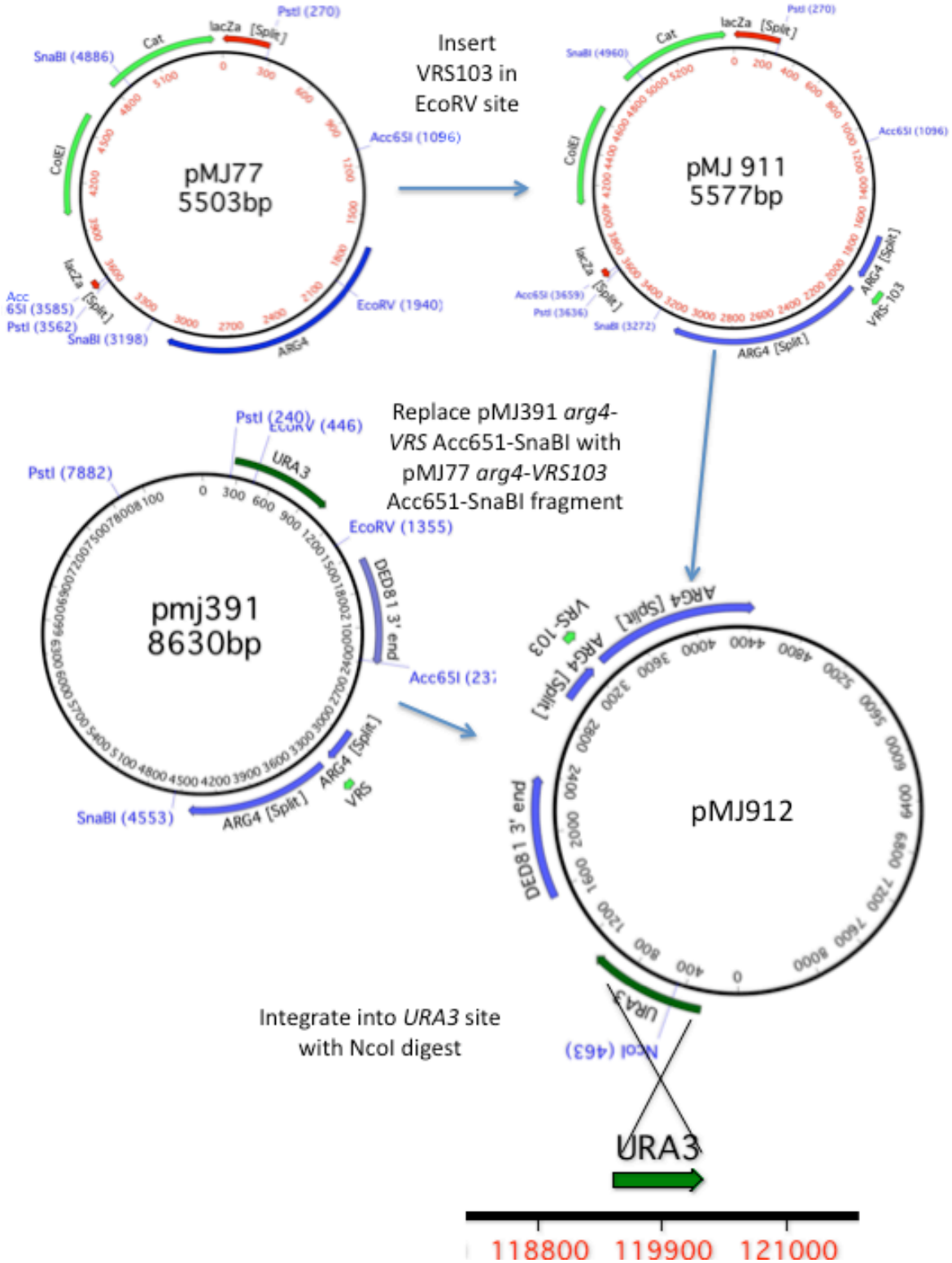

Figure 3-3 Scheme of cloning *arg4-VRS103* opposite *arg4-VRS* site on the homologue. The synthesized VRS103 sequence is inserted into the *ARG4* gene in pMJ77, and this *arg4-VRS103* allele is subsequently cloned into pMJ391, which contains the recombination reporter. The new plasmid pMJ912 is then integrated at *URA3* by an *Nco*I digest.

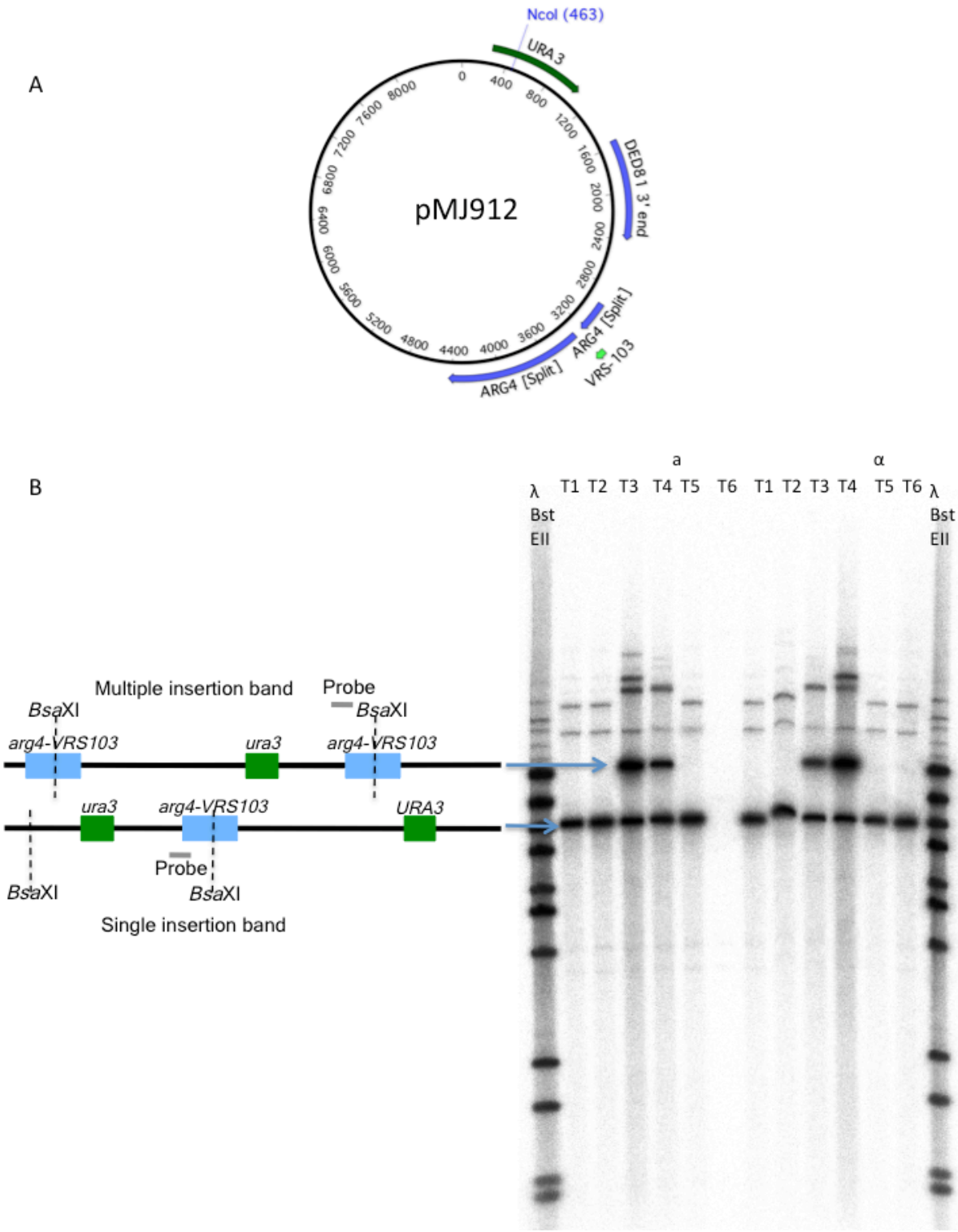

Figure 3-4 . Cloning *arg4-VRS103* to *URA3* locus
A) Plasmid map of pMJ912, which has *arg4-VRS* and *URA3*, *Nco*I digestion targets the plasmid to *URA3*
B) Southern blot of transformants after transformation of pMJ912, digested with *Bsa*XI, and probed with *ARG4* sequences. Map of digest bands are illustrated alongside the Southern blot, partial digests of products are seen above main bands.

3.4 Moving the VDE recombination reporter system to the *HIS4* locus

The VDE recombination reporter system was initially inserted at *URA3,* which had been previously determined as a Spo11 DSB-cold region using a precursor recombination reporter with *URA3* and *ARG4* sequences (Wu and Lichten. 1995, Borde et al. 1999). As discussed in the introduction section 1.4.10, meiotic axial element proteins Red1 and Hop1 are enriched in DSB-hot regions, and Spo11 then forms meiotic DSBs by interacting with the meiotic axis (Blat et al. 2002, Panizza et al. 2011). Consistent with this, the *URA3* locus, which is cold for Spo11 DSB formation, also does not show Red1 and Hop1 enrichment (Panizza et al. 2011). Therefore, the VDE DSB at *URA3* may be in a different chromosome context from most Spo11 DSBs. In order to determine if the chromosome context affects DSB repair, we moved the recombination reporter to the well-known meiotic DSB hot-spot, *HIS4* (Detloff et al. 1992, White and Petes. 1994, Fan et al. 1995, Borde el al. 1999), which also shows enrichment for the meiotic axial elements Red1 and Hop1 (Panizza et al. 2011).

The scheme for moving the *arg4-VRS* chromatid to the *HIS4* locus is described in Figure 3-5. The plasmid pMJ913 contains *arg4-VRS013* in a recombination cassette that can be targeted to *HIS4* (Figure 3-6A). The final transformants were genetically tested (data not shown). Genomic DNA was then extracted as before, digested with PI*Sce*I, which cuts within *arg4-VRS*, and *Hind*III, which cuts in flanking regions (Figure 3-6B). As before, probing with *arg4* sequences gives one band, for single insertion, while multiple insertions gives 2 bands due to multiple *arg4* copies. No multiple insertions were seen in Southern blot (Figure 3-6B). As with the recombination reporter at *ura3,* the flanking *his4'* homologies generated by the integration were then removed by sequential transformation of *NatMX* upstream of *arg4-VRS* and *KlTRP1* downstream of *arg4-VRS* (Figure 3-7A). Transformants were tested by HindIII digestion of their genomic DNA, which was then probed by *KlTRP1* sequences (Figure 3-7B).

The scheme for moving the opposite homologous *arg4-VRS103* chromatid to *HIS4* is described in Figure 3-8, by creating the plasmid pMJ914, which contains *arg4-VRS103* with a recombination cassette that can be targeted to *HIS4* (Figure 3-9A). Transformants were genetically tested (data not shown) and then genomic DNA was extracted for Southern blots. Genomic DNA was digested with *Bsr*GI, which cuts within *arg4*, and *Bst*EII, which cuts in flanking regions (Figure 3-9B). Probing with *arg4* sequences gives one band, for single insertion, while multiple insertions gives 2 bands due to multiple *arg4* copies. No multiple insertions were seen in Southern blots (Figure 3-9B).

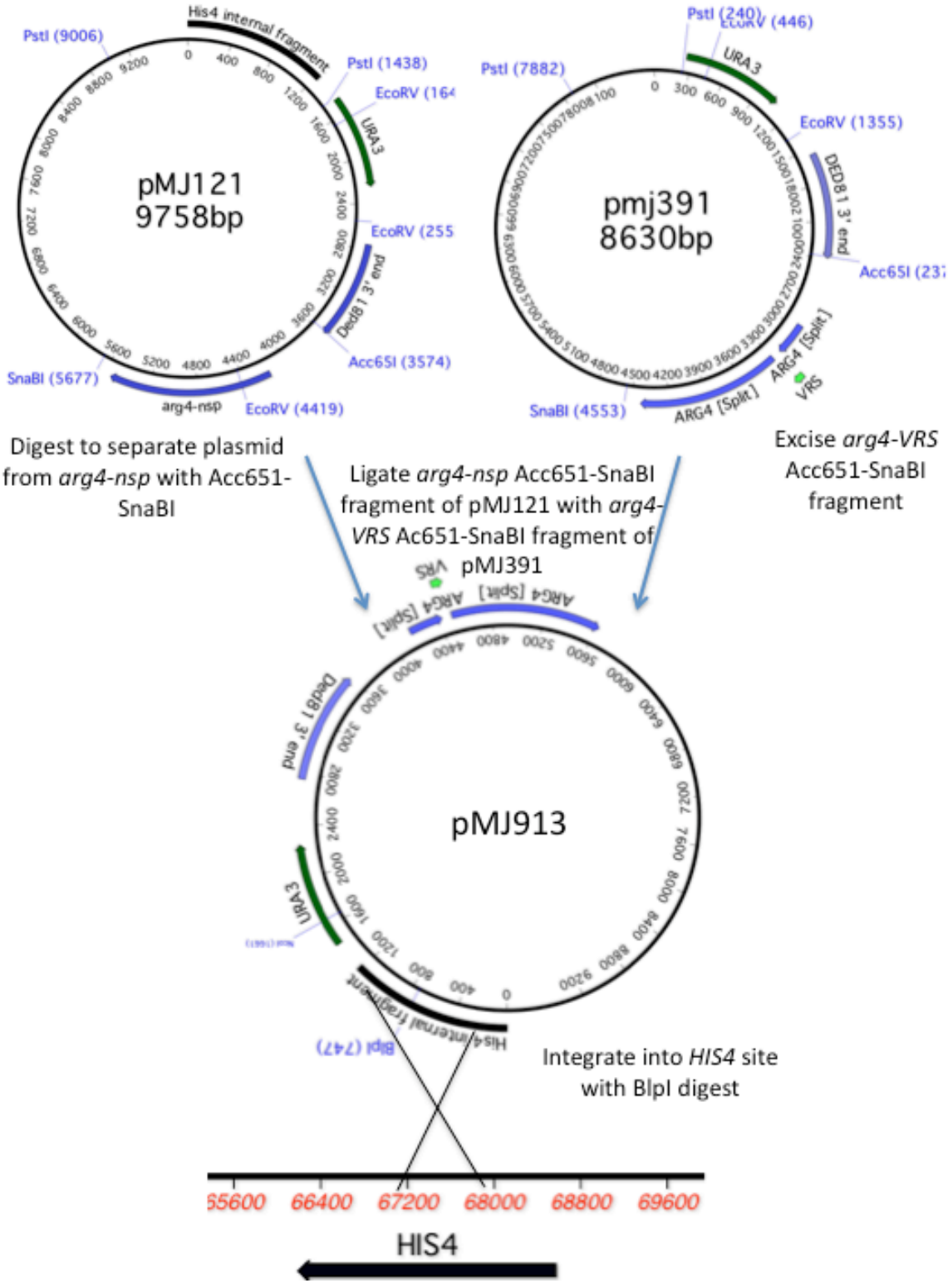

Figure 3-5 Scheme of moving *arg4-VRS* recombination reporter to *HIS4*. The *arg4-VRS* fragment from pMJ391 was excised and put in pMJ121 in place of *arg4-nsp* to form pMJ913 with *his4'* internal fragment and the recombination reporter cassette. pMJ913 was then integrated at *HIS4* by BlpI digest.

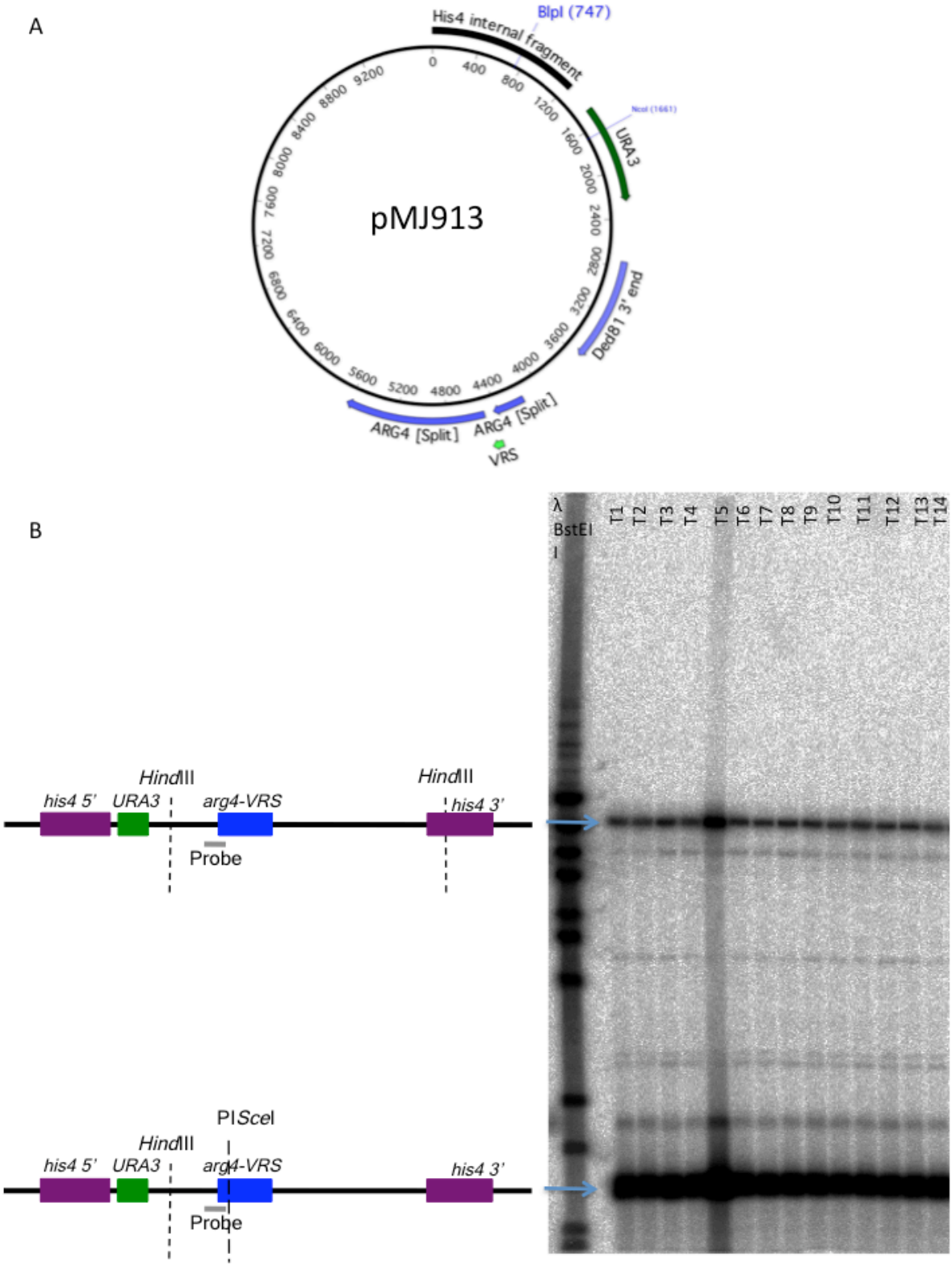

Figure 3-6 Cloning *arg4-VRS* to *HIS4* locus
A) Plasmid map of pMJ913, which has *ar4-VRS, URA3* and *his4* internal fragment (*his4'*), *Blp*I digest within *his4'* targets plasmid to *HIS4.*
B) Southern blot of transformants after transformation of pMJ913, digested with *Hind*III and PI*Sce*I, and probed with *ARG4* sequences. Map of digest bands are illustrated alongside the Southern blot, partial digests of products are seen above main bands. Sub stoichiometric higher band is caused by partial digestion by PISceI.

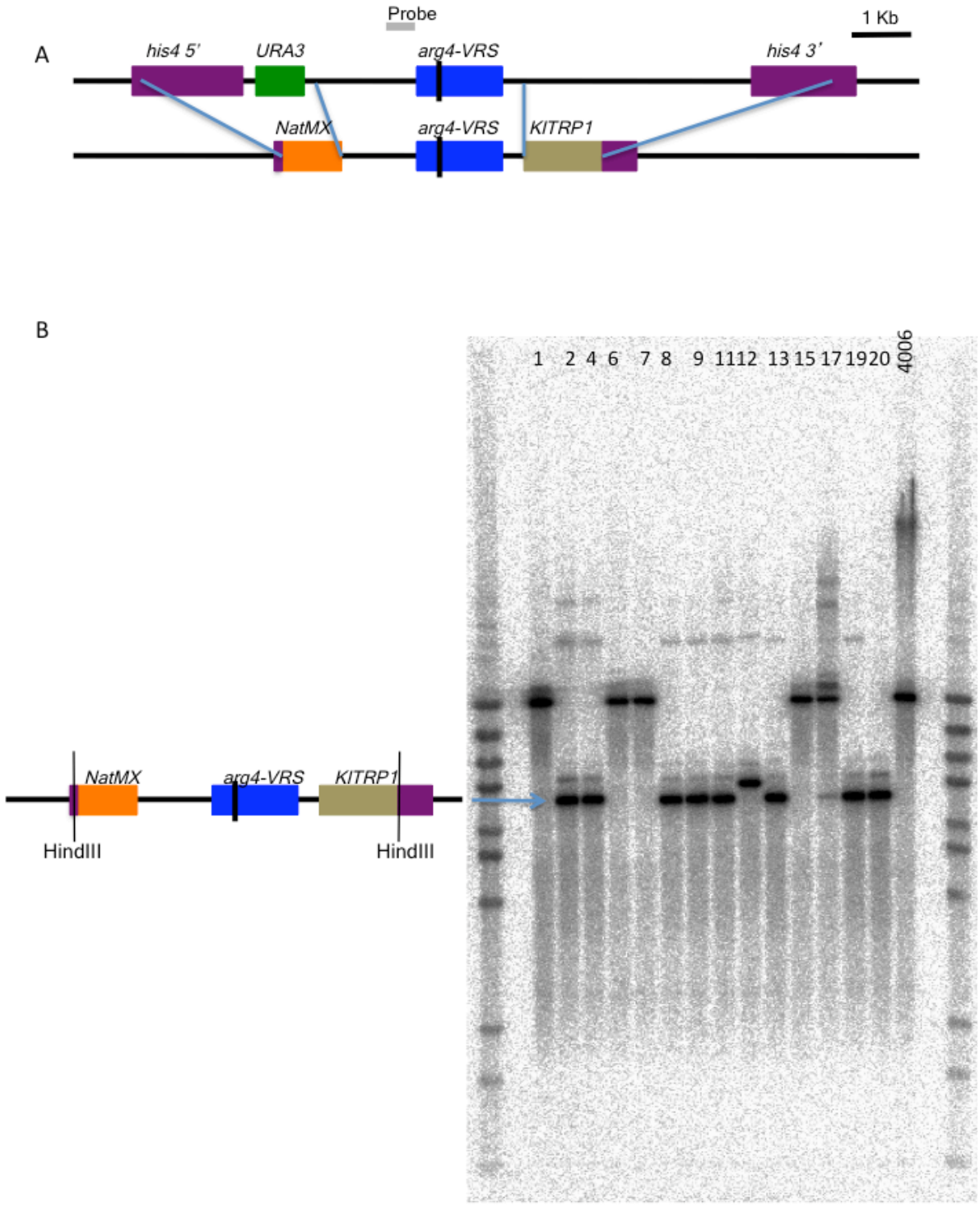

Figure 3-7 Removing flanking *his4'* homologies.
A) Construct maps of recombination cassette at *HIS4* before and after transformation of *NatMX* to remove upstream *HIS4* sequences and *KlTRP1* to remove downstream *HIS4* sequences.
B) Southern blot of transformants after transformation of pMJ913, digested with *Hind*III and probed with *ARG4* sequences. Map of digest band from correct integration of *NatMX* and *KlTRP1* is illustrated alongside the Southern blot; digests bands above are form incorrect integration.

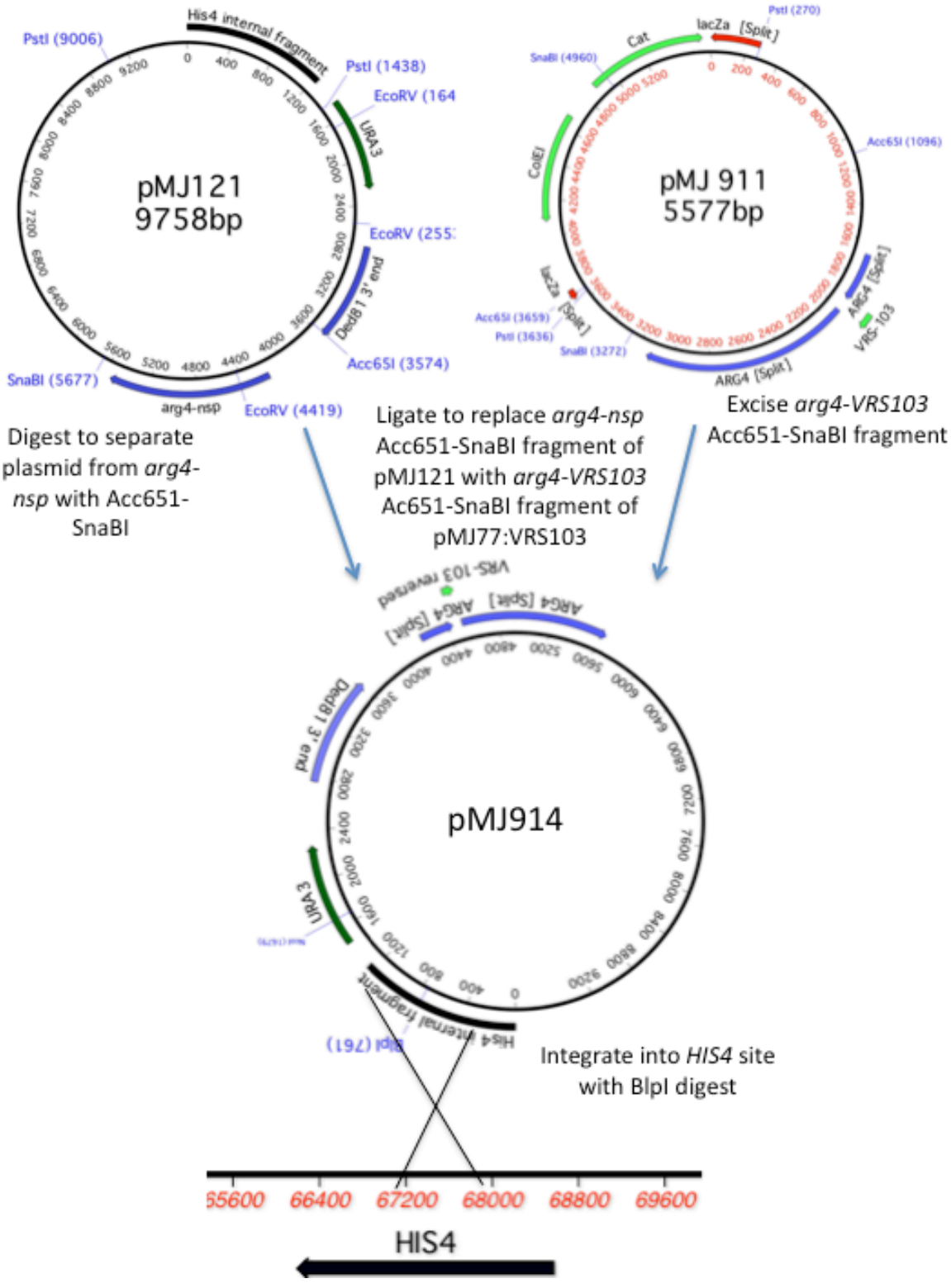

Figure 3-8 Scheme of moving *arg4-VRS103* to *HIS4*. The *arg4-VRS103* fragment, which had been cloned into pMJ911, is excised and put into pMJ121 replacing *arg4-nsp* to give pMJ914. pMJ914 is also then also integrated at *HIS4* by digesting with *Blp*I to complete the recombination reporter.

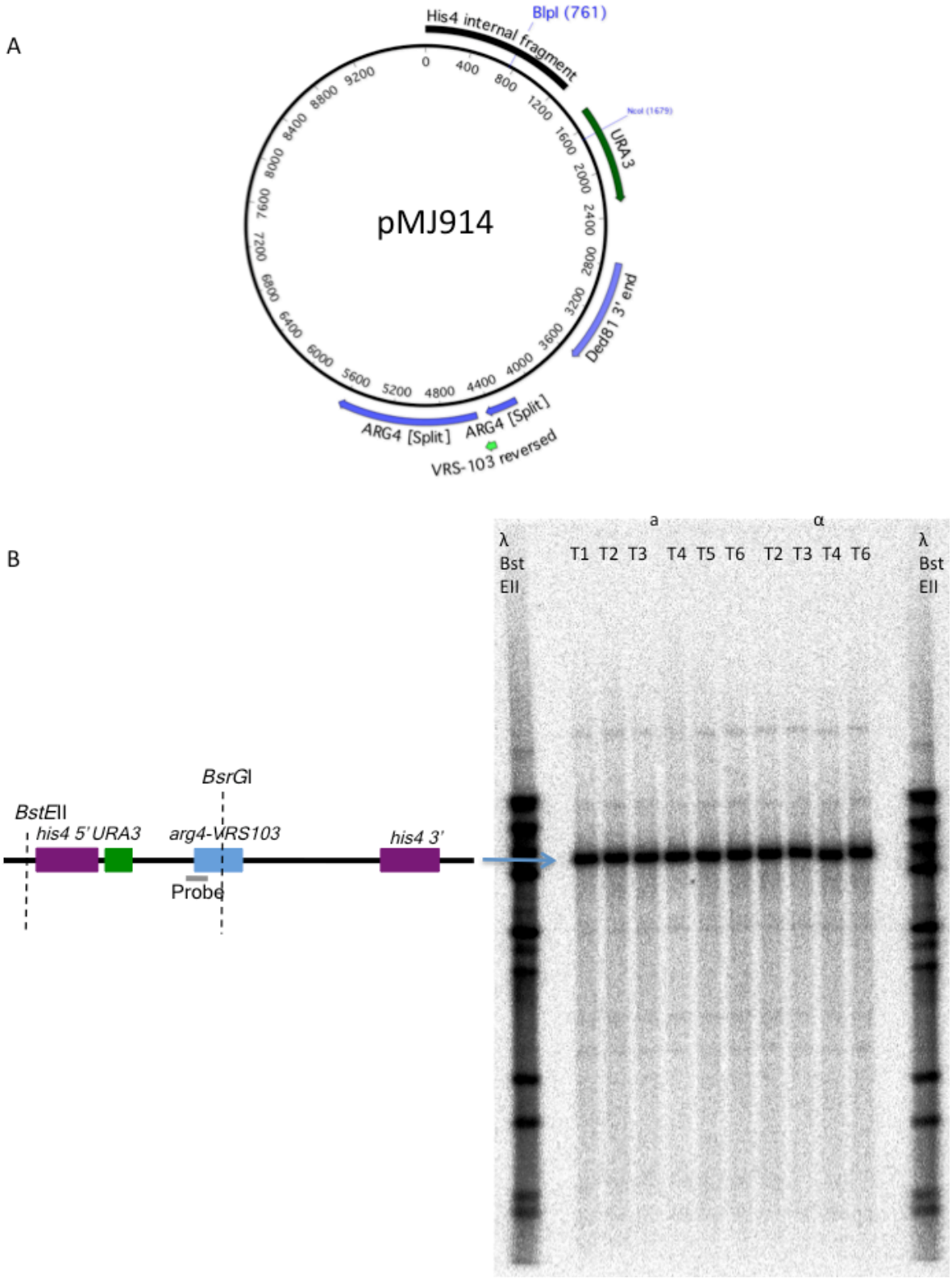

Figure 3-9 Cloning *arg4-VRS103* to *His4* locus
A) Plasmid map of pMJ914, which has *ar4-VRS103, URA3* and *his4* internal fragment. *Blp*I digest targets plasmid to *HIS4.*
B) Southern blot of transformants after transformation of pMJ914, digested with *BstE*II and *BsrG*I and probed with *ARG4* sequences. Map of digest band from single integration of is illustrated alongside the Southern blot. No multiple insertions are seen.

3.5 Cloning VDE under the copper inducible pCUP1 promoter and determining Cu induction conditions.

As mentioned previously, another issue of the existing recombination reporter system is that DSBs and COs are detected in Southern blots at the 0hr time-point, and reciprocal COs are not at equal levels (Figure 3-2A,E; Figure 4-1A,B). These results are inconsistent with COs arising from HR during meiosis, which should be at roughly equal levels. Instead, they suggest pre-meiotic recombination events, which is possible as the VDE protein is constitutively expressed. Therefore, we sought to limit the expression of VDE, by cloning VDE under a copper inducible *CUP1* promoter (*pCUP1*), which can be used in meiosis (Boselli et al. 2009) and can restrict *VDE* expression.

The scheme of this cloning is depicted in Figure 3-10. The VDE gene was cloned under the *pCUP1* promoter and subsequently integrated at the *CUP1* locus. Transformants were selected for G418 resistance and then genomic DNA was digested with *Xba*I and probed with *VDE* internal sequences. Genomic DNA from a *VMA1::VDE* strain was used as a positive control. Also, single copy insertion of *VDE* was determined by comparing the signal in the *pCUP1-VDE* bands to the *VMA1::VDE* band, which is present as a single copy in the genome.

A temporary diploid was made with *VDE* under *pCUP1* in a strain with the heterologous recombination reporter. VDE protein was induced with 10μM $CuSo_4$ in the sporulation medium. DSB formation for *pCUP1-VDE* diploid began 2 hrs after meiotic induction rather than at 1 hr as for previous *VMA1::VDE* strains (Figure 3-11D). Peak DSB levels are reached at 4-5 hrs rather than 3 hrs (Figure 3-11D). Thus the new time frame of VDE DSB formation is much closer to that of Spo11 DSB formation during meiosis (De Muyt et al. 2012). Also, the levels of the CO products were roughly equal to each other in the *pCUP1-VDE* strain (Figure 3-11E), indicating that the previous disparity in COs may have indeed come from pre-meiotic recombination.

Since putting *VDE* under *pCUP1* meant that DSB formation in all sporulations had to be induced by adding $CuSO_4$ to the sporulation medium, it was important to determine if adding copper had any adverse affect on meiosis. Increasing amounts of $CuSo_4$ from 40μM had a pronounced affect on meiotic progression while 10μM $CuSo_4$ had minimal affect (Figure 3-12A,B). Subsequently, levels of DSB formation from induction with 10 μM $CuSo_4$ were compared with DSB formation from basal induction of *pCUP1-VDE* without any added $CuSO_4$. Though DSBs are formed even without any added copper, the kinetics of these DSBs is not comparable to the endogenous meiotic DSBs formed by Spo11, as there are late DSBs under these conditions (Figure 3-12B,D). On the other hand, DSB kinetics, when *pCUP1-VDE* is induced with 10μM $CuSO_4$, mostly resemble kinetics of Spo11 DSBs (Figure 3-12B,C).

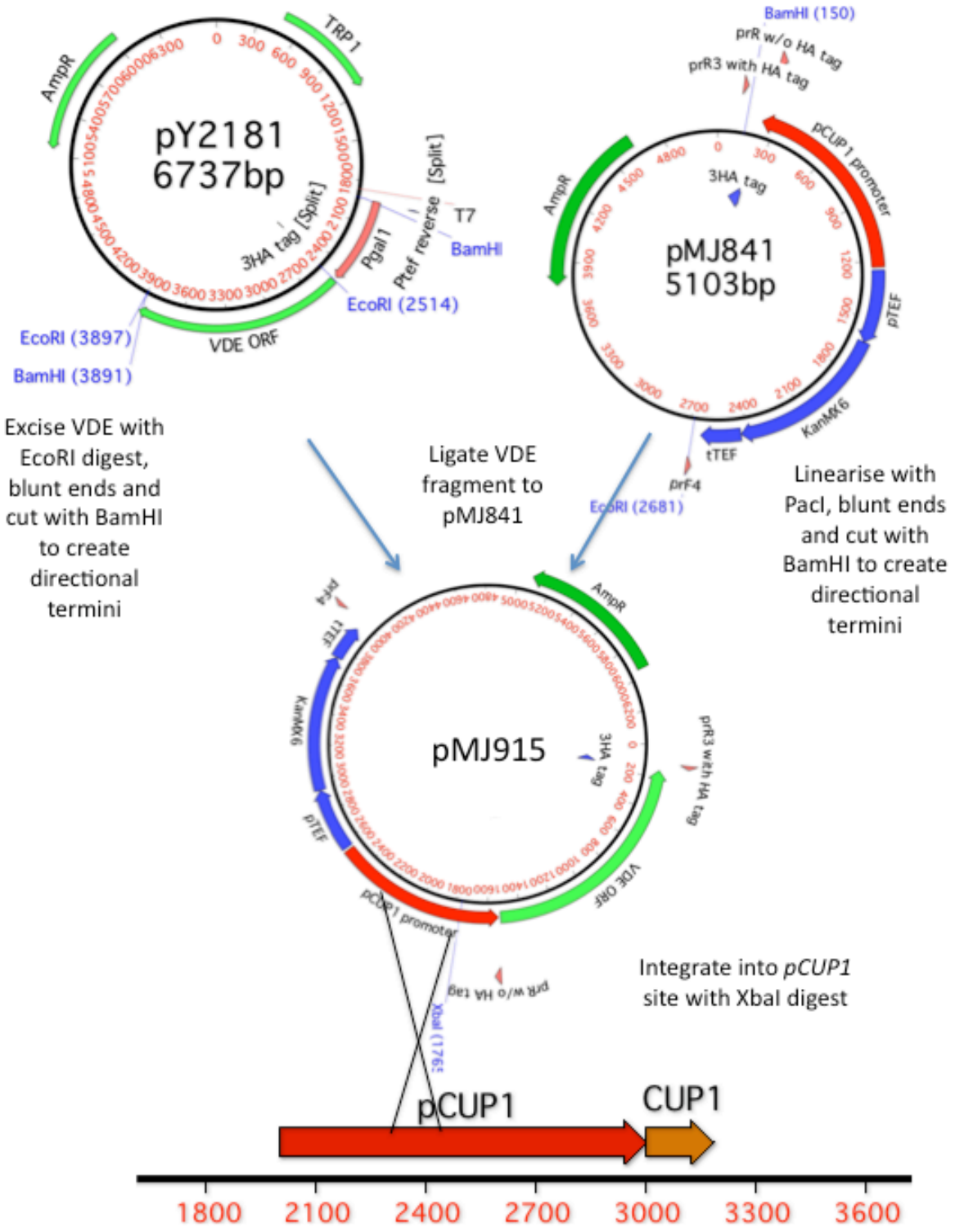

Figure 3-10 Scheme of cloning *VDE* under *pCUP1* into the genome VDE, cloned as an independent gene under GAL1 promoter was present on plasmid pYO2181 (gift from Dr. Sotaru Nogami, Ohya lab). The VDE gene was excised from this plasmid and inserted downstream of the *CUP1* promoter in plasmid pMJ841 to give pMJ915. pMJ915 was then integrated in the genome upstream of the *CUP1* locus by digesting with *Xba*I which cuts within *pCUP1*.

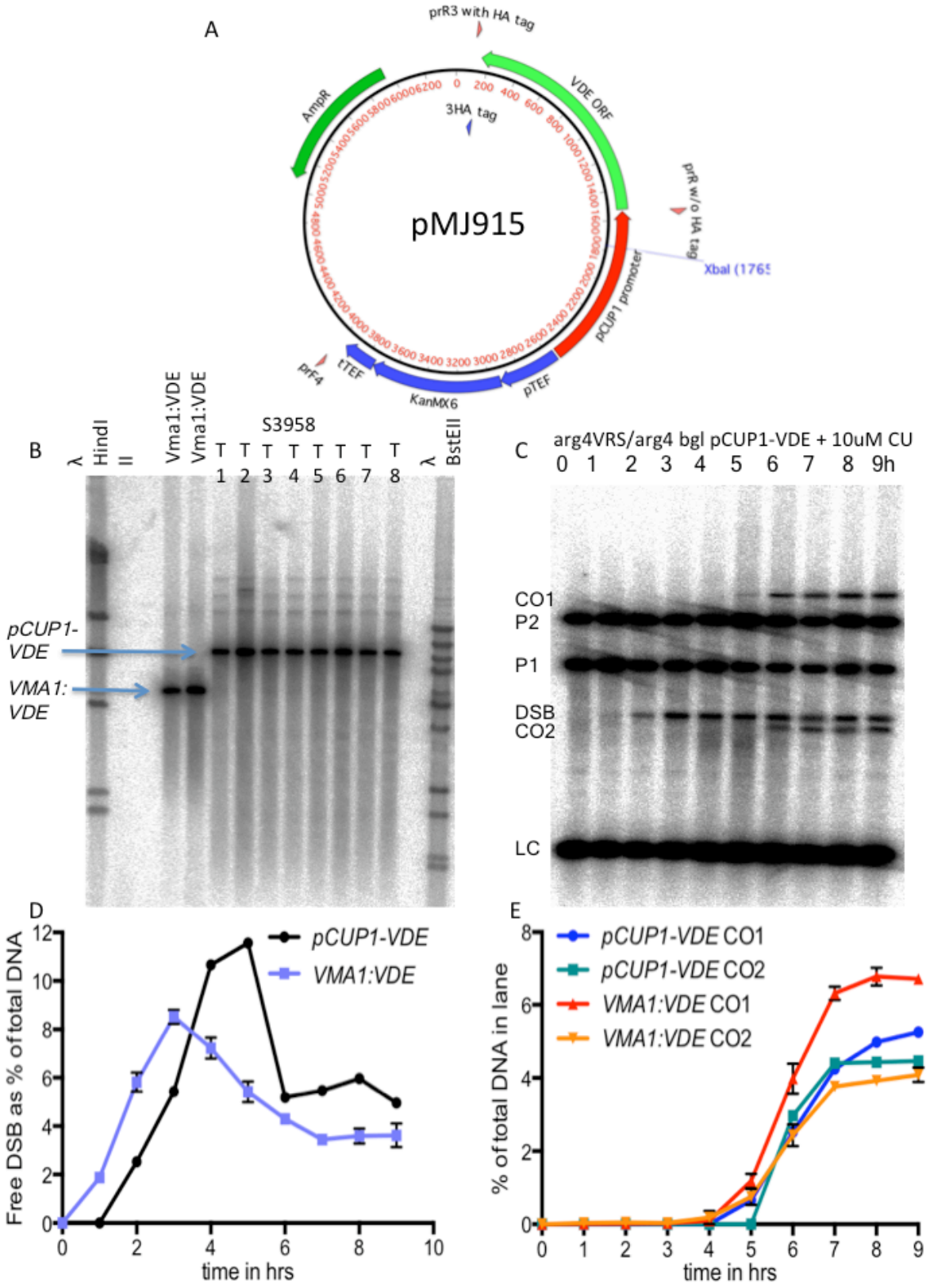

Figure 3-11 Transforming and testing pCUP1-VDE
A) Plasmid map of pMJ915 with *VDE* under *pCUP1-VDE* and *KanMX*, *Xba*I digestion is used to target plasmid to the *CUP1* locus.
B) Transformants are tested by Southern blotting with a VDE internal probe and *VMA1::VDE* strains as positive control. Since *VMA1::VDE* is present in a single copy, signal

levels from *pCUP1-VDE* bands were compared to signal from *VMA1::VDE* level to confirm single insertion.
C) A diploid with *arg4-VRS/arg4-bgl* with *pCUP1-VDE* is tested for DSB formation in meiosis with 10um Cu.
D) Break levels are comparable to DSBs produced by *VMA1:VDE* strains, and the timing of break formation for *pCUP1-VDE* is closer to Spo11 DSBs
E) CO levels are comparable to *VMA1-VDE* strains, and CO1 and CO2 levels are now roughly equal.

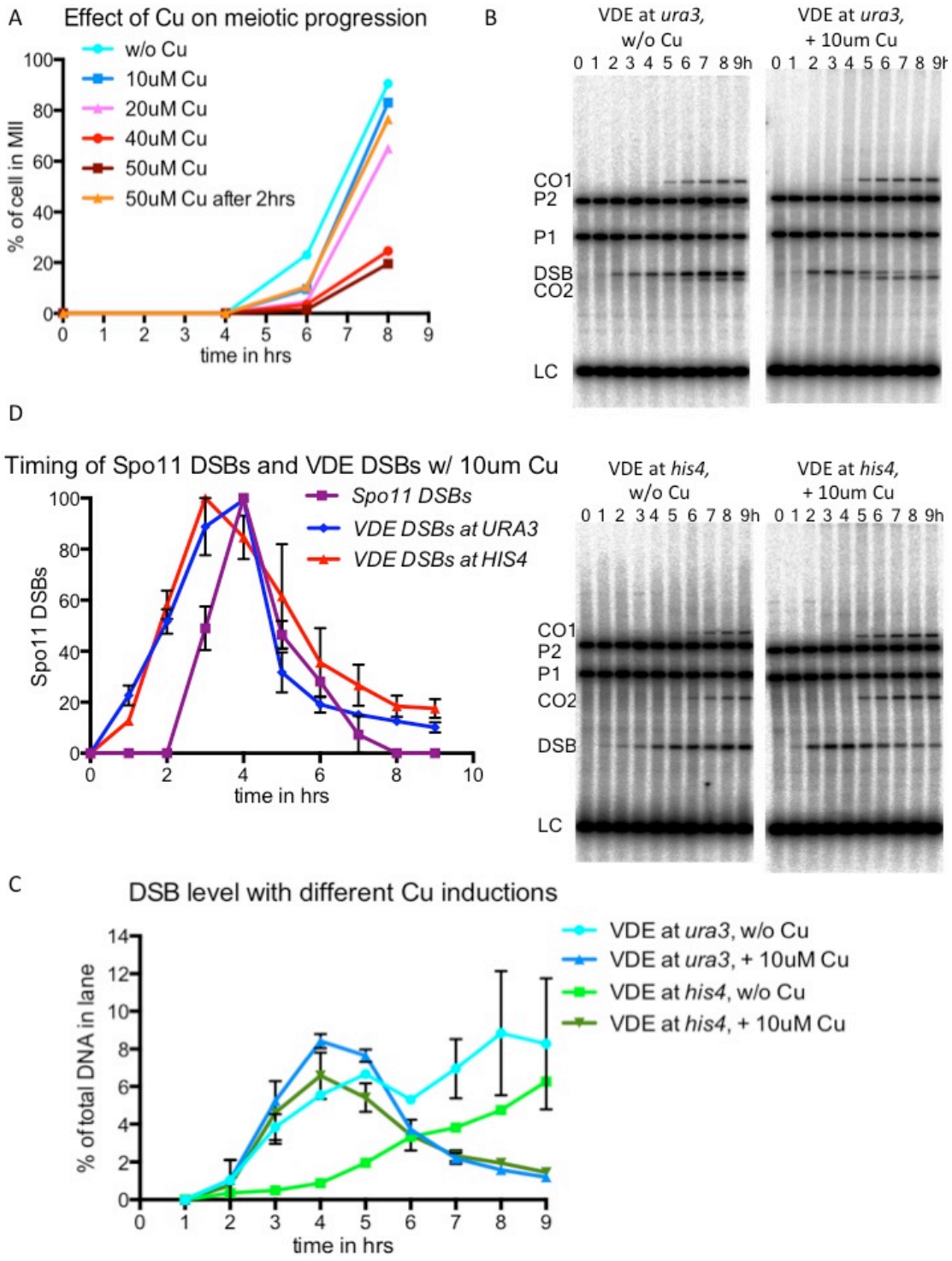

Figure 3-12 Testing the effect of copper on meiotic proegression and determining optimum copper level for VDE induction.
A) Timing of completion of meiosis II for sporulations with 6 different amounts of Cu. Cu^+ levels ≥ 40μM cause a pronounced delay in meiotic progression.
B) Southern blots to determine timing and level of VDE DSBs at both *URA3* and *HIS4* loci in WT strains MJL3624 and MJL3618 with and without added $CuSO_4$.
C) VDE DSB levels under basal induction without any added Cu^+ have a high level of late DSBs, while inducing VD with 10uM $CuSO_4$ gives DSB kinetics which are comparable to endogenous Spo11 DSBs.

D) Kinetics of VDE DSBs at *URA3* and *HIS4* are comparable to Spo11 DSBs, though earliest VDE DSBs are detected an hour earlier than Spo11 DSBs.

3.6 Crossing VMA1-103 allele into strains to remove VDE initiated DSB at natural VMA1 locus.

The final modification to the VDE recombination system was to remove the naturally occurring VDE DSB form the *VMA1* locus, as mentioned in section 3.2. *VDE* exists as an intein in the yeast *VMA1* gene and cleaves the *VMA1* allele that lacks the intein during meiosis to propagate itself via homing (Bremer et al. 1992, Gimble and Thorner. 1992). In this study of meiotic recombination, VDE has been used to make Spo11-independent DSBs to better understand HR in meiosis. However, in order to limit the timing of such DSBs in meiosis, VDE was cloned as an independent gene under the *pCUP1* promoter and integrated at the *CUP1* locus. However, this VDE protein now expressed with copper could still cleave the natural *VMA1* genes present on both homologues during meiosis. DSBs formed on all four chromatids would leave no intact template for repair and this could be very deleterious, as even a single unrepaired DSB causes mitotic *S. cerevisiae* cells to arrest before metaphase through the action of Mec1 (Paciotti et al. 2000, Melo et al. 2001). Also, persistent DSBs that fail to repair can lead to loss of chromosomes (Bennett et al. 1997). Having cleavage resistant *VMA1::VDE* alleles was also not an option as these would result in constitutive VDE expression and defeat the purpose of cloning *VDE* under *pCUP1.* Therefore, to avoid having persistent unrepairable DSBs in the yeast genome without having extra copies of *VDE*, we crossed the *VMA1-103* allele into our strains, which is resistant to cleavage by VDE, but does not contain the *VDE* intein (Gimble and Stephens. 1995). The haploids were tested for *VMA1-103*, by PCR of the gene and digestion with PI*Sce*I (Figure 3-13B), the WT *VMA1* allele is cleaved to about 50% completion while *VMA1-103* is completely resistant to cleavage.

A

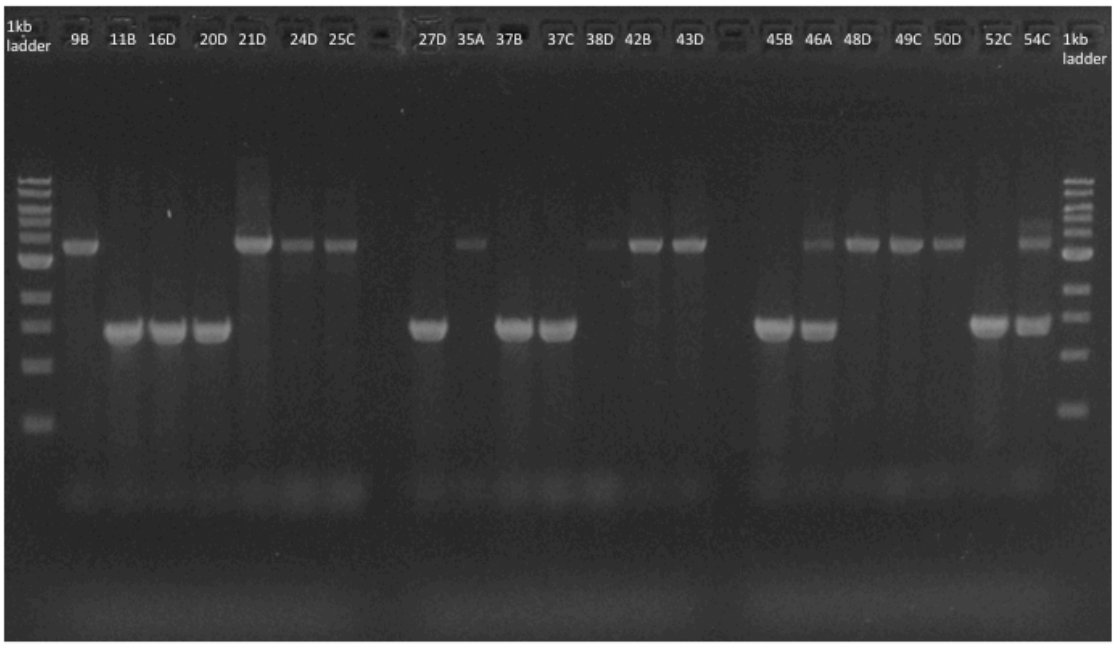

B

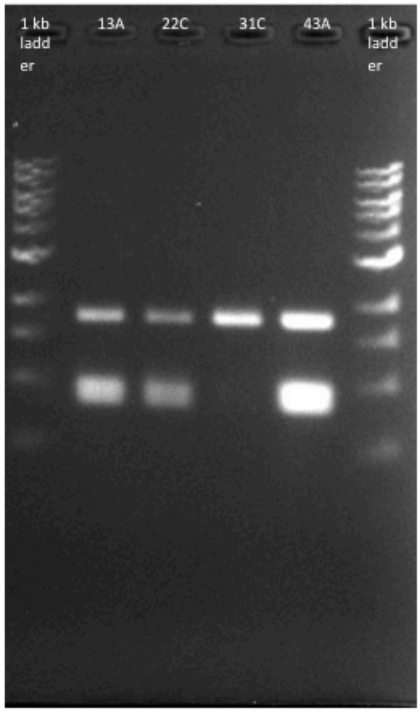

Figure 3-13 Testing *arg4Δ(eco47iii-hpaI) and VMA1-103* by PCR.
A) PCR with primers upstream and downstream of the *ARG4* locus gives an 3.3 Kb band for *arg4-nsp,bgl* and a 2.2 Kb band for *arg4Δ(eco47iii-hpaI)*.
B) PCR product of *VMA1* upstream and downstream primers is digested with PI*Sce*I to test for the *VMA1-103* allele, Lane 4 with haploid 31C contains the *VMA1-103* allele.

3.7 Efficient DSB repair, increased interhomologue recombinants and reduced loss of chromosome material in new homologous cassettes

The initial VDE recombination reporter system had *arg4-VRS* on one homologue opposite an *arg4-bgl* allele on the other, and as a result had 74 bps of heterology right at the DSB site. Sequence heterology in DNA is known to inhibit HR (Datta et al. 1996), and consistent with this, ~5% of VDE DSBs in this heterologous reporter persist in an unrepaired state even after 9 hrs in meiosis (Figure 3-2B) and there is a loss of chromosome material from the *arg4-VRS* chromatids, this rises from 50% in WT strain to 86% in the *spo11 ndt80* strain (Figure 3-2D). Tetrad dissections also showed severe spore inviability in these strains (Table 3-2). This problem was addressed by cloning *arg4-VRS103* opposite *arg4-VRS* in the recombination reporter; this reduced the sequence heterology for 32 bps, which is 40% of an average 80 bp homologous synapsis region in strand invasion (van der Heijden et al. 2008), to 4 bp mismatches, which is 0.05%. Along with the new reporter at *URA3,* the recombination reporter was also moved to *HIS4*, to allow the examination of locus specific properties of meiotic recombination. In addition, *VDE* was cloned under copper inducible *pCUP1* promoter and removed form its endogenous *VMA1* promoter; and VDE cleavage resistant *VMA1:103* was crossed into the strains at both endogenous *VMA1* loci.

These new cassettes will be henceforth referred to as the homologous cassettes. As with the strains carrying the heterologous reporter, genomic DNA was extracted from the new homologous reporter strains, digested with *Hind*III to monitor free DSB levels, and probed with *DED81* sequences to allow comparison with the natural *arg4* locus as a loading control (Figure 3-14A). The level of residual DSBs in the new reporters is <1% (Figure 3-14B). Also, the total level of *arg4-VRS* chromatid material was monitored in comparison with the loading control, and the loss of *arg4-VRS* chromosome material in the homologous strains is ~25% at *URA3* and ~28% at *HIS4,* compared to ~53% in the heterologous reporter strain, which is 2 fold less (Figure 3-14C). Thus, the efficiency of HR in the repair of VDE DSBs in improved 2 fold with the removal of heterology at the DSB site. Additionally, tetrad dissection of the homologous reporter strain at *URA3*, with *pCUP1-VDE* induced with 10μM $CuSO_4$ showed a 96% spore viability, with 92% *arg4-VRS* spore viability and greater parity between COs (Table 3-3).

These analyses therefore show that a 74 bp stretch of heterology at the DSB site, which is ~32 bp of heterology on the invading strand, reduces the efficiency of HR by ~50%. Unlike inbred laboratory strains, diploid budding yeast cells in the wild may have significant polymorphisms between their corresponding "homologous" chromosomes, including such heterologous stretches. Meiotic recombination initiated by DSBs in such regions on the genome can be efficiently repaired by intersister HR (Goldfarb and Lichten. 2010), and in the case that intersister repair does

not occur, 74 bp stretch of heterology can still be dealt with in interhomologue recombination. Such robustness in the process of HR may be thus highly relevant to budding yeast in the wild, which are not perfectly homologous like inbred lab strains.

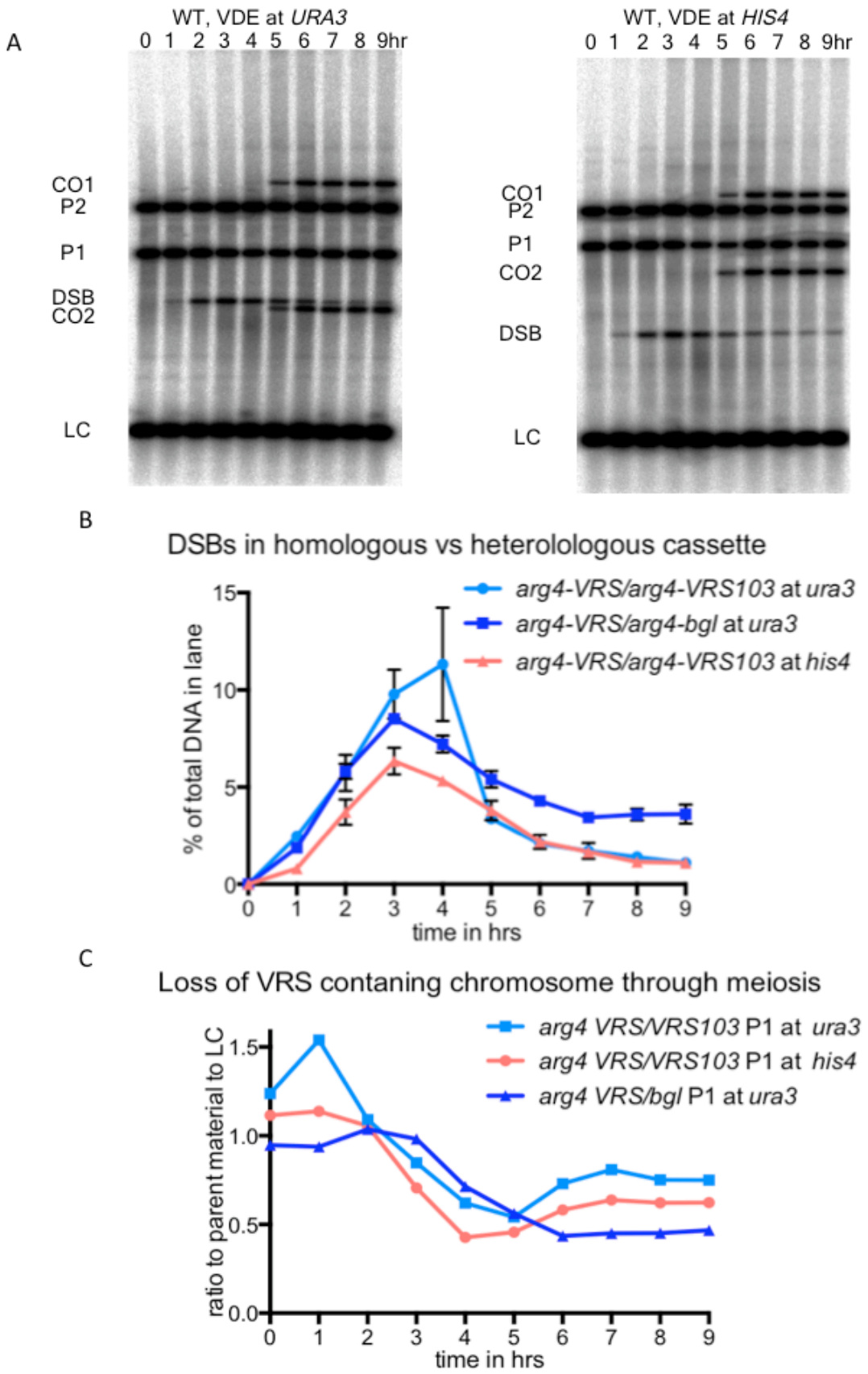

Figure 3-14 Efficient VDE DSB repair in the homologous recombination reporter
A) Southern blots of WT homologous strains with reporter inserts at *URA3* and *HIS4* (MJL3624 and MJL3618). Genomic DNA is digested with *Hind*III to detect free DSBs and

probed with *DED81* sequences, which also detect the endogenous *ARG4* locus as a loading control. Results are from two biological replicates for each strain, error bars indicate standard error of mean (SEM). P1 refers to the *arg4-VRS* parent, P2 the *arg4-VRS103* parent, interhomologue crossovers are denoted CO1 and CO2, the VDE DSB is referred to as DSB and the *ARG4* natural locus is denoted as the loading control (LC). For construct maps explaining these digest, refer to Figure 5-3.
B) Homologous strains are referred to as *arg4 VRS/VRS103*, while heterologous strain MJL 3549 is denoted *arg4 VRS/bgl*. VDE DSBs are efficiently repaired at both *URA3* and *HIS4* with <1% residual breaks, as compared to ~5% in heterologous insert.
C) Loss of *arg4-VRS* containing chromosomes is reduced in new strains without heterology at DSB site. At the 9 hr timepoint, remaining *arg4-VRS* chromosomes are at 75% at *URA3* and 62% at *HIS4* for the arg4 VRS/VRS103 strains with homologous inserts. Remaining *arg4-VRS* chromosomes are at 47% for the *arg4 VRS/bgl* strain with heterologous inserts.

Tetrads dissected	Viable spores	Spore viability	P1 spores	P2 spores	CO1 spores	CO2 spores	VRS chromatids spore viabilty $\frac{(P1+CO1)}{(P2+CO2)}$	$\frac{CO1}{CO2}$ ratio
48	186	0.97	60	76	29	21	0.92	1.38

Table 3-3 Genetic analysis of VDE DSB repair by tetrad dissection in homologous reporter strain MJL 3624.

The level of IH recombinants in the new homologous cassette at *URA3* reaches 30%, as compared to ~15% in the heterologous cassette at same locus (Figure 3-15B). This is again consistent with a 32 bp heterology in the invading strand causing a 2-fold reduction in homologous recombination as compared to a 4 bp mismatch, which also correspondingly increases loss of chromosome material by 2 fold (Figure 3-14C)

However, the increase in recombinants is not evenly distributed between NCOs and COs, NCOs are increased by 2.2 fold while COs are increased by 1.4 fold (Figure 3-15C). Therefore, there is a greater loss of NCOs than COs in the heterologous cassette versus the homologous cassette. Therefore, these results suggest that heterology at the site of DSB affects NCO formation more than CO formation. In both yeast and male mouse meiosis, the gene conversion tracts associated with COs are longer than gene conversion tracts for NCOs (Terasawa et al. 2007, Mancera et al. 2008, Mitchel et al. 2010, Cole et al. 2010), which has been suggested to reflect increased DNA synthesis associated with CO formation. The increased DNA synthesis in CO formation may arise from a more stable association between the synaptic filament and donor strand, which inhibits the anti-recombinase function of helicases and allows longer tracts of DNA synthesis. Martini et al. (2011) reported that heteroduplex patterns associated with CO are more complex than NCOs, and suggest that phenomenon such as multiple strand invasions and template switching may be more commonly associated with COs. Such mechanisms

may also permit CO forming pathways to more easily circumnavigate the impediment to strand invasion caused by a stretch of heterology at the break site, as template switching and multiple rounds of strand invasion could also lead to a more stable strand invasion intermediate.

Finally, there also appears to be a timing difference in the appearance of interhomologue recombinants in the homologous cassette versus the heterologous cassette. Both NCOs and COs in the homologous cassette appearing about an hour earlier than the heterologous cassette (Figure 3-15D). Heterology at the DSB site may delay the homology search due to reduced efficiency of initial homologue synapsis. Also, heterology at the DSB site may require longer tracts of synthesis and more template switching to cope. These could contribute to a delay in appearance of HR repair products.

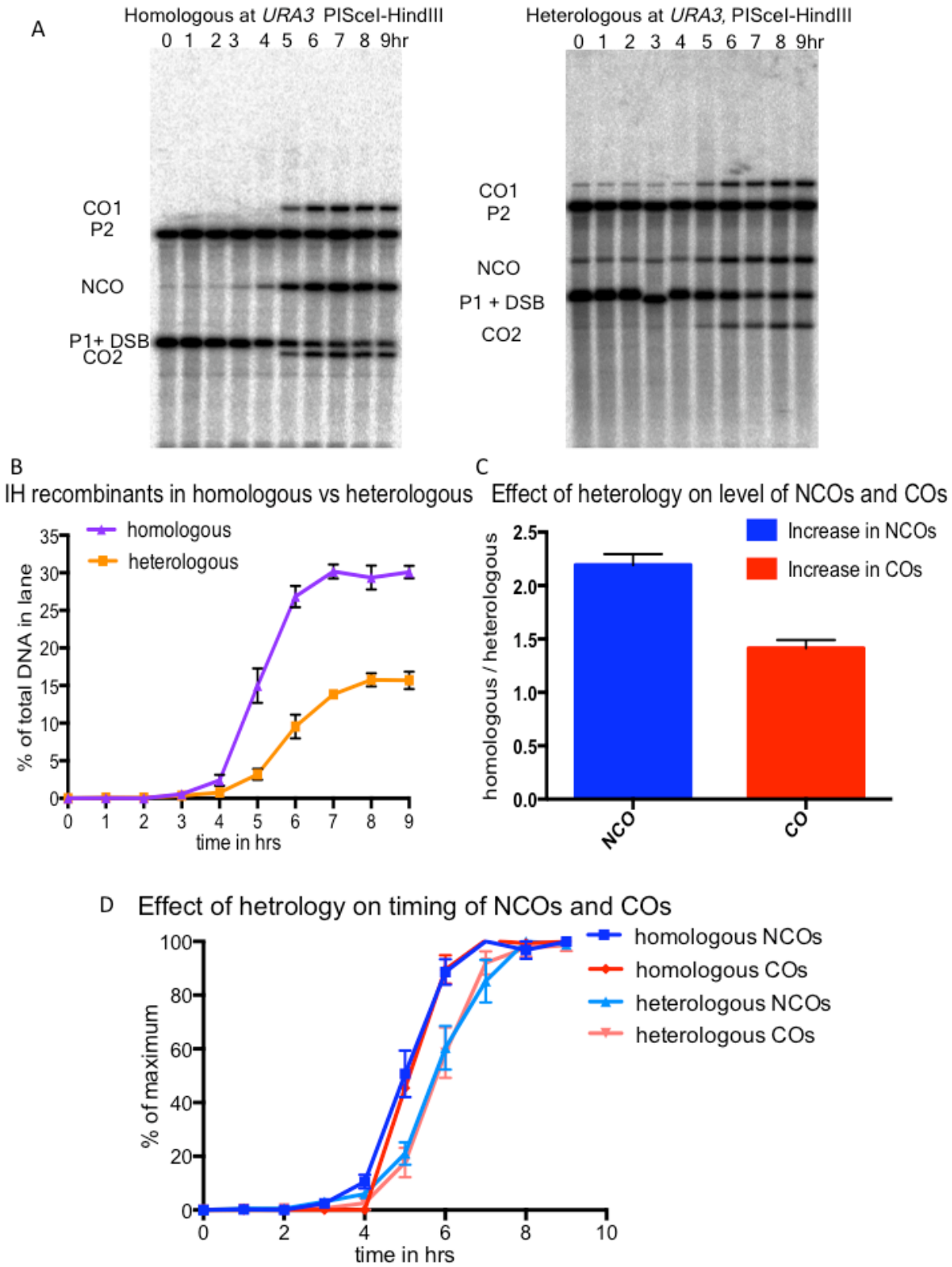

Figure 3-15 Effect of heterology on level and timing of NCOs and COs at *URA3*.
A) Southern blots of WT strains at *URA3* with homologous and heterologous cassettes respectively.
B) Level of IH recombinants is increased 2 fold in homologous cassette as compared to heterologous cassette.
C) Heterology does not equally affect both COs and NCOs, NCOs are increased 2.2 fold in homologous cassette compared to heterologous, while COs are increased 1.4 fold. D) IH

recombinants in homologous cassette appear ~1hr earlier as compared to the heterologous cassette.

3.8 Insertion of VDE recombination reporter cassettes does not alter endogenous Spo11 DSB activity of loci

I created a VDE recombination reporter system, which can be used to examine meiotic HR events at two different loci, *URA3,* which is a cold spot for Spo11 DSBs and is likely to be away from the meiotic axis, and *HIS4*, which is a hot-spot for Spo11 DSBs and should be in the vicinity of the axis (Panizza et al. 2011). However, in order to be able to determine if these two loci had any unique recombination properties, it is important that the endogenous Spo11 DSB activity and meiotic chromatin state remained unaltered with the reporter inserts. I discussed previously in section 1.4.4 that Spo11 DSB activity in a locus is dependent on chromosome context rather than primary sequence. Replacing DNA sequences around a DSB site does not alter DSB formation (de Massy and Nicolas. 1993), and similarly, moving a DSB hot sequence like the promoter region of *ARG4* to the DSB cold *MAT* region does not increase DSB formation at *MAT*. Also, the VDE recombination reporter I used is based on an older recombination reporter with *URA3* and *arg4* sequences, and this had been used by Wu and Lichten (1995) and Borde et al. (1999) to determine the endogenous recombination frequencies at various hot and cold loci in the genome, with no indication that insertion of the reporter altered recombination activity in any loci.

In order to determine if Spo11 activity in the *URA3* cold-spot and the *HIS4* hotspot remained intact, *sae2 vdeΔ* strains were examined to directly determine Spo11 DSB levels at *URA3* and *HIS4*. *vdeΔ* strains were used to prevent any interference by VDE in Spo11 DSB formation, as VDE targeting has been reported to reduce proximal hot-spot activity (Fukuda et al. 2008). Spo11 DSBs remain in an unrepaired unresected state in *sae2* mutants (Keeney and Kleckner. 1995). 5 times as many Spo11 DSBs are detected at *HIS4* compared to *URA3*, and DSB levels are consistent with those detected at *URA3* and HIS4 in *sae2* strains by Borde et al. (1999). Therefore, insertion of the recombination reporters does not alter Spo11 initiated recombination activity at *URA3* and *HIS4*. CO formation was also examined in a *vdeΔ* strain, which was otherwise WT, to obtain an indirect readout for Spo11 activity, as *sae2* mutants are known to alter DSB formation in cold regions (Buhler et al. 2007). However, consistent with DSB levels in the *sae2 vdeΔ* strains, 5 times as many Spo11 initiated COs form at *HIS4* compared to *URA3*. Therefore, insertion of the recombination reporters does not alter Spo11 DSB activity at these loci. Genome wide Red1 and Hop1 ChIP data from Panizza et al. 2011 show that Red1 and Hop1 are at median levels at *URA3*, while they are enriched at *HIS4.* Since Spo11 DSB activity remains unchanged at *URA3* and *HIS4* with the VDE recombination reporter insert, Red1 and Hop1 enrichment at these loci are also likely to remain unchanged from endogenous levels.

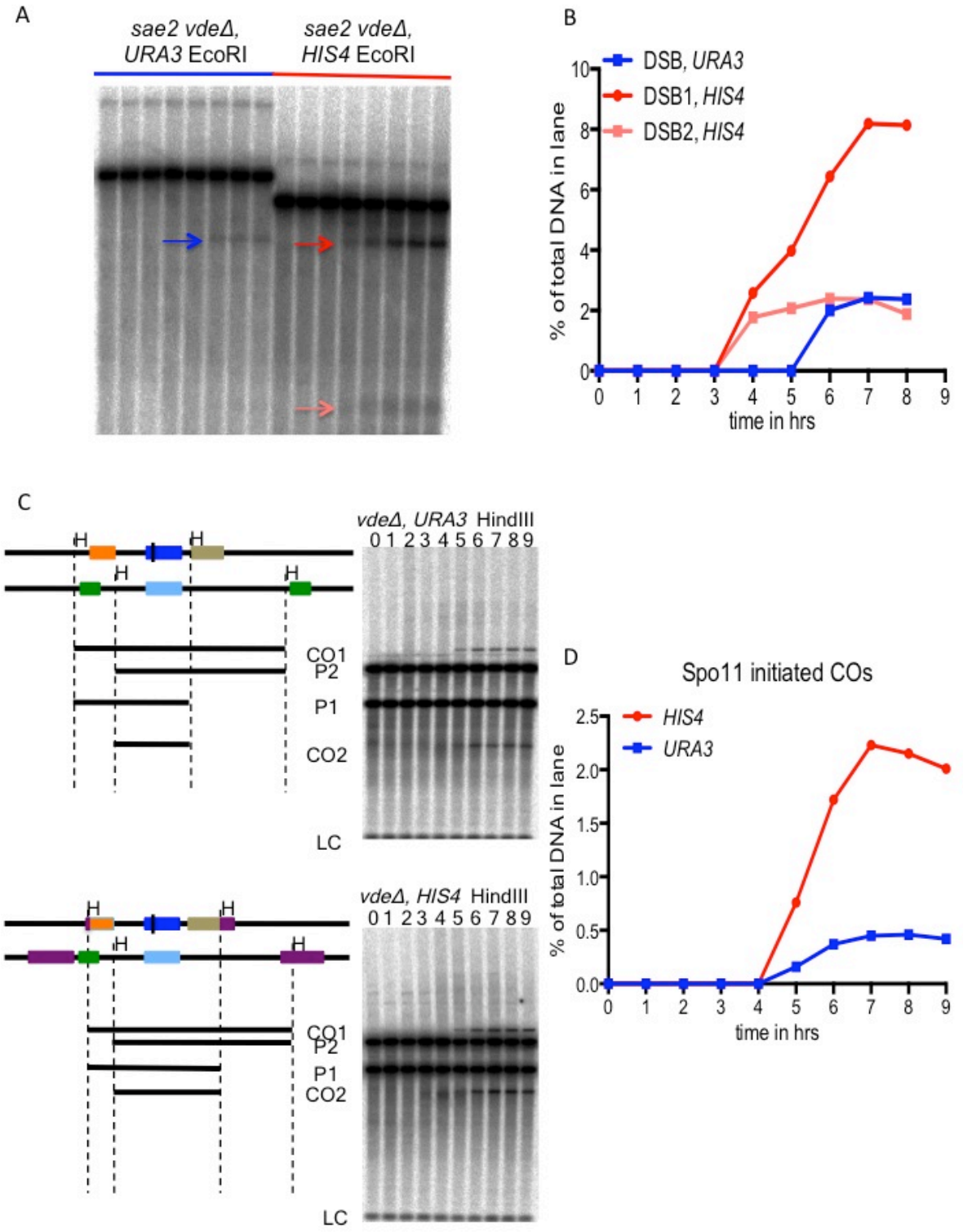

Figure 3-16 VDE recombination reporter inserts do not alter Spo11 DSB formation at *URA3* and *HIS4.*

A) Southern blots with corresponding maps of meiotic DNA digested with *Eco*RI from sae2 *vde*⁻ at *URA3* strain MJL3643 and *sae2 vde*⁻ at *HIS4* strain MJL3645, probed with *arg4-VRS103* specific pbr322 probe. Data is from a single experiment.

B) Spo11 DSBs detected at *HIS4* are at 10.6% of *arg4-VRS013* chromatids, while they are compared at 2.4% at *URA3*, which is a 5X excess at *HIS4.*

C) Southern blot and corresponding construct map of meiotic DNA from *vde*⁻ strain at *URA3* MJL 3627 and *vde*⁻ strain at *HIS4* MJL3617, digested with *Hind*III. The band labeled LC

is a loading control from *ded81* contamination in the *arg4* probe. All subsequent Southern blots of *Hind*III digests will be labeled in the same way. Data is from a single experiment. D) Spo11 CO1 levels are 2.5% at *HIS4* and 0.5% at *URA3,* which is also a 5X excess at *HIS4*.

3.9 Spo11 initiated repair events can be distinguished from VDE initiated repair events

Having established the homologous recombination reporter system at both *URA3* and *HIS4*, I set to determine if VDE initiated events could be effectively distinguished from Spo11 initiated events. This is of particular importance at the *HIS4* Spo11 hotspot, where there is a significant level of Spo11 initiated recombination (Figure 3-16B,D). The VDE recombination reporter system initiates meiotic recombination via a DSB at *arg4-VRS* chromosome, which is subsequently repaired from *arg4-VRS103* chromosome. This leads to gene conversion of the *VRS* site to *VRS103* in all products of homologous recombination, which can be physically tested for by digesting meiotic DNA with VDE/PI*Sce*I. All VDE initiated recombinants are resistant to cleavage (Figure 3-17A,B). This feature also allows VDE initiated NCOs to be effectively separated from the parental DNA fragment, which is still cleaved by PI*Sce*I (Figure 3-17A,B). Therefore, we used this feature of recombination system to also see Spo11 initiated recombination events also lead to gene conversion of *VRS* to *VRS103*, as this will indicate how much many recombinant products in our recombination reporters could actually arise from Spo11 DSBs.

Southern blots of meiotic DNA from WT (*VDE*$^{+}$) and *vdeΔ* strains at both *URA3* and *HIS4* were digested with *Hind*III and PI*Sce*I. *VDE+* strains show VDE-resistant NCOs, but *vdeΔ* strains do not show any VDE resistant NCOs (the faint band is due to incomplete cleavage by the enzyme, and this band does not change its level from 0-9 hrs. Therefore it does not represent a meiotic recombinant) (Figure 3-17A,B). For *VDE*$^{+}$ strains, both CO1 and CO2 are resistant to cleavage by VDE and present at roughly equal levels. However, as regards Spo11-initiated COs, CO1 is resistant to cutting by VDE for at both *URA3* and *HIS4*, but there is no VDE resistant CO2 at *URA3* and the level of VDE resistant CO2 at *HIS4* is about 0.5% of total DNA (Figure 3-17A,B). Levels of VDE resistant CO1 in the *vdeΔ* strains arise due to the position of the DSB at *URA3* and *HIS4,* which is upstream of *arg4-VRS103*, and thus CO1 usually receives the *arg4-VRS103* allele. A smaller fraction of DSBs at *HIS4* are also downstream of *arg4-VRS103*, this probably creates the VDE resistant CO2 population in *vdeΔ* at *HIS4*. Thus, there is little gene conversion of *VRS* to *VRS103* by Spo11 initiated recombination. Also, Spo11 DSBs are located on the *arg4-VRS103* chromatid; therefore gene conversion from the *arg4-VRS* chromatid would make all products of meiosis cleavable by VDE/PI*Sce*I. The maximum fraction of COs in our analysis, which could be attributable to Spo11 initiated recombination in our inserts, is about 0.05% of total events, which is a very minor fraction (Figure 3-17C,D).

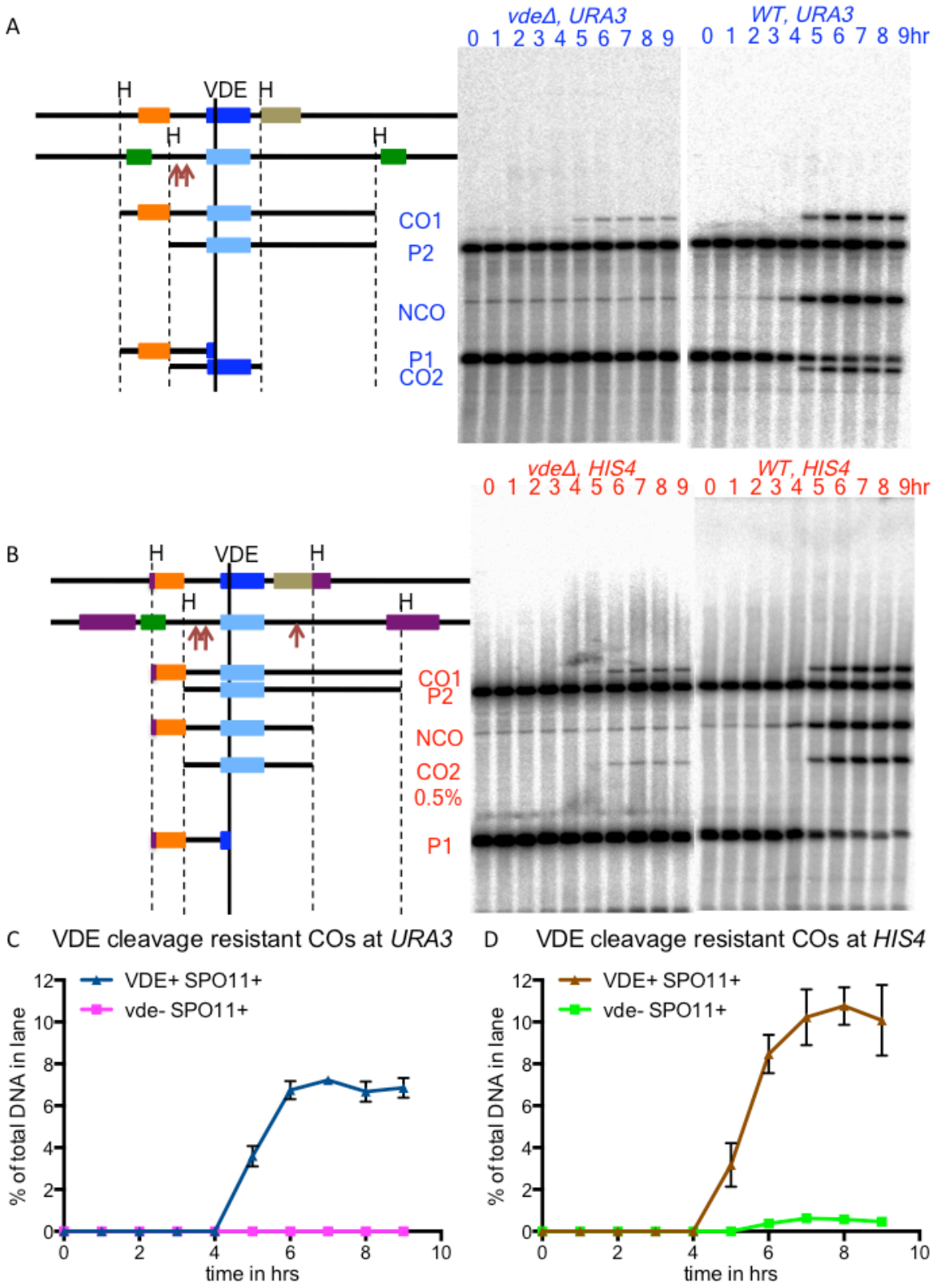

Figure 3-17 Spo11 initiated recombinants can be effectively distinguished from VDE initiated recombinants
A) Southern blots with corresponding maps of meiotic DNA digested with *HInd*III PI*Sce*I from *vdeΔ* and WT *(VDE⁺)* strains at *URA3* strain MJL3627 and MJL3624 respectively. These are probed with *arg4* sequences.

B) Southern blots with corresponding maps of meiotic DNA digested with *HInd*III PI*Sce*I from *vdeΔ* and WT *(VDE+)* strains at *URA3* strain MJL3617 and MJL3618 respectively. These are probed with *arg4* sequences.
C) VDE resistant CO2 levels are at 7% in WT*/VDE+* but undetectable in *vdeΔ* strains at *URA3.* WT data is from two biological replicates, *vdeΔ* is form a single experiment.
D) C) VDE resistant CO2 levels are at 10.8% in WT*/VDE+* and at 0.6% in *vdeΔ* strains at *HIS4.* WT data is from two biological replicates, *vdeΔ* is form a single experiment.

3.10 Current progress and future work on the VDE recombination reporter system

I have created a recombination reporter system that effectively initiates Spo11 independent recombination at two different loci in the genome, and this recombination forms NCOs and COs with reasonable efficiency. The primary features of the recombination reporter that differentiates it from previous VDE recombination reporters are as follows:

1. The VDE DSB site at *arg4-VRS* is flanked by heterologous markers. This means that repair of the VDE DSB has to proceed by interhomologue recombination (Table 3-1); there is no flanking homology that allows intra-strand repair of DSB by SSA.
2. The heterologous markers that flank *arg4-VRS* allow COs to be easily detected in genetic and physical assays. Also, since VDE recombination always initiates on the *arg4-VRS* chromosome and repairs from the *arg4-VRS103* chromosome, NCOs can also be easily detected in physical assays as they can be separated from the *arg4-VRS* parent based on resistance to cleavage by VDE/PI*Sce*I (Figure 3-17).
3. All VDE recombination reporter strains carry *arg4Δ (eco47iii-hpaI)*(Figure 3-13), thus there is no opportunity for ectopic repair events, and Southern blots can be probed with *arg4* sequences without picking up the endogenous *ARG4* locus.
4. Previous recombination reporters using site specific endonucleases such as HO (Malkova et al. 2000) or I-*Sce*I (Ho et al. 2010, Bzymek et al. 2010) usually have heterology right at the DSB site, as the recognition sequence is only present on one homologue. As demonstrated in Figure 3-14 and Figure 3-15, this heterology has significant consequences for DSB repair by HR. The heterology between both homologues in the current VDE recombination reporter system is 4 bps, which effectively removes any issues that arise from heterology (Figure 3-14 and Figure 3-15).
5. VDE protein expression in the current VDE recombination reporter strains is under the control of the *pCUP1* promoter, which is inducible with copper and can be used for meiotic induction (Boselli et al. 2009). This acts as an additional layer of regulation, on top of the naturally regulated meiosis-specific import of VDE into the nucleus (Nagai et al. 2003). These ensure that the VDE DSB formation is effectively restricted to meiotic cells only (Figure 3-11 and Figure 3-12).

6. Replacement of the endogenous *VMA1* loci with *VMA1-103* (Figure 3-13) ensures that the VDE DSB is targeted to only the recombination cassettes, and there are no additional sites for DSB formation by VDE.
7. Finally, the VDE recombination reporter inserts can be used to study meiotic recombination at different loci, without altering the endogenous recombination properties of these loci (Figure 3-16). Also, scoring for gene conversion of *arg4-VRS* to *arg4-VRS103* in physical assays for recombination by digesting with PI*Sce*I can effectively differentiate between VDE-initiated and Spo11-initiated events, even at a Spo11 DSB hot-spot like *HIS4* (Figure 3-17).

However, in spite of the above, there are still aspects of the VDE recombination reporter system, which limit its use in the study of recombination.

1. The VDE DSB is very efficient and site-specific. It cleaves 90% of its target sequences by 9 hrs in meiosis (Figure 4-1 and Figure 5-1). This means that both sister chromatids are being cleaved, and this prevents us from addressing any aspect of partner choice in recombination. Spo11 DSBs are formed on only a single chromatid (Zhang et al. 2011), this allows the Spo11 DSB to choose between the sister chromatid or the homologous chromosomes as a template partner for repair. Since both sister chromatids are cleaved by VDE, the homologous chromosomes are the only option as a repair partner. Reducing VDE expression is ineffective with *pCUP1-VDE,* as even in sporulations where no copper is added, the basal transcription level, possibly driven by trace copper in media and water, creates significant DSB levels (Figure 3-12C). Also, after DSB formation, it is unclear if the VDE protein is actively ejected from the nucleus, as basal induction of VDE gives rise to the late DSBs (Figure 3-12C), which probably arise from cleavage of uncut *VRS* sites by residual VDE protein in the nucleus. A more efficient method of controlling VDE cleavage might be to mutate the *VRS* cleavage site of VDE, to reduce the efficiency of VDE DSB formation and restrict break formation to only one sister chromatid.
2. The current recombination cassettes were created in plasmids meant for site specific targeting. This makes moving the VDE recombination reporter to other genomic loci a very cumbersome process. Redesigning the plasmids would allow quicker targeting of VDE recombination reporter cassettes anywhere in the genome.
3. The first version of the recombination reporter had *arg4* with a *VRS* sequence inserted at *Eco*RV, opposite an *arg4-bgl* allele. Thus, VDE recombinants could also be genetically detected by looking for arginine prototrophs. However, removing the heterology in the reporter system by cloning *arg4-VRS103* on the other homologue has removed the potential to generate *ARG⁺* prototrophs from VDE initiated recombination. Moving the *VRS* sequences outside *ARG4* could allow NCO and CO recombinants to also be genetically detected by looking for *ARG⁺* prototrophs.

4 Homologous recombination at *URA3* in *arg4-VRS/arg4-bgl* heterologous cassette

4.1 VDE DSB are repaired in meiosis to give an excess of NCOs over COs

The initial experiments to examine VDE DSB repair in meiosis were performed with strains containing the heterologous inserts, with *arg4-VRS* on one homologue and *arg4-bgl* on the other. Repair of VDE DSBs in this reporter system is not efficient; this is described in section 3.2 and Figure 3-2. In addition, I also determined the efficiency of interhomologue recombination by comparing the cumulative level of DSB formation to the cumulative level of interhomologue (IH) recombinants. The cumulative level of VDE DSBs was determined by monitoring the loss of intact *arg4-VRS* chromatids during meiosis using an *Eco*RV-*Bgl*II digest, which separates the uncut *arg4-VRS* parent from all cut and repaired chromatids (Figure 4-1A). The level of *arg4-VRS* chromatids go from ~50% at the beginning of meiosis (half the total DNA detected by *arg4* probe) to ~5% by the end. Therefore, 45% of total DNA i.e. 90% of *arg4-VRS* chromatids are being cut by VDE. However, the level of interhomologue (IH) recombinants is ~15% by the end of meiosis, which accounts for only 1/3 of the total VDE DSBs formed (Figure 4-1C). Subsequent experiments done with the homologous reporter show a higher level of IH recombinants (see section 5.1). Therefore the 74 bp heterology at the site of a DSB reduces the efficiency of interhomologue recombination. Also, since ~90% *arg4-VRS* sister chromatids are cut during meiosis, the VDE recombination reporter system cannot be used to study partner choice during meiotic recombination.

IH recombinant levels were determined by digesting genomic DNA with PI*Sce*I(VDE)-*Hind*III, which separates NCOs and COs from parental bands due to gene conversion of the *arg4-VRS* site (Figure 4-1B). The level of VDE initiated NCOs formed during meiosis is ~10%, while VDE initiated COs form to only ~5% (Figure 4-1D). Therefore, there is a 2-fold excess of NCOs over COs in VDE DSB repair during meiosis. As discussed in the introduction (section 1.3), both locus specific and genome wide studies have determined that meiotic HR repair of Spo11 DSBs gives at least as many COs as NCOs (Keeney and Kleckner. 1995, De Muyt et al. 2012, Mancera et al. 2008, Qi et al. 2009, Esberg et al. 2011), while an excess of NCOs is feature of mitotic HR (Bzymek et al. 2010, Pâques et al. 1998, Virgin et al. 2001, Stark and Jasin. 2003, Nassif et al. 1994, Mitchel et al. 2010, Mitchel et al. 2013). Thus, HR repair of VDE DSBs seems closer to DSB repair that occurs in mitosis, despite occurring in meiosis.

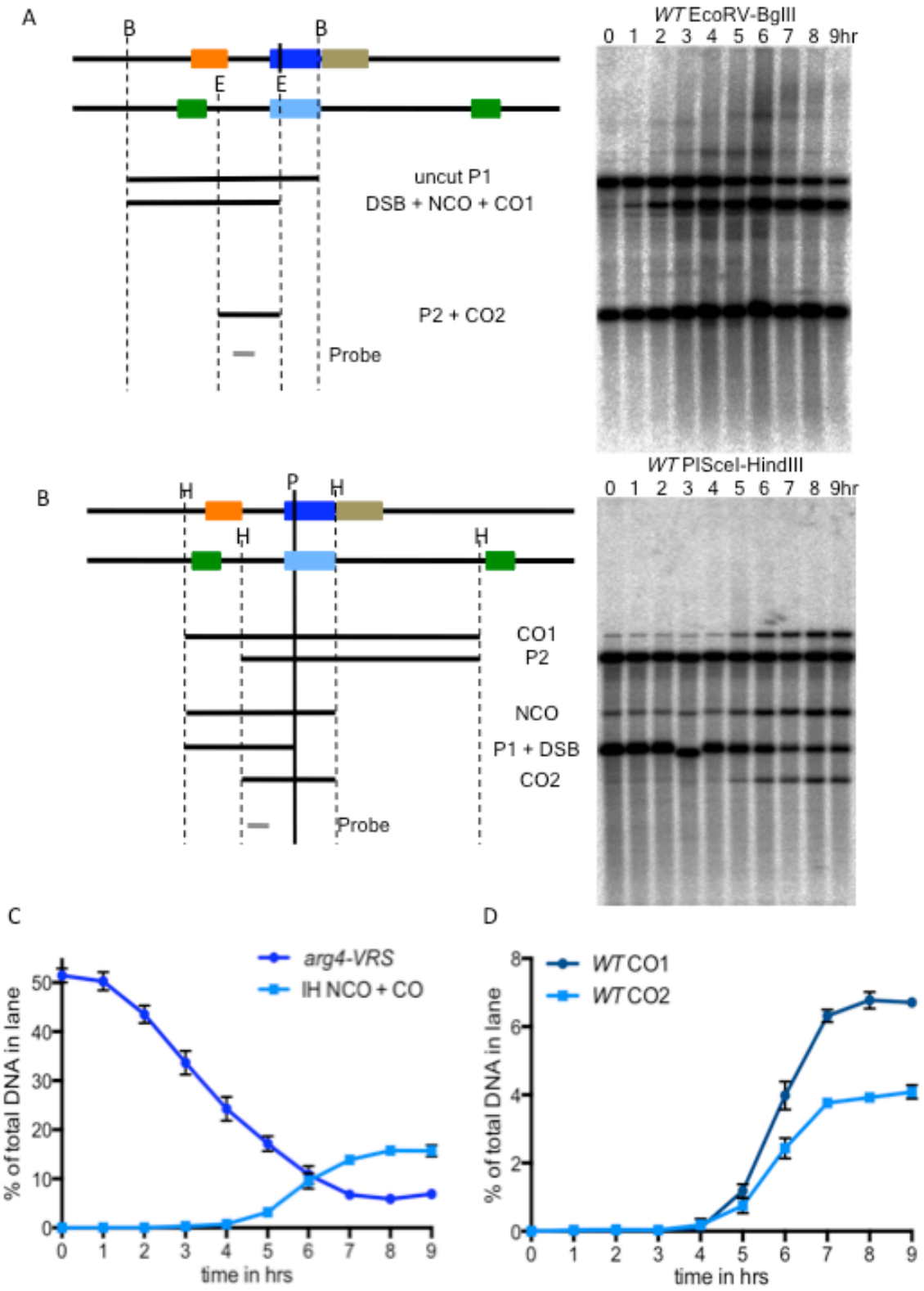

Figure 4-1 VDE DSB repair during meiosis gives a low level of interhomologue recombinants and excess of NCOs

A) Construct map and Southern blot of meiotic DNA from WT strain MJL3549, digested with *Eco*RV-B*gl*II and probed with *arg4* sequences, which separates the uncut *arg4-VRS* chromatid, and loss of this band gives a measure of cumulative DSB level. The *arg4-VRS* chromatid is referred to as uncut P1. The second band represents the VDE DSB or chromatids where the *VRS* site has been gene converted to *Eco*RV, these consist of the

NCOs and CO1. The bottom band contains all *arg4-bgl* chromatids and contains P2 + CO2. The same labeling is used as in Figure 3-2, and all subsequent Southern blots of this type shall also use this labeling. All results are from two biological replicates and error bars indicate standard error of mean.
B) Construct map and Southern blot of meiotic DNA from WT strain MJL3549, digested with PI*Sce*I- *Hind*III to look at COs and NCOs. The same labeling is used as in Figure 3-2, but in this digest, the PI*Sce*I/VDE cleavage causes the *arg4-VRS* (P1) to comigrate with the VDE DSB (DSB), while the NCO band is separated from the *arg4-VRS* parent as it is resistant to PI*Sce*I/VDE cleavage due to gene conversion of VRS site. The same labeling will be used in all subsequent Southern blots of this type. All results are from two biological replicates and error bars indicate standard error of mean.
C) The level of the *arg4-VRS* chromatids reduces from ~50% (1/2 of total DNA) to ~5%. Therefore, 45% of the total DNA, or 90% of *arg4-VRS* chromatids, are cut by VDE during meiosis. Interhomologue recombinants account for only ~15% of DNA, which is 1/3 of total VDE DSBs formed.
D) In WT cells, peak NCO levels are ~10% . CO levels are calculated as the mean of CO1 and CO2 and peak at ~5%. Therefore, there is a 2-fold excess of NCOs.

VDE DSBs are made independently of Spo11 and axis proteins (Fukuda et al. 2008), but it is not known if their repair is anyway dependent on Spo11. In *S. cerevisiae,* there are ~170 DSBs per meiotic cell (Buhler et al. 2007, Pan et al. 2011). Therefore the absence of these DSBs in a *spo11* mutant will alter the global recombination state of a meiotic cell. I wanted to test the effect of this change on VDE initiated HR. Malkova et al. (2000) reported that repair of *SPO13::HO* DSBs is affected in trans by the lack of Spo11. Therefore, to examine if there are similar effects on VDE DSB repair, I studied VDE catalyzed recombination in *spo11Y135F* mutants that have a catalytically dead Spo11 protein; this will be subsequently referred to as *spo11*. Since Malkova et al. (2000) used a *spo11Δ*, it might be possible that the effect they saw is due to some other function of Spo11, and the Spo11Y135F protein should retain these functions. Sasanuma et al. (2007) reported that a Spo11Y135F-Gal4BD fusion protein is still able to form the pre-initiation complex with the Spo11 accessory proteins (see section 1.4.2) at Gal4 binding sites.

The *spo11* mutation had no effect on the rate and level of VDE DSB formation (Figure 4-2B). However, with regard to IH recombinants, the excess of NCOs over COs further increased in *spo11* mutants compared to WT, such that there was a ~3 fold excess of NCOs over COs (Figure 4-2D). This increased NCO/CO ratio is due to a greater loss of COs compared to NCOs in *spo11* cells (Figure 4-2E,F). Therefore, in the absence of global DSB formation, VDE DSB repair is driven towards an even more mitotic outcome, due to selective loss of COs. This is consistent with the reduction of COs arising from the *SPO13::HO* DSB reported by Malkova et al. (2000). The presence of genome wide Spo11 DSBs therefore has a trans effect on meiotic CO formation.

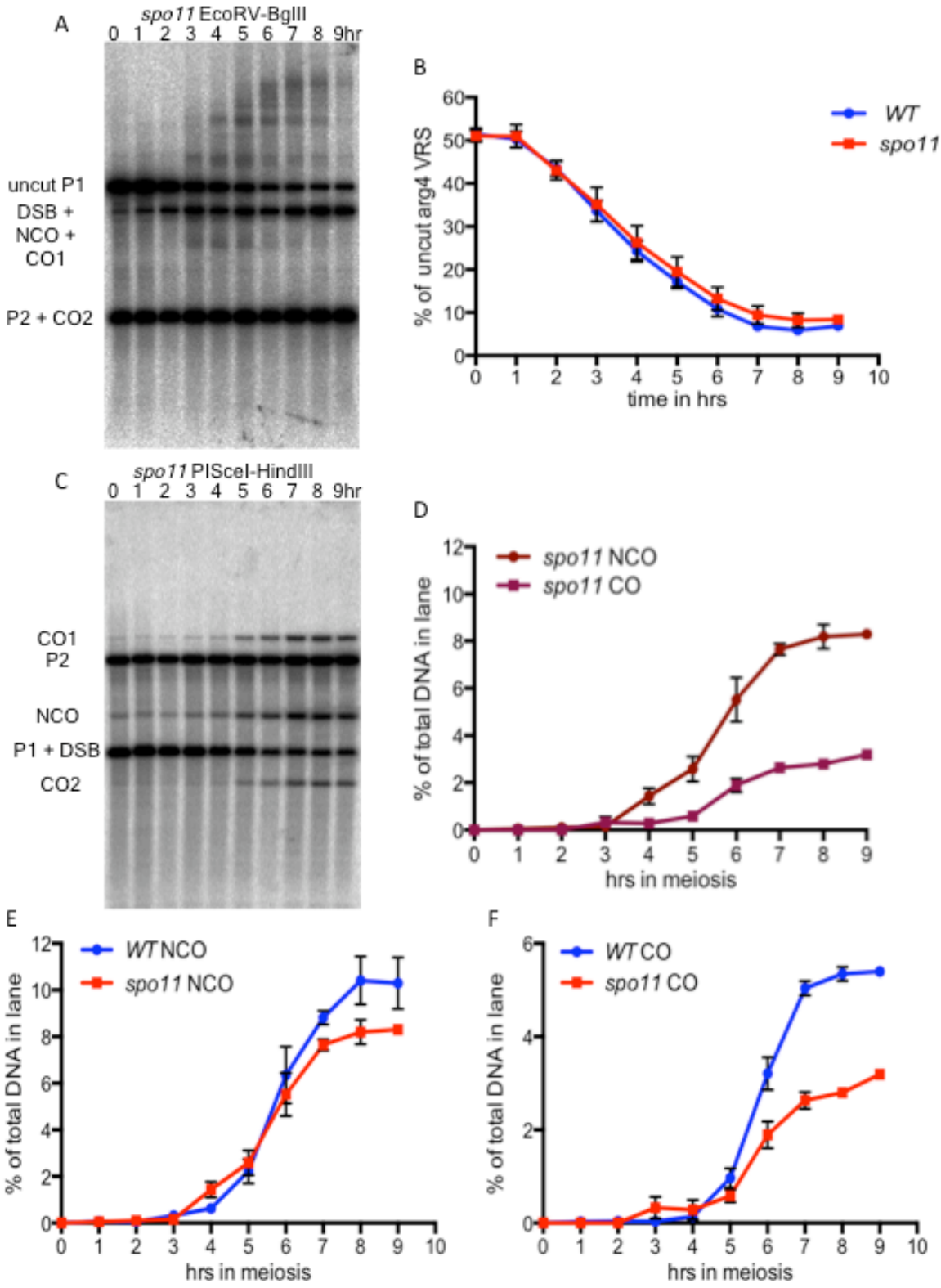

Figure 4-2 NCOs are in further excess over COs for VDE DSB repair in *spo11* mutants, as COs are selectively reduced.
A) Southern blot of meiotic DNA from *spo11* strain MJL3529 digested with *Eco*RV-*Bgl*II to examine cumulative DSB levels. All results are from two biological replicates and error bars indicate standard error of mean.
B) VDE DSB formation in independent of Spo11.

C) Southern blot of meiotic DNA from *spo11* strain MJL3529, digested with PI*Sce*I-*Hind*III to examine COs and NCOs. All results are from two biological replicates and error bars indicate standard error of mean
D) NCOs levels peak at ~8.3%. CO levels are calculated as the mean of CO1 and CO2 and peak at 3.2%. NCOs are in ~3 fold excess over COs.
E) NCOs in WT are 1.25 times NCOs in *spo11*.
F) COs in WT are 1.7 times COs in *spo11.*

4.2 VDE DSB formation is independent of Red1 and the effect of Red1 on VDE DSB repair phenocopies Spo11

The *spo11* mutation causes a loss of COs from VDE initiated recombination. Since a catalytically dead *spo11Y135F* mutant was used, we presume that this loss of COs is due to loss of Spo11 DSBs, and not some other function. To further validate this conclusion, VDE DSB repair was examined in *red1* mutants. Red1 defines domains of DSB hot regions (Blat et al. 2002, Panizza et al. 2011) and is required for Spo11 DSB formation (Mao-Draayer et al. 1996, Schwacha and Kleckner 1997). Examining VDE catalyzed recombination in *red1* mutants will also enquire if genome wide axis enrichment has any effect on VDE DSB repair, beyond the expected effect brought about by reduced genome wide DSB formation.

Red1 has no effect on VDE DSB formation (Figure 4-3B), which is consistent with VDE DSBs being able to effectively form in both hot-spots and cold-spots (Fukuda et al. 2008) i.e. in axis-enriched and axis-depleted regions (Panizza et al. 2011). Both NCOs and COs are reduced in *red1* mutants, and COs are reduced to a greater extent (Figure 4-3D,E). This phenotype of *red1* directly copies that of *spo11,* and as mentioned previously, Spo11 DSBs are reduced in *red1* mutants. Therefore, the *red1* and *spo11* mutants have identical phenotypes regarding VDE DSB repair, and the reduction or absence of genome wide DSBs is able to somehow inhibit VDE initiated CO formation.

Martini et al. (2006) showed that in hypomorphs of Spo11, which have decreasing levels of genome wide DSB formation, CO frequencies are actually increased at the expense of NCOs, this is referred to as CO homeostasis. However, the effect of *spo11* and *red1* mutants show that there is a threshold level of DSB formation required for CO homeostasis, as *red1* mutants still retain some DSB formation, but not enough to trigger CO homeostasis (Mao-Draayer et al. 1996, Schwacha and Kleckner. 1997).

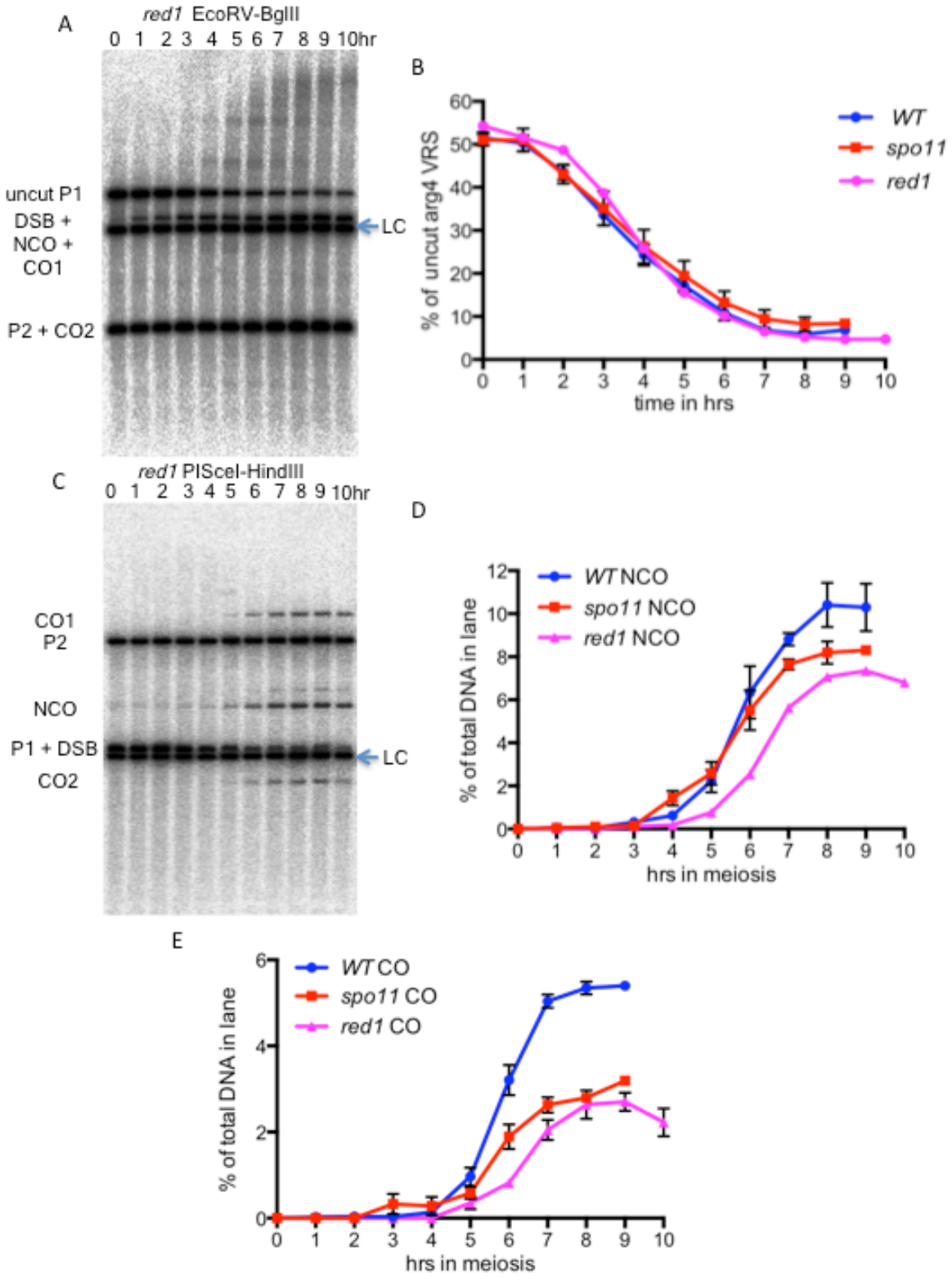

Figure 4-3 Red1 does not directly affect VDE DSB repair
A) Southern blot of meiotic DNA from *red1* strain MJL3677, digested with *Eco*RV-*Bgl*II to examine cumulative DSB levels. The blue arrow indicates a loading control band arising due to contamination in the probe. Results are from a single experiment.
B) VDE DSB formation is independent of Red1.

C) Southern blot of meiotic DNA from *red1* strain MJL3677 digested with PI*Sce*I-*Hind*III to examine COs and NCOs. The blue arrow indicates a loading control band. Results are from a single experiment
D) NCOs in *red1* peak at at 7.35%, which is close to peak NCOs levels of 8.35% in *spo11* mutants.
E) COs, depicted as the average of CO1 and CO2, peak at at 2.7% in *red1* mutants, which is also close to peak COs of 3.2% in *spo11* mutants.

4.3 Dmc1 is not essential for catalyzing strand invasion in VDE initiated HR

Studies in WT and *spo11* cells show that the repair of VDE DSBs gives an excess of NCOs over COs, akin to mitotic DSB repair. I therefore sought to examine the affect of meiosis-specific recombination factors on VDE DSB repair, starting with the meiosis-specific recombinase Dmc1. Bishop et al. (1992) showed that Spo11 DSBs remain in an unrepaired resected state in *dmc1* mutants, so it is essential for HR repair of Spo11 DSBs in meiosis.

In *dmc1* mutants with the heterologous recombination reporter at *URA3*, the rate of loss of intact *arg4-VRS* chromatids is slower, and they also persist at a higher level at 9 hrs (Figure 4-4C). The altered rate of *arg4-VRS* loss could be due to less cleavage by VDE, or alternatively, there could be higher level of intersister recombination in *dmc1* mutants that restores the uncut *arg4-VRS* chromatids. Also, very few NCOs and almost no COs form in *dmc1* mutants (Figure 4-4D,E). However, Spo11 DSBs also remain in an unrepaired resected state in *dmc1* mutants, and this could indirectly affect VDE DSB repair by titrating other HR proteins. Johnson et al. 2007 reported that VDE DSB repair by SSA is also inhibited in *dmc1* mutants due to the presence of excess ssDNA arising from unrepaired Spo11 DSBs. Upon combining the *dmc1* mutation with *spo11* or *hop1*, which eliminate or reduce DSB formation respectively, there was no longer any defect in VDE DSB repair by SSA due to lack of Dmc1. Similarly, the lack of HR repair in *dmc1* mutants in VDE DSB repair by HR does not necessarily mean that Dmc1 is essential for VDE initiated recombination. The excess of unrepaired Spo11 DSBs in the *dmc1* mutants could also titrate off repair factors. Another possibility is that the genome wide DNA damage response from unrepaired Spo11 DSBs could inhibit Rad51 activity, which is also present in meiotic cells. The meiotic signaling kinase Mek1 is activated by Spo11 DSB formation in meiosis (Rockmill and Roeder. 1991, Usui et al. 2001) and *mek1* mutants can alleviate the meiotic arrest of *dmc1* mutants (Xu et al. 1997). Therefore, the cell wide meiotic DNA damage signal in *dmc1* mutants could inhibit Rad51 function via Mek1. For Spo11 catalyzed recombination, this inhibition of Rad51 could ensure that Dmc1 mainly catalyzes meiotic recombination.

Therefore, to examine if Dmc1 was directly required for VDE initiated recombination, *spo11 dmc1* mutants were also examined for VDE DSB repair, as these would be free from the influence of other unrepaired DSBs in the cell. In contrast to *dmc1* mutants, loss of intact *arg4-VRS* is

very similar in *spo11 dmc1* to WT and *spo11* strains (Figure 4-4C). Thus there was no alteration of VDE DSB formation in *spo11 dmc1* mutants. Also, both NCOs and COs are formed in *spo11 dmc1* mutants, with COs being at comparable levels to *spo11* (Figure 4-4E). NCOs in *spo11 dmc1* are at higher levels than in either *spo11* or WT (Figure 4-4D), such that the excess of NCOs over COs is 4-fold. Thus, recombination in *spo11 dmc1* is even more mitotic. Also, this suggests that Dmc1 is not essential for VDE catalyzed IH recombination. In fact, total IH recombination is improved in *spo11 dmc1* compared to *spo11* cells due to increased NCO levels. In mitotic cells, Rad51 catalyzes strand invasion during HR (Shinohara et al. 1992), so if HR in this *spo11 dmc1* mutant is also being carried out by Rad51, this would suggest Rad51 is sufficient to carry out VDE catalyzed interhomologue strand invasion in meiosis. However, such Rad51 catalyzed HR in meiosis enriches for NCOs rather than COs. Since the recombination reporter used in this experiment has heterologous sequence right at the DSB site, it is possible that Rad51 may be more capable of catalyzing recombination in the presence of such heterology.

If Rad51 is indeed more efficient in catalyzing recombination between heterologous sequences, perhaps the Rad51 presynaptic filament requires less stable homologous contacts than Dmc1. In mitotic cells, a less stable synaptic association would also be more susceptible to disassociation catalyzed by helicases, which could then enrich for NCOs to prevent loss of heterozygosity. This is also consistent with the observation that NCOs are more reduced than COs in the heterologous VDE recombination reporter versus the homologous recombination reporter (Figure 3-15C), as heterology at the break site may require a longer more stable synaptic association, which would then be less susceptible to disassembly by helicases. However, no significant differences have been reported so far in the *in vitro* biochemical properties of the Rad51 and Dmc1 pre synaptic filaments (Sheridan et al. 2008), but different synaptic properties could also be attributed to the different accessory partners of the Rad51 and Dmc1 filaments *in vivo*.

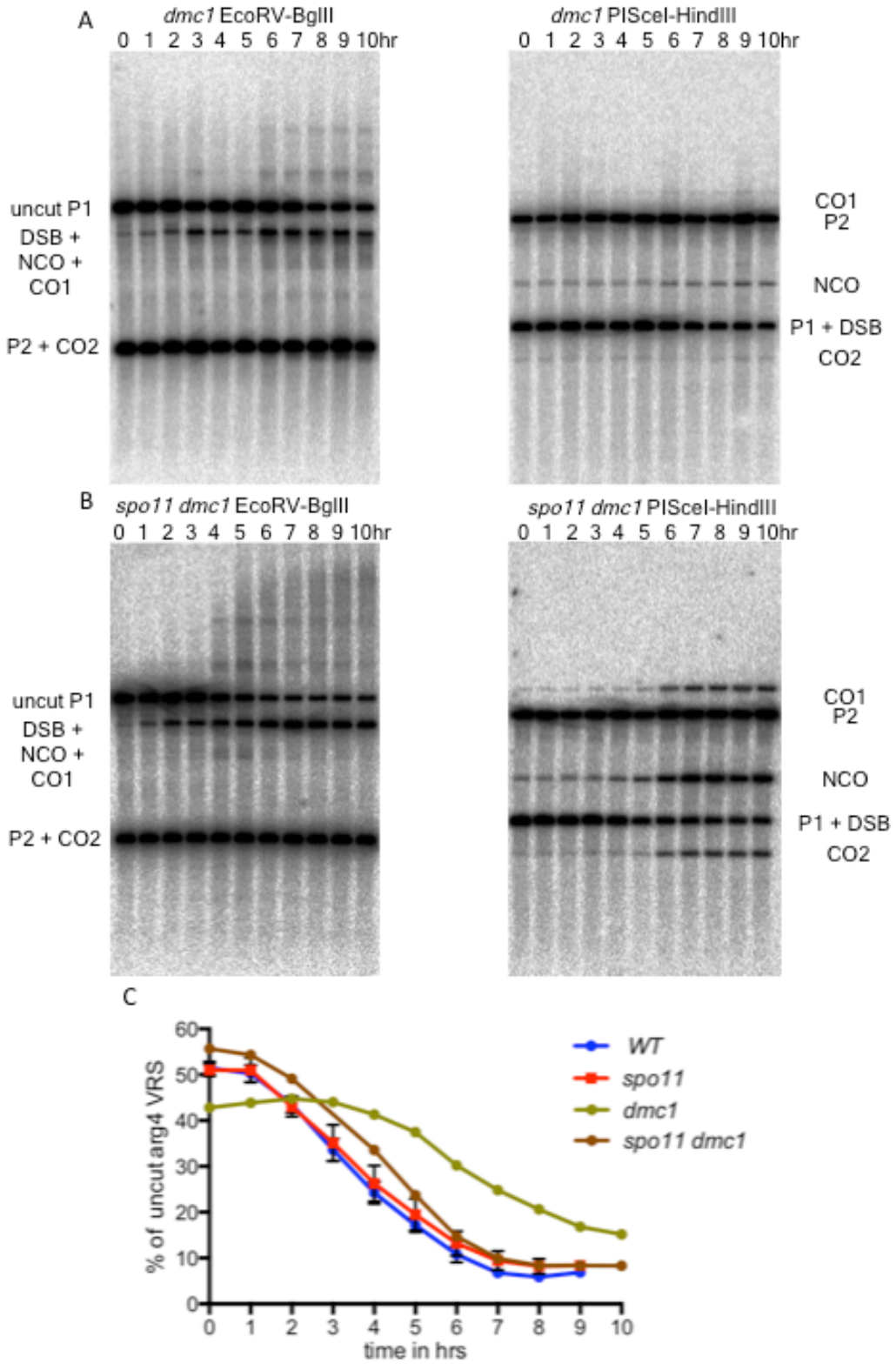
A
dmc1 EcoRV-BglII
0 1 2 3 4 5 6 7 8 9 10hr
uncut P1
DSB +
NCO +
CO1
P2 + CO2
dmc1 PIScel-HindIII
0 1 2 3 4 5 6 7 8 9 10hr
CO1
P2
NCO
P1 + DSB
CO2
B
spo11 dmc1 EcoRV-BglII
0 1 2 3 4 5 6 7 8 9 10hr
uncut P1
DSB +
NCO +
CO1
P2 + CO2
spo11 dmc1 PIScel-HindIII
0 1 2 3 4 5 6 7 8 9 10hr
CO1
P2
NCO
P1 + DSB
CO2
C
% of uncut arg4 VRS
time in hrs
WT
spo11
dmc1
spo11 dmc1

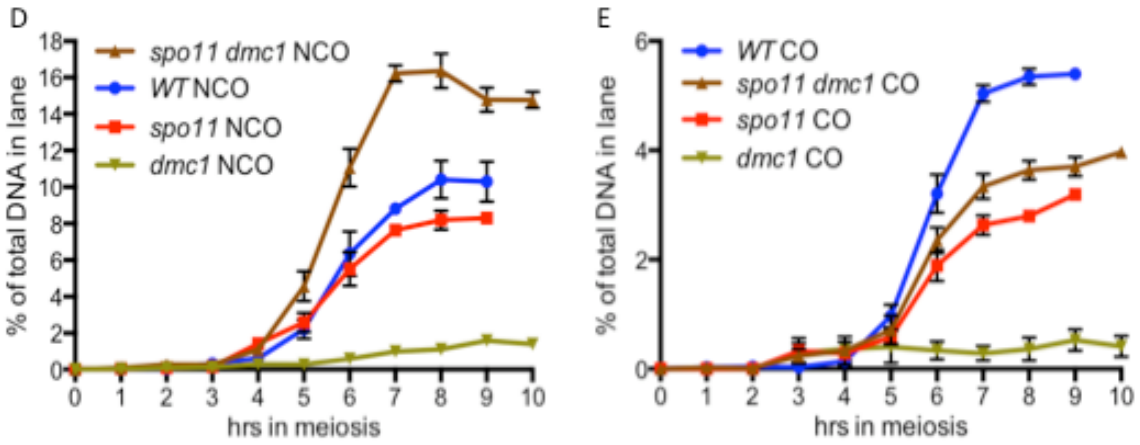

Figure 4-4 Dmc1 is not essential for VDE initiated NCOs and COs
A) Southern blot of meiotic DNA from *dmc1* strain MJL3673. The left Southern blot shows meiotic DNA digested with *Eco*Rv-*Bgl*II to determine cumulative VDE DSB levels. The right Southern blot shows meiotic DNA digested with PI*Sce*I-*Hind*III to examine COs and NCOs. Results are from a single experiment.
B) Southern blot of meiotic DNA from *spo11 dmc1* strain MJL3674. Results are from a single experiment. The left Southern blot shows meiotic DNA digested with EcoRv-BglII to examine cumulative VDE DSB levels. The right Southern blot shows meiotic DNA digested with PI*Sce*I-*Hind*III to examine COs and NCOs. Results are from two biological replicates and error bars indicate standard error of mean.
C) VDE DSB formation is altered in *dmc1* mutants, rate of loss of *arg4-VRS* is lower and the level of *arg4-VRS* chromatids at 10 hrs is at ~15% instead of ~8-5% for all other strains. *spo11 dmc1* form VDE DSBs identically to WT and *spo11* cells.
D) Very few NCOs are formed in *dmc1* mutants, NCOs are at 1.6% at 10 hrs. On the other hand, more NCOs are formed in *spo11 dmc1* than either *spo11* or WT cells. Peak NCO levels in *spo11 dmc1* are at 16.4%, compared to peak NCOs of 10.5 and 8.3% in WT and *spo11* respectively.
E) CO levels are calculated from the average of CO1 and CO2. Almost no COs form in *dmc1* mutants, while COs in *spo11 dmc1* reach a peak of 4.0% at 10 hrs, which is comparable to the peaks COs of 3.2% in *spo11* mutants.

4.4 VDE initiated COs and NCOs are dependent on Ndt80

Ndt80 is a meiosis-specific transcription factor that drives the exit from pachytene by activating the expression of the polo-like kinase Cdc5 (Xu et al. 1995, Chu and Herskowitz. 1998, Chu et al. 1998, Sourirajan and Lichten. 2008). dHJ JMs accumulate in *ndt80* (Allers and Lichten, 2001a) and the expression of Cdc5 in *ndt80* cells is sufficient to trigger the resolution of dHJ JMs to form COs (Sourirajan and Lichten. 2008). In the absence of Ndt80 or Cdc5, Spo11 initiated CO formation is reduced to ~1/5 of the WT levels and dHJ JMs persist (Allers and Lichten, 2001a, Sourirajan and Lichten. 2008). Since most of Spo11 initiated COs are dependent on Ndt80, I tested the effect of Ndt80 on VDE initiated COs, both in *ndt80* and *spo11 ndt80* mutants.

VDE DSB formation in both *ndt80* and *spo11 ndt80* mutants is unaffected (Figure 4-5B). Also, both *ndt80* and *spo11 ndt80* mutants accumulate high

molecular weight species (marked with a blue arrow in Figure 4-5C), which are consistent in size to joint molecules (JMs). In *ndt80* mutants, these JMs accumulate to a level of 2.9% of total DNA, while in *spo11 ndt80* mutants, they accumulate to 2.4% of total DNA (Figure 4-5D). Spo11 DSBs at the *HIS4-LEU2* hotspot reach ~20% of total DNA (Keeney and Kleckner. 1995), while JMs accumulated in *ndt80* mutants at *HIS4-LEU2* reach 4.5% of total DNA by 7 hrs (Allers and Lichten. 2001a). Therefore, a greater proportion of Spo11 DSBs form detectable JMs, and this is consistent with a greater proportion of Spo11 DSBs giving rise to COs, as compared to VDE DSBs. Also, JMs for Spo11 DSB repair appear as early as 4 hrs (Allers and Lichten. 2001a), while in this reporter system, the earliest detectable JMs for VDE DSB repair appear at 6 hrs in *ndt80* and 8 hrs in *spo11 ndt80* (Figure 4-5D). Since both Spo11 and VDE form DSBs during meiosis, they are in comparable cellular environments, but the Spo11 DSBs maybe in a unique local environment that promotes JM formation. VDE initiated COs in the heterologous reporter are both delayed and reduced in *ndt80* and *spo11 ndt80* (Figure 4-5G), as is the case with Spo11 initiated COs (Allers and Lichten. 2001a). Very few COs form in *spo11 ndt80*, which is greater than the CO loss in *spo11* and *ndt80* mutants. Therefore the lack of genome wide DSBs and the reduction of JM resolution function both contribute to CO loss.

The ZMM synapsis promoting proteins promote CO formation during Spo11 DSB repair (Börner et al. 2004) and associate with Spo11 CO sites (Fung et al. 2004). ZMM proteins have also been shown to associate with Holliday junctions (Snowden et al. 2004) and antagonize the activity of the Sgs1 helicase during meiosis (Jessop et al. 2006). As helicases can dissolve JMs by dissolution (Wu et al. 2006, Raynard et al. 2006. Raynard et al. 2008)(see section 1-25), the ZMM proteins may locally associate with chromatin around Spo11 DSBs to stabilize JMs and promote CO enrichment. On the other hand, ZMM proteins may be absent from VDE DSBs in the heterologous recombination reporter at *URA3*, which would reduce JM and CO formation during the repair of VDE DSBs.

NCOs are slightly delayed in *ndt80* mutants, but reach WT level at 8 hrs. NCOs continue to form past 8 hrs unlike in WT cells (Figure 4-5F). These late NCOs may arise from continued Spo11 DSB formation in *ndt80* mutants (Allers and Lichten. 2001a). In contrast, Spo11 initiated NCOs are not affected in *ndt80* mutants (Allers and Lichten. 2001a). Spo11 initiated NCOs in meiosis are believed to form primarily via SDSA (Martini et al. 2011)(section 1-24), which does not involve JM intermediates, while COs form from Ndt80 dependent JM resolution (Allers and Lichten. 2001a, Sourirajan and Lichten. 2008). On the other hand, formation of VDE initiated NCOs is delayed *ndt80* mutants, which suggest some VDE initiated NCOs may form via JM intermediates. The loss of VDE initiated NCOs in even more severe in *spo11 ndt80* mutants (Figure 4-5F), thus most VDE initiated NCOs are resolvase dependent in *spo11 ndt80* cells. The residual VDE initiated NCOs and COs in mutants lacking Ndt80 may

arise from leaky JM resolution by partially active resolvases (Matos et al. 2011). NCOs could also arise from the dissolution of JMs by Sgs1-TopIIIα-RmiI complex (Wu et al. 2006, Raynard et al. 2006. Raynard et al. 2008). However, the dissolution activity of Sgs1-TopIIIα-RmiI in *spo11 ndt80* cells is not able to restore NCO formation to WT*/ndt80* levels. Also, the level of accumulated JMs in the discrete band does not account for all the lost COs and NCOs, especially in *spo11 ndt80* mutants. Therefore these VDE initiated JMs in the heterologous reporter at *URA3* may represent intermediates, which are different from dHJ JM intermediates that arise from Spo11 DSB repair. Hence, they do not migrate as discrete bands by our assays and may have different susceptibilities to resolution or dissolution compared to Spo11 initiated JMs.

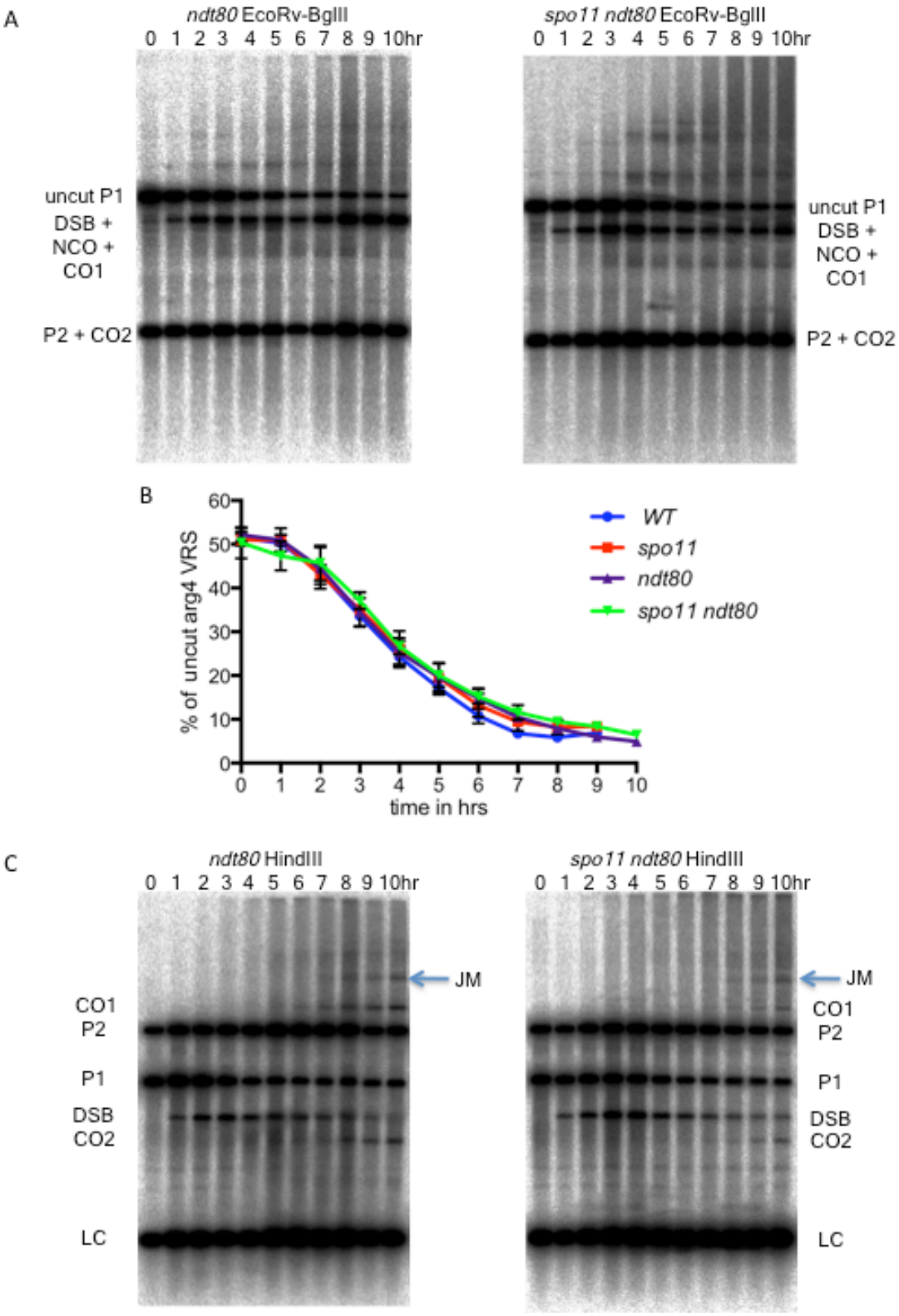
A
ndt80 EcoRv-BglII
0 1 2 3 4 5 6 7 8 9 10hr
spo11 ndt80 EcoRv-BglII
0 1 2 3 4 5 6 7 8 9 10hr
uncut P1
DSB +
NCO +
CO1
P2 + CO2
uncut P1
DSB +
NCO +
CO1
P2 + CO2
B
% of uncut arg4 VRS
time in hrs
WT
spo11
ndt80
spo11 ndt80
C
ndt80 HindIII
0 1 2 3 4 5 6 7 8 9 10hr
spo11 ndt80 HindIII
0 1 2 3 4 5 6 7 8 9 10hr
JM
CO1
P2
P1
DSB
CO2
LC
JM
CO1
P2
P1
DSB
CO2
LC

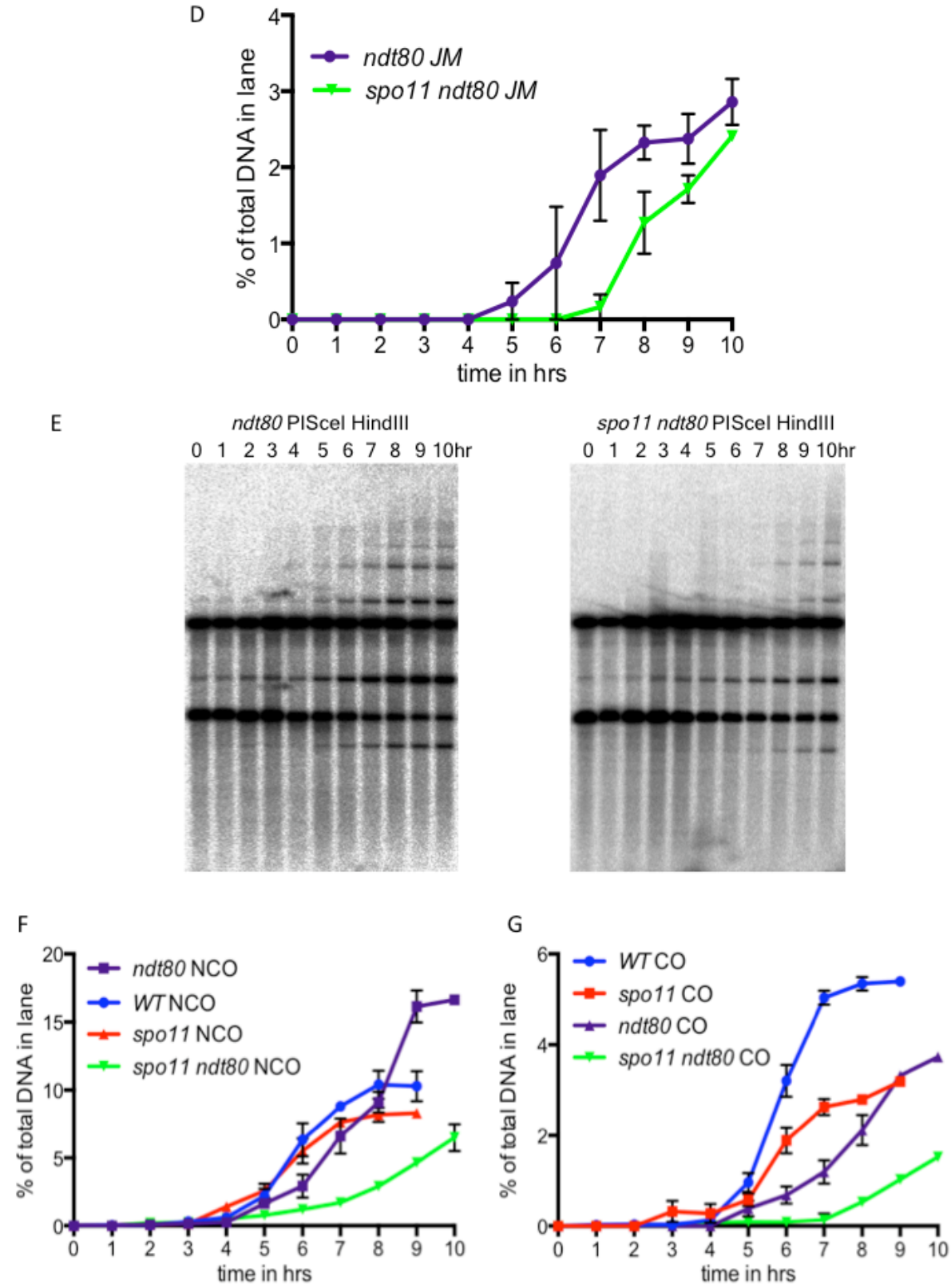

Figure 4-5 VDE initiated COs and NCOs are dependent on Ndt80
All results are from two biological replicates and error bars depict standard error of mean.
A) Southern blot of meiotic DNA from *ndt80* strain MJL3550 and *spo11 ndt80* strain MJL3675 digested with *Eco*RV-*Bgl*II to detect cumulative DSB levels.
B) VDE DSB formation in unaffected in *ndt80* and *spo11 ndt80* mutants.

C) Southern blot of meiotic DNA from *ndt80* strain MJL3550 and *spo11 ndt80* strain MJL3675 digested with *Hind*III to examine levels of JMs, indicated with the solid blue arrow.
D) *ndt80* mutants accumulate JMs at 2.9%, while *spo11 ndt80* mutants accumulate JMs at 2.4%.
E) Southern blot of meiotic DNA from *ndt80* strain MJL3550 and *spo11 ndt80* strain MJL3675 digested with PI*Sce*I-*Hind*III to examine COs and NCOs.
F) NCO formation in *ndt80* is slightly delayed initially, but reach ~88% of WT NCO levels at 8 hrs, and NCOs keep accumulate past 8 hrs, unlike in WT where they plateau. NCOs in *spo11 ndt80* are delayed and reach about 63% of WT NCOs and 78% of *spo11* NCOs by 10 hrs.
G) CO levels are calculated as the mean of CO1 and CO2. CO formation is significantly delayed in *ndt80* mutants and COs reach ~69% of WT COs at 10 hrs. COs are even further delayed in *spo11 ndt80* mutants, and reach ~28% of WT COs and 48% of *spo11* COs.

4.5 The mitotic CO resolvase Mus81-Mms4 forms the majority of VDE initiated COs

VDE initiated COs show dependence on Ndt80, and in the absence of Ndt80, few VDE initiated COs form initially, but CO formation gradually increases past 6 hrs. In mitotic cells, Mus81-Mms4 is the primary resolvase that form COs and Yen1 is its backup (Ho et al. 2010). Matos et al. 2011 showed that the Mms4, which is the partner of Mus81, is phosphorylated by Cdc5 in meiosis I which hyperactivates it, while Yen1 in activated in meiosis II by dephosphorylation. However, Mus81-Mms4 would still retain some activity in the absence of Ndt80, which could form the residual COs in *ndt80* mutants, I therefore looked at meiotic null mutants of Mms4 (*mms4-mn*) and mutants of Yen1 to examine if Mus81-Mms4 and Yen1 were responsible for VDE initiated CO formation in the heterologous reporter at *URA3.* Using meiotic null mutant for Mms4 ensures that the phenotypes seen are not a result of accumulation of mitotic DNA damage, as Mus81 is required for efficient mitotic recombination (Mazón and Symington. 2013) and resistance of mitotic cells to DNA damage (Ho et al. 2010).

The *mms4-mn* and *yen1* mutants have no effect of VDE DSB formation (Figure 4-6B), and Yen1 does not affect NCO or CO formation as well (Figure 4-6E,F). On the other hand, the *mms4-mn* behaves like a less severe version of *ndt80* (Figure 4-6E,F). JM accumulation is seen to a lesser extent in *mms4-mn* than *ndt80* (Figure 4-6D). NCOs are slightly delayed but their levels are unaffected, while COs are again delayed but their levels reach ~86% of WT by 8 hrs (Figure 4-6E,F). These data are consistent with Mus81-Mms4 being the primary resolvase for VDE initiated CO formation, and the leaky resolvase activity in *ndt80* mutants may be from partially active Mus81-Mms4 (Matos et al. 2011). Also, Mus81-Mms4 is believed to be an unbiased resolvase that can form both NCOs and COs (De Muyt et al. 2012). This is again consistent with a fraction of VDE initiated JMs also forming NCOs. Yen1 may perform a backup role for late VDE initiated CO formation, and may be responsible

for some of the late resolvase activity in *ndt80* mutants and the major resolvase in *mms4-mn* mutants, as Yen1 activation does not required Ndt80 activation of Cdc5 phosphorylation (Matos et al. 2011). On the other hand, Spo11 initiated COs are very modestly affected by *mms4-mn, yen1* and even *mms4-mn yen1* double mutants show COs at 80-90% of levels seen in wild type cells (De Muyt et al. 2012 Zakharyevich et al. 2013). Therefore, in terms of CO formation, yet again VDE DSB repair in the heterologous recombination reporter at *URA3* shares more features with mitotic rather than meiotic recombination.

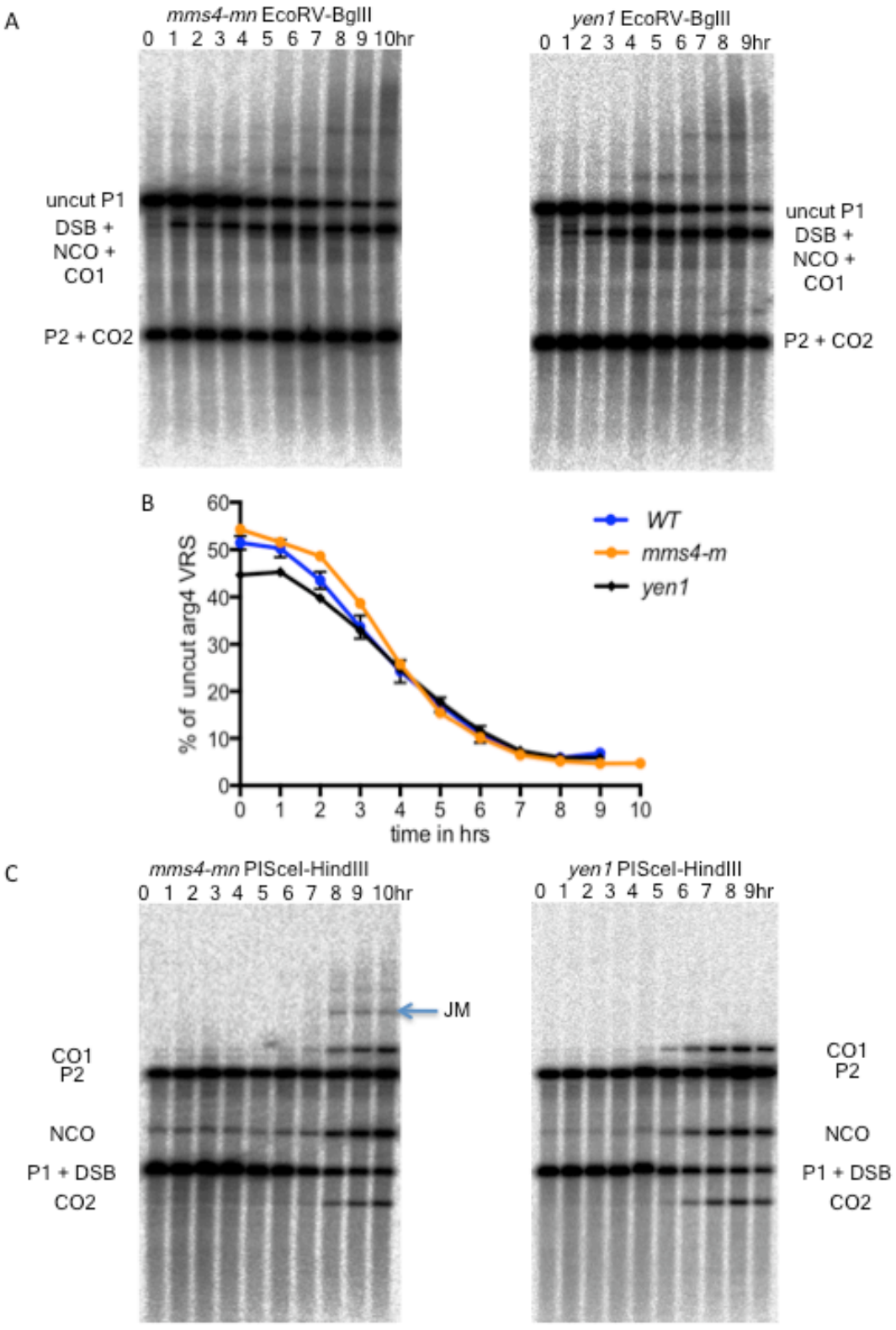
A
mms4-mn EcoRV-BglII
0 1 2 3 4 5 6 7 8 9 10hr
yen1 EcoRV-BglII
0 1 2 3 4 5 6 7 8 9hr
uncut P1
DSB +
NCO +
CO1
P2 + CO2
uncut P1
DSB +
NCO +
CO1
P2 + CO2
B
WT
mms4-m
yen1
% of uncut arg4 VRS
time in hrs
C
mms4-mn PIScel-HindIII
0 1 2 3 4 5 6 7 8 9 10hr
yen1 PIScel-HindIII
0 1 2 3 4 5 6 7 8 9hr
JM
CO1
P2
NCO
P1 + DSB
CO2
CO1
P2
NCO
P1 + DSB
CO2

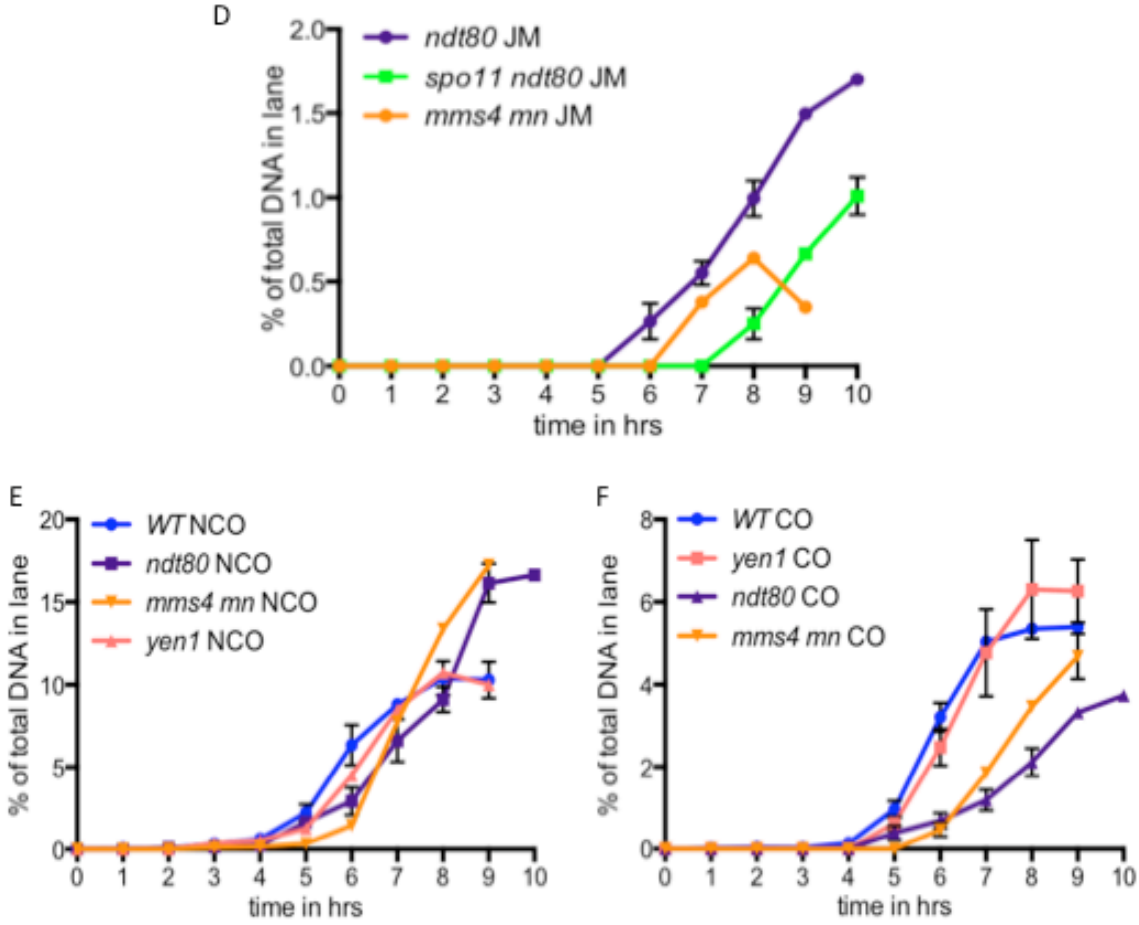

Figure 4-6 Mus81-Mms4 is the primary resolvase for VDE initiated COs
A) Southern blot of meiotic DNA from *mms4-mn* strain MJL3676 and *yen1* strain MJL3560 digested with *Eco*RV-*Bgl*II to examine cumulative DSB levels. Results are from a single experiment.
B) VDE DSB formation is unaffected in *mms4-mn* and *yen1*.
C) Southern blot of meiotic DNA from *mms4-mn* strain MJL3676 and *yen1* strain MJL3560 digested with with PISceI-HindIII to examine COs and NCOs. Results are from a single experiment.
D) JMs (marked with a blue arrow on C) accumulate in *mms4-mn*, but might begin to resolve after 8 hrs.
E) NCOs are unaffected in both *mms4-mn* and *yen1,* although they are slightly delayed in *mms4-mn*, akin to *ndt80* mutants.
F) CO levels, calculated as the mean of CO1 and CO2, are unaffected in *yen1*, while COs are significantly delayed in *mms4-mn*, but reach ~86% of WT by 8 hrs. Once again, the *mms4-mn* phenotype is similar to that of *ndt80* mutants.

5 Homologous recombination at *URA3* and *HIS4* in *arg4-VRS/arg4-VRS103* homologous cassette

5.1 Repair of VDE DSBs by HR in homologous cassettes still gives an excess of NCOs over COs, but with locus-specific differences

The initial experiments, done in the heterologous cassette with *arg4-VRS* opposite *arg4-bgl*, indicated that VDE DSB repair in meiosis is more akin to mitotic DSB repair. However, VDE DSB repair by HR in this system is not efficient (Figure 3-2B,C,E), and interhomologue recombinants account for only 1/3 of total DSBs (Figure 4-1C). To improve the efficiency of HR repair, I cloned a VDE cleavage resistant *arg-VRS103* allele opposite *arg4-VRS* (Figure 3-14C,D). This reduces the 74 bp heterology at the DSB site to a 4 bp mismatch; I refer to this new system as the homologous cassettes/reporters. Also, the VDE protein in the early experiments was constitutively expressed from its native *VMA1* promoter, which resulted in significant DSB formation prior to 2 hrs, which is also the time for meiotic DNA replication (Williamson et al. 1983, Padmore et al. 1991). For subsequent experiments, I cloned *VDE* downstream of the *pCUP1* promoter in the plasmid pMJ915, which was then integrated at the *CUP1* locus using the homology in the promoter region (Figure 3-10), such that VDE expression could now be controlled by copper. Correspondingly, the natural *VMA1::VDE* genes were replaced with *VMA1-103,* which does not express the VDE intein but is still resistant to cleavage by VDE (Figure 3-13). Meiotic induction of VDE with Cu^{+} resulted in DSB kinetics that are closer to endogenous Spo11 DSBs in meiosis (Figure 3-11D, Figure 3-12D). These modifications to the VDE recombination reporter allow more efficient repair of the VDE DSB by HR (Figure 3-14,Figure 3-15A, Table 3-3), which allows it to be more comparable to Spo11 DSB repair in meiosis.

In addition to the above, VDE recombination was initially studied only at *URA3*. The *URA3* locus was shown to be a meiotic DSB cold-spot (Wu and Lichten. 1995, Borde et al. 1999), using a recombination reporter containing *URA3* and *arg4* sequences. As discussed in the introduction section 1-42, Spo11 forms meiotic DSBs by interacting with the meiosis-specific axial element components Rad1 and Hop1, and enrichment of Red1 and Hop1 differentiates DSB hot regions from DSB cold regions (Blat et al. 2002, Panizza et al. 2011). As per data from Panizza et al. 2011, the DSB cold *URA3* region shows only median levels of Red1 and Hop1. Therefore, the VDE DSB at *URA3* could form in a different chromosome context from the majority of Spo11 DSBs. In order to determine if the chromosome context, in addition to influencing meiotic DSB formation, could also affect DSB repair, we moved the VDE DSB recombination reporter to *HIS4* (Figure 3-5, Figure 3-6, Figure 3-7, Figure 3-8 and Figure 3-9). The *HIS4* locus is a known meiotic DSB hotspot (Detloff et al. 1992,

White and Petes. 1994, Fan et al. 1995), and shows enrichment for the meiotic axial elements Red1 and Hop1 (Panizza et al. 2011). Wu and Lichten (1995) and Borde el al. (1999) also showed that there are more Spo11 DSBs in a recombination reporter inserted at *HIS4* than in the same reporter inserted at *URA3.* To confirm that the insertion of VDE recombination reporters at *URA3* and *HIS4* did not change their endogenous Spo11 activity (and correspondingly axial enrichment), Spo11 DSB formation and Spo11 CO formation were examined at *URA3* and *HIS4.* The insert of *HIS4* showed five times more Spo11 initiated recombination compared to the insert at *URA3* (Figure 3-16).

Having accomplished these modifications to the recombination reporter system, I studied VDE initiated meiotic recombination at both *URA3* and *HIS4* loci. As with the previous system, I first determined the efficiency of interhomologue recombination in the new system. VDE DSB levels were determined by looking at the loss of uncut parent, which was done by subtracting the levels of free DSB band from *Hind*III digests (Figure 3-14A,B) from the levels of *arg4-VRS* + DSB band in PI*Sce*I-*Hind*III digests (Figure 5-1A,B). The level of the VRS parental band goes from ~50% to ~5% at both *ura3* and *his4* (Figure 5-1C). Thus, as before, 45% of *arg4-VRS* chromatids i.e. 90% of *VRS* sites were cleaved by VDE. This means that both *VRS* sister chromatids are being cleaved, so partner choice can't be studied in the new system as well. But, unlike Spo11 DSBs, VDE DSBs form at both loci at equal levels and with similar kinetics. Also, level of IH recombinants at *URA3* and *HIS4* in the new homologous cassettes reaches ~30% (Figure 5-1D), this allows for more comparable meiotic recombination scenarios at *URA3* and *HIS4.*

Also, as previously mentioned, the level of IH recombinants in the new homologous cassettes reaches ~30% (Figure 5-1D) as compared to ~15% in the heterologous cassette (Figure 4-1C). Therefore 2/3 of VDE DSBs are repaired to give IH recombinants, which is twice as many as with the heterologous cassette. This suggests that the 74 bp heterology opposite the DSB site causes a 2-fold reduction in recombination efficiency.

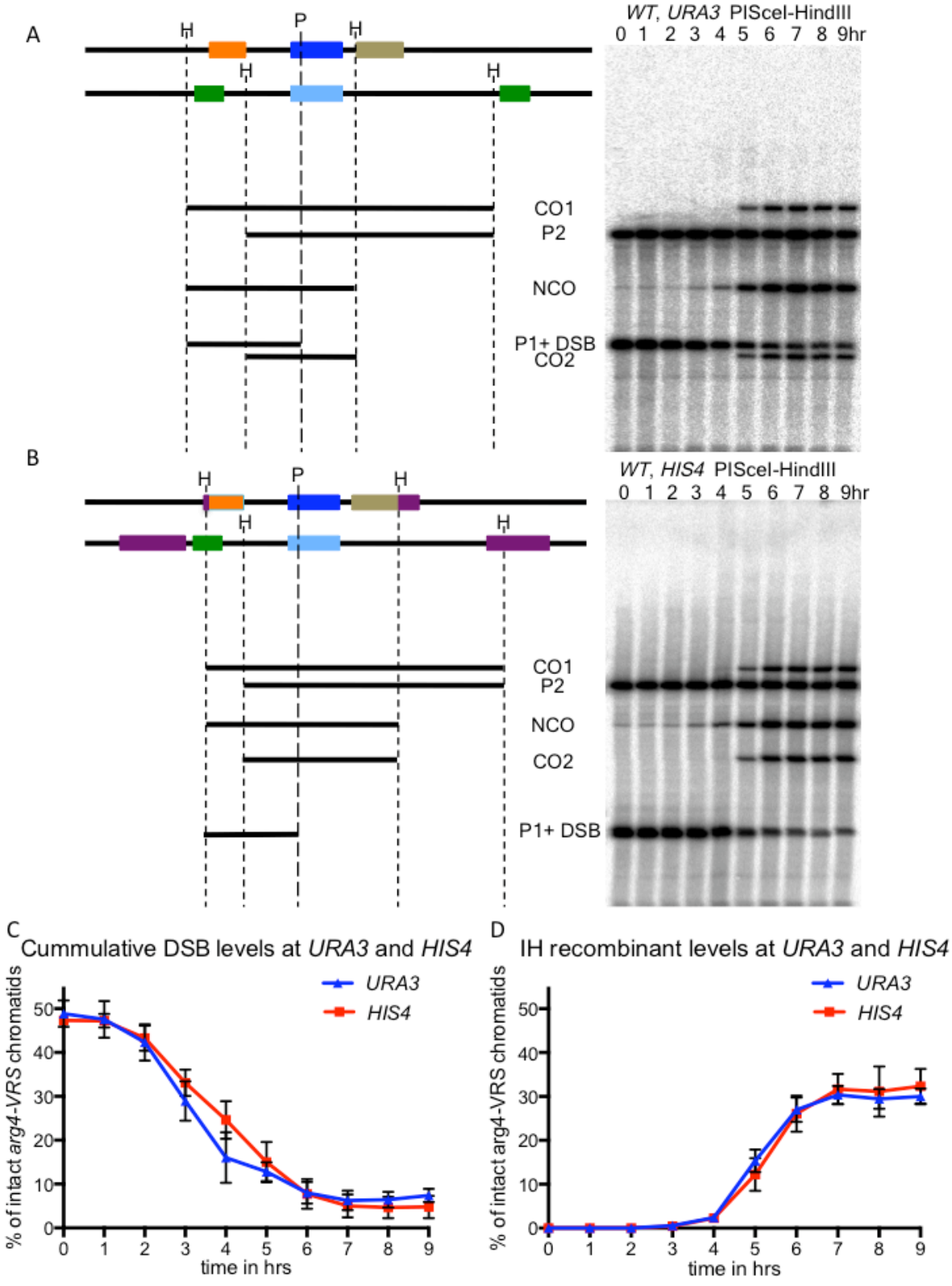

Figure 5-1 VDE DSBs are formed at equal levels at both the *URA3* cold-spot and the *HIS4* hot-spot, and subsequently both loci also form roughly equal levels of interhomologue recombinants

A) Southern blot with corresponding construct map of PI*Sce*I-*Hind*III digest of meiotic DNA from WT, *URA3* strain MJL 3624. The identity of each band is described to the left of the blot. Subsequent blots with this digest will use a shorter annotation for the bands, which is shown to the right.

B) Southern blot with corresponding construct map of PI*Sce*I-*Hind*III digest of meiotic DNA from WT, *HIS4* strain MJL 3618.
C) The level of the *arg4-VRS* band from both *URA3* and *HIS4* reporters goes from ~50% to ~5%, so 45% of chromosomes, or 90% of *VRS* sites are being cleaved.
D) IH recombinants at both loci form to ~30%. All results are from two biological replicates and error bars depict standard error of mean.

Of the total IH recombinants that form in the homologous cassettes, NCOs are in excess of COs at *URA3* by 3-fold (Figure 5-2B). The excess of NCO over COs in the heterologous cassette at *URA3* is 2-fold (Figure 4-1D). NCO levels are at 22.5% in the homologous cassette at *ura3* while they are at 10.4% in the heterologous cassette at *URA3*. Thus there is a 2.2 fold decrease in NCOs due to the heterology. On the other hand, CO levels are at 7.85% in the homologous cassette and 5.4% in the heterologous cassette, which is a 1.4 fold decrease (Figure 3-15C). Therefore, as mentioned earlier, there is a greater loss of NCOs than COs in the heterologous cassette versus the homologous cassette (Figure 3-15C). Therefore, heterology at the site of DSB affects IH NCO formation more than IH CO formation.

NCOs are also in excess over COs in the homologous reporter cassette at *HIS4,* by 2-fold (Figure 5-2C). Thus the bias towards NCO is lower at *HIS4* than at *URA3.* NCOs are at roughly equal levels at both loci (Figure 5-2D), but there are 1.3 times more COs at *HIS4* than at *URA3* (Figure 5-2E). The difference in COs between *HIS4* and *URA3* loci cannot be accounted for by simply adding up the Spo11 initiated COs, which would be more abundant in the *HIS4* hot-spot. As mentioned previously, all VDE initiated COs are resistant to cleavage by VDE/PI*Sce*I, while only 0.5% of Spo11 initiated COs are PI*Sce*I resistant, and the difference in COs between *URA3* and *HIS4* is 2.6%. Therefore, VDE DSB repair has a stronger NCO bias at *URA3* compared to *HIS4.*

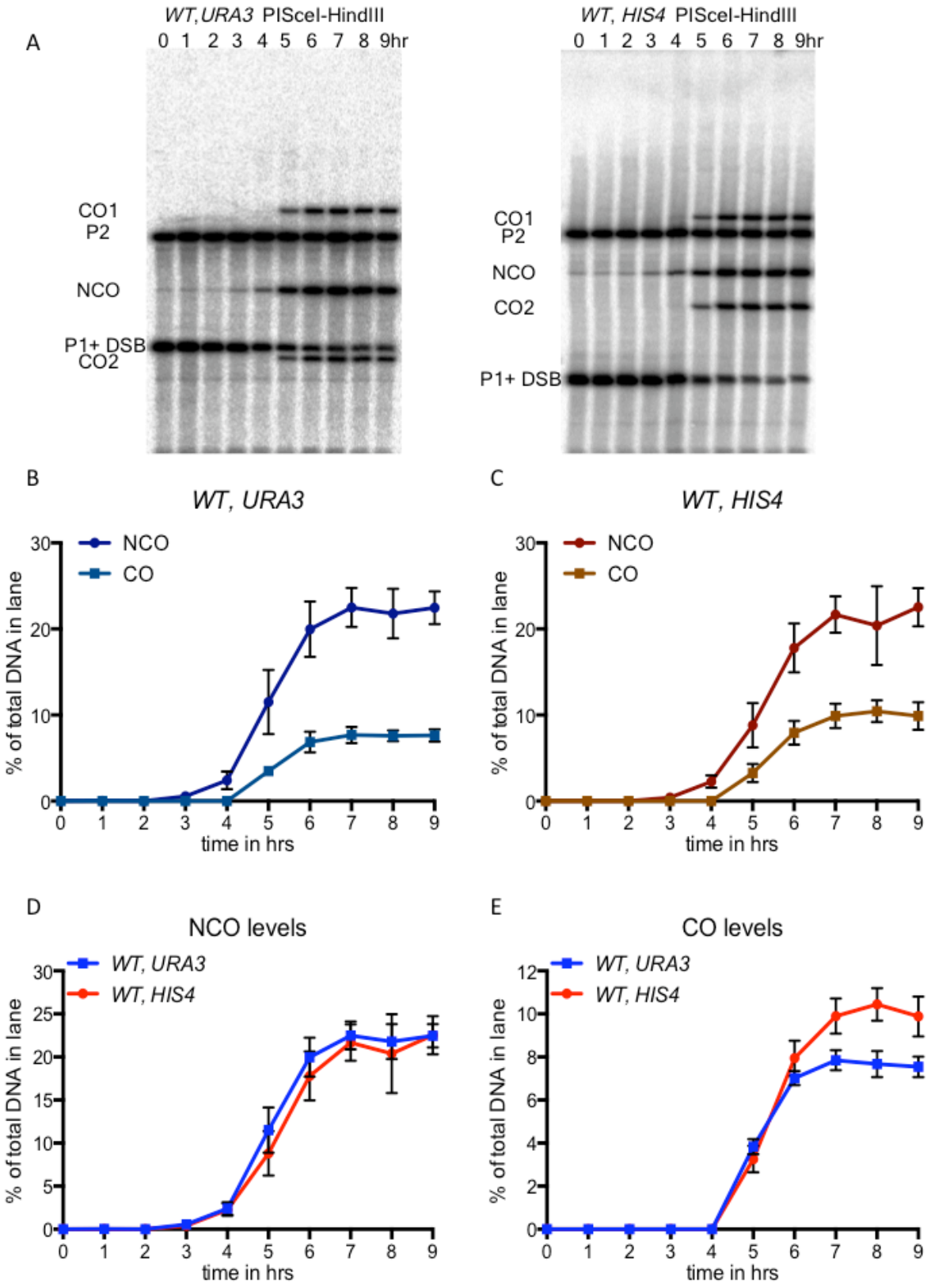

Figure 5-2 VDE DSB repair in meiosis gives an excess of NCOs over COs at both loci, but more COs form at *HIS4*.
A) Southern blots of meiotic DNA from WT, *URA3* strain MJL3624 and WT, *HIS4* strain MJL3618 digested with PIScel-HindIII to look at NCOs and COs. All results are from two biological replicates for each strain. All results are from two biological replicates and error bars depict standard error of mean.

B) In WT, *URA3,* NCOs are at 22.5% and CO are at 7.7%, which is ~3 fold excess of NCOs.
C) In WT, *HIS4,* NCOs are at 22.5% and CO are at 10.4%, which is ~2 fold excess of NCOs
D) Roughly equal NCOs form at both *URA3* and *HIS4* in WT strains.
E) CO levels are calculated as the average of CO1 and CO2. CO levels are at *HIS4* are at 1.33 times greater level than COs at *URA3* in WT strains

5.2 VDE DSB repair in *spo11* strains is even more biased towards NCOs, and both loci behave identically

As with the previous experiments, I sought to determine if the lack of genome wide meiotic DSBs also had an effect on VDE DSB repair in the homologous cassettes. The kinetics of formation and repair of VDE DSBs remain unchanged in *spo11* mutants as compared to WT strains at both loci (Figure 5-3B,C)

NCOs are in 2-3 fold excess over COs for VDE DSB repair at *URA3* and *HIS4* respectively in WT strains. This bias in NCOs is further increased in *spo11* strains, NCOs are now in 5.6 fold excess over COs at *HIS4* and 5.4 fold at *URA3.* NCO levels in *spo11* mutants are at 24.4% and 25% at *URA3* and *HIS4* respectively, which is close to NCO levels in WT strains (Figure 5-4B,C,D). However, CO levels in *spo11* mutants are 4.6% at both loci, which is a reduction of 1.7 and 2.3 times at *URA3* and *HIS4* respectively (Figure 5-4B,C,E). Thus, there is a selective loss of COs in the absence of genome wide DSBs, an affect that is also seen in the heterologous cassette. This loss of COs at either loci cannot be due to the *cis* effect of losing Spo11 DSBs in the insert. The maximum level of Spo11 initiated PI*Sce*I resistant COs is 0.5%, while the CO loss at *URA3* and *HIS4* in *spo11* mutants is 3.25% and 5.85% respectively. Therefore, there is a *trans* effect of losing genome wide Spo11 DSBs on VDE DSB repair. This is consistent with earlier studies on *SPO13::HO* DSBs by Malkova et al. (2000).

Another observation of note is that unlike in WT cells where there are 2.6% more COs at *HIS4* than *URA3*, s*po11* mutants form COs at an equal frequency at both loci. If there are any locus specific recombination properties at *HIS4*, that allow an increase in CO formation, this appears to be lost in the absence of genome wide DSBs. Therefore, CO enrichment in meiosis requires global DSB formation.

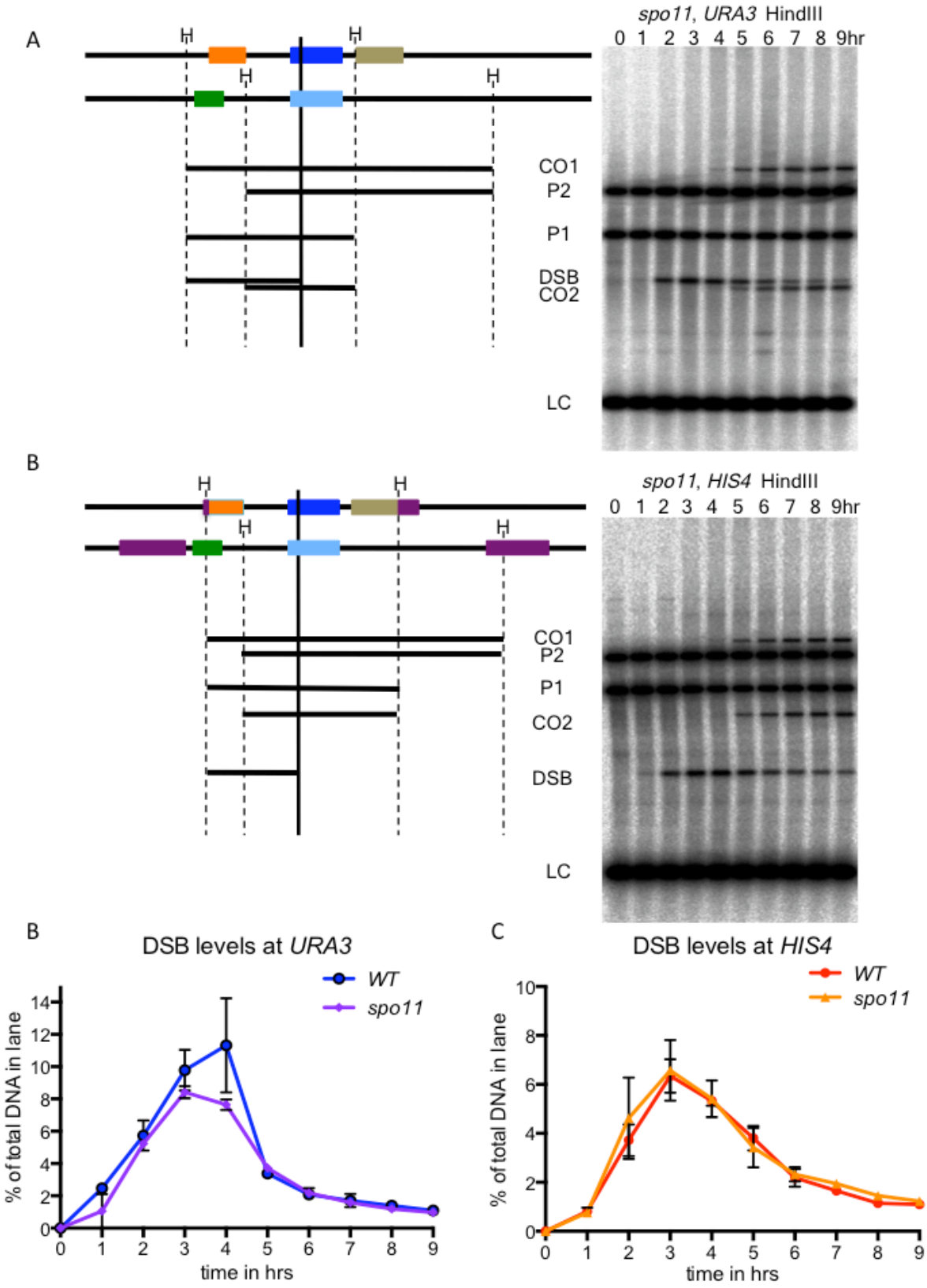

Figure 5-3 *spo11* mutation has no effect on the kinetics of VDE DSB formation and repair
A) Southern blot with corresponding construct map of meiotic DNA from *spo11, URA3* strain MJL 3605 digested with *Hind*III. The identity of each band is described to the left of the blot. Subsequent blots with this digest will use a shorter annotation for the bands, which is shown to the right.

B) Southern blot with corresponding construct map of *Hind*III digest of meiotic DNA from *spo11, HIS4* strain MJL 3606. The identity of each band is described to the left of the blot. Subsequent blots with this digest will use a shorter annotation for the bands, which is shown to the right.
C,D) Kinetics of DSB formation are similar in WT and *spo11* strains at both loci. Results are from two biological replicates for each strain. All results are from two biological replicates and error bars depict standard error of mean.

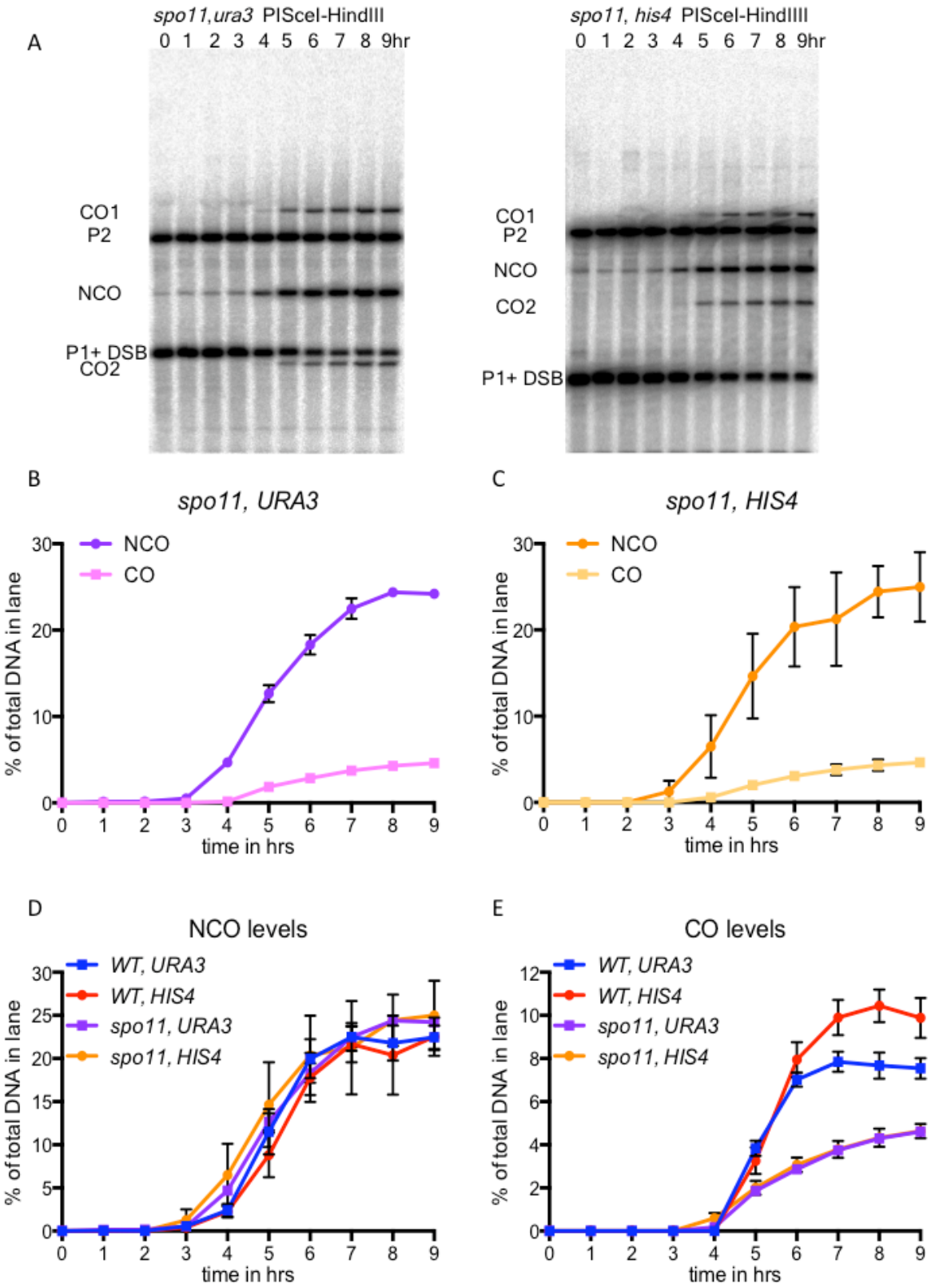

Figure 5-4 VDE DSB repair becomes more mitotic in *spo11* strains, and both loci behave identically

A) Southern blots of meiotic DNA from *spo11, URA3* strain MJL3605 and *spo11, HIS4* strain MJL3606 digested with PIScel-HindIII to look at NCOs and COs. All results are from two biological replicates for each strain

B,C) NCOs in *spo11, URA3* are at 24.4% and CO are at 4.6%, which is a ~5.3 fold excess of NCOs. In *spo11, HIS4,* NCOs are at 25% and CO are at 4.6%, which is ~5.4 fold excess of NCOs
D) NCO levels are unaffected in *spo11* mutants
E) CO levels are calculated as the average of CO1 and CO2. COs are reduced from 7.9% to 4.6% at *URA3* and 10.4% to 4.6% at *HIS4*, which is a reduction of 1.7 fold and 2.3 fold respectively. CO levels are now identical between *URA3* and *HIS4.*

Having observed a reduction of COs in *spo11* mutants in all strains examined so far (Figure 4-2F, Figure 5-4E), I sought to better understand the basis of this *trans* affect of Spo11 in CO enrichment. The absence of genome wide DSBs can lead to an altered DNA damage response and availability of repair factors. In addition, homologous pairing in *Saccharomyces cerevisiae* is dependent on DSB formation, and *spo11* mutants are known to exhibit pairing defects (Weiner and Kleckner. 1994, Loidl et al. 1994, Henderson and Keeney. 2004). NCO formation by SDSA requires only a single strand invasion event, with no second capture of the D-loop. On the other hand, CO formation via DSBR requires a second strand annealing event between the displaced D-loop of the donor to the second end of the DSB, and this may require close juxtapositioning of both chromosomes. Therefore, to separate the effects of altered DSB signaling and titration of repair proteins from pairing, I tested VDE initiated recombination in an ectopic context in WT cells, with a VDE DSB in *arg4-VRS* at *URA3* repairing from *arg4-VRS103* at *HIS4;* this strain is referred to as WT*, URA3/HIS4.* Ectopic recombination was also tested in a strain with the *arg4-VRS* at *HIS4* repairing from *arg4-VRS103* at *URA3;* this strain is referred to as WT*, HIS4/URA3.*

The ectopic strains do not differ in VDE DSB kinetics (Figure 5-5B,D). However, the level of intact *arg4-VRS* chromatids is higher than WT allelic strains from 4 hrs onwards in strains with the insert at *URA3* and 6 hrs onwards in strains with the insert at *HIS4* (Figure 5-5E,F). Also, total IH recombinant levels are reduced from ~30% in allelic strains to 13% and 19% in the *URA3/HIS4* and *HIS4/URA3* ectopic strains respectively (Figure 5-5E,F). This indicates that, in WT strains, recombination between ectopic inserts on heterologous chromosomes is less efficient that between allelic inserts on homologous chromosomes. This is consistent with past studies by Goldman and Lichten (2000), which showed interhomologue pairing in WT strains reduces ectopic recombination. These ectopic strains may also have a greater level of intersister recombination, which causes the intact *arg4-VRS* chromatids to persist at a higher level. Both NCOs and COs are also subsequently reduced in the ectopic strains (Figure 5-5G,H,I,J). However, the NCO to CO ratio is higher in both ectopic WT strains than in the allelic WT strains. The NCO to CO ratio in the ectopic *HIS4/URA3* strain is 5.3, which is very close to the NCO:CO ratio of 5.6 in *spo11* strain with allelic inserts at *HIS4.* The NCO to CO ratio for the ectopic *URA3/HIS4* strain is 4.2,which is about halfway between the NCO:CO ratio of 3 in WT and 5.4 in *spo11* strains with allelic inserts at *URA3*. Thus these results indicate that the lack of pairing

between the recombination reporter inserts can bias the outcome of HR more towards NCOs, and this may be partially responsible for the loss of COs observed in the absence of genome wide DSB formation in meiosis.

Goldman and Lichten (1996) looked at Spo11 initiated ectopic recombination between dispersed sequences during meiosis, and CO frequency in ectopic recombination between six loci on non homologous chromosomes was still enriched to ~50% frequency. This would suggest that Spo11 initiated recombination is enriched for CO formation in both allelic and ectopic contexts, while VDE initiated ectopic recombination has lower CO frequency than allelic recombination. Thus, Spo11 DSB repair in meiosis seems to be always enriched for CO formation, in both allelic and ectopic recombination. Spo11 DSB formation is dependent on axis proteins (Mao-Draayer et al. 1996, Schwacha and Kleckner 1997) and the RMM sub-complex of the meiotic DSB forming complex directly associates with axial elements (Panizza et al. 2011), therefore Spo11 DSBs are perhaps always repaired within the context of the axis. VDE DSBs, on the other hand, can be formed independently of axis proteins (Fukuda et al. 2008), and the VDE protein reportedly does not have any direct interactions with axis proteins, so even at the axis enriched *HIS4* locus, VDE DSBs may be mostly repaired outside the context of the meiotic axis. Therefore, Spo11 DSBs are always enriched for CO formation, while VDE DSBs more frequently form NCOs.

Another interesting observation is that the *HIS4/URA3* ectopic setup, where the DSB is at *HIS4*, has 1.5 times more ectopic recombinants than *URA3/HIS4,* where the DSB is at *URA3* (Figure 5-5E,F). Also kinetics for loss of *arg4-VRS* in the *HIS4/URA3* closely resembles the allelic reporter at *HIS4* up to 6 hrs. On the other hand, kinetics for loss of *arg4-VRS* at *URA3/HIS4* start deviating from the allelic reporter at *URA3* from 4 hrs, which may be due to increased intersister recombination that restores *arg4-VRS* chromatids. Thus, the VDE DSB insert at *HIS4* is more capable of ectopic recombination than the VDE DSB insert at *URA3*. *HIS4* is a Spo11 DSB hot-spot that is also enriched for Red1 (Panizza et al. 2011), and Red1 is known to be required for the interhomologue bias in Spo11 initiated recombination (Schwacha and Kleckner 1997, Hong et al. 2013). Thus the increased presence of Red1 at *HIS4* may prevent VDE DSB repair via intersister recombination at this locus, which then increases the level of ectopic recombination.

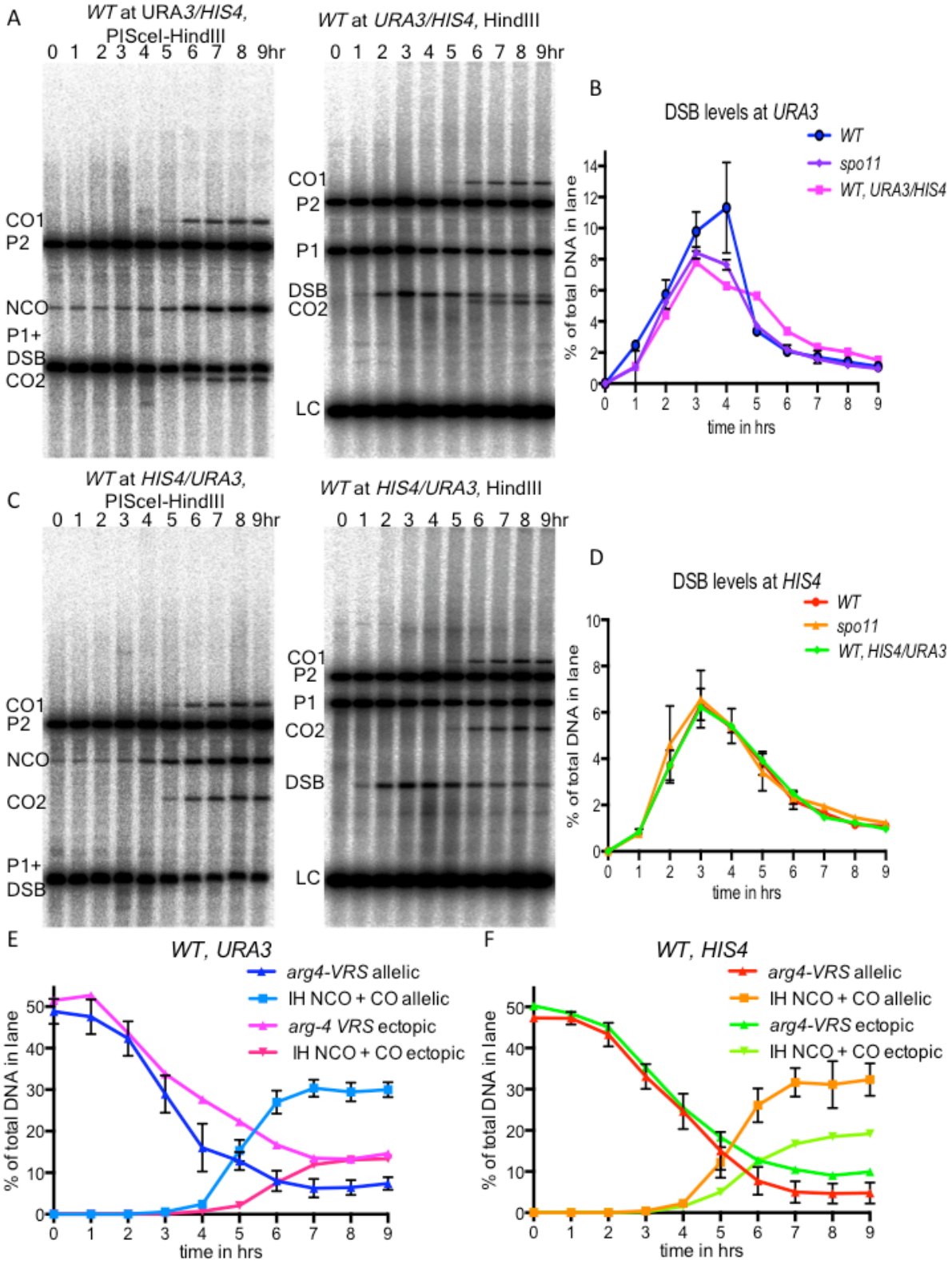
A
WT at URA3/HIS4, PIScel-HindIII
0 1 2 3 4 5 6 7 8 9hr
CO1
P2
NCO
P1+
DSB
CO2
WT at URA3/HIS4, HindIII
0 1 2 3 4 5 6 7 8 9hr
CO1
P2
P1
DSB
CO2
LC
B
DSB levels at URA3
WT
spo11
WT, URA3/HIS4
% of total DNA in lane
time in hrs
C
WT at HIS4/URA3, PIScel-HindIII
0 1 2 3 4 5 6 7 8 9hr
CO1
P2
NCO
CO2
P1+
DSB
WT at HIS4/URA3, HindIII
0 1 2 3 4 5 6 7 8 9hr
CO1
P2
P1
CO2
DSB
LC
D
DSB levels at HIS4
WT
spo11
WT, HIS4/URA3
% of total DNA in lane
time in hrs
E
WT, URA3
arg4-VRS allelic
IH NCO + CO allelic
arg-4 VRS ectopic
IH NCO + CO ectopic
% of total DNA in lane
time in hrs
F
WT, HIS4
arg4-VRS allelic
IH NCO + CO allelic
arg4-VRS ectopic
IH NCO + CO ectopic
% of total DNA in lane
time in hrs

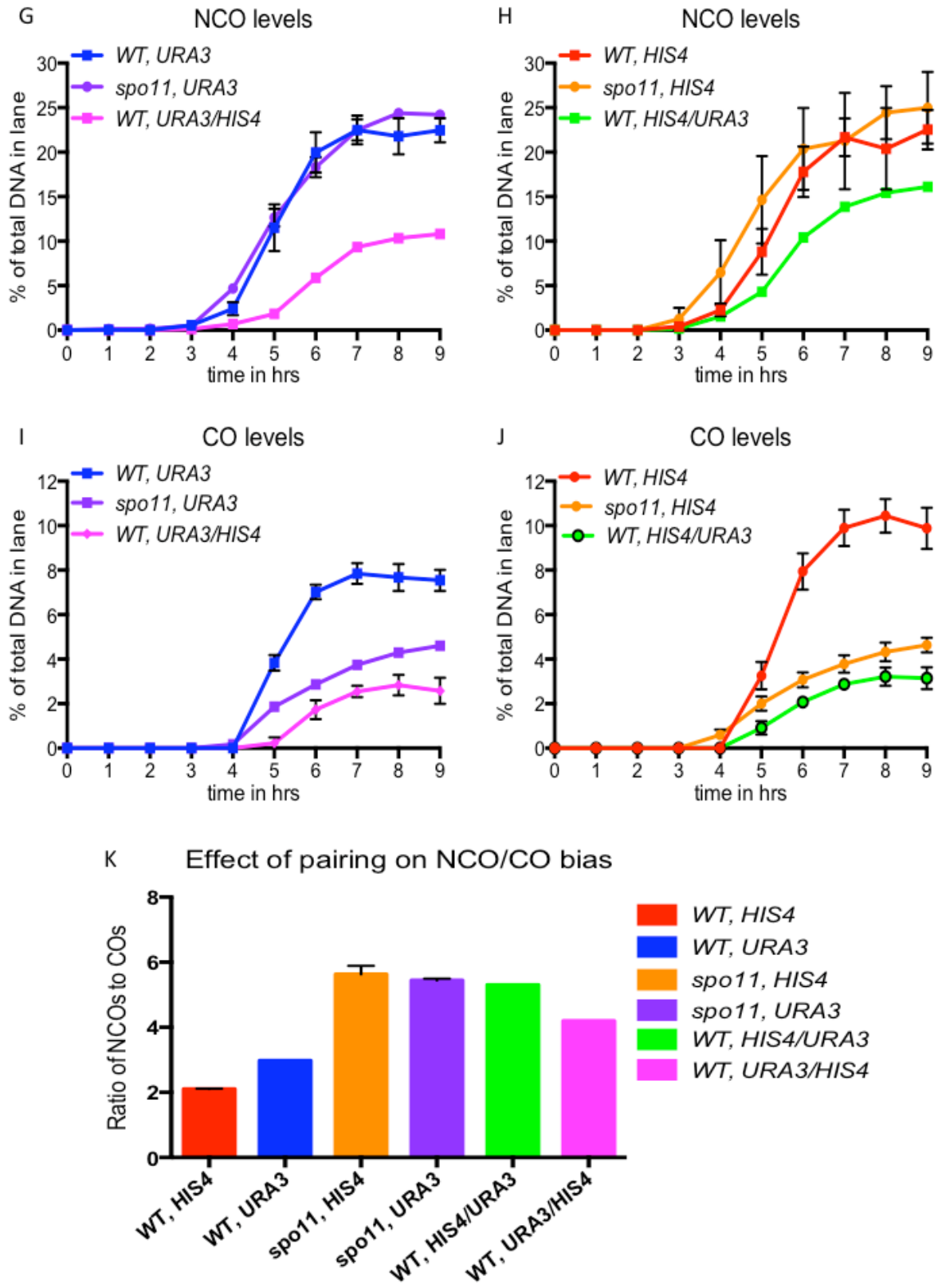

Figure 5-5 VDE initiated interhomologue recombination is reduced in ectopic strains and NCO to CO ratio is increased, similarly to *spo11* mutants.
A) Southern blots of meiotic DNA digested with *Hind*III to monitor DSBs and PI*Sce*I-*Hind*III to monitor NCOs and COs in WT, *URA3/HIS4* strain MJL3659. Results are from a single experiment.

C) Southern blots of meiotic DNA digested with *Hind*III to monitor DSBs and PI*Sce*I-*Hind*III to monitor NCOs and COs for WT, *HIS4/URA3* strain MJL3660. Results are from a single experiment.
B,D) DSB kinetics are not altered in both ectopic strains, compared to WT or *spo11* allelic strains.
E) LevelS of *arg4-VRS* band in WT, *URA3/HIS4* goes from ~50% to ~15% and levels of IH recombinants are reduced relative to WT, *URA3* strain from ~30% to ~13%.
F) Level of *arg4-VRS* band in WT at *HIS4/URA3 goes* from ~50% to ~10% and levels of IH recombinants are reduced relative to WT, *HIS4* strain from ~32% to ~19%.
G) NCOs are reduced from 22.5% and 24.2% in allelic WT and *spo11 URA3* insert strains to 10.8% of total DNA in the *URA3/HIS4* ectopic strain.
H) NCOs are reduced from 22.5 and 25 % in allelic WT and *spo11 HIS4* insert strains to 16.1% in the *HIS4/URA3* ectopic strain.
I) CO levels (average of CO1 and CO2) are reduced from 7.9% and 4.6 % in allelic WT and *spo11 URA3* insert strains to 2.8% in the *URA3/HIS4* ectopic strain.
J) CO levels are the average of CO1 and CO2. COs are reduced from 10.44% and 4.6 % in allelic WT and *spo11 HIS4* insert strains to 3.15% in the ectopic strain
K) The NCO to CO ratio is 5.3 for the WT, *HIS4/URA3* strain, which is almost equal to the NCO over CO ratio for the *spo11, HIS4* strain. The NCO to CO ratio is 4.2 for the WT *URA3/HIS4* strain, which is about half the NCO to CO ratio in *spo11, URA3* strain.

5.3 JMs accumulate at both loci in *ndt80* mutants, but more so at *HIS4,* and CO formation is also affected at both loci, but more so at *URA3.*

Since the VDE initiated NCOs and COs in the heterologous cassette are affected in *ndt80* mutants, I examined if these NCOs and COs were also affected in the homologous cassettes. The *ndt80* mutation does not affect DSB kinetics at either locus (Figure 5-6B,C). JMs accumulate at both loci, and the total signal in the higher molecular weight region is 2.3 times greater at *HIS4* than at *URA3* (Figure 5-6D). COs are reduced compared to WT strains at both loci but not equally. Compared to *NDT80* strains, in *ndt80* mutants, there is a 3.3 fold loss of COs at *URA3,* while COs at *HIS4* are less affected and show a 2.5 fold loss (Figure 5-7B,C).

The increased JM accumulation at *HIS4* compared to a greater CO loss at *URA3* appears to be contradictory at first, as CO loss should be greater at the locus where more JMs accumulate. However, *ndt80* mutants are not absolutely resolvase deficient, so another way to understand this observation is to consider the properties of both loci in terms of both the propensity to form JMs, and then to protect these JMs from dissolution when resolution is deficient. The Sgs1 helicase is believed to limit JM formation by increasing the disassociation of strand invasion intermediates and shuttling them to SDSA (De Muyt et al. 2012). Sgs1 can also act at a later stage of recombination, as JMs can also be dissolved by the Sgs1-TopIIIα-RmiI complex (Wu et al. 2006, Raynard et al. 2006. Raynard et al. 2008). ZMM associated recombination events are believed to be protected from the action of helicases (Jessop et al. 2006). The *HIS4* locus, which is a Spo11 DSB hot-spot, and these Spo11 DSBs later form ZMM dependent COs (Lynn et al. 2007, Börner et al. 2004). *URA3* is cold for Spo11 DSB formation, and therefore consequently may not be ZMM associated.

Therefore, if VDE initiated recombination at *HIS4* was also in the context of the ZMM proteins, there would also be more VDE initiated JMs at *HIS4* than *URA3.* This would also result in more VDE initiated JM accumulation at *HIS4* than *URA3* in *ndt80*, which is observed (Figure 5-6D). In addition to stimulating JM formation, ZMM proteins also further protect JMs from dissolution by helicases later, to ensure CO formation. This property of ZMM proteins hence ensures that Spo11 initiated JMs in meiosis form exclusively COs (Sourirajan and Lichten. 2008). Therefore, the VDE initiated JMs at *HIS4,* which may be ZMM associated, would then also be less susceptible to dissolution and some of them may be are eventually resolved to give COs. Consistent with this assumption, accumulated JMs can account for almost all of the lost COs at *HIS4* (Figure 5-6D, Figure 5-7C). On the other hand, VDE initiated JMs at *URA3* on the may not be ZMM associated. Thus, VDE recombination at *URA3* forms fewer JMs (Figure 5-6D), and VDE initiated JMs at *URA3* could also be more susceptible to dissolution in resolution deficient mutants. Again, consistent with this, JMs accumulate to half the level of lost COs at *URA3* (Figure 5-6D, Figure 5-7C). Also, there is ~6% increase in mean NCOs in *ndt80* compared to WT at *URA3* (Figure 5-7D), which would account for the ~5.5% loss of COs in *ndt80* compared to WT (Figure 5-7B).

In the previous experiments in the heterologous cassette at *URA3*, NCO formation is delayed in *ndt80* mutants but their levels catch up to those seen in WT by 8 hrs (Figure 4-5F). In contrast, in the homologous cassette at *URA3*, NCO levels are unaffected in *ndt80*. Ndt80 induces Cdc5, which then activates resolvases that act upon JMs (Sourirajan and Lichten 2008). JM resolution in the same orientation can also form NCOs. Therefore, it is possible that in the *ndt80* strains with the heterologous cassette at *URA3*, some NCOs are formed from JM resolution, and thus the lack of Cdc5 activation would result in low resolvase activity, which consequently delays NCO formation. This would mean that fewer NCOs form from SDSA, which is independent of JM resolution, in the heterologous strains. *ndt80* mutants show very little effect on Spo11 initiated NCOs (Allers and Lichten 2001a), as the majority of these NCOs are believed to be formed by SDSA (Martini et al. 2011). Similarly, *ndt80* mutation has no effect on NCO formation in strains with homologous cassettes, suggesting that these NCO may also form mostly by SDSA. Thus, It appears that heterology at the break repair site can affect the balance between SDSA and JM formation, which in turn affects how NCOs form in heterologous versus homologous contexts.

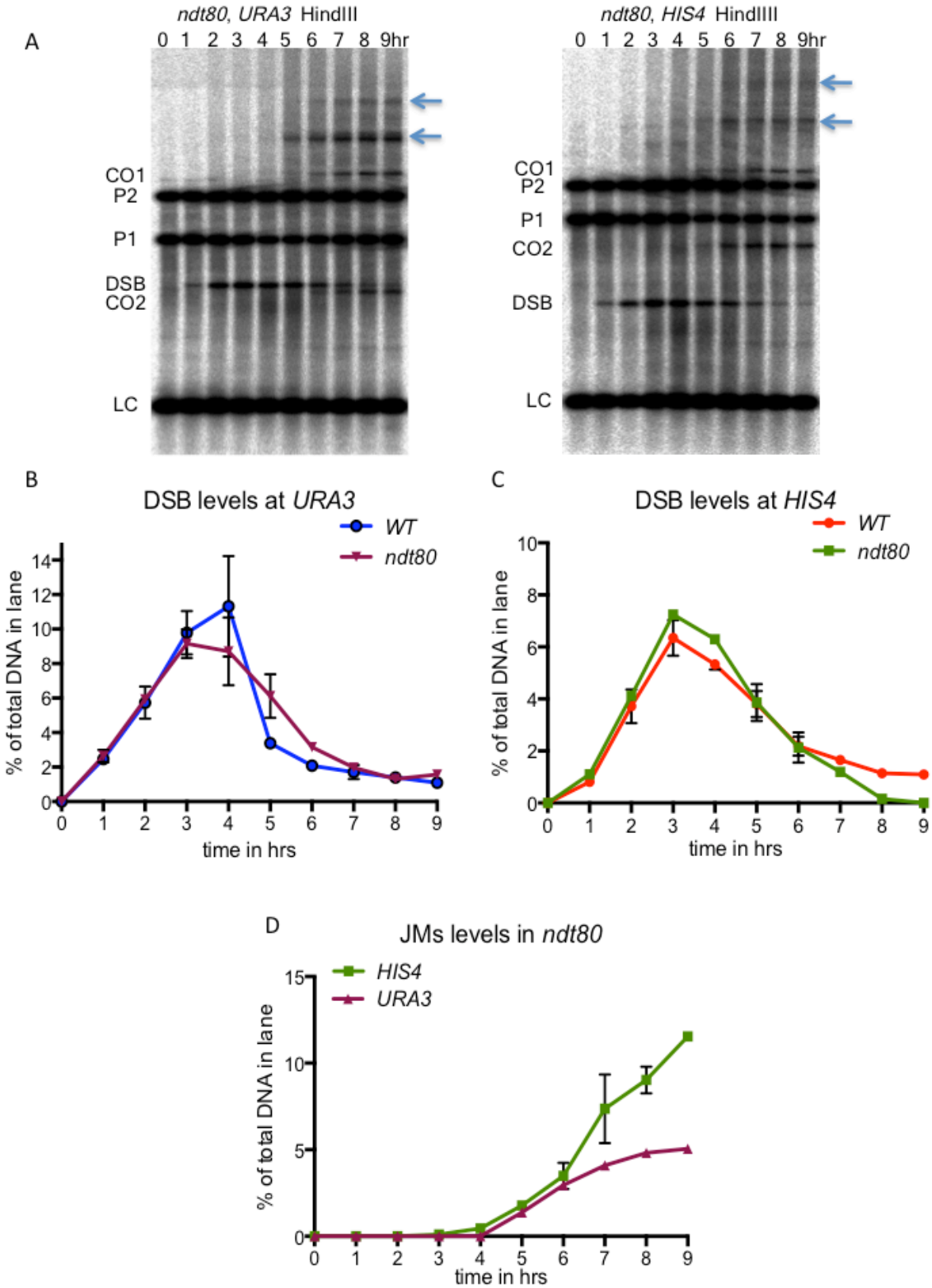

Figure 5-6 *ndt80* strains do not affect DSB kinetics, but do accumulate JMs, at a higher levels at *HIS4* than *URA3*.
A) Southern blots of meiotic DNA digested with *Hind*III to look at JMs and DSBs for *ndt80, URA3* strain MJL3630 and *ndt80, HIS4* strain MJL3631. All results are from two biological replicates for each strain and error bars indicate standard error of mean. Blue arrows indicate discrete JM peaks that were quantified.

B,C) *ndt80* mutants do not affect DSB kinetics
D) The total level of JMs accumulation is 2X higher at *HIS4* (11.5%) than at *URA3* (5.1%) at 9 hrs.

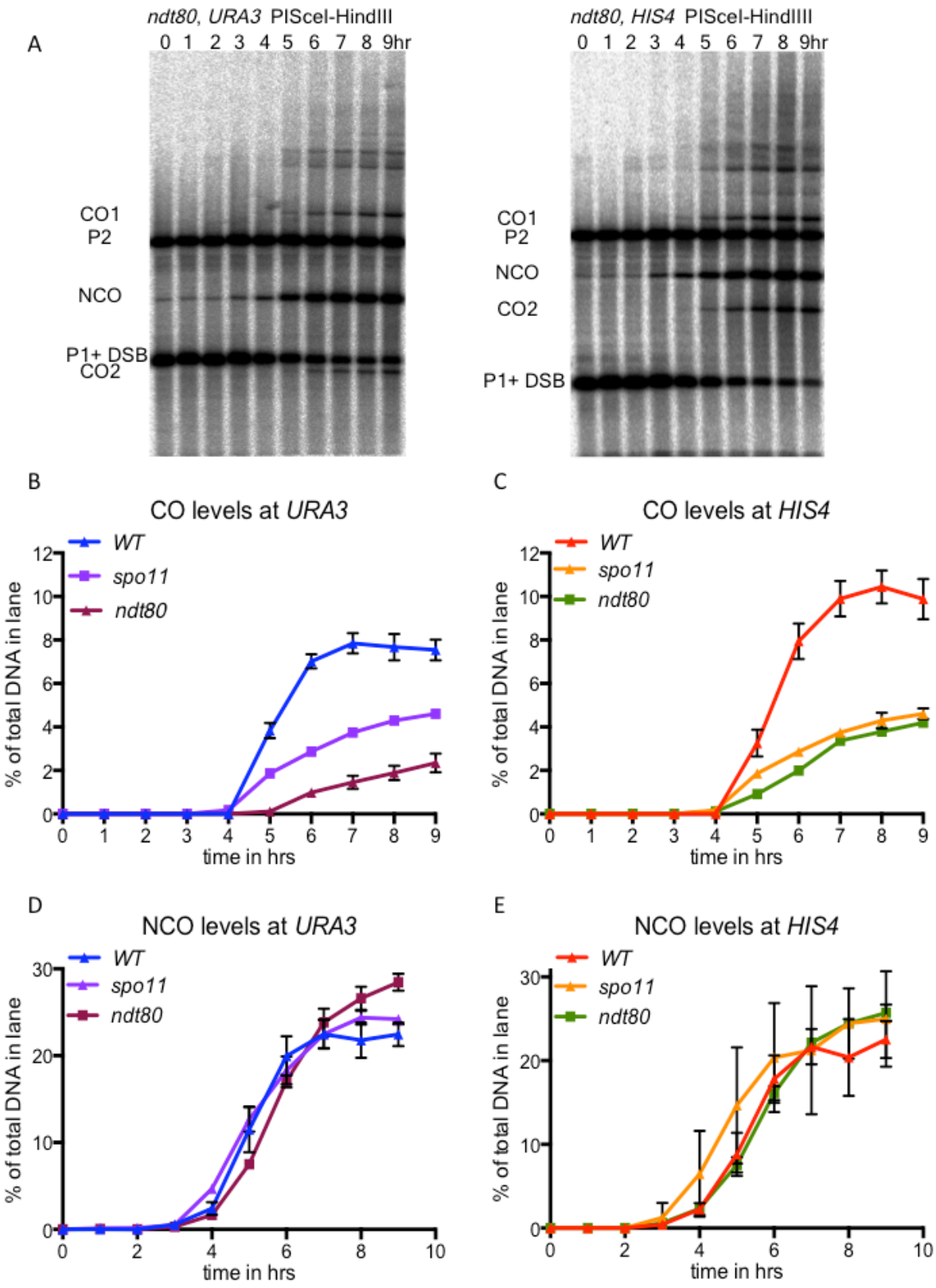

Figure 5-7 Ndt80 affects VDE initiated COs at both loci, and the effect is greater at *URA3*. NCOs are unaffected.
A) Southern blots of meiotic DNA digested with PI*Sce*I-*Hind*III to look at NCOs and COs for *ndt80, URA3* strain MJL3630 and *ndt80, HIS4* strain MJL3631. All results are from two biological replicates for each strain and error bars indicate standard error of mean.
B) COs (mean of CO1 and CO2) at *URA3* reduce from 7.9% to 2.4%, which is 3.3 fold loss.

C) COs (mean of CO1 and CO2) at *HIS4* reduce from 10.4% to 4.2%, which is 2.5 fold loss. D)E) NCOs are at 28.5% at *URA3* and 25.7% at *HIS4,* which are both close to WT levels.

5.4 *spo11 ndt80* mutants affect COs at both *URA3* and *HIS4*, and NCOs at *URA3* are also slightly affected.

Both COs and NCOs are both severely delayed and reduced in *spo11 ndt80* mutants in the heterologous cassette at *URA3,* which suggested that both NCOs and COs in these mutants are formed via JM resolution. Therefore, I also sought to examine if the DSB repair in the homologous cassettes was similarly affected. *spo11 ndt80* mutants do not alter DSB kinetics (Figure 5-8B,C). JMs also accumulate at both loci, but now, the total signal at *URA3* and *HIS4* is much closer (Figure 5-8D). This is consistent with the observation that both loci behave more similarly in the absence of genome wide DSBs 9(Figure 5-4E), and residual COs in *spo11 ndt80* strains are also equal (Figure 5-9B,C). Thus, the lack of genome wide DSBs in addition to a reduction in resolvase activity can almost eliminate CO enrichment in meiosis.

NCOs at *URA3* are slightly delayed and reduced in *spo11 ndt80*, but are not affected at *HIS4* (Figure 5-9D,E). This suggests that almost all NCOs at *HIS4* are JM independent, however some of the NCOs at *URA3* may arise from JMs. This effect of increased NCO dependence on Ndt80 at *URA3* is only seen in the absence of genome wide Spo11 DSBs. Furthermore, heterology at the site of DSB, as seen in *ndt80* at *URA3* with heterologous cassette, also increases dependence of NCOs on Ndt80. And, both the lack of DSBs and heterology have an additive effect on NCOs in the *spo11 ndt80* mutant at *URA3* with the heterologous cassette, where most VDE initiated NCOs become resolvase dependent. This effect is similar to effect of *sgs1 ndt80* mutants on Spo11 initiated NCOs (De Muyt et al. 2012).

Sgs1 is postulated to disassemble early strand invasion intermediates to promote NCO formation by SDSA. Early NCOs are lost in *sgs1* mutants, and all recombinants, including NCOs, become dependent on the resolution of JMs in *sgs1 ndt80* mutants (De Muyt et al. 2012). The *sgs1* mutation may therefore increase JM formation by stabilizing strand invasion. The lack of genome wide DSBs and heterology also increases NCO dependence on JM resolution. But, there is no corresponding increase in JMs in the heterologous reporter strains (Figure 4-5D), though it is possible hat these JMs do not migrate as detectable bands in our physical assays. In the homologous cassette, there is indeed a 2 times increase in accumulated JMs at *URA3* in *spo11 ndt80* compared to *ndt80* (Figure 5-9F). The lack of genome wide DSBs is known to increase resection for VDE DSBs (Neale et al. 2002, Johnson et al. 2007), and heterology at the DSB site may also enforce increased resection to initiate homologue synapsis by exposing ssDNA beyond the region of heterology. Therefore, similar to the *sgs1* mutants, *spo11* mutants or strains with heterology at the DSB site may also lead to more stable strand invasion, which then

increases the balance of recombination towards more JM formation and less SDSA. And this will be reflected in the greater dependence of NCOs on JM resolution. The lack of Sgs1, genome wide DSBs and heterology at DSB site may therefore shift recombination to more JM formation by the same mechanism of more stable strand invasion.

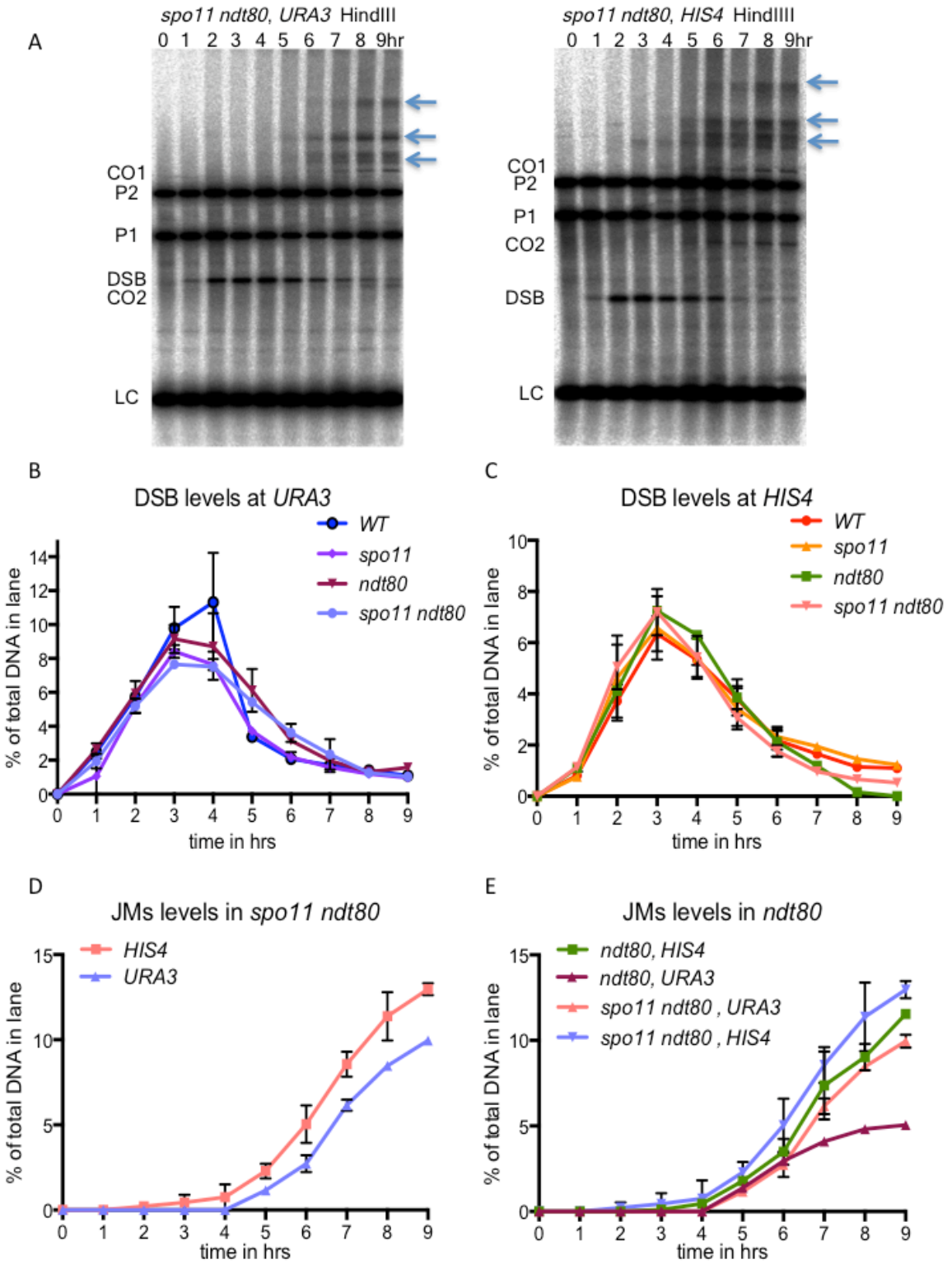

Figure 5-8 *spo11 ndt80* strains show normal DSB kinetics, but again accumulate JMs, but at more similar level at *HIS4* and *URA3*. This is as JM levels at *URA3* are increased 2 fold in *spo11 ndt80* strain compared to the *ndt80*. All results are from two biological replicates for each strain and error bars indicate standard error of mean.
A) Southern blots of meiotic DNA digested with *Hind*III to look at JMs and DSBs for *spo11 ndt80, URA3* strain MJL3621 and *spo11 ndt80, HIS4* strain MJL3640. Blue arrows indicate discrete JM peaks which were quantified.
B,C) *spo11 ndt80* mutants show normal DSB kinetics.
D) JM accumulation at 9 hrs is slightly higher at *HIS4* (13%) than *URA3* (10%).

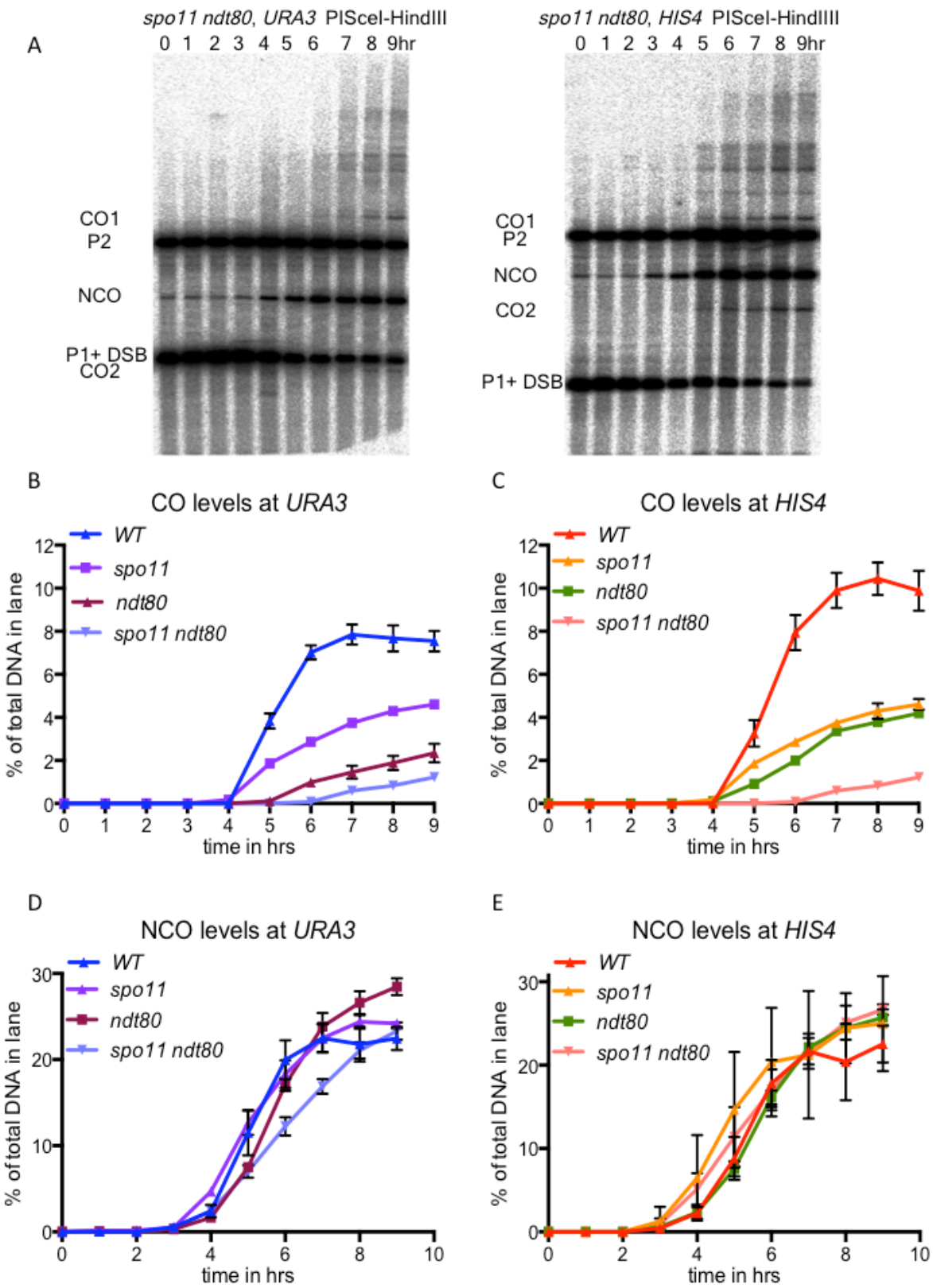

Figure 5-9 *spo11 ndt80* mutants have reduced VDE initiated COs at both loci, while NCOs are only affected at *URA3*. All results are from two biological replicates for each strain and error bars indicate standard error of mean.
A) Southern blots of meiotic DNA digested with PI*Sce*I-*Hind*III to look at NCOs and COs for *spo11 ndt80, URA3* strain MJL3621 and *spo11 ndt80, HIS4* strain MJL3640.

B,C) COs (mean of CO1 and CO2) at both loci reduce from 4.6% in *spo11* to 1.2% in *spo11 ndt80*, which is a 3.7 fold loss.
D) NCOs are slightly delayed and reduced at *URA3.* At 7hrs, NCOs are at 17% in *spo11 ndt80* compared to ~20% for all other strains.
E) NCOs are at *HIS4* are at 26.67% in *spo11 ndt80*, which is comparable to all other strains.

5.5 Mitotic resolvases Mus81-Mms4 and Yen1 have a greater effect on CO formation at *URA3* compared to CO formation at *HIS4.*

Mus81-Mms4 appeared to be the primary resolvase for VDE DSB repair at *URA3* in the heterologous cassette. Yen1 by itself had no effect, but in mitotic cells, Yen1 is known to play a back-up role to Mus81-Mms4 (Ho et al. 2010). Therefore, I tested the effect of *mms4-mn* and *mms4-mn yen1* on VDE initiated recombination at both *URA3* and *HIS4* loci in the homologous cassettes. VDE DSB kinetics are similar in *mms4-mn* and WT strains (Figure 5-10B,C). But, unlike WT strains, *mms4-mn* strains show transient JM accumulation at both loci. These JMs accumulate an hour earlier at *HIS4* than *URA3,* and JM levels at *HIS4* are slightly higher at *HIS4* at 4.4%, compared to 3.6% at *URA3* (Figure 5-10D,E). This may indicate an earlier role for Mus81-Mms4 at *HIS4* to limit JM formation, but JM peaks are at fairly equal levels between *URA3* and *HIS4*, before their resolution.

COs in *mms4-mn* at *URA3* are at 63% of WT levels at 7 hrs, and reach 85% of WT levels by 9 hrs, while COs in *mms4-mn* at *HIS4* are at 85% of WT CO levels at 7 hrs and are at WT levels by 9 hrs (Figure 5-11B,C). Also COs in *mms4-mn yen1* at *URA3* at 7 hrs are at 50% of WT levels, and reach 63% of WT levels by 9 hrs, while COs in *mms4-mn yen1* at *HIS4* peak at 69% of WT levels (Figure 5-12B,C). Hence, there is a greater effect of the mitotic resolvases Mus81-Mms4 and Yen1 on CO formation at *URA3* compared to *HIS4.* Spo11 initiated COs in reporter constructs at the *HIS4-LEU2* are also modestly reduced (by 10-30%) in *mms4-mn yen1* mutants (De Muyt et al. 2012, Zakharyevich et al. 2013). Similar to this, in the absence of Mus81-Mms4 and Yen1, VDE initiated recombination at *HIS4* loses about 30% COs, compared to a loss of 40-50% COs for VDE initiated recombination at *URA3.* Thus, CO formation at *URA3* is more dependent on Mus81 and Yen1, similar to mitosis.

The effect of transient JM accumulation and reduced CO formation was also seen in the *URA3* heterologous cassette, although at 7 hrs rather than at 5 hrs for the homologous cassette (Figure 4-6D). Consistent with this, COs were also delayed in the heterologous cassette at *URA3*, reaching only 87% of WT by 9 hrs (Figure 4-6F). Thus, heterology at the break site may delay JM formation. Also, NCO formation in the heterologous cassette at *URA3* was also slightly delayed in *mms4-mn* mutants (Figure 4-6E), but not in the strains with the homologous cassette (Figure 5-11D). This is consistent with most NCOs in the homologous cassette forming

independently of JMs, while NCOs in the heterologous cassette are more dependent on JM resolution.

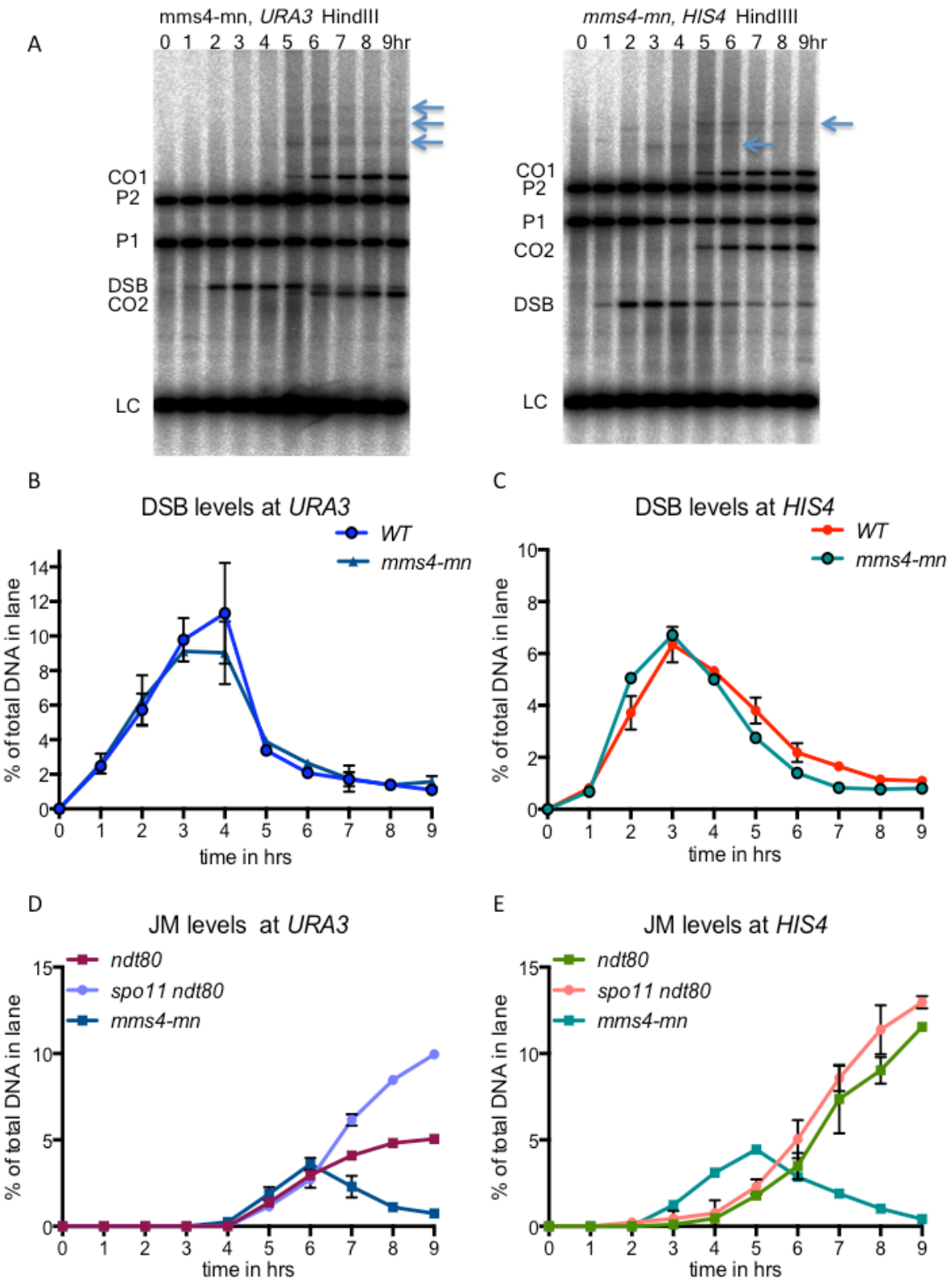

Figure 5-10 *mms4-mn* mutants show normal DSB formation and transient JM accumulation, at a higher level and earlier at *HIS4* compared to *URA3.*
A) Southern blots of meiotic DNA digested with *Hind*III to detect JMs and DSBs for *mms-mn, URA3* strain MJL3665 and *mms4-mn, HIS4* strain MJL3666. Results are from two biological replicates. Blue bands indicate discrete JM peaks, which are quantified.
B,C) *mms4-mn* mutants do not affect DSB kinetics

D)E) JMs accumulate transiently at *URA3* to a peak of 3.6% at 6 hrs, and also at *HIS4* to a peak of 4.4% at 5 hrs and resolve thereafter. JMs accumulate an hour earlier at *HIS4.*

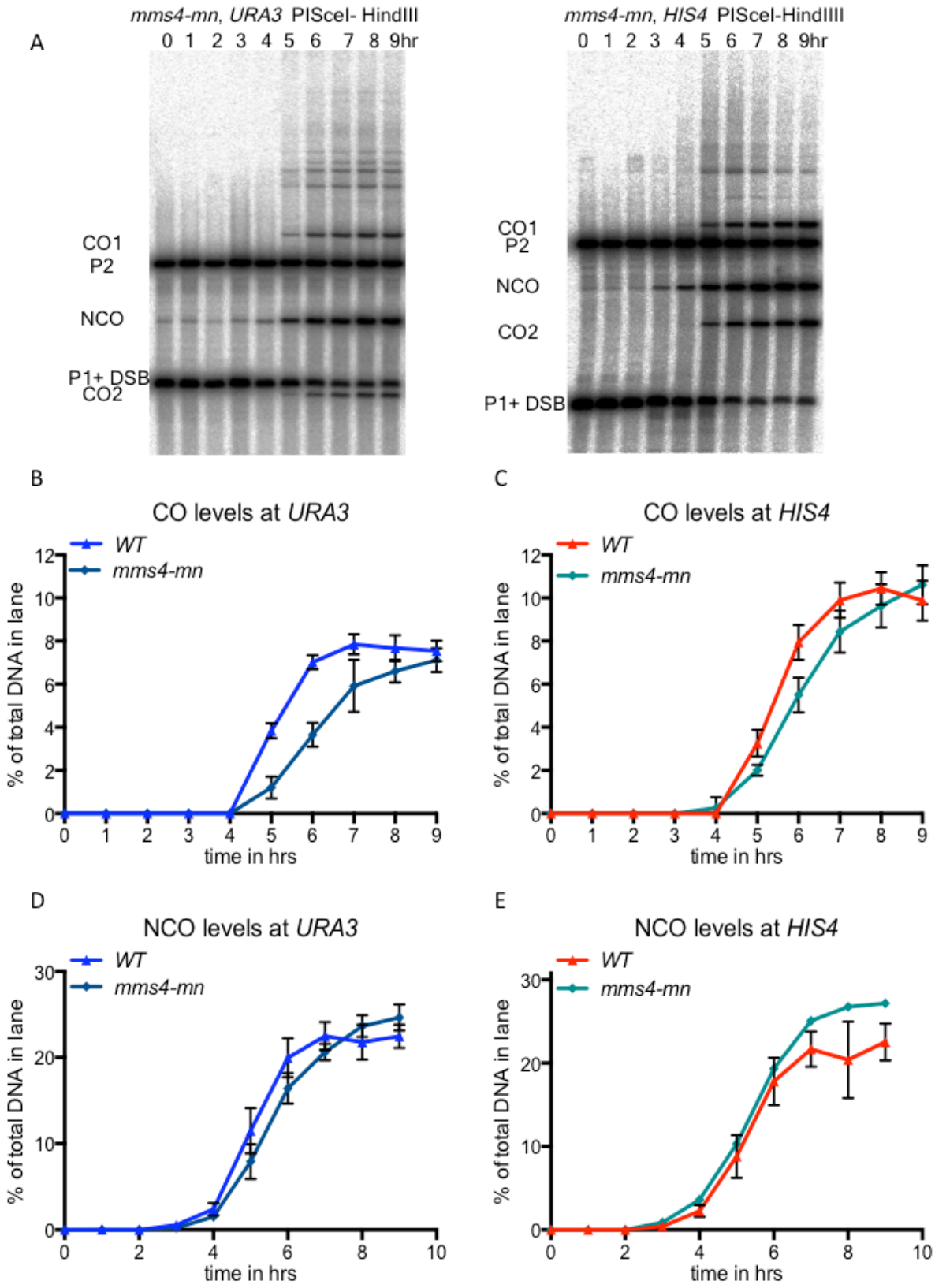

Figure 5-11 *mms4-mn* mutants affect COs at *URA3* more than COs at *HIS4*.
A) Southern blots of meiotic DNA digested with PI*Sce*I-*Hind*III to detect NCOs and COs in *mms4-mn, URA3* strain MJL3665 and *mms4-mn, HIS4* strain MJL3665. Results are from two biological replicates.

B) COs (mean of CO1 and CO2) at 7 hrs reach 7.85% of total DNA in WT at *URA3*, while COs in *mms4-mn* at *URA3* lag behind at 5% or ~63% of WT levels. At 9 hrs however, COs in *mms4-mn* reach 6.7%, which is ~85% of COs in WT.
C) COs at 7 hrs to reach 9.9% of total DNA in WT at *HIS4* while COs in *mms4-mn* at *HIS4* also lag behind at 8.4% or ~85% of WT levels. At 9 hrs, COs in *mms4-mn* reach 10.6%, which is very similar WT levels. Therefore, *mms4-mn* affects CO formation at both loci, but the effect is larger at *URA3.*
D)E) NCO formation at both *URA3* and *HIS4* is not affected by *mms4-mn.*

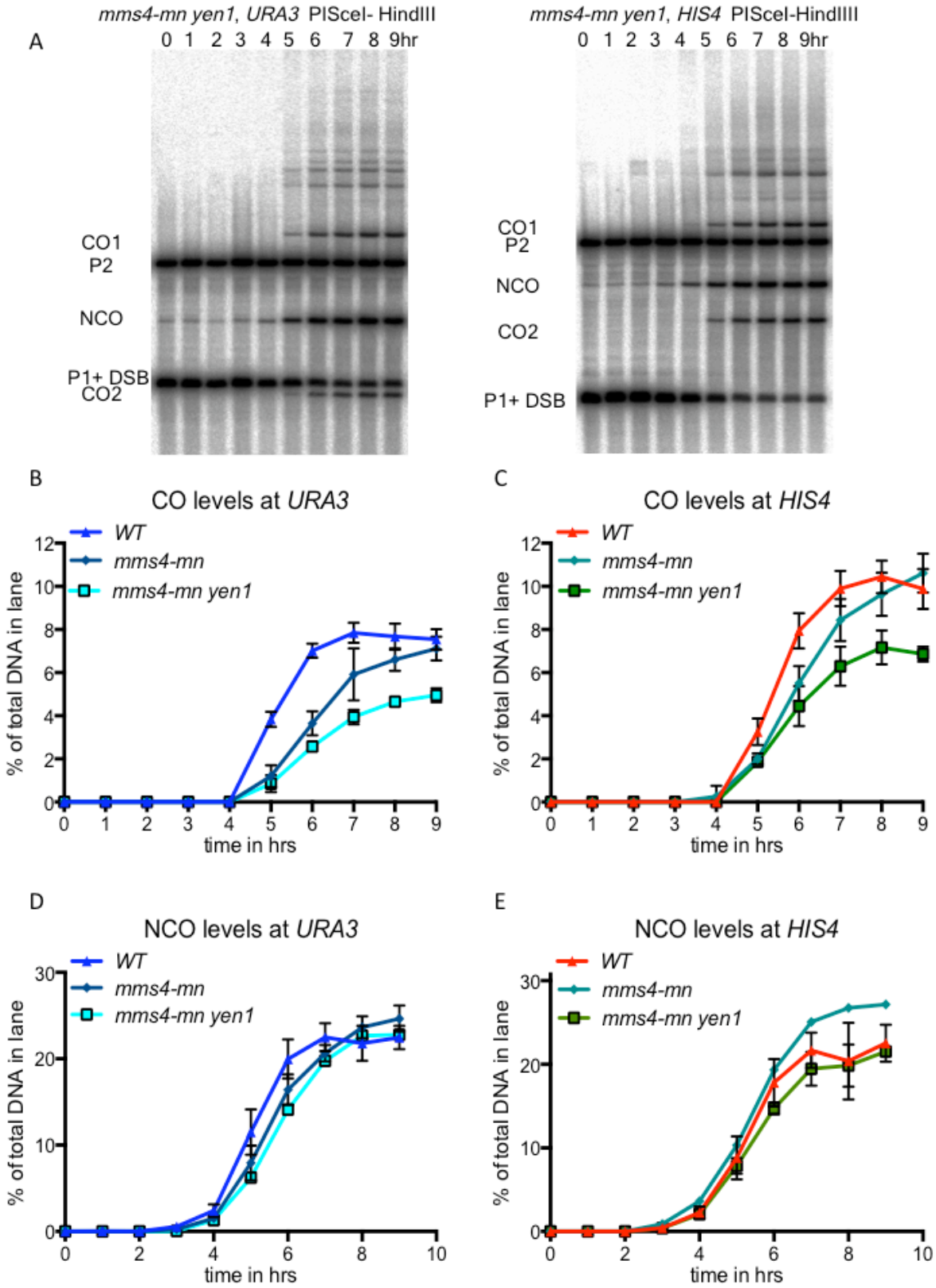

Figure 5-12 *mms4-mn yen1* mutants also affect COs at *URA3* more than COs at *HIS4*.
A) Southern blots of meiotic DNA digested with PI*Sce*I-*Hind*III to detect NCOs and COs in *mms4-mn yen1, URA3* strain MJL3681 and *mms4-mn yen1, HIS4* strain MJL3682. Results are from a single experiment.

B) COs (mean of CO1 and CO2) at 7 hrs reach 7.85% of total DNA in WT at *URA3*, while COs in *mms4-mn yen1* at *URA3* lag behind at 3.94% or ~50% of WT levels. At 9 hrs, COs in *mms4-mn yen1* reach 4.96%, which is ~63% of COs in WT.
C) COs at 7 hrs to reach 9.9% of total DNA in WT at *HIS4* while COs in *mms4-mn yen1* at *HIS4* also lag behind at 6.3% or ~63% of WT levels. COs in *mms4-mn yen1* finally peak at 7.17%, which is very ~69% of WT levels. Therefore, *mms4-mn yen1* again affects CO formation at both loci, but the effect is larger at *URA3.*
D)E) NCO formation at both *URA3* and *HIS4* is not affected by *mms4-mn yen1.*

5.6 The ZMM resolvase Mlh3 only affects CO formation at HIS4, and has no effect on CO formation at URA3

Since the mitotic resolvases Mus81 and Yen1 differentially affected CO formation at *URA3* and *HIS4*, I sought to determine if CO formation at both loci would also differ in the effects of the meiosis-specific ZMM resolvase complex Mlh1-Mlh3-Exo1 (Wang et al. 1999, Zakharyevich et al. 2010 and Zakharyevich et al. 2012). Therefore, I examined VDE DSB repair at *URA3* and *HIS4* in *mlh3* mutants. The *mlh3* mutants have normal VDE DSB kinetics, and like *mms4-mn* and *mms4-mn yen1* mutants, also accumulate some JMs, an hour earlier at *HIS4* compared to *URA3* (Figure 5-13D,E). However, unlike *mms4-mn* and *mms4-mn yen1* mutants, which accumulate roughly equal JMs at *URA3* and *HIS4* (20% difference), *mlh3* mutants accumulate 44% fewer JMs at *URA3* compared to *HIS4* (Figure 5-13D,E). This may reflect the greater propensity of the Spo11 DSB hot-spot *HIS4* to be ZMM associated.

Consistently, *mlh3* mutants are also very different from *mms4-mn* and *mmns4-mn yen1* mutants in terms of CO formation. CO formation in *mlh3* mutants at *URA3* is largely unaffected, COs in *mlh3* at *URA3* are 88% of WT levels (Figure 5-14B). However, CO formation in *mlh3* at *HIS4* goes down to 43% of WT, which is greater than a 2 fold loss (Figure 5-14C). Spo11 initiated COs are also reduced by 2 fold in *HIS4-LEU2* and other genetic intervals in *mlh3* mutants (Wang et al. 1999, Abdullah et al. 2004). Thus, VDE initiated COs at *HIS4* are very similar in their ZMM dependence to Spo11 initiated COs, while VDE initiated COs at *URA3* are mostly ZMM independent.

The differing CO dependencies of VDE initiated COs at *URA3* and *HIS4* presents a very intriguing possibility that only axis enriched Spo11 hot-spot loci are capable of association with ZMM proteins. This would then mean that axis enrichment sites are pre selected for later ZMM association, and eventual CO formation.

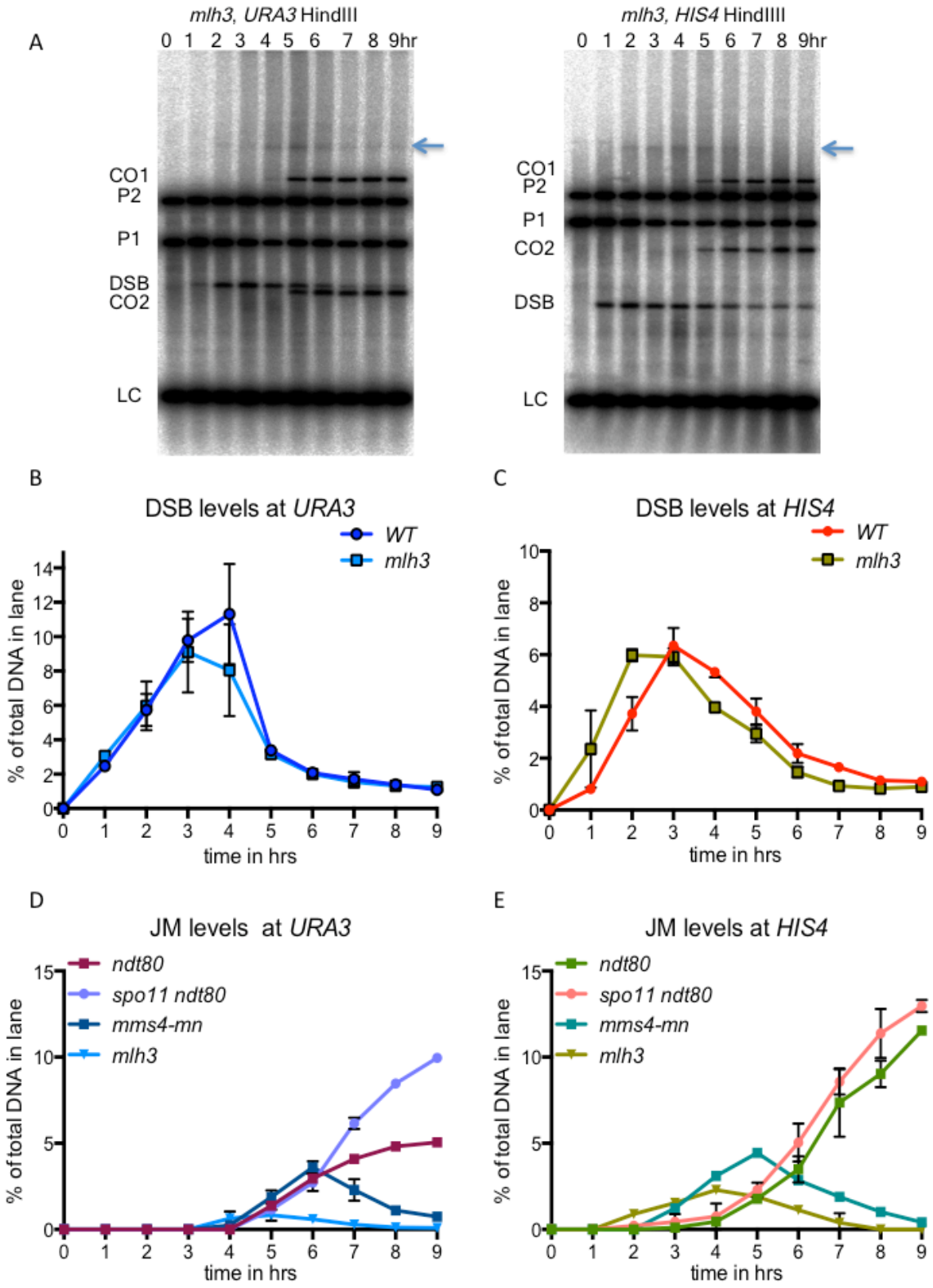

Figure 5-13 *mlh3* mutants show normal DSB formation and also transient JM accumulation, at a much higher level and earlier at *HIS4* compared to *URA3*.
A) Southern blots of meiotic DNA digested with *Hind*III to detect JMs and DSBs for *mlh3, URA3* strain MJL3669 and *mlh3, HIS4* strain MJL3670. Results are from two biological replicates. Blue bands indicate discrete JM peaks, which are quantified.
B,C) *mms4-mn* mutants do not affect DSB kinetics

D)E) Very few JMs accumulate transiently at *URA3* to a peak of 0.83% at 5 hrs. On the other hand, JMs accumulate to a higher level at *HIS4* to a peak of 2.3% at 4 hrs and resolve thereafter.

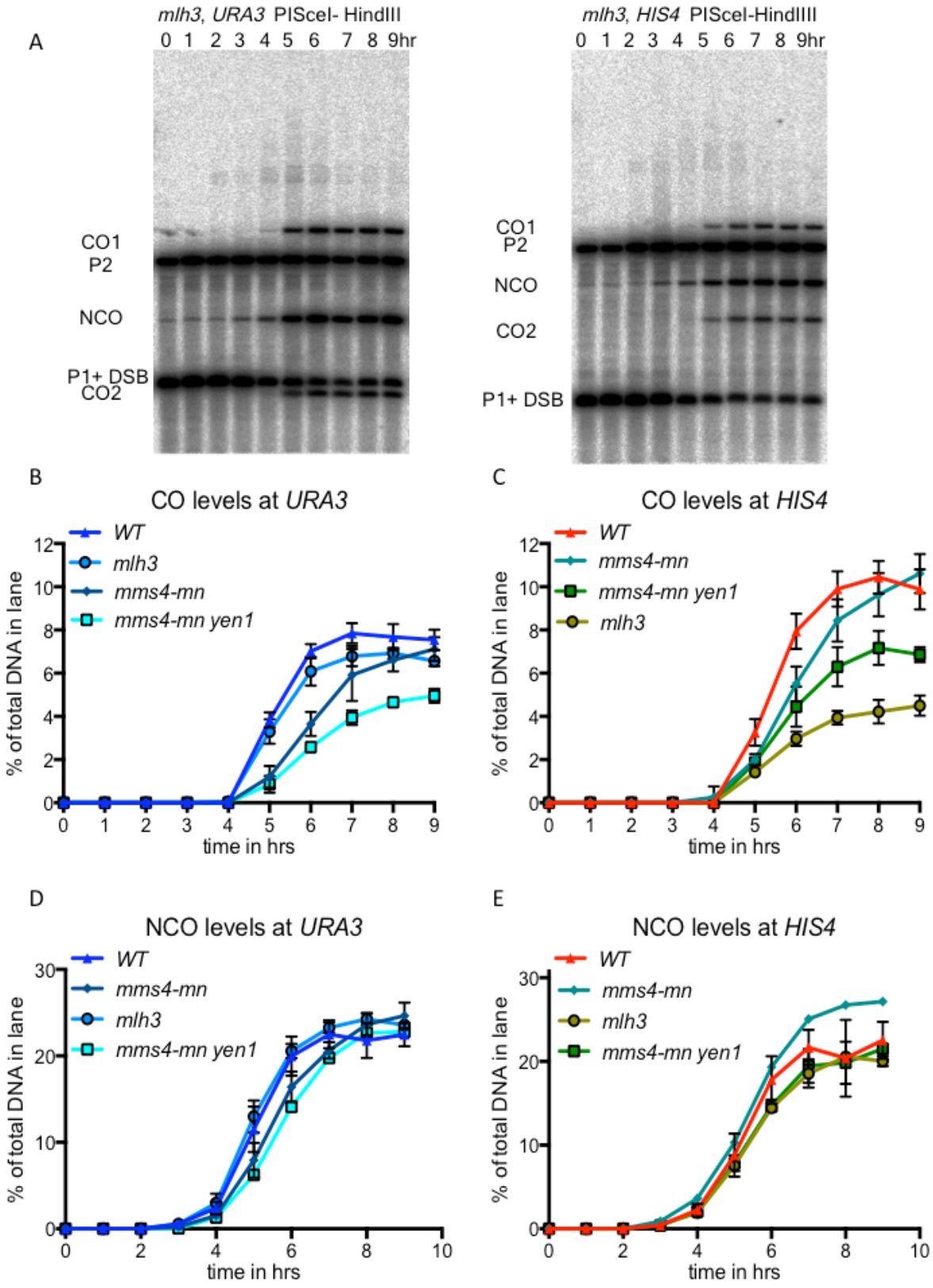

Figure 5-14 *mlh3* mutants affect COs at *HIS4* only.
A) Southern blots of meiotic DNA digested with PI*Sce*I-*Hind*III to detect NCOs and COs in *mlh3, URA3* strain MJL3669 and *mlh3, HIS4* strain MJL3670. Results are from a two biological replicates.
B) COs in *mlh3* at *URA3* reach a peak of 6.93%, which is ~88% of WT.

C) COs in *mlh3* at *HIS4* reach a peak of 4.5%, which is ~43% of WT. Therefore, *mlh3* results in a 2 fold loss of COs at *HIS4,* while COs at *URA3* are almost unaffected.
D)E) NCO formation at both *URA3* and *HIS4* is not affected by *mlh3.*

6 Conclusions and future work

DSBs are formed in chromatin loops (Kleckner. 2006) during meiosis via the interaction between Spo11, its accessory factors and meiotic axial elements (Blat et al. 2002, Panizza et al. 2011). The meiotic axis therefore plays a role in determining the sites of DSB formation, and it has been postulated that DNA sequences in loops are physically brought in proximity to the axis for DSB formation (Kleckner. 2006). If this is so, meiotic DSB repair would also take place within the axis environment, and thus, the axis may also influence Spo11 DSB repair during meiosis. On the other hand, meiotic cells also express meiosis-specific recombination proteins, and these may alter the recombination environment, such that all DSBs formed in meiosis are repaired to enrich for COs. Study of Spo11 DSBs is unable to address this problem, as Spo11 DSBs do not form efficiently outside of axis enriched regions. Therefore, their repair cannot differentiate between the local influence of the meiotic axis and the cell wide influence of meiosis-specific recombination proteins.

I addressed this problem by studying the repair of VDE DSBs, which can form in regions both with and without axis enrichment (Fukuda et al. 2008). Therefore, VDE DSB repair can be studied outside the meiotic axis environment, and I can ask if this differentiates VDE repair from the repair of Spo11 DSBs within the axis. We tested this hypothesis by creating a recombination reporter system that forms VDE DSBs in meiosis, in an axis depleted Spo11 DSB cold-region *URA3* (Panizza et al. 2011, Wu and Lichten. 1995, Borde et al. 1999). This would allow us to determine if these VDE DSBs, which were likely to be away from the meiotic axis, would be repaired similarly or differently from Spo11 DSBs. We also recreated the VDE recombination reporter in an axis enriched Spo11 DSB hot-region *HIS4* (Panizza et al. 2011, Wu and Lichten. 1995, Borde et al. 1999), to further examine if placing a VDE DSB in the vicinity of the meiotic axis could have any effect on its repair. This would further strengthen our hypothesis that DSB repair in meiosis is influenced by the local chromosome context. Also, insertion of the recombination reporter should not alter the local chromatin context in hot-spots like *HIS4*, as Spo11 DSB activity at these loci is maintained even with reporter insertions (Wu and Lichten 1995, Borde et al. 1999, Figure 3-16). Therefore, if VDE DSB repair at *HIS4* is still different from the repair of Spo11 DSBs, this may suggest additional factors other than the local chromosome context that contribute to high frequency of COs from Spo11 DSB repair in meiosis.

Our results indicate that VDE DSB repair at *URA3* greatly favours NCOs over COs, such that there is a 3-fold excess of NCOs compared to COs (Figure 5-2). Also, the VDE initiated COs formed at *URA3* are independent of the Mlh3, which is part of the ZMM resolvase complex Mlh1-Mlh3-Exo1 (Figure 5-14) (Wang et al. 1999, Zakharyevich et al. 2010 and Zakharyevich et al. 2012), but more dependent on the “mitotic” resolvases

Mua81-Mms4 and Yen1 (Figure 5-11, Figure 5-12). Thus, VDE DSBs at *URA3* are repaired in a more "mitotic" manner, which shows that DSBs, which are in a meiotic cell but outside the local chromatin context of the meiotic axis, are repaired more like mitotic DSBs.

On the other hand, VDE DSBs at *HIS4* are repaired differently from VDE DSBs at *URA3*. NCO still form in excess of COs, but they are in 2 fold excess compared to 3-fold excess at *URA3.* Also, VDE DSBs at *HIS4* are repaired to give ~25% more COs than at *URA3* (Figure 5-2). These VDE-initiated COs at *HIS4* are less dependent on the mitotic resolvases Mus81-Mms4 and Yen1 (Figure 5-11, Figure 5-12) than VDE-initiated COs at *URA3.* VDE-initiated COs at *HIS4* however do show dependence on Mlh3, which is part of the ZMM resolvase complex Mlh1-Mlh3-Exo1 ((Figure 5-14) (Wang et al. 1999, Zakharyevich et al. 2010 and Zakharyevich et al. 2012), to the same extent as do Spo11 initiated COs. Therefore, the VDE DSBs at the axis enriched *HIS4* locus show more "meiotic" repair. CO frequencies for VDE DSB repair at *HIS4* however is 33%, while Spo11 DSBs form COs at 50% frequency, indicating that VDE DSB repair at *HIS4* is still less "meiotic" then Spo11 DSB repair. This may be due to the fact that Spo11 DSBs almost always form in the context of the axis, while the VDE DSB at *HIS4* will form irrespective of axis enrichment. Also, the RMM sub-complex, which is part of Spo11 pre initiation complex, interacts with Red1 and Hop1 (Panizza et al. 2011), which may cause the Spo11 DSB to be directly recruited to the axis. On the other hand, recruitment of the VDE DSB to the axis may be dependent on fortuitous contacts between the DSB and the axis.

These results demonstrate that the local axial environment of Red1 and Hop1 enrichment has an influence on meiotic DSB repair, in addition to stimulating DSB formation by Spo11 (Blat et al. 2002, Panizza et al. 2011). The VDE DSB at the axis-enriched *HIS4* region is able to form more COs than the VDE DSB at axis-depleted region *URA3*, and these VDE-initiated COs at *HIS4* show ZMM dependence, like Spo11 initiated COs. The ZMM pathway is unique to meiosis, and loss of ZMM proteins leads to reduced CO formation (Lynn et al. 2007, Börner et al. 2004) and subsequent non-disjunction of homologues in meiosis I (Engebrecht et al. 1990, Nakagawa and Ogawa. 1999, Khazanehdari and Borts. 2000). The ZMM pathway is therefore critical for CO enrichment in meiosis, and the differing dependencies of VDE initiated COs at *URA3* and *HIS4* on the ZMM resolvase Mlh3 indicates that axis-enriched sites in the genome are pre selected for later ZMM association, and eventual CO formation. This points to a partitioning of the genome in meiosis between regions that are pre-conditioned for "meiotic"/ZMM associated recombination and regions that show "mitotic" recombination. We speculate that this pre-conditioning is based on the enrichment of axis proteins in certain genomic regions early in meiosis.

The ZMM proteins promote CO formation during meiosis by associating with Spo11 DSBs (Fung et al. 2004). ZMM proteins Msh4-Msh5 are able to associate with Holliday junctions (Snowden et al. 2004) and antagonize the activity of the Sgs1 helicase during meiosis (Jessop et al. 2006). As helicases can dissolve JMs by dissolution (see section 1-25), the ZMM proteins may locally associate with the chromatin around Spo11 DSBs to stabilize JMs and promote CO enrichment (De Muyt et al. 2012). VDE initiated at *HIS4* are also dependent on the ZMM resolvase, hence VDE DSB repair at *HIS4* should be in the context of the ZMM pathway. Consistent with this, more VDE initiated JMs form at *HIS4* than *URA3* (Figure 5-6D). And in addition to stimulating JM formation (De Muyt et al. 2012), ZMM-associated JMs are then resolved to exclusively form COs (Sourirajan and Lichten. 2008). Therefore, the VDE-initiated JMs at *HIS4,* which also should be ZMM associated, should be less susceptible to dissolution. Consistent with this assumption, accumulated JMs in the *ndt80* mutant at *HIS4* can account for almost all of the lost COs at *HIS4* (Figure 5-6D, Figure 5-7C). This suggests that JMs at *HIS4* are CO designated, and cannot be dissolved to give NCOs only. VDE initiated COs at *URA3*, on the other hand, are independent of the ZMM resolvase. Therefore these DSBs are not repaired via the ZMM pathway. Again, consistent with this assumption, VDE DSBs at *URA3* forms fewer JMs (Figure 5-6D) and have increased NCOs compared to WT (Figure 5-7D,E). This indicates that JMs at *URA3* in the absence of resolvase activity are more susceptible to be dissolved to form NCOs. These differences between VDE initiated recombination between *URA3* and *HIS4* are consistent with the properties of Spo11 initiated recombination via to the ZMM pathway. Since this pathway is unique to meiosis, this is what primarily differentiates meiotic recombination from mitotic, and VDE initiated recombination at *HIS4* and *URA3* are also more reminiscent of meiosis and mitosis respectively. These findings suggest that the local axial environment primarily differentiates homologous recombination in meiosis from mitosis, via directing repair through the ZMM pathway.

Although there are distinct differences in VDE DSB repair at *URA3* versus *HIS4,* these differences are fairly small. Overall, VDE DSBs at *URA3* and *HIS4* are similarly repaired in WT cells, to form an excess of NCOs over COs. This would therefore argue that in most cases, VDE DSB repair at *URA3* is indistinguishable from VDE DSB repair at *HIS4*. However, it is important to consider that while the formation of VDE DSBs is an almost obligate event, as ~90% of VRS sites at both *URA3* and *HIS4* are cleaved (Figure 5-1), Spo11 DSBs infrequently form at any locus. Even in the *HIS4* hot-spot, the cumulative frequency of Spo11 DSBs is ~10% (Figure 3-16), and if this is believed to be a reflection of axis enrichment, then the axis proteins are also enriched at *HIS4* in only ~10% of cells. If this is indeed the case, for most meiotic cells (~90%), both *URA3* and *HIS4* are similar in their local axial environment, and correspondingly, VDE DSB repair in most cells is also similar between *URA3* and *HIS4* to give mostly NCOs.

Previous studies of Spo11 independent *SPO13::HO* DSB by Malkova et al. (2000), reported that the repair of this DSB resembled Spo11 DSB repair. This would argue that all DSBs in meiosis are similarly repaired. However, Malkova et al. (2000) limited their analysis to the *LEU2* locus, which is a hot-spot for meiotic recombination (White and Petes. 1994). Since my results show that VDE DSB repair at another hot-spot (*HIS4*) shares features with Spo11 DSB repair, the behaviour of the *SPO13::HO* DSB at *LEU2* is consistent with my findings. Expanding the scope of the study of Spo11 independent DSBs to cold-spots, such as VDE DSB repair at *URA3*, allows me to conclude that all DSBs in meiosis are not equally repaired.

Malkova et al. (2000) reported 52% CO frequency for the *SPO13::HO* DSB at *LEU2*, this was calculated only for tetrads which showed 3:1 segregation of Leu^+ prototrophs. 3:1 segregation arises when only of the two *leu2::HO cutsite* sister chromatids is cleaved. On the other hand, for 4:0 Leu^+ tetrads where both *leu2::HO cutsite* chromatids are cleaved, CO frequency is reduced to 23%. The CO frequency at *HIS4* from my physical assays is 33%. Since the physical assay is performed with DNA extracted from population of meiotic cells, all recombinant chromatids from 2:2, 3:1, 4:0 and even tetrads without 4 viable spores, would be represented in this assay. Therefore, 33% CO frequency at *HIS4* is relatively close to the 37.5% average CO frequency at *LEU2* in Malkova et al. (2000) when both 3:1 and 4:0 recombination events are considered. Also, genetic studies by tetrad analysis can only be preformed on 4 spore viable tetrads, which may lead to a slight bias of CO enrichment, as COs are essential for viable segregation of chromosomes in meiosis (Engebrecht et al. 1990, Nakagawa and Ogawa. 1999, Khazanehdari and Borts. 2000). In addition to the above, the experimental setup for Malkova et al. (2000) had a 113 bp *HO* DSB site inserted on one homologue, with no homology on the other homologue. Heterology right at the DSB site affects the NCO to CO ratio. NCOs are reduced more in the presence of heterology than COs (Figure 3-15), thus the 113 bp heterology at the site of the DSB in Malkova et al. (2000) may have also caused an enrichment of COs in successful repair events. Therefore, considering the above, the results of VDE DSB repair at *HIS4* are consistent with the results of *SPO13::HO* repair at *LEU2* from Malkova et al. (2000).

VDE DSB repair, at *URA3* and also *HIS4,* overall shows more features of mitotic DSB repair than meiotic, and this is also consistent with previous studies on genome wide exogenous DSB repair in meiotic cells. Cartagena-Lirola et al. (2008) generated exogenous DSBs in meiotic cells by treatment with phleomycin. They found that these exogenous DSBs are able to trigger both Rad53 and Mek1 phosphorylation, whereas Spo11 DSBs only trigger Mek1 phosphorylation. Only fusing Rad53 to Ddc2, which is the partner of Mec1, allows Rad53 activation by Spo11 DSBs. This suggests that Rad53 itself cannot access endogenous Spo11 DSBs in meiosis, while Rad53 can access a subset of exogenous DSBs in meiosis. Since phleomycin would create DSBs in meiotic cells both within and

outside the axis, it is consistent that their signaling behaviour would also reflect that of both mitotic and meiotic DSBs. Also, Youds et al. (2010) showed that exogenous DSBs in *C. elegans* generated by ionizing radiation are primarily repaired as NCOs via the action of the RTEL-1 helicase, and this is also consistent with the VDE DSBs being repaired mostly as NCOs.

Future studies can expand on the correlation between local axis environment and "meiotic" ZMM dependent DSB repair by directly recruiting axis elements to cold loci. If axis element enrichment is indeed able to drive DSB repair towards the ZMM pathway, then repair at a cold-loci may also be changed towards more ZMM dependent CO formation by tethering axis elements to a particular locus.

Genome wide Spo11 DSBs are also required for CO formation in meiosis. In the absence of these DSBs, VDE DSB repair becomes even more biased towards NCOs, and this is driven by a selective loss of COs (Figure 5-4). As explained previously, the loss of COs in *spo11* mutants cannot be made up by adding back Spo11 initiated COs at both *URA3* and HIS4, therefore Spo11 DSBs have a trans effect on CO formation, this was also reported by Malkova et al. (2000). Martini et al. 2006 showed that when DSB formation is reduced in meiosis with Spo11 hypomorhs, CO levels are maintained at the expense of NCOs. However, there could to be a minimum threshold of DSB formation by Spo11 that is required for efficient CO formation during meiosis. Another observation of note is that unlike in WT cells where there are more VDE initiated COs at *HIS4* than *URA3*, s*po11* mutants form COs at an equal frequency at both loci. If there are any locus specific recombination properties at *HIS4* that allow an increase in CO formation, this appears to be lost in the absence of genome wide DSBs. Therefore, CO enrichment in meiosis requires global DSB formation.

I further elaborated on the trans effect of Spo11 DSBs on COs by studying VDE repair in ectopic inserts. VDE repair in ectopic inserts partially recapitulates the pairing defect of *spo11* mutants (Weiner and Kleckner. 1994, Loidl et al. 1994, Henderson and Keeney. 2004), without affecting genome wide DNA damage signaling. Ectopic strains had a VDE DSB in *arg4-VRS* at *URA3* repairing from *arg4-VRS103* at *HIS4;* this strain was referred to as WT*, URA3/HIS4.* Ectopic recombination was also tested in a strain with the VDE DSB in *arg4-VRS* at *HIS4* repairing from *arg4-VRS103* at *URA3;* this strain is referred to as WT*, HIS4/URA3.* Both *URA3/HIS4* and the *HIS4/URA3* strains had a lower level of interhomologue recombinants, as ectopic inserts have a pairing defect in WT cells (Goldman and Lichten. 1996). Repair of VDE DSBs in WT cells in ectopic contexts (*URA3/HIS4* and *HIS4/URA3*) showed an increase in NCO bias (Figure 5-5), therefore, the reduction of COs due to the loss of genome wide DSBs in *spo11* mutants can be partially attributed to the loss of pairing in these mutants.

The meiotic axial elements form the lateral components of the tripartite synaptonemal complex (SC), and formation of the SC happens concomitantly with meiotic DSB repair. Components of the SC such as the Zip1, Zip2 and Zip3 are required for CO formation during meiosis (Börner et al. 2004), and Serrentino et al. (2013) have recently demonstrated that Zip3 first associates with centromeres, and then localizes to a subset of DSBs, which are designated to form COs. This re-localization of Zip3 from the centromere requires DSB formation by Spo11 (Serrentino et al. 2013). These Zip3 loci then mark the sites of SC initiation and as well as CO-designated recombination sites (Agarwal and Roeder. 2000, Henderson and Keeney 2004, Serrentino et al. 2013). Spo11 DSB formation therefore affects both pairing and subsequent SC formation by ZMM proteins. ZMM proteins are also required for CO enrichment in meiosis (Lynn et al. 2007, Börner et al. 2004). Thus, a minimum threshold of genome wide DSBs may be required for ZMM recruitment to DSBs and subsequent pairing and CO biased repair. This would also suggest that COs formed during *spo11* meiosis are not ZMM dependent.

Spo11 initiated recombination in meiosis shows a bias for using the homologous chromosomes i.e. non-sister chromatids as a template for repair (Schwacha and Kleckner 1997, Hong et al. 2013). However, Goldfarb and Lichten (2010) showed that Spo11 DSBs can also be efficiently repaired using the sister chromatid, in the absence of homology on the "homologous" non-sister chromatids. We studied ectopic repair between reporter inserts at *URA3* and *HIS4*, with the VDE DSB placed in both orientations at *URA3* and *HIS4,* denoted *URA3/HIS4* and *HIS4/URA3* respectively. Such ectopic repair is less efficient than allelic recombination in WT strains (Figure 5-5G,H), and Goldman and Lichten (1996) showed that this is an affect of pairing between homologous chromosomes. As such, intersister recombination may be elevated in these ectopic strains. Intersister recombination re-creates the intact *arg4-VRS* chromatid, and this could cause the reduction in the rate of loss of *arg4-VRS* chromatids and the increased levels of residual *arg4-VSR* chromatids in the ectopic versus the allelic strains (Figure 5-5E,F). However, between them, the *HIS4/URA3* and the *URA3/HIS4* orientations do not behave identically. Level of residual *arg4-VRS* chromatids in *HIS4/URA3* more closely resembles the allelic reporter at *HIS4* up to 6 hrs, while loss of *arg4-VRS* at *URA3/HIS4* is slower than the allelic reporter at *URA3* from 4 hrs onwards (Figure 5-5E,F). Also, the *HIS4/URA3* orientation makes has 1.5 times more ectopic recombinants than *URA3/HIS4* (Figure 5-5E,F). These data suggest that the *URA3/HIS4* orientation may have a greater level of intersister recombination than the *HIS4/URA3*. *HIS4* is a Spo11 DSB hot-spot that is also enriched for Red1 (Panizza et al. 2011), and Red1 has a known role in suppressing intersister recombination in meisois (Schwacha and Kleckner 1997, Hong et al. 2013), thereby causing a lower level of intersister recombination in *HIS4/URA3.* This difference in the level of recombinants between the ectopic strains is however very small, and there is no difference in

recombinant levels between the allelic strains at *URA3* and *HIS4* (Figure 5-1D). This is because 85-90% of *arg4-VRS* chromatids are cleaved by VDE in the ectopic and allelic strains, which means both sister chromatids are frequently cleaved and the sister chromatid is thus no longer available as a repair template. Therefore, if there are indeed differences in partner choice bias between VDE DSBs at *URA3* and *HIS4*, I require an experiential system with reduced cleavage efficiency such that only one sister chromatid is cleaved. Nevertheless, the observations in the ectopic strains do suggest that the VDE DSB at *HIS4* may be more repressed for intersister recombination than the VDE DSB at *URA3.*

Initial studies using the heterologous cassette showed that heterology at the site of DSB can inhibit DSB repair, by lowering the level of interhomologue recombinants by 2 fold (Figure 3-15). Correspondingly, the loss of *arg4-VRS* chromatids was also 2 fold greater in the heterologous reporter compared to the homologous reporter (Figure 3-14). These results are consistent with earlier studies that show that sequence divergence inhibits homologous recombination (Datta et al. 1996).

Unlike inbred laboratory strains, diploid budding yeast cells in the wild may have significant polymorphisms between their corresponding "homologous" chromosomes, including such heterologous stretches. Meiotic recombination initiated by DSBs in such regions on the genome can be efficiently repaired by intersister HR (Goldfarb and Lichten. 2010), and in the case that intersister repair does not occur, heterology can still be dealt with in interhomologue recombination. Such robustness in the process of HR may be thus highly relevant to budding yeast in the wild, which are not perfectly homologous like inbred lab strains.

I observed that interhomologue recombinants appear earlier in the homologous cassette versus the heterologous cassette. Both NCOs and COs in the homologous cassette appear about an hour earlier than the heterologous cassette (Figure 3-15D). Heterology at the DSB site may delay the homology search due to reduced efficiency of initial homologue synapsis. Also, heterology at the DSB site may require longer tracts of synthesis and more template switching to cope. These could contribute to a delay in appearance of HR repair products.

The loss of interhomologue recombinants in the heterologous reporter is not evenly distributed between NCOs and COs. NCOs show a greater loss of 2.2 fold while COs are lost by 1.4 fold (Figure 3-15C). Therefore, heterology at the site of DSB affects NCO formation more than CO formation. Gene conversion tracts associated with COs are longer than gene conversion tracts for NCOs in budding yeast and mice (Terasawa et al. 2007, Mancera et al. 2008, Mitchel et al. 2010, Cole et al. 2010), and this could reflect increased DNA synthesis in CO formation. Correspondingly, this increased DNA synthesis in CO formation may arise

from a more stable association between the synaptic filament and donor strand, which inhibits the anti-recombinase function of helicases. Martini et al. (2011) reported that heteroduplex patterns associated with CO are more complex than NCOs, and suggest that phenomenon such as multiple strand invasions and template switching may be more commonly associated with COs. Such mechanisms may also permit CO forming pathways to more easily circumnavigate the impediment to strand invasion caused by a stretch of heterology at the break site, as template switching and multiple rounds of strand invasion could also lead to a more stable strand invasion intermediate. This also suggest that the stability of the strand invasion intermediate can affect recombination outcome

In addition to more NCOs being lost in the heterologous reporter, the residual NCOs formed are also more dependent on Ndt80. In the heterologous cassette at *URA3*, NCOs formation is delayed in *ndt80* mutants but their levels catch up to those seen in WT by 8 hrs (Figure 4-5), unlike the homologous cassette at *URA3* where NCO levels are unaffected in *ndt80*. Transcription of the yeast polo like kinase Cdc5 is induced by Ndt80, which then activates resolvases that act upon JMs (Sourirajan and Lichten. 2008). JM resolution in the same orientation can also form NCOs. Therefore, in the *ndt80* strains with the heterologous cassette at *URA3*, it is possible that JM resolution also leads to some NCO formation, and therefore the lack of Cdc5 transcription would result in low resolvase activity, which consequently delays NCO formation. This also means that fewer NCOs in the heterologous reporter form from SDSA, which is independent of JM resolution. This is in stark contrast to Spo11 initiated NCOs, which are completely independent of Ntd80 in WT cells. (Allers and Lichten. 2001a). The majority of Spo11 initiated NCOs are believed to be formed by SDSA (Martini et al. 2011).

ndt80 mutation also has no effect on NCO formation in strains with homologous cassettes, suggesting that these NCOs may also form mostly by SDSA. Thus, It appears that heterology at the break repair site can affect the balance between SDSA and JM formation. This may be due to a greater level of resection, which is required to uncover homologous sequences beyond the region of heterology. This in turn could also lead to a more stable strand invasion intermediate, and thereby increase JM formation at the expense of SDSA. The *spo11* mutants also have increased resection for VDE DSBs (Neale et al. 2002, Johnson et al. 2007), and this could again create more stable strand invasion, which then leads to more JM formation. Consistently, I can detect a 2 fold increase in JM population in *spo11 ndt80* versus *ndt80* strains in the homologous cassette at *URA3* (Figure 5-8). NCOs are also slightly delayed in *spo11 ndt80* strain with the homologous reporter at *URA3,* similar to the *ndt80* strain with the heterologous reporter at *URA3*. Thus, NCOs in *spo11* mutants also show more Ndt80 dependence.

Thus, both heterology and the lack of genome wide DSB formation are able to increase NCO dependence on resolvases. This could be because of the common effect of increased resection in both contexts, which stabilizes strand invasion. This is further evident in the *spo11 ndt80* mutants with the heterologous reporter at *URA3,* where almost all NCOs become resolvase dependent (Figure 4-5). However, unlike in the homologous reporter strains, I cannot detect an increase in JMs in the heterologous strains in *spo11 ndt80* compared to *ndt80.* In fact, in the heterologous strains, I cannot even detect enough JMs to account for the lost COs. Thus these JMs may not be detectable by the physical assay I use.

For Spo11 initiated recombination, NCOs form earlier via SDSA (Allers and Lichten. 2001a, Martini et al. 2011, De Muyt et al. 2012). The formation of these early NCOs is dependent on the helicase Sgs1 (De Muyt et al. 2012). Sgs1 has been hypothesized to destabilize strand invasion intermediates, which are then shuttled into the SDSA pathway (see section 1.1.3). Also, in *sgs1* mutants, early NCO formation is lost and NCOs become dependent on resolvase activity (De Muyt et al. 2012). Therefore Sgs1 may also permit increased resection and more stable strand invasion, which shifts the balance of recombination towards more JM formation and away from SDSA.

Therefore, there appears to exist a state of balance in meiosis between resection and DNA synthesis, which stabilize strand invasion, versus Sgs1 and potentially other helicases, which destabilize strand invasion. Increasing strand invasion stability can then push repair towards more JM formation and eventually CO outcomes, while decreasing strand invasion stability would push repair towards an NCO outcome. This can be tested for by directly assaying for resection levels in homologous versus heterologous reporters.

In the absence of genome wide DSBs, Dmc1 also does not appear to be essential for interhomologue recombination in the heterologous reporter at *URA3.* This effect could be because the Dmc1 requirement for DSB repair in meiosis is also stipulated by the axis, thus the off-axis VDE DSB at *URA3* would not require Dmc1. On the other hand, there could also be enough Rad51 activity in meiotic cells to repair a single DSB in the absence of Dmc1. Since interhomologue recombination is more efficient in the homologous reporter system, we can ask if there is any interhomologue recombination in *dmc1* mutants in *SPO11* cells in the homologous VDE recombination reporters. Alternatively, Spo11 hypomorphs could be used to lower DSB levels, to ask if VDE DSB repair is indeed independent of Dmc1. The effect of Rad51 on VDE recombination also remains to be tested.

The *spo11 dmc1* mutants also showed that NCOs are at higher levels than in either *spo11* or WT, such that the excess of NCOs over COs is 4-fold (Figure 4-4). Thus, recombination in *spo11 dmc1* is even more mitotic.

This suggests that Dmc1 is not essential for VDE catalyzed IH recombination. In fact, total IH recombination is improved in *spo11 dmc1* compared to *spo11* cells due to increased NCO levels (Figure 4-4). In mitotic cells, Rad51 catalyzes strand invasion during HR (Shinohara et al. 1992), so if HR in this *spo11 dmc1* mutant is also being carried out by Rad51, this would suggest Rad51 is more capable of catalyzing recombination in the presence of such heterology.

If Rad51 is indeed more efficient in catalyzing recombination between heterologous sequences, perhaps the Rad51 presynaptic filament requires less stable homologous contacts than Dmc1. These differences in synaptic properties could also play a role in NCO versus CO formation in mitosis and meiosis. In mitotic cells, a less stable synaptic association by Rad51 could enrich for NCOs by SDSA and prevents deleterious CO events that can lead to loss of heterozygosity or chromosome translocations. Conversely, meiotic cells inhibit Rad51 to allow Dmc1 to catalyze recombination, which then leads to a more stable synaptic association promoted by Dmc1 which enriches for COs. However, no significant differences have been reported so far in the *in vitro* biochemical properties of the Rad51 and Dmc1 pre synaptic filaments (Sheridan et al. 2008). But Rad51 and Dmc1 also have different accessory partners, which could differentiate the Rad51 and Dmc1 filaments *in vivo*.

A common theme that ties the above observations is that affecting the stability of strand invasion can alter the balance between NCOs arising from SDSA versus COs arising via JM resolution. Both heterology at the DSB site and a lack of genome-wide DSB formation seems to decrease the level of NCOs arising from SDSA. In addition, Rad51 catalyzed recombination in *spo11 dmc1* heterologous strains forms additional NCOs compared to *spo11* strains. If these additional NCOs formed from JM resolution, additional COs should also arise from these events, but no additional COs are seen in *spo11 dmc1* compared to *spo11.* Thus again, a different recombinase activity, that could affect the strand invasion intermediate, is able to alter the balance between SDSA and JM formation.

7 Bibliography

Abdullah MF, Hoffmann ER, Cotton VE, Borts RH. A role for the MutL homologue *MLH2* in controlling heteroduplex formation and in regulating between two different crossover pathways in budding yeast. Cytogenet Genome Res (2004) vol. 107 (3-4) pp. 180-90

Acquaviva L, Székvölgyi L, Dichtl B, Dichtl BS, de La Roche Saint André C, Nicolas A, Géli V. The COMPASS subunit *Spp1* links histone methylation to initiation of meiotic recombination. Science (2013) vol. 339 (6116) pp. 215-8

Agarwal S and Roeder GS. *Zip3* provides a link between recombination enzymes and synaptonemal complex proteins. Cell (2000) vol. 102 (2) pp. 245-55

Ajimura M, Leem SH, Ogawa H. Identification of new genes required for meiotic recombination in *Saccharomyces cerevisiae*. Genetics (1993) vol. 133 (1) pp. 51-66

Alani E, Padmore R, Kleckner N. Analysis of wild-type and *rad50* mutants of yeast suggests an intimate relationship between meiotic chromosome synapsis and recombination. Cell (1990) vol. 61 (3) pp. 419-36

Alani E, Thresher R, Griffith JD, Kolodner RD. Characterization of DNA-binding and strand-exchange stimulation properties of y-RPA, a yeast single-strand-DNA-binding protein. J Mol Biol (1992) vol. 227 (1) pp. 54-71

Albini SM and Jones GH. Synaptonemal complex spreading in *Allium cepa* and *A. fistulosum*. I. The initiation and sequence of pairing. *Chromosoma* (1987) vol. 95 pp. 324–38

Allers T and Lichten M. A method for preparing genomic DNA that restrains branch migration of Holliday junctions. Nucleic Acids Research (2000) vol. 28 (2) pp. e6

Allers T and Lichten M. Differential timing and control of noncrossover and crossover recombination during meiosis. Cell (2001a) vol. 106 (1) pp. 47-57

Allers T and Lichten M. Intermediates of yeast meiotic recombination contain heteroduplex DNA. Molecular Cell (2001b) vol. 8 (1) pp. 225-31

Anderson LK, Stack SM, Sherman JD. Spreading synaptonemal complexes from *Zea mays*. I. No synaptic adjustment of inversion loops during pachytene. Chromosoma (1988) vol. 96 (4) pp. 295-305

Argueso JL, Wanat J, Gemici Z, Alani E. Competing crossover pathways act during meiosis in Saccharomyces cerevisiae. Genetics (2004) vol. 168 (4) pp. 1805-16

Arora C, Kee K, Maleki S, Keeney S. Antiviral protein *Ski8* is a direct partner of Spo11 in meiotic DNA break formation, independent of its cytoplasmic role in RNA metabolism. Mol Cell (2004) vol. 13 (4) pp. 549-59

Averbeck D, Laskowski W, Eckardt F, Lehmann-Brauns E. Four radiation sensitive mutants of *Saccharomyces.* Survival after UV- and x-ray-irradiation as well as UV-induced reversion rates from isoleucine-valine dependence to independence. Mol Gen Genet (1970) vol. 107 (2) pp. 117-27

Bailis JM, Roeder GS. Synaptonemal complex morphogenesis and sister-chromatid cohesion require Mek1-dependent phosphorylation of a meiotic chromosomal protein. Genes Dev (1998) vol. 12 (22) pp. 3551-63

Baker TG and Franchi LL. The structure of the chromosomes in human primordial oocytes. Chromosoma (1967) vol. 22 (3) pp. 358-377

Barlow JH, Faryabi RB, Callén E, Wong N, Malhowski A, Chen HT, Gutierrez-Cruz G, Sun HW, McKinnon P, Wright G, Casellas R, Robbiani DF, Staudt L, Fernandez-Capetillo O, Nussenzweig A. Identification of early replicating fragile sites that contribute to genome instability. Cell (2013) vol. 152 (3) pp. 620-32

Baudat F, Buard J, Grey C, Fledel-Alon A, Ober C, Przeworski M, Coop G, de Massy B. *PRDM9* is a major determinant of meiotic recombination hotspots in humans and mice. Science (2010) vol. 327 (5967) pp. 836-40

Baudat F, Nicolas A.Clustering of meiotic double-strand breaks on yeast chromosome III. Proceedings of the National Academy of Sciences (1997) vol. 94 (10) pp. 5213-5218

Bennett CB, Snipe JR, Resnick MA. A persistent double-strand break destabilizes human DNA in yeast and can lead to G2 arrest and lethality. Cancer Res (1997) vol. 57 (10) pp. 1970-80

Berg IL, Neumann R, Lam KW, Sarbajna S, Odenthal-Hesse L, May CA, Jeffreys AJ. *PRDM9* variation strongly influences recombination hot-spot activity and meiotic instability in humans. Nat Genet (2010) vol. 42 (10) pp. 859-63

Bergerat A, de Massy B, Gadelle D, Varoutas PC, Nicolas A, Forterre P. An atypical topoisomerase II from Archaea with implications for meiotic recombination. Nature (1997) vol. 386 (6623) pp. 414-7

Bickel SE and Orr-Weaver TL. Holding chromatids together to ensure they go their separate ways. Bioessays (1996) vol. 18 (4) pp. 293-300

Bishop DK, Nikolski Y, Oshiro J, Chon J, Shinohara M, Chen X. High copy number suppression of the meiotic arrest caused by a dmc1 mutation: *REC114* imposes an early recombination block and *RAD54* promotes a *DMC1*-independent DSB repair pathway. Genes Cells (1999) vol. 4 (8) pp. 425-44

Bishop DK, Park D, Xu L, Kleckner N. DMC1: a meiosis-specific yeast homolog of *E. coli recA* required for recombination, synaptonemal complex formation, and cell cycle progression. Cell (1992) vol. 69 (3) pp. 439-56

Bishop DK. RecA homologs Dmc1 and Rad51 interact to form multiple nuclear complexes prior to meiotic chromosome synapsis. Cell (1994) vol. 79 (6) pp. 1081-92

Blanck S, Kobbe D, Hartung F, Fengler K, Focke M, Puchta H. A *SRS2* homolog from Arabidopsis thaliana disrupts recombinogenic DNA intermediates and facilitates single strand annealing. Nucleic Acids Research (2009) vol. 37 (21) pp. 7163-76

Blat Y, Protacio RU, Hunter N, Kleckner N. Physical and functional interactions among basic chromosome organizational features govern early steps of meiotic chiasma formation. Cell (2002) vol. 111 (6) pp. 791-802

Bleazard T, Ju YS, Sung J, Seo JS. Fine-scale mapping of meiotic recombination in Asians. BMC Genet (2013) vol. 14 pp. 19

Blitzblau HG and Hochwagen A. ATR/Mec1 prevents lethal meiotic recombination initiation on partially replicated chromosomes in budding yeast. Elife (2013) vol. 2 pp. e00844

Blitzblau HG, Bell GW, Rodriguez J, Bell SP, Hochwagen A. Mapping of meiotic single-stranded DNA reveals double-stranded-break hotspots near centromeres and telomeres. Curr Biol (2007) vol. 17 (23) pp. 2003-12

Boddy MN, Gaillard PH, McDonald WH, Shanahan P, Yates JR 3rd, Russell P. Mus81-Eme1 are essential components of a Holliday junction resolvase. Cell (2001) vol. 107 (4) pp. 537-48

Bojko M. Human meiosis VIII. Chromosome pairing and formation of the synaptonemal complex in oocytes. Carlsberg Research Communications (1983) vol. 48 (4) pp. 457-483

Bojko M. Two kinds of "recombination nodules" in *Neurospora crassa*. Genome (1989) vol. 32 (2) pp. 309-17

Borde V, de Massy B. Programmed induction of DNA double strand breaks during meiosis: setting up communication between DNA and the chromosome structure. Current opinion in genetics & development (2013) vol. 23 (2) pp. 147-55

Borde V, Lin W, Novikov E, Petrini JH, Lichten M, Nicolas A. Association of Mre11p with Double-Strand Break Sites during Yeast Meiosis. Molecular Cell (2004) vol. 13 (3) pp. 389-401

Borde V, Robine N, Lin W, Bonfils S, Géli V, Nicolas A. Histone H3 lysine 4 trimethylation marks meiotic recombination initiation sites. EMBO J (2009) vol. 28 (2) pp. 99-111

Borde V, Wu TC, Lichten M. Use of a recombination reporter insert to define meiotic recombination domains on chromosome III of *Saccharomyces cerevisiae*. Mol Cell Biol (1999) vol. 19 (7) pp. 4832-42

Borde V. The multiple roles of the Mre11 complex for meiotic recombination. Chromosome research : an international journal on the molecular, supramolecular and evolutionary aspects of chromosome biology (2007) vol. 15 (5) pp. 551-563

Börner GV, Kleckner N, Hunter N. Crossover/noncrossover differentiation, synaptonemal complex formation, and regulatory surveillance at the leptotene/zygotene transition of meiosis. Cell (2004) vol. 117 (1) pp. 29-45

Boselli M, Rock J, Unal E, Levine SS, Amon A. Effects of age on meiosis in budding yeast. Dev Cell (2009) vol. 16 (6) pp. 844-55

Bremer MC, Gimble FS, Thorner J, Smith CL. VDE endonuclease cleaves *Saccharomyces cerevisiae* genomic DNA at a single site: physical mapping of the VMA1 gene. Nucleic Acids Res (1992) vol. 20 (20) pp. 5484

Brick K, Smagulova F, Khil P, Camerini-Otero RD, Petukhova GV. Genetic recombination is directed away from functional genomic elements in mice. Nature (2012) vol. 485 (7400) pp. 642-5

Brunborg G, Resnick MA, Williamson DH. Cell-cycle-specific repair of DNA double strand breaks in *Saccharomyces cerevisiae*. Radiat Res (1980) vol. 82 (3) pp. 547-58

Buard J, Barthès P, Grey C, de Massy B. Distinct histone modifications define initiation and repair of meiotic recombination in the mouse. EMBO J (2009) vol. 28 (17) pp. 2616-24

Buhler C, Borde V, Lichten M. Mapping meiotic single-strand DNA reveals a new landscape of DNA double-strand breaks in *Saccharomyces cerevisiae*. PLoS Biol (2007) vol. 5 (12) pp. e324

Buonomo SB, Clyne RK, Fuchs J, Loidl J, Uhlmann F, Nasmyth K. Disjunction of homologous chromosomes in meiosis I depends on proteolytic cleavage of the meiotic cohesin Rec8 by separin. Cell (2000) vol. 103 (3) pp. 387-98

Busygina V, Sehorn MG, Shi IY, Tsubouchi H, Roeder GS, Sung P. Hed1 regulates Rad51-mediated recombination via a novel mechanism. Genes Dev (2008) vol. 22 (6) pp. 786-95

Bzymek M, Thayer NH, Oh SD, Kleckner N, Hunter N. Double Holliday junctions are intermediates of DNA break repair. Nature (2010) vol. 464 (7290) pp. 937-41

Cannavo E, Cejka P, Kowalczykowski SC. Relationship of DNA degradation by *Saccharomyces cerevisiae* Exonuclease 1 and its stimulation by RPA and Mre11-Rad50-Xrs2 to DNA end resection. Proc Natl Acad Sci USA (2013) vol. 110 (18) pp. E1661-8

Cao L, Alani E, Kleckner N. A pathway for generation and processing of double-strand breaks during meiotic recombination in *S. cerevisiae.* Cell (1990) vol. 61 (6) pp. 1089-101

Carpenter ATC. Electron microscopy of meiosis in Drosophila melanogaster females. Chromosoma (1975) vol. 51 (2) pp. 157-182

Cartagena-Lirola H, Guerini I, Manfrini N, Lucchini G, Longhese MP. Role of the Saccharomyces cerevisiae Rad53 checkpoint kinase in signaling double-strand breaks during the meiotic cell cycle. Mol Cell Biol (2008) vol. 28 (14) pp. 4480-93

Casper AM, Greenwell PW, Tang W, Petes TD. Chromosome aberrations resulting from double-strand DNA breaks at a naturally occurring yeast fragile site composed of inverted ty elements are independent of Mre11p and Sae2p. Genetics (2009) vol. 183 (2) pp. 423-39, 1SI-26SI

Cejka P, Cannavo E, Polaczek P, Masuda-Sasa T, Pokharel S, Campbell JL, Kowalczykowski SC. DNA end resection by Dna2-Sgs1-RPA and its stimulation by Top3-Rmi1 and Mre11-Rad50-Xrs2. Nature (2010a) vol. 467 (7311) pp. 112-6

Cejka P, Plank JL, Bachrati CZ, Hickson ID, Kowalczykowski SC. Rmi1 stimulates decatenation of double Holliday junctions during dissolution by Sgs1-Top3. Nat Struct Mol Biol (2010b) vol. 17 (11) pp. 1377-82

Cervantes MD, Farah JA, Smith GR. Meiotic DNA breaks associated with recombination in *S. pombe*. Molecular Cell (2000) vol. 5 (5) pp. 883-8

Chandley AC. A model for effective pairing and recombination at meiosis based on early replicating sites (R-bands) along chromosomes. Hum Genet (1986) vol. 72 (1) pp. 50-7

Chelysheva L, Gendrot G, Vezon D, Doutriaux MP, Mercier R, Grelon M. Zip4/Spo22 is required for class I CO formation but not for synapsis completion in *Arabidopsis thaliana*. PLoS Genet (2007) vol. 3 (5) pp. e83

Chelysheva L, Vezon D, Chambon A, Gendrot G, Pereira L, Lemhemdi A, Vrielynck N, Le Guin S, Novatchkova M, Grelon M. The *Arabidopsis HEI10* is a new ZMM protein related to Zip3. PLoS Genet (2012) vol. 8 (7) pp. e1002799

Chen C, Zhang W, Timofejeva L, Gerardin Y, Ma H. The *Arabidopsis ROCK-N-ROLLERS* gene encodes a homolog of the yeast ATP-dependent DNA helicase *MER3* and is required for normal meiotic crossover formation. Plant J (2005) vol. 43 (3) pp. 321-34

Chen X, Niu H, Chung WH, Zhu Z, Papusha A, Shim EY, Lee SE, Sung P, Ira G. Cell cycle regulation of DNA double-strand break end resection by Cdk1-dependent Dna2 phosphorylation. Nat Struct Mol Biol (2011) vol. 18 (9) pp. 1015-9

Cheng CH, Lo YH, Liang SS, Ti SC, Lin FM, Yeh CH, Huang HY, Wang TF. SUMO modifications control assembly of synaptonemal complex and polycomplex in meiosis of *Saccharomyces cerevisiae*. Genes Dev (2006) vol. 20 (15) pp. 2067-81

Cherest H, Surdin-Kerjan Y. Genetic analysis of a new mutation conferring cysteine auxotrophy in *Saccharomyces cerevisiae*: updating of the sulfur metabolism pathway. Genetics (1992) vol. 130 (1) pp. 51-8

Chlebowicz E, Jachymczyk WJ. Repair of MMS-induced DNA double-strand breaks in haploid cells of *Saccharomyces cerevisiae*, which requires the presence of a duplicate genome. Mol Gen Genet (1979) vol. 167 (3) pp. 279-86

Chu S, DeRisi J, Eisen M, Mulholland J, Botstein D, Brown PO, Herskowitz I. The transcriptional program of sporulation in budding yeast. Science (1998) vol. 282 (5389) pp. 699-705

Cloud V, Chan YL, Grubb J, Budke B, Bishop DK. Rad51 is an accessory factor for Dmc1-mediated joint molecule formation during meiosis. Science (2012) vol. 337 (6099) pp. 1222-5

Coïc E, Gluck L, Fabre F. Evidence for short-patch mismatch repair in Saccharomyces cerevisiae. EMBO J (2000) vol. 19 (13) pp. 3408-17

Cole F, Kauppi L, Lange J, Roig I, Wang R, Keeney S, Jasin M. Homeostatic control of recombination is implemented progressively in mouse meiosis. Nat Cell Biol (2012) vol. 14 (4) pp. 424-30

Cole F, Keeney S, Jasin M. Comprehensive, fine-scale dissection of homologous recombination outcomes at a hot spot in mouse meiosis. Molecular Cell (2010) vol. 39 (5) pp. 700-10

Comings DE and Okada TA. Whole mount electron microscopy of meiotic chromosomes and the synaptonemal complex. Chromosoma (1970) vol. 30 (3) pp. 269-286

Copenhaver GP, Housworth EA, Stahl FW. Crossover interference in *Arabidopsis.* Genetics (2002) vol. 160 (4) pp. 1631-9

Couteau F, Belzile F, Horlow C, Grandjean O, Vezon D, Doutriaux MP. Random chromosome segregation without meiotic arrest in both male and female meiocytes of a dmc1 mutant of *Arabidopsis*. Plant Cell (1999) vol. 11 (9) pp. 1623-34

D'Andrea AD. Susceptibility pathways in Fanconi's anemia and breast cancer. N Engl J Med (2010) vol. 362 (20) pp. 1909-19

Daniel K, Lange J, Hached K, Fu J, Anastassiadis K, Roig I, Cooke HJ, Stewart AF, Wassmann K, Jasin M, Keeney S, Tóth A. Meiotic homologue alignment and its quality surveillance are controlled by mouse *HORMAD1*. Nat Cell Biol (2011) vol. 13 (5) pp. 599-610

Datta A, Adjiri A, New L, Crouse GF, Jinks Robertson S. Mitotic crossovers between diverged sequences are regulated by mismatch repair proteins in Saccaromyces cerevisiae. Mol Cell Biol (1996) vol. 16 (3) pp. 1085-93

Dayani Y, Simchen G, Lichten M. Meiotic recombination intermediates are resolved with minimal crossover formation during return-to-growth, an analogue of the mitotic cell cycle. PLoS Genet (2011) vol. 7 (5) pp. e1002083

de los Santos T, Hunter N, Lee C, Larkin B, Loidl J, Hollingsworth NM. The Mus81/Mms4 endonuclease acts independently of double-Holliday junction resolution to promote a distinct subset of crossovers during meiosis in budding yeast. Genetics (2003) vol. 164 (1) pp. 81-94

de Massy B and Nicolas A. The control in cis of the position and the amount of the *ARG4* meiotic double-strand break of *Saccharomyces cerevisiae*. EMBO J (1993) vol. 12 (4) pp. 1459-66

de Massy B, Rocco V, Nicolas A. The nucleotide mapping of DNA double-strand breaks at the *CYS3* initiation site of meiotic recombination in *Saccharomyces cerevisiae*. EMBO J (1995) vol. 14 (18) pp. 4589-98

De Muyt A, Jessop L, Kolar E, Sourirajan A, Chen J, Dayani Y, Lichten M. BLM Helicase Ortholog Sgs1 Is a Central Regulator of Meiotic Recombination Intermediate Metabolism. Molecular Cell (2012) vol. 46 (1) pp. 43-53

Dernburg AF, McDonald K, Moulder G, Barstead R, Dresser M, Villeneuve AM. Meiotic recombination in *C. elegans* initiates by a conserved mechanism and is dispensable for homologous chromosome synapsis. Cell (1998) vol. 94 (3) pp. 387-98

Detloff P, White MA, Petes TD. Analysis of a gene conversion gradient at the *HIS4* locus in *Saccharomyces cerevisiae*. Genetics (1992) vol. 132 (1) pp. 113-23

Di Giacomo M, Barchi M, Baudat F, Edelmann W, Keeney S, Jasin M. Distinct DNA-damage-dependent and -independent responses drive the loss of oocytes in recombination-defective mouse mutants. Proc Natl Acad Sci USA (2005) vol. 102 (3) pp. 737-42

Dietrich AJJ and de Boer P. A sequential analysis of the development of the synaptonemal complex in spermatocytes of the mouse by electron microscopy using hydroxyurea and agar filtration. Genetica (1983) vol. 61 (2) pp. 119-129

Doe CL, Ahn JS, Dixon J, Whitby MC. Mus81-Eme1 and Rqh1 involvement in processing stalled and collapsed replication forks. J Biol Chem (2002) vol. 277 (36) pp. 32753-9

Dresser ME and Giroux CN. Meiotic chromosome behavior in spread preparations of yeast. The Journal of Cell Biology (1988) vol. 106 (3) pp. 567-73

Dutta SK, Jones AS, Stacey M The separation of desoxypentosenucleic acids and pentosenucleic acids. Biochim Biophys Acta (1953) vol. 10 (4) pp. 613-22

Engebrecht J, Hirsch J, Roeder GS. Meiotic gene conversion and crossing over: their relationship to each other and to chromosome synapsis and segregation. Cell (1990) vol. 62 (5) pp. 927-37

Engebrecht JA, Voelkel-Meiman K, Roeder GS. Meiosis-specific RNA splicing in yeast. Cell (1991) vol. 66 (6) pp. 1257-68

Entian KD, Schuster T, Hegemann JH, Becher D, Feldmann H, Güldener U, Götz R, Hansen M, Hollenberg CP, Jansen G, Kramer W, Klein S, Kötter P, Kricke J, Launhardt H, Mannhaupt G, Maierl A, Meyer P, Mewes W, Munder T, Niedenthal RK, Ramezani Rad M, Röhmer A, Römer A, Hinnen A, et al. Functional analysis of 150 deletion mutants in *Saccharomyces cerevisiae* by a systematic approach. Mol Gen Genet (1999) vol. 262 (4-5) pp. 683-702

Esashi F, Christ N, Gannon J, Liu Y, Hunt T, Jasin M, West SC. CDK-dependent phosphorylation of BRCA2 as a regulatory mechanism for recombinational repair. Nature (2005) vol. 434 (7033) pp. 598-604

Esberg A, Muller LA, McCusker JH. Genomic structure of and genome-wide recombination in the *Saccharomyces cerevisiae* S288C progenitor isolate EM93. PLoS ONE (2011) vol. 6 (9) pp. e25211

Esposito MS, Esposito RE. Genes controlling meiosis and spore formation in yeast. Genetics (1974) vol. 78 (1) pp. 215-25

Esposito MS, Esposito RE. The genetic control of sporulation in *Saccharomyces*. I. The isolation of temperature-sensitive sporulation-deficient mutants. Genetics (1969) vol. 61 (1) pp. 79-89

Esposito RE, Frink N, Bernstein P, Esposito MS. The genetic control of sporulation in *Saccharomyces.* II. Dominance and complementation of mutants of meiosis and spore formation. Mol Gen Genet (1972) vol. 114 (3) pp. 241-8

Fan Q, Xu F, Petes TD. Meiosis-specific double-strand DNA breaks at the *HIS4* recombination hot spot in the yeast *Saccharomyces cerevisiae*: control in cis and trans. Mol Cell Biol (1995) vol. 15 (3) pp. 1679-88

Fawcett DW. The fine structure of chromosomes in the meiotic prophase of vertebrate spermatocytes. J Biophys Biochem Cytol (1956) vol. 2 (4) pp. 403-6

Fiorentini P, Huang KN, Tishkoff DX, Kolodner RD, Symington LS. Exonuclease I of *Saccharomyces cerevisiae* functions in mitotic recombination in vivo and in vitro. Mol Cell Biol (1997) vol. 17 (5) pp. 2764-73

Fogel S, Mortimer R, Lusnak K, Tavares F. Meiotic gene conversion: a signal of the basic recombination event in yeast. Cold Spring Harbor Symp. Quant. Biol. (1978) 43, 1325-1341.

Fogel S, Mortimer RK. Informational transfer in meiotic gene conversion. Proc Natl Acad Sci USA (1969) vol. 62 (1) pp. 96-103

Freudenreich CH. Chromosome fragility: molecular mechanisms and cellular consequences. Front Biosci (2007) vol. 12 pp. 4911-24

Friedman DB, Hollingsworth NM, Byers B. Insertional mutations in the yeast HOP1 gene: evidence for multimeric assembly in meiosis. Genetics (1994) vol. 136 (2) pp. 449-64

Fukuda T, Kugou K, Sasanuma H, Shibata T, Ohta K. Targeted induction of meiotic double-strand breaks reveals chromosomal domain-dependent regulation of Spo11 and interactions among potential sites of meiotic recombination. Nucleic Acids Research (2008) vol. 36 (3) pp. 984-97

Fukuda T, Ohya Y. Recruitment of RecA homologs Dmc1p and Rad51p to the double-strand break repair site initiated by meiosis-specific endonuclease VDE (PI-SceI). Mol Genet Genomics (2006) vol. 275 (2) pp. 204-14

Fung JC, Rockmill B, Odell M, Roeder GS. Imposition of crossover interference through the nonrandom distribution of synapsis initiation complexes. Cell (2004) vol. 116 (6) pp. 795-802

Gallie BL, Worton RG. Somatic events unmask recessive cancer genes to initiate malignancy. J Cell Biochem (1986) vol. 32 (3) pp. 215-22

Game JC, Mortimer RK. A genetic study of x-ray sensitive mutants in yeast. Mutat Res (1974) vol. 24 (3) pp. 281-92

Gangloff S, McDonald JP, Bendixen C, Arthur L, Rothstein R. The yeast type I topoisomerase Top3 interacts with Sgs1, a DNA helicase homolog: a potential eukaryotic reverse gyrase. Mol Cell Biol (1994) vol. 14 (12) pp. 8391-8

Gangloff S, Soustelle C, Fabre F. Homologous recombination is responsible for cell death in the absence of the Sgs1 and Srs2 helicases. Nat Genet (2000) vol. 25 (2) pp. 192-4

Garcia V, Phelps SE, Gray S, Neale MJ. Bidirectional resection of DNA double-strand breaks by Mre11 and Exo1. Nature (2011) pp.

Gerton JL, DeRisi J, Shroff R, Lichten M, Brown PO, Petes TD. Global mapping of meiotic recombination hotspots and coldspots in the yeast *Saccharomyces cerevisiae*. Proceedings of the National Academy of Sciences (2000) vol. 97 (21) pp. 11383-11390

Getz TJ, Banse SA, Young LS, Banse AV, Swanson J, Wang GM, Browne BL, Foss HM, Stahl FW. Reduced mismatch repair of heteroduplexes reveals "non"-interfering crossing over in wild-type Saccharomyces cerevisiae. Genetics (2008) vol. 178 (3) pp. 1251-69

Gilbertson LA and Stahl FW. A test of the double-strand break repair model for meiotic recombination in Saccharomyces cerevisiae. Genetics (1996) vol. 144 (1) pp. 27-41

Gilbertson LA and Stahl FW. Initiation of meiotic recombination is independent of interhomologue interactions. Proc Natl Acad Sci USA (1994) vol. 91 (25) pp. 11934-7

Gimble FS and Stephens BW. Substitutions in conserved dodecapeptide motifs that uncouple the DNA binding and DNA cleavage activities of PI-*Sce*I endonuclease. J Biol Chem (1995) vol. 270 (11) pp. 5849-56

Gimble FS and Thorner J. Homing of a DNA endonuclease gene by meiotic gene conversion in *Saccharomyces cerevisiae*. Nature (1992) vol. 357 (6376) pp. 301-6

Gimble FS, Thorner J. Purification and characterization of VDE, a site-specific endonuclease from the yeast Saccharomyces cerevisiae. J Biol Chem (1993) vol. 268 (29) pp. 21844-53

Glover TW, Berger C, Coyle J, Echo B. DNA polymerase alpha inhibition by aphidicolin induces gaps and breaks at common fragile sites in human chromosomes. Hum Genet (1984) vol. 67 (2) pp. 136-42

Goldfarb T and Lichten M. Frequent and efficient use of the sister chromatid for DNA double-strand break repair during budding yeast meiosis. PLoS Biol (2010) vol. 8 (10) pp. e1000520

Goldman AS and Lichten M. Restriction of ectopic recombination by interhomolog interactions during *Saccharomyces cerevisiae* meiosis. Proc Natl Acad Sci USA (2000) vol. 97 (17) pp. 9537-42

Goldman AS and Lichten M. The efficiency of meiotic recombination between dispersed sequences in *Saccharomyces cerevisiae* depends upon their chromosomal location. Genetics (1996) vol. 144 (1) pp. 43-55

Goodyer W, Kaitna S, Couteau F, Ward JD, Boulton SJ, Zetka M. *HTP-3* links DSB formation with homolog pairing and crossing over during *C. elegans* meiosis. Dev Cell (2008) vol. 14 (2) pp. 263-74

Gorbalenya AE, Koonin EV, Donchenko AP, Blinov VM. A novel superfamily of nucleoside triphosphate-binding motif containing proteins which are probably involved in duplex unwinding in DNA and RNA replication and recombination. FEBS Lett (1988) vol. 235 (1-2) pp. 16-24

Goyon C and Lichten M. Timing of molecular events in meiosis in *Saccharomyces cerevisiae*: stable heteroduplex DNA is formed late in meiotic prophase. Mol Cell Biol (1993) vol. 13 (1) pp. 373-82

Grey C, Barthès P, Chauveau-Le Friec G, Langa F, Baudat F, de Massy B. Mouse *PRDM9* DNA-Binding Specificity Determines Sites of Histone H3 Lysine 4 Trimethylation for Initiation of Meiotic Recombination. PLoS Biol (2011) vol. 9 (10) pp. e1001176

Grushcow JM, Holzen TM, Park KJ, Weinert T, Lichten M, Bishop DK. Saccharomyces cerevisiae checkpoint genes *MEC1, RAD17* and *RAD24* are required for normal meiotic recombination partner choice. Genetics (1999) vol. 153 (2) pp. 607-20

Haber JE, Weiffenbach B, Rogers DT, McCusker J, Rowe LB. Chromosomal Rearrangements Accompanying Yeast Mating-type Switching: Evidence for a Gene-conversion Model. Cold Spring Harb Symp Quant Biol (1981) vol. 45 (0) pp. 991-1002

Haber JE. Mating-type genes and *MAT* switching in *Saccharomyces cerevisiae*. Genetics (2012) vol. 191 (1) pp. 33-64

Haldane JBS. The Cytological Basis of Genetical Interference TI -. CYTOLOGIA (1931) vol. 3 (1) pp. 54-65

Hastings PJ, Quah SK, von Borstel RC. Spontaneous mutation by mutagenic repair of spontaneous lesions in DNA. Nature (1976) vol. 264 (5588) pp. 719-22

Henderson KA and Keeney S. Tying synaptonemal complex initiation to the formation and programmed repair of DNA double-strand breaks. Proc Natl Acad Sci USA (2004) vol. 101 (13) pp. 4519-24

Henderson SA. Grades of chromatid organisation in mitotic and meiotic chromosomes I. Chromosoma (1971) vol. 35 (1) pp. 28-40

Heng HH, Tsui LC, Moens PB. Organization of heterologous DNA inserts on the mouse meiotic chromosome core. (1994) vol. 103 (6) pp. 401-407

Heyting C. Synaptonemal complexes: structure and function. Curr Opin Cell Biol (1996) vol. 8 (3) pp. 389-96

Higgins JD, Armstrong SJ, Franklin FC, Jones GH. The *Arabidopsis* MutS homolog *AtMSH4* functions at an early step in recombination: evidence for two classes of recombination in Arabidopsis. Genes Dev (2004) vol. 18 (20) pp. 2557-70

Ho CK, Mazón G, Lam AF, Symington LS. Mus81 and Yen1 promote reciprocal exchange during mitotic recombination to maintain genome integrity in budding yeast. Molecular Cell (2010) vol. 40 (6) pp. 988-1000|

Hodgson A, Terentyev Y, Johnson RA, Bishop-Bailey A, Angevin T, Croucher A, Goldman AS. Mre11 and Exo1 contribute to the initiation and processivity of resection at meiotic double-strand breaks made independently of Spo11. DNA Repair (2011) vol. 10 (2) pp. 138-48

Holliday R. A mechanism for gene conversion in fungi. Genetical Research Cambridge (1964) vol. 5 (2) pp. 282-304

Hollingsworth NM and Byers B. *HOP1*: a yeast meiotic pairing gene. Genetics (1989) vol. 121 (3) pp. 445-62

Hollingsworth NM and Johnson AD. A conditional allele of the *Saccharomyces cerevisiae HOP1* gene is suppressed by overexpression of two other meiosis-specific genes: *RED1* and *REC104*. Genetics (1993) vol. 133 (4) pp. 785-97

Hollingsworth NM and Brill SJ. The Mus81 solution to resolution: generating meiotic crossovers without Holliday junctions. Genes Dev (2004) vol. 18 (2) pp. 117-25

Hollingsworth NM, Goetsch L, Byers B. The *HOP1* gene encodes a meiosis-specific component of yeast chromosomes. Cell (1990) vol. 61 (1) pp. 73-84

Hollingsworth NM, Ponte L, Halsey C. *MSH5*, a novel MutS homolog, facilitates meiotic reciprocal recombination between homologs in *Saccharomyces cerevisiae* but not mismatch repair. Genes Dev (1995) vol. 9 (14) pp. 1728-39

Holm P. Three-dimensional reconstruction of chromosome pairing during the zygotene stage of meiosis in Lilium longiflorum. Carlsberg Research Communications (1977) vol. 42 (2) pp. 103-151

Hong S, Sung Y, Yu M, Lee M, Kleckner N, Kim KP. The logic and mechanism of homologous recombination partner choice. Molecular Cell (2013) vol. 51 (4) pp. 440-53

Housworth EA and Stahl FW. Crossover interference in humans. Am J Hum Genet (2003) vol. 73 (1) pp. 188-97

Huertas P and Jackson SP. Human CtIP mediates cell cycle control of DNA end resection and double strand break repair. J Biol Chem (2009) vol. 284 (14) pp. 9558-65

Huertas P, Cortés-Ledesma F, Sartori AA, Aguilera A, Jackson SP. CDK targets Sae2 to control DNA-end resection and homologous recombination. Nature (2008) vol. 455 (7213) pp. 689-92

Hunter N and Kleckner N. The single-end invasion: an asymmetric intermediate at the double-strand break to double-holliday junction transition of meiotic recombination. Cell (2001) vol. 106 (1) pp. 59-70

Hussin J, Roy-Gagnon MH, Gendron R, Andelfinger G, Awadalla P. Age-dependent recombination rates in human pedigrees. PLoS Genet (2011) vol. 7 (9) pp. e1002251

Hyppa RW and Smith GR. Crossover Invariance Determined by Partner Choice for Meiotic DNA Break Repair. Cell (2010) vol. 142 (2) pp. 243-255

Ira G, Malkova A, Liberi G, Foiani M, Haber JE. Srs2 and Sgs1-Top3 suppress crossovers during double-strand break repair in yeast. Cell (2003) vol. 115 (4) pp. 401-11

Ira G, Pellicioli A, Balijja A, Wang X, Fiorani S, Carotenuto W, Liberi G, Bressan D, Wan L, Hollingsworth NM, Haber JE, Foiani M. DNA end resection, homologous recombination and DNA damage checkpoint activation require *CDK1*. Nature (2004) vol. 431 (7011) pp. 1011-7

Jackson SP and Bartek J. The DNA-damage response in human biology and disease. Nature (2009) vol. 461 (7267) pp. 1071-8

Janssens FAIM. La Theorie de la Chiasmatypie, Nouvelle interprétation des cinèses de maturation (1909) Translated by Koszul R and Zickler D. Genetics (2012) vol. 191 (2) pp. 319-46

Jessop L and Lichten M. Mus81/Mms4 endonuclease and Sgs1 helicase collaborate to ensure proper recombination intermediate metabolism during meiosis. Molecular Cell (2008) vol. 31 (3) pp. 313-23

Jessop L, Rockmill B, Roeder GS, Lichten M. Meiotic chromosome synapsis-promoting proteins antagonize the anti-crossover activity of Sgs1. PLoS Genet (2006) vol. 2 (9) pp. e155

Johnson R, Borde V, Neale MJ, Bishop-Bailey A, North M, Harris S, Nicolas A, Goldman AS. Excess single-stranded DNA inhibits meiotic double-strand break repair. PLoS Genet (2007) vol. 3 (11) pp. e223

Jones AS. The isolation of bacterial nucleic acids using cetyltrimethylammonium bromide (cetavlon). Biochim Biophys Acta (1953) vol. 10 (4) pp. 607-12

Kauppi L, Barchi M, Baudat F, Romanienko PJ, Keeney S, Jasin M. Distinct properties of the XY pseudoautosomal region crucial for male meiosis. Science (2011) vol. 331 (6019) pp. 916-20

Kee K, Protacio RU, Arora C, Keeney S. Spatial organization and dynamics of the association of Rec102 and Rec104 with meiotic chromosomes. EMBO J (2004) vol. 23 (8) pp. 1815-24

Kee K, Protacio RU, Arora C, Keeney S. Covalent protein-DNA complexes at the 5' strand termini of meiosis-specific double-strand breaks in yeast. Proc Natl Acad Sci USA (1995) vol. 92 (24) pp. 11274-8

Keeney S, Giroux CN, Kleckner N. Meiosis-specific DNA double-strand breaks are catalyzed by Spo11, a member of a widely conserved protein family. Cell (1997) vol. 88 (3) pp. 375-84

Keeney S. Mechanism and control of meiotic recombination initiation. Curr Top Dev Biol (2001) vol. 52 pp. 1-53

Keyl HG. Lampbrush chromosomes in spermatocytes of *Chironomus*. (1975) vol. 51 (1) pp. 75-91

Khazanehdari KA and Borts RH. EXO1 and MSH4 differentially affect crossing-over and segregation. Chromosoma (2000) vol. 109 (1-2) pp. 94-102

Kim KP, Weiner BM, Zhang L, Jordan A, Dekker J, Kleckner N. Sister cohesion and structural axis components mediate homolog bias of meiotic recombination. Cell (2010) vol. 143 (6) pp. 924-37

Kitani Y and Whitehouse HLK. Aberrant ascus genotypes from crosses involving mutants at the g locus in Sordaria fimicola. Genetical Research (2008) vol. 24 (3) pp. 229-250

Klapholz S, Waddell CS, Esposito RE. The role of the *SPO11* gene in meiotic recombination in yeast. Genetics (1985) vol. 110 (2) pp. 187-216

Klar AJ, Fogel S, Lusnak K. Gene conversion of the mating-type locus in Saccharomyces cerevisiae. Genetics (1979) vol. 92 (3) pp. 777-82

Kleckner N. Chiasma formation: chromatin/axis interplay and the role(s) of the synaptonemal complex. Chromosoma (2006) vol. 115 (3) pp. 175-94

Kohli J and Bähler J. Homologous recombination in fission yeast: absence of crossover interference and synaptonemal complex. Experientia (1994) vol. 50 (3) pp. 295-306

Kolodkin AL, Klar AJ, Stahl FW. Double-strand breaks can initiate meiotic recombination in *S. cerevisiae*. Cell (1986) vol. 46 (5) pp. 733-40

Kon N, Krawchuk MD, Warren BG, Smith GR, Wahls WP. Transcription factor Mts1/Mts2 (Atf1/Pcr1, Gad7/Pcr1) activates the *M26* meiotic recombination hotspot in *Schizosaccharomyces pombe*. Proc Natl Acad Sci USA (1997) vol. 94 (25) pp. 13765-70

Koszul R, Meselson M, Van Doninck K, Vandenhaute J, Zickler D. The centenary of Janssens's chiasmatype theory. Genetics (2012) vol. 191 (2) pp. 309-17

Krejci L, Altmannova V, Spirek M, Zhao X. Homologous recombination and its regulation. Nucleic Acids Research (2012) vol. 40 (13) pp. 5795-818

Krejci L, Van Komen S, Li Y, Villemain J, Reddy MS, Klein H, Ellenberger T, Sung P. DNA helicase Srs2 disrupts the Rad51 presynaptic filament. Nature (2003) vol. 423 (6937) pp. 305-9

Krogh BO and Symington LS. Recombination proteins in yeast. Annu Rev Genet (2004) vol. 38 pp. 233-71

Kugou K, Fukuda T, Yamada S, Ito M, Sasanuma H, Mori S, Katou Y, Itoh T, Matsumoto K, Shibata T, Shirahige K, Ohta K. Rec8 guides canonical Spo11 distribution along yeast meiotic chromosomes. Mol Biol Cell (2009) vol. 20 (13) pp. 3064-76

Lamb NE, Feingold E, Savage A, Avramopoulos D, Freeman S, Gu Y, Hallberg A, Hersey J, Karadima G, Pettay D, Saker D, Shen J, Taft L, Mikkelsen M, Petersen MB, Hassold T, Sherman SL. Characterization of susceptible chiasma configurations that increase the risk for maternal nondisjunction of chromosome 21. Hum Mol Genet (1997) vol. 6 (9) pp. 1391-9

Langerak P, Mejia-Ramirez E, Limbo O, Russell P. Release of Ku and MRN from DNA ends by Mre11 nuclease activity and Ctp1 is required for homologous recombination repair of double-strand breaks. PLoS Genet (2011) vol. 7 (9) pp. e1002271

Larsen NB, Hickson ID. RecQ Helicases: Conserved Guardians of Genomic Integrity. Adv Exp Med Biol (2013) vol. 767 pp. 161-84

Lee PS, Greenwell PW, Dominska M, Gawel M, Hamilton M, Petes TD. A fine-structure map of spontaneous mitotic crossovers in the yeast *Saccharomyces cerevisiae*. PLoS Genet (2009) vol. 5 (3) pp. e1000410

Lee SK, Johnson RE, Yu SL, Prakash L, Prakash S. Requirement of yeast *SGS1* and *SRS2* genes for replication and transcription. Science (1999) vol. 286 (5448) pp. 2339-42

Lemoine FJ, Degtyareva NP, Kokoska RJ, Petes TD. Reduced levels of DNA polymerase delta induce chromosome fragile site instability in yeast. Mol Cell Biol (2008) vol. 28 (17) pp. 5359-68

Lemoine FJ, Degtyareva NP, Lobachev K, Petes TD. Chromosomal translocations in yeast induced by low levels of DNA polymerase a model for chromosome fragile sites. Cell (2005) vol. 120 (5) pp. 587-98

Lengsfeld BM, Rattray AJ, Bhaskara V, Ghirlando R, Paull TT. Sae2 is an endonuclease that processes hairpin DNA cooperatively with the Mre11/Rad50/Xrs2 complex. Molecular Cell (2007) vol. 28 (4) pp. 638-51

Li J, Hooker GW, Roeder GS. Saccharomyces cerevisiae Mer2, Mei4 and Rec114 form a complex required for meiotic double-strand break formation. Genetics (2006) vol. 173 (4) pp. 1969-81

Lichten M. Meiotic Chromatin: The Substrate for Recombination Initiation. Recombination and Meiosis Models, Means, and Evolution (2008) vol. 3 pp. 165-193

Lieber MR. The mechanism of double-strand DNA break repair by the nonhomologous DNA end-joining pathway. Annu Rev Biochem (2010) vol. 79 pp. 181-211

Lindegren CC. Gene Conversion in *Saccharomyces*. Journal of Genetics (1953) vol. 51 (1) pp. 625-637

Lisby M, Barlow JH, Burgess RC, Rothstein R. Choreography of the DNA damage response: spatiotemporal relationships among checkpoint and repair proteins. Cell (2004) vol. 118 (6) pp. 699-713

Llorente B, Smith CE, Symington LS. Break-induced replication: what is it and what is it for?. Cell Cycle (2008) vol. 7 (7) pp. 859-64

Lobachev KS, Gordenin DA, Resnick MA. The Mre11 complex is required for repair of hairpin-capped double-strand breaks and prevention of chromosome rearrangements. Cell (2002) vol. 108 (2) pp. 183-93

Loidl J, Klein F, Scherthan H. Homologous pairing is reduced but not abolished in asynaptic mutants of yeast. The Journal of Cell Biology (1994) vol. 125 (6) pp. 1191-200

Lu BC. Meiosis in *Coprinus lagopus*: a comparative study with light and electron microscopy. J Cell Sci (1967) vol. 2 (4) pp. 529-36

Lu BC. Spreading the synaptonemal complex of *Neurospora crassa*. Chromosoma (1993) vol. 102 (7) pp. 464-72

Lydall D, Nikolsky Y, Bishop DK, Weinert T. A meiotic recombination checkpoint controlled by mitotic checkpoint genes. Nature (1996) vol. 383 (6603) pp. 840-3

Lynn A, Koehler KE, Judis L, Chan ER, Cherry JP, Schwartz S, Seftel A, Hunt PA, Hassold TJ. Covariation of synaptonemal complex length and mammalian meiotic exchange rates. Science (2002) vol. 296 (5576) pp. 2222-5

Lynn A, Soucek R, Börner GV. ZMM proteins during meiosis: crossover artists at work. Chromosome research (2007) vol. 15 (5) pp. 591-605

Mahadevaiah SK, Turner JM, Baudat F, Rogakou EP, de Boer P, Blanco-Rodríguez J, Jasin M, Keeney S, Bonner WM, Burgoyne PS. Recombinational DNA double-strand breaks in mice precede synapsis. Nat Genet (2001) vol. 27 (3) pp. 271-6

Majka J, Binz SK, Wold MS, Burgers PM. Replication protein A directs loading of the DNA damage checkpoint clamp to 5'-DNA junctions. J Biol Chem (2006a) vol. 281 (38) pp. 27855-61

Majka J, Niedziela-Majka A, Burgers PM. The checkpoint clamp activates Mec1 kinase during initiation of the DNA damage checkpoint. Molecular Cell (2006b) vol. 24 (6) pp. 891-901

Maleki S, Neale MJ, Arora C, Henderson KA, Keeney S. Interactions between Mei4, Rec114, and other proteins required for meiotic DNA double-strand break formation in *Saccharomyces cerevisiae*. Chromosoma (2007) vol. 116 (5) pp. 471-86

Mancera E, Bourgon R, Brozzi A, Huber W, Steinmetz LM. High-resolution mapping of meiotic crossovers and non-crossovers in yeast. Nature (2008) vol. 454 (7203) pp. 479-85

Manfrini N, Guerini I, Citterio A, Lucchini G, Longhese MP. Processing of meiotic DNA double strand breaks requires cyclin-dependent kinase and multiple nucleases. Journal of Biological Chemistry (2010) vol. 285 (15) pp. 11628-37

Mantiero D, Clerici M, Lucchini G, Longhese MP. Dual role for Saccharomyces cerevisiae Tel1 in the checkpoint response to double-strand breaks. EMBO reports (2007) vol. 8 (4) pp. 380-7

Mao-Draayer Y, Galbraith AM, Pittman DL, Cool M, Malone RE. Analysis of meiotic recombination pathways in the yeast Saccharomyces cerevisiae. Genetics (1996) vol. 144 (1) pp. 71-86

Martini E, Borde V, Legendre M, Audic S, Regnault B, Soubigou G, Dujon B, Llorente B. Genome-wide analysis of heteroduplex DNA in mismatch repair-deficient yeast cells reveals novel properties of meiotic recombination pathways. PLoS Genet (2011) vol. 7 (9) pp. e1002305

Martini E, Diaz RL, Hunter N, Keeney S. Crossover homeostasis in yeast meiosis. Cell (2006) vol. 126 (2) pp. 285-95

Matos J, Blanco MG, Maslen S, Skehel JM, West SC. Regulatory control of the resolution of DNA recombination intermediates during meiosis and mitosis. Cell (2011) vol. 147 (1) pp. 158-72

Matos J, Blanco MG, West SC. Cell-cycle kinases coordinate the resolution of recombination intermediates with chromosome segregation. Cell Rep (2013) vol. 4 (1) pp. 76-86

Mazón G and Symington LS. Mph1 and Mus81-Mms4 Prevent Aberrant Processing of Mitotic Recombination Intermediates. Molecular Cell (2013) vol. 52 (1) pp. 63-74

Mazón G, Mimitou EP, Symington LS. SnapShot: Homologous recombination in DNA double-strand break repair. Cell (2010) vol. 142 (4) pp. 646, 646.e1

McGill C, Shafer B, Strathern J. Coconversion of flanking sequences with homothallic switching. Cell (1989) vol. 57 (3) pp. 459-67

McMahill MS, Sham CW, Bishop DK. Synthesis-dependent strand annealing in meiosis. PLoS Biol (2007) vol. 5 (11) pp. e299

Meetei AR, Medhurst AL, Ling C, Xue Y, Singh TR, Bier P, Steltenpool J, Stone S, Dokal I, Mathew CG, Hoatlin M, Joenje H, de Winter JP, Wang W. A human ortholog of archaeal DNA repair protein Hef is defective in Fanconi anemia complementation group M. Nat Genet (2005) vol. 37 (9) pp. 958-63

Melo JA, Cohen J, Toczyski DP. Two checkpoint complexes are independently recruited to sites of DNA damage in vivo. Genes Dev (2001) vol. 15 (21) pp. 2809-21

Mercier R, Jolivet S, Vezon D, Huppe E, Chelysheva L, Giovanni M, Nogué F, Doutriaux MP, Horlow C, Grelon M, Mézard C. Two meiotic crossover classes cohabit in *Arabidopsis*: one is dependent on *MER3*, whereas the other one is not. Curr Biol (2005) vol. 15 (8) pp. 692-701

Merker JD, Dominska M, Petes TD. Patterns of heteroduplex formation associated with the initiation of meiotic recombination in the yeast *Saccharomyces cerevisiae*. Genetics (2003) vol. 165 (1) pp. 47-63

Meselson MS and Radding CM.A general model for genetic recombination. Proc Natl Acad Sci USA (1975) vol. 72 (1) pp. 358-61

Mimitou EP and Symington LS. Nucleases and helicases take center stage in homologous recombination. Trends Biochem Sci (2009) vol. 34 (5) pp. 264-72

Mimitou EP and Symington LS. Sae2, Exo1 and Sgs1 collaborate in DNA double-strand break processing. Nature (2008) vol. 455 (7214) pp. 770-4

Mitchel K, Lehner K, Jinks-Robertson S. Heteroduplex DNA position defines the roles of the Sgs1, Srs2, and Mph1 helicases in promoting distinct recombination outcomes. PLoS Genet (2013) vol. 9 (3) pp. e1003340

Mitchel K, Zhang H, Welz-Voegele C, Jinks-Robertson S. Molecular structures of crossover and noncrossover intermediates during gap repair in yeast: implications for recombination. Molecular Cell (2010) vol. 38 (2) pp. 211-22

Møens PB and Pearlman RE. Chromatin organization at meiosis. Bioessays (1988) vol. 9 (5) pp. 151-153

Moens PB. The fine structure of meiotic chromosome polarization and pairing in Locusta migratoria spermatocytes. Chromosoma (1969) vol. 28 (1) pp. 1-25

Moore CW. Responses of radiation-sensitive mutants of *Saccharomyces cerevisiae* to lethal effects of bleomycin. Mutat Res (1978) vol. 51 (2) pp. 165-80

Moreau S, Morgan EA, Symington LS. Overlapping functions of the *Saccharomyces cerevisiae* Mre11, Exo1 and Rad27 nucleases in DNA metabolism. Genetics (2001) vol. 159 (4) pp. 1423-33

Morrison DP and Hastings PJ. Characterization of the mutator mutation *mut5-1*. Mol Gen Genet (1979) vol. 175 (1) pp. 57-65

Mosedale G, Niedzwiedz W, Alpi A, Perrina F, Pereira-Leal JB, Johnson M, Langevin F, Pace P, Patel KJ. The vertebrate Hef ortholog is a component of the Fanconi anemia tumor-suppressor pathway. Nat Struct Mol Biol (2005) vol. 12 (9) pp. 763-71

Moses MJ. Chromosomal structures in crayfish spermatocytes. J Biophys Biochem Cytol (1956) vol. 2 (2) pp. 215-8

Murakami H and Nicolas A. Locally, meiotic double-strand breaks targeted by Gal4BD-Spo11 occur at discrete sites with a sequence preference. Mol Cell Biol (2009) vol. 29 (13) pp. 3500-16

Murray MG and Thompson WF. Rapid isolation of high molecular weight plant DNA. Nucleic Acids Research (1980) vol. 8 (19) pp. 4321-5

Myers S, Freeman C, Auton A, Donnelly P, McVean G. A common sequence motif associated with recombination hot spots and genome instability in humans. Nat Genet (2008) vol. 40 (9) pp. 1124-9

Myung K, Datta A, Chen C, Kolodner RD. *SGS1*, the Saccharomyces cerevisiae homologue of *BLM* and *WRN*, suppresses genome instability and homeologous recombination. Nat Genet (2001) vol. 27 (1) pp. 113-6

Nagai Y, Nogami S, Kumagai-Sano F, Ohya Y. Karyopherin-mediated nuclear import of the homing endonuclease *VMA1*-derived endonuclease is required for self-propagation of the coding region. Mol Cell Biol (2003) vol. 23 (5) pp. 1726-36

Nakada D, Matsumoto K, Sugimoto K. ATM-related Tel1 associates with double-strand breaks through an Xrs2-dependent mechanism. Genes Dev (2003) vol. 17 (16) pp. 1957-62

Nakagawa T and Ogawa H. Involvement of the *MRE2* gene of yeast in formation of meiosis-specific double-strand breaks and crossover recombination through RNA splicing. Genes Cells (1997) vol. 2 (1) pp. 65-79

Nakagawa T and Ogawa H. The Saccharomyces cerevisiae MER3 gene, encoding a novel helicase-like protein, is required for crossover control in meiosis. EMBO J (1999) vol. 18 (20) pp. 5714-23

Nakai S and Matsumoto S. Two types of radiation-sensitive mutant in yeast. Mutat Res (1967) vol. 4 (2) pp. 129-36

Nandabalan K and Roeder GS. Binding of a cell-type-specific RNA splicing factor to its target regulatory sequence. Mol Cell Biol (1995) vol. 15 (4) pp. 1953-60

Nasmyth K. Molecular genetics of yeast mating type. Annu Rev Genet (1982) vol. 16 pp. 439-500

Nassif N, Penney J, Pal S, Engels WR, Gloor GB. Efficient copying of nonhomologous sequences from ectopic sites via P-element-induced gap repair. Mol Cell Biol (1994) vol. 14 (3) pp. 1613-25

Neale MJ, Ramachandran M, Trelles-Sticken E, Scherthan H, Goldman AS. Wild-type levels of Spo11-induced DSBs are required for normal single-strand resection during meiosis. Molecular Cell (2002) vol. 9 (4) pp. 835-46

Nebel BR and Coulon EM. The fine structure of chromosomes in pigeon spermatocytes. (1962) vol. 13 (3) pp. 272-291

Ng SW, Liu Y, Hasselblatt KT, Mok SC, Berkowitz RS. A new human topoisomerase III that interacts with SGS1 protein. Nucleic Acids Research (1999) vol. 27 (4) pp. 993-1000

Nickoloff JA, Chen EY, Heffron F. A 24-base-pair DNA sequence from the MAT locus stimulates intergenic recombination in yeast. Proc Natl Acad Sci USA (1986) vol. 83 (20) pp. 7831-5

Nicolas A, Treco D, Schultes NP, Szostak JW. An initiation site for meiotic gene conversion in the yeast *Saccharomyces cerevisiae.* Nature (1989) vol. 338 (6210) pp. 35-9

Niu H, Li X, Job E, Park C, Moazed D, Gygi SP, Hollingsworth NM. Mek1 kinase is regulated to suppress double-strand break repair between sister chromatids during budding yeast meiosis. Mol Cell Biol (2007) vol. 27 (15) pp. 5456-67

Niu H, Wan L, Baumgartner B, Schaefer D, Loidl J, Hollingsworth NM. Partner choice during meiosis is regulated by Hop1-promoted dimerization of Mek1. Mol Biol Cell (2005) vol. 16 (12) pp. 5804-18

Nogami S, Fukuda T, Nagai Y, Yabe S, Sugiura M, Mizutani R, Satow Y, Anraku Y, Ohya Y. Homing at an extragenic locus mediated by VDE (PI-SceI) in Saccharomyces cerevisiae. Yeast (2002) vol. 19 (9) pp. 773-82

Novak JE, Ross-Macdonald PB, Roeder GS. The budding yeast Msh4 protein functions in chromosome synapsis and the regulation of crossover distribution. Genetics (2001) vol. 158 (3) pp. 1013-25

Ogawa H, Johzuka K, Nakagawa T, Leem SH, Hagihara AH. Functions of the yeast meiotic recombination genes, *MRE11* and *MRE2*. Adv Biophys (1995) vol. 31 pp. 67-76

Oh SD, Lao JP, Hwang PY, Taylor AF, Smith GR, Hunter N. BLM ortholog, Sgs1, prevents aberrant crossing-over by suppressing formation of multichromatid joint molecules. Cell (2007) vol. 130 (2) pp. 259-72

Ohta K, Shibata T, Nicolas A. Changes in chromatin structure at recombination initiation sites during yeast meiosis. EMBO J (1994) vol. 13 (23) pp. 5754-63

Orr-Weaver T and Szostak JW.. Yeast recombination: the association between double-strand gap repair and crossing-over. Proc Natl Acad Sci USA (1983) vol. 80 (14) pp. 4417-21

Orr-Weaver TL, Szostak JW, Rothstein RJ. Yeast transformation: a model system for the study of recombination. Proc Natl Acad Sci USA (1981) vol. 78 (10) pp. 6354-8

Osman F, Dixon J, Doe CL, Whitby MC. Generating crossovers by resolution of nicked Holliday junctions: a role for Mus81-Eme1 in meiosis. Molecular Cell (2003) vol. 12 (3) pp. 761-74

Ozeri-Galai E, Bester AC, Kerem B. The complex basis underlying common fragile site instability in cancer. Trends Genet (2012) vol. 28 (6) pp. 295-302

Paciotti V, Clerici M, Lucchini G, Longhese MP. The checkpoint protein Ddc2, functionally related to S. pombe Rad26, interacts with Mec1 and is regulated by Mec1-dependent phosphorylation in budding yeast. Genes Dev (2000) vol. 14 (16) pp. 2046-59

Padmore R, Cao L, Kleckner N. Temporal comparison of recombination and synaptonemal complex formation during meiosis in *S. cerevisiae*. Cell (1991) vol. 66 (6) pp. 1239-56

Pan J, Sasaki M, Kniewel R, Murakami H, Blitzblau HG, Tischfield SE, Zhu X, Neale MJ, Jasin M, Socci ND, Hochwagen A, Keeney S. A Hierarchical Combination of Factors Shapes the Genome-wide Topography of Yeast Meiotic Recombination Initiation. Cell (2011) vol. 144 (5) pp. 719-31

Panizza S, Mendoza MA, Berlinger M, Huang L, Nicolas A, Shirahige K, Klein F. Spo11-accessory proteins link double-strand break sites to the chromosome axis in early meiotic recombination. Cell (2011) vol. 146 (3) pp. 372-83

Pâques F and Haber JE. Multiple pathways of recombination induced by double-strand breaks in *Saccharomyces cerevisiae*. Microbiol Mol Biol Rev (1999) vol. 63 (2) pp. 349-404

Pâques F, Leung WY, Haber JE. Expansions and contractions in a tandem repeat induced by double-strand break repair. Mol Cell Biol (1998) vol. 18 (4) pp. 2045-54

Parvanov ED, Petkov PM, Paigen K. Prdm9 controls activation of mammalian recombination hotspots. Science (2010) vol. 327 (5967) pp. 835

Pastink A, Eeken JC, Lohman PH. Genomic integrity and the repair of double-strand DNA breaks. Mutat Res (2001) vol. 480-481 pp. 37-50

Peciña A, Smith KN, Mézard C, Murakami H, Ohta K, Nicolas A. Targeted stimulation of meiotic recombination. Cell (2002) vol. 111 (2) pp. 173-84

Perkins DD. Crossing-over and interference in a multiply marked chromosome arm of *Neurospora.* Genetics (1962) vol. 47 pp. 1253-74

Pittman DL, Cobb J, Schimenti KJ, Wilson LA, Cooper DM, Brignull E, Handel MA, Schimenti JC. Meiotic prophase arrest with failure of chromosome synapsis in mice deficient for Dmc1, a germline-specific RecA homolog. Mol Cell (1998) vol. 1 (5) pp. 697-705

Plank JL, Wu J, Hsieh TS. Topoisomerase III alpha and Bloom's helicase can resolve a mobile double Holliday junction substrate through convergent branch migration. Proc Natl Acad Sci USA (2006) vol. 103 (30) pp. 11118-23

Porter SE, White MA, Petes TD. Genetic evidence that the meiotic recombination hotspot at the *HIS4* locus of *Saccharomyces cerevisiae* does not represent a site for a symmetrically processed double-strand break. Genetics (1993) vol. 134 (1) pp. 5-19

Prakash R, Satory D, Dray E, Papusha A, Scheller J, Kramer W, Krejci L, Klein H, Haber JE, Sung P, Ira G. Yeast Mph1 helicase dissociates Rad51-made D-loops: implications for crossover control in mitotic recombination. Genes Dev (2009) vol. 23 (1) pp. 67-79

Prieler S, Penkner A, Borde V, Klein F. The control of Spo11's interaction with meiotic recombination hotspots. Genes Dev (2005) vol. 19 (2) pp. 255-69

Qi J, Wijeratne AJ, Tomsho LP, Hu Y, Schuster SC, Ma H. Characterization of meiotic crossovers and gene conversion by whole-genome sequencing in *Saccharomyces cerevisiae*. BMC Genomics (2009) vol. 10 pp. 475

Qin J, Richardson LL, Jasin M, Handel MA, Arnheim N. Mouse strains with an active H2-Ea meiotic recombination hot spot exhibit increased levels of H2-Ea-specific DNA breaks in testicular germ cells. Mol Cell Biol (2004) vol. 24 (4) pp. 1655-66

Radman-Livaja M and Rando OJ. Nucleosome positioning: how is it established, and why does it matter?. Dev Biol (2010) vol. 339 (2) pp. 258-66

Rasmussen SW and Holm PB. Human meiosis II. Chromosome pairing and recombination nodules in human spermatocytes. Carlsberg Research Communications (1978) vol. 43 (5) pp. 275-327

Rasmussen SW and Holm PB. The synaptonemal complex, recombination nodules and chiasmata in human spermatocytes. Symp Soc Exp Biol (1984) vol. 38 pp. 271-92

Rasmussen SW, Holm PB, Lu BC, Zickler D, Sage J. Synaptonemal complex formation and distribution of recombination nodules in pachytene trivalents of triploid *Coprinus cinereus*. Carlsberg Research Communications (1982) vol. 46 pp. 347-60

Rasmussen SW. The meiotic prophase in *Bombyx mori* females analyzed by three-dimensional reconstructions of synaptonemal complexes. (1976) vol. 54 (3) pp. 245-293

Rattner JB, Goldsmith MR, Hamkalo BA. Chromosome organization during male meiosis in *Bombyx mori*. Chromosoma (1981) vol. 82 (3) pp. 341-351

Ray BL, White CI, Haber JE. Heteroduplex formation and mismatch repair of the "stuck" mutation during mating-type switching in *Saccharomyces cerevisiae*. Mol Cell Biol (1991) vol. 11 (10) pp. 5372-80

Ray JH and German J. Bloom's syndrome and EM9 cells in BrdU-containing medium exhibit similarly elevated frequencies of sister chromatid exchange but dissimilar amounts of cellular proliferation and chromosome disruption. Chromosoma (1984) vol. 90 (5) pp. 383-388

Ray JH, Louie E, German J. Different mutations are responsible for the elevated sister-chromatid exchange frequencies characteristic of Bloom's syndrome and hamster EM9 cells. Proc Natl Acad Sci USA (1987) vol. 84 (8) pp. 2368-71

Raynard S, Bussen W, Sung P. A double Holliday junction dissolvasome comprising BLM, topoisomerase IIIalpha, and BLAP75. J Biol Chem (2006) vol. 281 (20) pp. 13861-4

Raynard S, Zhao W, Bussen W, Lu L, Ding YY, Busygina V, Meetei AR, Sung P. Functional role of BLAP75 in BLM-topoisomerase IIIalpha-dependent holliday junction processing. J Biol Chem (2008) vol. 283 (23) pp. 15701-8

Resnick MA and Martin P. The repair of double-strand breaks in the nuclear DNA of *Saccharomyces cerevisiae* and its genetic control. Mol Gen Genet (1976) vol. 143 (2) pp. 119-29

Resnick MA. The repair of double-strand breaks in DNA; a model involving recombination. J Theor Biol (1976) vol. 59 (1) pp. 97-106

Robine N, Uematsu N, Amiot F, Gidrol X, Barillot E, Nicolas A, Borde V. Genome-wide redistribution of meiotic double-strand breaks in *Saccharomyces cerevisiae*. Mol Cell Biol (2007) vol. 27 (5) pp. 1868-80

Rockmill B and Roeder GS. A meiosis-specific protein kinase homolog required for chromosome synapsis and recombination. Genes Dev (1991) vol. 5 (12B) pp. 2392-404

Rockmill B and Roeder GS. Meiosis in asynaptic yeast. Genetics (1990) vol. 126 (3) pp. 563-74

Rockmill B and Roeder GS. *RED1*: a yeast gene required for the segregation of chromosomes during the reductional division of meiosis. Proc Natl Acad Sci USA (1988) vol. 85 (16) pp. 6057-61

Rockmill B, Sym M, Scherthan H, Roeder GS. Roles for two RecA homologs in promoting meiotic chromosome synapsis. Genes Dev (1995) vol. 9 (21) pp. 2684-95

Roeder GS. Meiotic chromosomes: it takes two to tango. Genes Dev (1997) vol. 11 (20) pp. 2600-21

Roman H. Gene conversion and crossing-over. Environ Mutagen (1985) vol. 7 (6) pp. 923-32

Ross-Macdonald P and Roeder GS. Mutation of a meiosis-specific MutS homolog decreases crossing over but not mismatch correction. Cell (1994) vol. 79 (6) pp. 1069-80

Saini N, Ramakrishnan S, Elango R, Ayyar S, Zhang Y, Deem A, Ira G, Haber JE, Lobachev KS, Malkova A. Migrating bubble during break-induced replication drives conservative DNA synthesis. Nature (2013) vol. 502 (7471) pp. 389-92

Sasaki M, Lange J, Keeney S. Genome destabilization by homologous recombination in the germ line. Nat Rev Mol Cell Biol (2010) vol. 11 (3) pp. 182-95

Sasanuma H, Hirota K, Fukuda T, Kakusho N, Kugou K, Kawasaki Y, Shibata T, Masai H, Ohta K. Cdc7-dependent phosphorylation of Mer2 facilitates initiation of yeast meiotic recombination. Genes Dev (2008) vol. 22 (3) pp. 398-410

Sasanuma H, Murakami H, Fukuda T, Shibata T, Nicolas A, Ohta K. Meiotic association between Spo11 regulated by Rec102, Rec104 and Rec114. Nucleic Acids Research (2007) vol. 35 (4) pp. 1119-33

Schatz DG and Ji Y. Recombination centres and the orchestration of V(D)J recombination. Nat Rev Immunol (2011) vol. 11 (4) pp. 251-63

Schmekel K and Daneholt B. The central region of the synaptonemal complex revealed in three dimensions. Trends Cell Biol (1995) vol. 5 (6) pp. 239-42

Schultes NP and Szostak JW. A poly(dA.dT) tract is a component of the recombination initiation site at the *ARG4* locus in Saccharomyces cerevisiae. Mol Cell Biol (1991) vol. 11 (1) pp. 322-8

Schwacha A and Kleckner N. Identification of double Holliday junctions as intermediates in meiotic recombination. Cell (1995) vol. 83 (5) pp. 783-91

Schwacha A and Kleckner N. Identification of joint molecules that form frequently between homologs but rarely between sister chromatids during yeast meiosis. Cell (1994) vol. 76 (1) pp. 51-63

Schwacha A and Kleckner N. Interhomolog bias during meiotic recombination: meiotic functions promote a highly differentiated interhomolog-only pathway. Cell (1997) vol. 90 (6) pp. 1123-35

Serrentino ME and Borde V. The spatial regulation of meiotic recombination hotspots: Are all DSB hotspots crossover hotspots?. Exp Cell Res (2012) pp.

Serrentino ME, Chaplais E, Sommermeyer V, Borde V. Differential association of the conserved SUMO ligase Zip3 with meiotic double-strand break sites reveals regional variations in the outcome of meiotic recombination. PLoS Genet (2013) vol. 9 (4) pp. e1003416

Sharif WD, Glick GG, Davidson MK, Wahls WP. Distinct functions of S. pombe Rec12 (Spo11) protein and Rec12-dependent crossover recombination (chiasmata) in meiosis I; and a requirement for Rec12 in meiosis II. Cell Chromosome (2002) vol. 1 (1) pp. 1

Sheridan SD, Yu X, Roth R, Heuser JE, Sehorn MG, Sung P, Egelman EH, Bishop DK. A comparative analysis of Dmc1 and Rad51 nucleoprotein filaments. Nucleic Acids Research (2008) vol. 36 (12) pp. 4057-66

Sherwood R, Takahashi TS, Jallepalli PV. Sister acts: coordinating DNA replication and cohesion establishment. Genes Dev (2010) vol. 24 (24) pp. 2723-31

Shilatifard A. Chromatin modifications by methylation and ubiquitination: implications in the regulation of gene expression. Annu Rev Biochem (2006) vol. 75 pp. 243-69

Shinohara A, Ogawa H, Ogawa T. Rad51 protein involved in repair and recombination in S. cerevisiae is a RecA-like protein. Cell (1992) vol. 69 (3) pp. 457-70

Shinohara M, Gasior SL, Bishop DK, Shinohara A. Tid1/Rdh54 promotes colocalization of Rad51 and Dmc1 during meiotic recombination. Proc Natl Acad Sci USA (2000) vol. 97 (20) pp. 10814-9

Shinohara M, Oh SD, Hunter N, Shinohara A. Crossover assurance and crossover interference are distinctly regulated by the ZMM proteins during yeast meiosis. Nat Genet (2008) vol. 40 (3) pp. 299-309

Smagulova F, Gregoretti IV, Brick K, Khil P, Camerini-Otero RD, Petukhova GV. Genome-wide analysis reveals novel molecular features of mouse recombination hotspots. Nature (2011) vol. 472 (7343) pp. 375-8

Smith AV and Roeder GS. The yeast Red1 protein localizes to the cores of meiotic chromosomes. The Journal of Cell Biology (1997) vol. 136 (5) pp. 957-67

Smith GR, Boddy MN, Shanahan P, Russell P. Fission yeast Mus81-Eme1 Holliday junction resolvase is required for meiotic crossing over but not for gene conversion. Genetics (2003) vol. 165 (4) pp. 2289-93

Sollier J, Lin W, Soustelle C, Suhre K, Nicolas A, Géli V, de La Roche Saint-André C. Set1 is required for meiotic S-phase onset, double-strand break formation and middle gene expression. EMBO J (2004) vol. 23 (9) pp. 1957-67

Sommermeyer V, Béneut C, Chaplais E, Serrentino ME, Borde V. Spp1, a member of the Set1 Complex, promotes meiotic DSB formation in promoters by tethering histone H3K4 methylation sites to chromosome axes. Molecular Cell (2013) vol. 49 (1) pp. 43-54

Sourirajan A and Lichten M. Polo-like kinase Cdc5 drives exit from pachytene during budding yeast meiosis. Genes Dev (2008) vol. 22 (19) pp. 2627-32

Stack SM and Anderson LK. Two-dimensional spreads of Synaptonemal complexes from solanaceous plants. II. Synapsis in *Lycopersicon esculentum*(tomato). *Am. J. Bot.* (1986) vol. 73 pp. 264–81

Stadler DR and Towe AM. Evidence for meiotic recombination in *Ascobolus* involving only one member of a tetrad. Genetics (1971) vol. 68 (3) pp. 401-13

Stahl FW, Foss HM, Young LS, Borts RH, Abdullah MF, Copenhaver GP. Does crossover interference count in *Saccharomyces cerevisiae*?. Genetics (2004) vol. 168 (1) pp. 35-48

Stahl FW. Genetic Recombination: Thinking about It in Phage and Fungi. (1979). (San Francisco: W. H. Freeman).

Stark JM and Jasin M. Extensive loss of heterozygosity is suppressed during homologous repair of chromosomal breaks. Mol Cell Biol (2003) vol. 23 (2) pp. 733-43

Stevens WL. The analysis of interference. Journal of Genetics (1936) vol. 32 (1) pp. 51-64

Stracker TH, Theunissen JW, Morales M, Petrini JH. The Mre11 complex and the metabolism of chromosome breaks: the importance of communicating and holding things together. DNA Repair (2004) vol. 3 (8–9) pp. 845-854

Sugawara N, Ira G, Haber JE. DNA length dependence of the single-strand annealing pathway and the role of Saccharomyces cerevisiae RAD59 in double-strand break repair. Mol Cell Biol (2000) vol. 20 (14) pp. 5300-9

Sun H, Treco D, Schultes NP, Szostak JW. Double-strand breaks at an initiation site for meiotic gene conversion. Nature (1989) vol. 338 (6210) pp. 87-90

Sun H, Treco D, Szostak JW. Extensive 3'-overhanging, single-stranded DNA associated with the meiosis-specific double-strand breaks at the *ARG4* recombination initiation site. Cell (1991) vol. 64 (6) pp. 1155-61

Sweeney FD, Yang F, Chi A, Shabanowitz J, Hunt DF, Durocher D. Saccharomyces cerevisiae Rad9 acts as a Mec1 adaptor to allow Rad53 activation. Curr Biol (2005) vol. 15 (15) pp. 1364-75

Sym M and Roeder GS. Crossover interference is abolished in the absence of a synaptonemal complex protein. Cell (1994) vol. 79 (2) pp. 283-92

Sym M, Engebrecht JA, Roeder GS. ZIP1 is a synaptonemal complex protein required for meiotic chromosome synapsis. Cell (1993) vol. 72 (3) pp. 365-78

Szostak JW, Orr-Weaver TL, Rothstein RJ, Stahl FW. The double-strand-break repair model for recombination. Cell (1983) vol. 33 (1) pp. 25-35

Tanaka K, Miyamoto N, Shouguchi-Miyata J, Ikeda JE. HFM1, the human homologue of yeast Mer3, encodes a putative DNA helicase expressed specifically in germ-line cells. DNA Seq (2006) vol. 17 (3) pp. 242-6

Tarsounas M, Morita T, Pearlman RE, Moens PB. RAD51 and DMC1 form mixed complexes associated with mouse meiotic chromosome cores and synaptonemal complexes. The Journal of Cell Biology (1999) vol. 147 (2) pp. 207-20

Terasawa M, Ogawa H, Tsukamoto Y, Shinohara M, Shirahige K, Kleckner N, Ogawa T. Meiotic recombination-related DNA synthesis and its implications for cross-over and non-cross-over recombinant formation. Proc Natl Acad Sci USA (2007) vol. 104 (14) pp. 5965-70

Terasawa M, Ogawa T, Tsukamoto Y, Ogawa H. Sae2p phosphorylation is crucial for cooperation with Mre11p for resection of DNA double-strand break ends during meiotic recombination in Saccharomyces cerevisiae. Genes Genet Syst (2008) vol. 83 (3) pp. 209-17

Terasawa M, Shinohara A, Hotta Y, Ogawa H, Ogawa T. Localization of RecA-like recombination proteins on chromosomes of the lily at various meiotic stages. Genes Dev (1995) vol. 9 (8) pp. 925-34

Terentyev Y, Johnson R, Neale MJ, Khisroon M, Bishop-Bailey A, Goldman AS. Evidence that *MEK1* positively promotes interhomologue double-strand break repair. Nucleic Acids Research (2010) pp.

Tsubouchi H and Ogawa H. A Novel *mre11* Mutation Impairs Processing of Double-Strand Breaks of DNA during Both Mitosis and Meiosis. Mol Cell Biol (1998) vol. 18 (1) pp. 260-268

Tsubouchi H and Ogawa H. Exo1 roles for repair of DNA double-strand breaks and meiotic crossing over in Saccharomyces cerevisiae. Mol Biol Cell (2000) vol. 11 (7) pp. 2221-33

Tsubouchi H and Roeder GS. Budding yeast Hed1 down-regulates the mitotic recombination machinery when meiotic recombination is impaired. Genes Dev (2006) vol. 20 (13) pp. 1766-75

Usui T, Ogawa H, Petrini JH. A DNA damage response pathway controlled by Tel1 and the Mre11 complex. Molecular Cell (2001) vol. 7 (6) pp. 1255-66

Valencia M, Bentele M, Vaze MB, Herrmann G, Kraus E, Lee SE, Schär P, Haber JE. *NEJ1* controls non-homologous end joining in Saccharomyces cerevisiae. Nature (2001) vol. 414 (6864) pp. 666-9

van der Heijden T, Modesti M, Hage S, Kanaar R, Wyman C, Dekker C. Homologous recombination in real time: DNA strand exchange by RecA. Molecular Cell (2008) vol. 30 (4) pp. 530-8

Vaze MB, Pellicioli A, Lee SE, Ira G, Liberi G, Arbel-Eden A, Foiani M, Haber JE. Recovery from checkpoint-mediated arrest after repair of a double-strand break requires Srs2 helicase. Mol Cell (2002) vol. 10 (2) pp. 373-85

Veaute X, Jeusset J, Soustelle C, Kowalczykowski SC, Le Cam E, Fabre F. The Srs2 helicase prevents recombination by disrupting Rad51 nucleoprotein filaments. Nature (2003) vol. 423 (6937) pp. 309-12

Vedel M and Nicolas A. *CYS3*, a hotspot of meiotic recombination in *Saccharomyces cerevisiae*. Effects of heterozygosity and mismatch repair functions on gene conversion and recombination intermediates. Genetics (1999) vol. 151 (4) pp. 1245-59

Vialard JE, Gilbert CS, Green CM, Lowndes NF. The budding yeast Rad9 checkpoint protein is subjected to Mec1/Tel1-dependent hyperphosphorylation and interacts with Rad53 after DNA damage. EMBO J (1998) vol. 17 (19) pp. 5679-88

Virgin JB, Bailey JP, Hasteh F, Neville J, Cole A, Tromp G. Crossing over is rarely associated with mitotic intragenic recombination in *Schizosaccharomyces pombe*. Genetics (2001) vol. 157 (1) pp. 63-77

Wagstaff JE, Klapholz S, Waddell CS, Jensen L, Esposito RE. Meiotic exchange within and between chromosomes requires a common Rec function in Saccharomyces cerevisiae. Mol Cell Biol (1985) vol. 5 (12) pp. 3532-44

Wang K, Tang D, Wang M, Lu J, Yu H, Liu J, Qian B, Gong Z, Wang X, Chen J, Gu M, Cheng Z. *MER3* is required for normal meiotic crossover formation, but not for presynaptic alignment in rice. J Cell Sci (2009) vol. 122 (Pt 12) pp. 2055-63

Wang TF, Kleckner N, Hunter N. Functional specificity of MutL homologs in yeast: evidence for three Mlh1-based heterocomplexes with distinct roles during meiosis in recombination and mismatch correction. Proc Natl Acad Sci USA (1999) vol. 96 (24) pp. 13914-9

Watt PM and Hickson IH. Failure to unwind causes cancer. Genome stability. Curr Biol (1996) vol. 6 (3) pp. 265-7

Watt PM, Louis EJ, Borts RH, Hickson ID. Sgs1: a eukaryotic homolog of E. coli RecQ that interacts with topoisomerase II in vivo and is required for faithful chromosome segregation. Cell (1995) vol. 81 (2) pp. 253-60

Webb AJ, Berg IL, Jeffreys A. Sperm cross-over activity in regions of the human genome showing extreme breakdown of marker association. Proc Natl Acad Sci USA (2008) vol. 105 (30) pp. 10471-6

Weiner BM and Kleckner N. Chromosome pairing via multiple interstitial interactions before and during meiosis in yeast. Cell (1994) vol. 77 (7) pp. 977-91

Weintraub H and Groudine M. Chromosomal subunits in active genes have an altered conformation. Science (1976) vol. 193 (4256) pp. 848-56

Westergaard M and von Wettstein D. Studies on the mechanism of crossing over. IV. The molecular organization of the synaptinemal complex in *Neottiella* (Cooke) *saccardo* (Ascomycetes). C R Trav Lab Carlsberg (1970) vol. 37 (11) pp. 239-68

Westergaard M and von Wettstein D. The synaptinemal complex. Annu Rev Genet (1972) vol. 6 pp. 71-110

Whitby MC, Osman F, Dixon J. Cleavage of model replication forks by fission yeast Mus81-Eme1 and budding yeast Mus81-Mms4. J Biol Chem (2003) vol. 278 (9) pp. 6928-35

White MA and Petes TD. Analysis of meiotic recombination events near a recombination hotspot in the yeast *Saccharomyces cerevisiae*. Curr Genet (1994) vol. 26 (1) pp. 21-30

White MA, Detloff P, Strand M, Petes TD. A promoter deletion reduces the rate of mitotic, but not meiotic, recombination at the *HIS4* locus in yeast. Curr Genet (1992) vol. 21 (2) pp. 109-16

White MA, Wierdl M, Detloff P, Petes TD. DNA-binding protein Rap1 stimulates meiotic recombination at the *HIS4* locus in yeast. Proc Natl Acad Sci USA (1991) vol. 88 (21) pp. 9755-9

Williamson DH, Johnston LH, Fennell DJ, Simchen G. The timing of the S phase and other nuclear events in yeast meiosis. Exp Cell Res (1983) vol. 145 (1) pp. 209-17

Winkler H (1930): "Die Konversion der Gene." Jena: Verlag Gustav Fischer

Wu L and Hickson ID. The Bloom's syndrome helicase suppresses crossing over during homologous recombination. Nature (2003) vol. 426 (6968) pp. 870-4

Wu L, Bachrati CZ, Ou J, Xu C, Yin J, Chang M, Wang W, Li L, Brown GW, Hickson ID. BLAP75/RMI1 promotes the BLM-dependent dissolution of homologous recombination intermediates. Proc Natl Acad Sci USA (2006) vol. 103 (11) pp. 4068-73

Wu TC and Lichten M. Factors that affect the location and frequency of meiosis-induced double-strand breaks in *Saccharomyces cerevisiae*. Genetics (1995) vol. 140 (1) pp. 55-66

Wu TC and Lichten M. Meiosis-induced double-strand break sites determined by yeast chromatin structure. Science (1994) vol. 263 (5146) pp. 515-8

Xu L, Ajimura M, Padmore R, Klein C, Kleckner N. *NDT80*, a meiosis-specific gene required for exit from pachytene in Saccharomyces cerevisiae. Mol Cell Biol (1995) vol. 15 (12) pp. 6572-81

Xu L, Weiner BM, Kleckner N. Meiotic cells monitor the status of the interhomolog recombination complex. Genes Dev (1997) vol. 11 (1) pp. 106-18

Xu X, Aprelikova O, Moens P, Deng CX, Furth PA. Impaired meiotic DNA-damage repair and lack of crossing-over during spermatogenesis in *BRCA1* full-length isoform deficient mice. Development (2003) vol. 130 (9) pp. 2001-12

Yoshida K, Kondoh G, Matsuda Y, Habu T, Nishimune Y, Morita T. The mouse RecA-like gene Dmc1 is required for homologous chromosome synapsis during meiosis. Mol Cell (1998) vol. 1 (5) pp. 707-18

Youds JL, Mets DG, McIlwraith MJ, Martin JS, Ward JD, ONeil NJ, Rose AM, West SC, Meyer BJ, Boulton SJ. RTEL-1 enforces meiotic crossover interference and homeostasis. Science (2010) vol. 327 (5970) pp. 1254-8

Young JA, Hyppa RW, Smith GR. Conserved and nonconserved proteins for meiotic DNA breakage and repair in yeasts. Genetics (2004) vol. 167 (2) pp. 593-605

Zakharyevich K, Ma Y, Tang S, Hwang PY, Boiteux S, Hunter N. Temporally and biochemically distinct activities of Exo1 during meiosis: double-strand break resection and resolution of double Holliday junctions. Molecular Cell (2010) vol. 40 (6) pp. 1001-15

Zakharyevich K, Tang S, Ma Y, Hunter N. Delineation of joint molecule resolution pathways in meiosis identifies a crossover-specific resolvase. Cell (2012) vol. 149 (2) pp. 334-47

Zalevsky J, MacQueen AJ, Duffy JB, Kemphues KJ, Villeneuve AM. Crossing over during *Caenorhabditis elegans* meiosis requires a conserved MutS-based pathway that is partially dispensable in budding yeast. Genetics (1999) vol. 153 (3) pp. 1271-83

Zenvirth D, Arbel T, Sherman A, Goldway M, Klein S, Simchen G. Multiple sites for double-strand breaks in whole meiotic chromosomes of *Saccharomyces cerevisiae*. EMBO J (1992) vol. 11 (9) pp. 3441-7

Zenvirth D, Richler C, Bardhan A, Baudat F, Barzilai A, Wahrman J, Simchen G. Mammalian meiosis involves DNA double-strand breaks with 3' overhangs. Chromosoma (2003) vol. 111 (6) pp. 369-76

Zhang L, Kim KP, Kleckner NE, Storlazzi A. Meiotic double-strand breaks occur once per pair of (sister) chromatids and, via Mec1/ATR and Tel1/ATM, once per quartet of chromatids. Proc Natl Acad Sci USA (2011) vol. 108 (50) pp. 20036-41

Zhu Z, Chung WH, Shim EY, Lee SE, Ira G. Sgs1 helicase and two nucleases Dna2 and Exo1 resect DNA double-strand break ends. Cell (2008) vol. 134 (6) pp. 981-94

Zickler D and Sage J. Synaptonemal complexes with modified lateral elements in *Sordaria humana*: development of and relationship to the “recombination nodules”. Chromosoma (1981) vol. 84 (3) pp. 305-318

Zickler D. Development of the synaptonemal complex and the "recombination nodules" during meiotic prophase in the seven bivalents of the fungus *Sordaria macrospora Auersw*. Chromosoma (1977) vol. 61 (4) pp. 289-316

Zou L and Elledge SJ. Sensing DNA damage through ATRIP recognition of RPA-ssDNA complexes. Science (2003) vol. 300 (5625) pp. 1542-8

Zou L, Liu D, Elledge SJ. Replication protein A-mediated recruitment and activation of Rad17 complexes. Proc Natl Acad Sci USA (2003) vol. 100 (24) pp. 13827-32